Titre: Title:	Conditional Mean Spectra, Spectral Correlation Coefficients, and High Damping Spectral Amplitudes for Seismic Design and Evaluation in Canada
Auteur: Author:	Poulad Daneshvar
Date:	2015
Type:	Mémoire ou thèse / Dissertation or Thesis
Référence: Citation:	Daneshvar, P. (2015). Conditional Mean Spectra, Spectral Correlation Coefficients, and High Damping Spectral Amplitudes for Seismic Design and Evaluation in Canada [Ph.D. thesis, École Polytechnique de Montréal]. PolyPublie. https://publications.polymtl.ca/1740/

UNIVERSITÉ DE MONTRÉAL

CONDITIONAL MEAN SPECTRA, SPECTRAL CORRELATION COEFFICIENTS, AND HIGH DAMPING SPECTRAL AMPLITUDES FOR SEISMIC DESIGN AND EVALUATION IN CANADA

POULAD DANESHVAR

DÉPARTEMENT DES GÉNIES CIVIL, GÉOLOGIQUE, ET DES MINES

ÉCOLE POLYTECHNIQUE DE MONTRÉAL

THÈSE PRÉSENTÉE EN VUE DE L'OBTENTION

DU DIPLÔME DE PHILOSOPHIAE DOCTOR

(GÉNIE CIVIL)

MARS 2015

UNIVERSITÉ DE MONTRÉAL

ÉCOLE POLYTECHNIQUE DE MONTRÉAL

Cette thèse intitulée :

CONDITIONAL MEAN SPECTRA, SPECTRAL CORRELATION COEFFICIENTS, AND HIGH DAMPING SPECTRAL AMPLITUDES FOR SEISMIC DESIGN AND EVALUATION IN CANADA

présentée par : DANESHVAR Poulad

en vue de l'obtention du diplôme de : Philosophiae Doctor

a été dûment acceptée par le jury d'examen constitué de :

Mme KOBOEVIC Sanda, Ph. D., présidente

M. BOUAANANI Najib, Ph. D., membre et directeur de recherche

M. JAMES Michael, Ph. D., membre

Mme NOLLET Marie-José, Ph. D., membre

DEDICATION

To Nassim who did not let my feet touch the ground…

ACKNOWLEDGEMENTS

No research endeavor is ever carried out in solitude. I owe my deep gratitude to a great number of people. I would like to thank my supervisor, Dr. Najib Bouaanani, who provided invaluable academic support, advice and attention and guided me through all these years of research.

I would also like to thank my parents, Masoud and Forough, and my brother Hirad, who followed my progress with worried eyes and encouraged me to follow my dreams.

Special thanks to my parents-in-law, Dariush and Nayereh, who inspired me with their concern and warmth.

My gratitude also goes to my friends and the kind staff at Polytechnique Montreal who helped me throughout the research process. Special thanks to Morteza Dehghani, Armin Sadeghian, Ilona Bartosh and Fabien Lagier for their support and always being available for discussions and sharing ideas.

I would also like to acknowledge the financial support of Natural Sciences and Engineering Research Council of Canada (NSERC), the Canadian Seismic Research Network (CSRN), and the Quebec Fund for Research on Nature and Technology (FRQNT).

Performing this research would not have been possible for me if it were not for Nassim. Nassim, you were the one I came to, whenever I was worried, frustrated or hopeless. You tolerated me when I was not myself and made me go forward. I dedicate this thesis to you, although it is not even comparable to the wings you have given me.

RÉSUMÉ

Les séismes présentent une menace majeure contre l'intégrité des structures dans plusieurs zones géographiques du monde. Au Canada, aussi bien à l'Est qu'à l'Ouest, une attention particulière est dédiée à l'évaluation de l'aléa sismique et du risque associé, notamment dans les grands centres urbains tels que Montréal et Vancouver. Il va sans dire que cette évaluation est d'autant plus importante que bon nombre de structures dans ces régions subissent un vieillissement significatif.

Par conséquent, les normes et guides de calcul traitant de la conception parasismique sont constamment mis à jour pour prendre en considération les progrès technologiques et ceux en recherche. Les clauses et recommandations énoncées dans ces documents sont principalement fondées, soit directement sur des études des secousses sismiques, ou sur des leçons tirées des expériences passées en comparaison avec les modèles analytiques et/ou numériques. Les dernières versions du Code National du Bâtiment du Canada et du Code canadien sur le Calcul des Ponts Routiers contiennent deux principaux outils qui sont directement développés à partir de séismes et de leurs caractéristiques, à savoir : le spectre d'aléa uniforme (SAU) et le facteur de réduction d'amortissement.

Un SAU a tendance à fournir des amplitudes spectrales très conservatrices pour la majorité des périodes de vibrations considérées. Ceci s'explique par le fait qu'il ne représente pas un spectre de réponse spécifique de n'importe quel accélérogramme. En conséquence, le spectre moyen conditionnel (SMC) a été proposé comme approche alternative pour l'évaluation de l'aléa sismique d'une région. En Amérique du Nord, le SMC a fait l'objet de plusieurs recherches aux États-Unis. Au Canada, des études ont été menées considérant l'aléa sismique en vigueur à l'Ouest canadien mais pas à l'Est en raison de l'absence de certains paramètres régionaux nécessaires au calcul du SMC.

Pour pallier à ces lacunes, cette thèse de doctorat présente les étapes de calcul du SMC pour l'Est canadien en utilisant les paramètres disponibles actuellement, alors que les paramètres manquants sont mis en évidence. L'application du SMC dans le cadre de l'analyse spectrale d'un bâtiment à Montréal démontre une réduction significative des indicateurs de réponse sismique affectés par les modes supérieurs, par exemple, le cisaillement à la base du bâtiment. L'étude du SMC dans l'Est canadien est ensuite approfondie pour déterminer quelques paramètres régionaux manquants. Il est

démontré que le choix des lois d'atténuation peut affecter de manière significative les amplitudes spectrales du SMC, surtout pour les plus courtes périodes. Les coefficients de corrélation des accélérations spectrales sont déterminés pour l'Est du Canada en se basant sur des enregistrements sismiques historiques. Des coefficients de corrélation plus élevés sont observés dans l'Est comparativement à ceux obtenus à partir d'un modèle correspondant à l'Ouest. Le coefficient de corrélation déterminé pour l'Est ne dépend que légèrement de la magnitude et de la distance. Il est démontré que cette dépendance a peu d'effet sur le SMC pour de plus courtes périodes.

Les amplitudes spectrales à des niveaux d'amortissement plus grand que 5% sont couramment utilisées dans les méthodes simplifiées de conception et d'évaluation parasismiques. Ces amplitudes peuvent être obtenues en calculant les réponses spectrales pour le niveau d'amortissement désiré ou en appliquant des facteurs de réduction d'amortissement aux amplitudes spectrales correspondant à 5% d'amortissement, généralement disponibles. Les lois d'atténuation prédisant des amplitudes spectrales à des niveaux d'amortissement plus élevés que 5% ne sont pas disponibles actuellement pour l'Est canadien. En plus, les facteurs de réduction d'amortissement prévus par les normes canadiennes sont principalement basés sur des séismes correspondant à des régions ayant des caractéristiques généralement différentes de ceux de l'Est canadian, telles que l'ouest de l'Amérique du Nord. Dans cette thèse, une base de données de séismes hybrides est adoptée et les amplitudes spectrales pour des périodes allant jusqu'à 2 s, correspondant à des niveaux d'amortissement entre 5% et 30% sont déterminées. Une loi d'atténuation est proposée pour prédire les déplacements spectraux d'amortissement élevés en considérant un nombre de paramètres sismiques déterminés par des analyses de régression. Les facteurs de réduction d'amortissement obtenus par les prédictions sont vérifiés avec ceux calculés à partir des enregistrements. Bien que les dernières versions des normes canadiennes prescrivent des facteurs de réduction d'amortissement basés sur des données sismique de l'Ouest, ces facteurs correspondent principalement à des séismes peu profonds par rapport à la croute terrestre et négligeant la contribution des événements plus profonds ainsi que ceux caractéristiques de la zone de subduction de Cascadia. Dans cette thèse de doctorat, une vaste base de données d'enregistrement de séismes est compilée et les facteurs de réduction d'amortissement pour la ville de Vancouver sont déterminés par une sélection d'enregistrements de désagrégation considérant les trois types de séismes pouvant se produire à l'Ouest canadien. Il est démontré que le contenu des hautes fréquences des enregistrements profond entraine des facteurs de réduction

d’amortissement considérablement dépendants des périodes, alors qu’ils sont plutôt indépendants pour des enregistrements d’interface en raison d’une durée relativement plus longue. On observe également que les facteurs de réductions d’amortissement à l’Ouest sont pratiquement similaires pour des sites de classes C et D. Une équation prédisant les facteurs de réduction d’amortissement correspondant à chaque événement est proposée et les coefficients correspondants sont déterminés par des analyses de régression. La thèse de doctorat se conclut par un chapitre incluant des exemples d’application des paramètres développés pour la conception parasismique d’un bâtiment et de deux ponts.

ABSTRACT

Seismic loads are a major source of threat against the integrity of structures in many parts of the world. In Canada, considerable contribution of ground motions to the forces acting on structures is expected in the eastern and western parts of the country where a number of major urban centers such as Montreal and Vancouver are located. This makes Eastern and Western Canada two zones of significant seismic risk. Thus attention has to be paid to the corresponding seismic risk when it comes to urban development and also maintenance and retrofit of the aging structures, particularly in these regions. As a result, seismic design codes and guidelines are constantly being updated to take account of advancements in technology and research. Prescriptions of these documents are mainly based on either direct studies of ground motions or the analyses and past experiences regarding structures and their analytical models. The recent versions of the National Building Code of Canada (NBCC) and the Canadian Highway Bridge Design Code (CHBDC), contain two major design tools which are directly developed from ground motions and their corresponding characteristics: Uniform Hazard Spectrum (UHS) and Damping Reduction Factors.

A UHS tends to provide over-conservative spectral amplitudes at the majority of the vibration periods considered mainly due to the fact that it does not represent a specific spectrum from any accelerogram. Therefore, Conditional Mean Spectrum (CMS) has been proposed as an alternative approach towards evaluation of seismic hazard in a region. Considering North America, CMS has been given great attention in the United States. In Canada, studies have been conducted for western Canada, however, this is not the case in the east mainly due to the lack of some underlying regional parameters needed to compute CMS. To address this issue, in this thesis, a step by step computation of CMS for Eastern Canada using the currently available constituents of CMS is provided and the missing parameters are pinpointed. Through application of the computed CMS to response spectrum analysis of a building in Montreal, it is shown that there is a considerable reduction in the response when the response parameter is also affected by the higher modes, e.g. base shear. The investigation of computation of CMS in Eastern Canada is continued through an in depth look at the missing regional constituents. It is shown that selection of the underlying ground motion prediction equations can significantly affect the spectral amplitudes of a CMS particularly at shorter periods. Spectral acceleration correlation coefficients are determined for Eastern Canada based on historical events. Higher correlation coefficients are observed in the east in comparison

to those obtained from a western based model. Minor dependence of the determined eastern correlation coefficients on magnitude and distance is observed. This dependence is shown to have slight effects on the CMS at shorter periods.

High damping spectral amplitudes are widely used in simplified structural seismic design and evaluation methods and can be obtained either by computing the spectral amplitudes at the desired damping level or applying damping reduction factors to the available 5%-damped amplitudes. Ground motion prediction equations providing spectral amplitudes at higher damping levels are not currently available for Eastern Canada. In addition, the damping reduction factors provided by the Canadian codes are mainly based on ground motions from regions with high seismicity such as Western North America (WNA). In this thesis, a database of hybrid ground motions is adopted and spectral amplitudes for periods up to 2 s corresponding to damping levels between 5% and 30% are determined. A model equation to predict high damping spectral displacements considering a number of ground motion parameters is proposed and the corresponding coefficients are determined through regression analyses. The damping reduction factors obtained from the predictions are verified against those computed from the records in the database. Although the latest versions of the Canadian codes prescribe WNA-based damping reduction factors, these are mainly based on shallow crustal ground motions and neglect the contribution of inslab and interface events from the Cascadia Subduction zone. In this thesis, an extensive database of ground motion records is compiled and damping reduction factors for the city of Vancouver are determined through a deaggregation-based record selection considering the three ground motion types in Western Canada. It is shown that high frequency content of the inslab records result in considerably period dependent damping reduction factors, whereas these factors are rather period independent for interface records due to the relatively longer duration. It is also shown that WNA damping reduction factors are practically similar for site classes C and D. A model equation for prediction of damping reduction factors corresponding to each event type is proposed and the corresponding coefficients are determined through regression analyses. This doctoral thesis ends with a chapter including examples of application of the developed parameters to seismic design of a building and two bridges.

TABLE OF CONTENTS

LIST OF TABLES

LIST OF FIGURES

LIST OF SYMBOLS AND ABBREVIATIONS

Abbreviations

CHBDC	Canadian Highway Bridge Design Code
CEUS	Central and Eastern United States
CMS	Conditional Mean Spectrum
DBD	Displacement-based design
ENA	Eastern North America
GMPE	Ground motion prediction equation
GSC	Geological Survey of Canada
NBCC	National Building Code of Canada
NEHRP	National Earthquake Hazard Reduction Program
NGA West	Next Generation Attenuation Relationships for Western USA
PBSD	Performance-based seismic design
PEER	Pacific Earthquake Engineering Research Center
PSA	Pseudo spectral acceleration
PSHA	Probabilistic seismic hazard analysis
UHS	Uniform hazard spectrum
USGS	United States Geological Survey
WNA	Western North America
WUS	Western United States

Symbols

M	Magnitude
M_{V}	Elastic higher mode shear amplification factor

M_{b}	Body wave magnitude
M_{N}	Nuttli's magnitude
M_{S}	Surface wave magnitude
M_{W}	Moment magnitude
R	Distance
R_{h}	Hypocentral distance
R_{jb}	Joyner-Boore distance
R_{RUP}	Rupture distance
S_{a}	Spectral acceleration
$S_{\mathrm{a}}(T,\xi)$	Spectral acceleration at a period T and an equivalent damping ratio of ξ
S_{d}	Spectral displacement
$S_{\mathrm{d}}(T,\xi)$	Spectral displacement at a period T and an equivalent damping ratio of ξ
T	Period of vibration
T^*	Period at which the CMS is anchored to the UHS
ξ	Equivalent damping ratio
η	Damping reduction factor
V_{S30}	Time-averaged shear-wave velocity in the top 30m of the subsurface profile
$\varepsilon(T)$	The difference between the spectral amplitudes of the UHS and the predicted accelerations measured at a period T as the number of standard deviations
$\mu_{\ln S_{\mathrm{a}}(T)}^{(\mathrm{CMS})}$	Spectral accelerations given by CMS
$\sigma_{\ln\, S_{\mathrm{a}}}$	Standard deviation in logarithmic units provided by the GMPE
$\sigma_{\ln S_{\mathrm{a}}(T)}^{(\mathrm{CMS})}$	Standard deviation in logarithmic units associated with CMS
$\rho(T,T^*)$	Spectral acceleration correlation coefficient

CHAPTER 1 INTRODUCTION

This chapter introduces the context of this study, specifically the problem it addresses and its area of application. The objectives of this work and the methodology by which these objectives are accomplished are explained. This is followed by a description of the scope and the original contributions of this study. Finally, the organization of the thesis is presented.

1.1 Problem statement

Seismic loads are a major source of threat against the integrity of structures in many parts of the world. In Canada, considerable contribution of ground motions to the forces acting on structures is expected in the eastern and western parts of the country where a number of major urban centers such as Montreal and Vancouver are located. This makes Eastern and Western Canada two zones of significant seismic risk. Thus attention has to be paid to the corresponding seismic risk when it comes to urban development and also maintenance and retrofit of the aging structures, particularly in these regions. As a result, seismic design codes and guidelines are constantly being updated to take account of advancements in technology and research. Prescriptions of these documents are mainly based on either direct studies of ground motions or the analyses and past experiences regarding structures and their analytical models. The recent versions of the National Building Code of Canada (NBCC) and the Canadian Highway Bridge Design Code (CHBDC), prescribe two major design tools which are directly developed from ground motions and their corresponding characteristics: Uniform Hazard Spectra and Damping Reduction Factors.

A Uniform Hazard Spectrum (UHS) provides spectral amplitudes having the same seismic hazard level at all periods as it represents the envelope of the spectral amplitudes that are exceeded with a certain probability, e.g. 2% in 50 years. Thus over-conservative spectral amplitudes are observed at the majority of the vibration periods considered. This is mainly due to the fact that it does not represent a specific spectrum from any accelerogram. The results of probabilistic seismic hazard analysis (PSHA) can show that at each period there are different events contributing to the hazard and occurrence of the spectral amplitude given by the UHS. Therefore, Conditional Mean Spectrum

(CMS) has been proposed (Baker 2011) as an alternative approach towards evaluation of seismic hazard in a region. CMS is and to the UHS at a specific period and usually has lower spectral amplitudes than the UHS at other periods. In other words, the spectral amplitudes given by CMS are of lower probabilities of exceedance at periods other than the anchoring period. This results in a reduced conservatism in the spectral amplitudes. Considering North America, CMS has been given great attention in the United States with the United States Geological Survey (USGS 2010) providing CMS for various locations within the American borders. In Canada, studies on computation and application of CMS have been focused on Western Canada, e.g. Goda and Atkinson 2009. However, this is not the case in the east mainly due to the lack of some underlying regional parameters needed to compute CMS. Although parameters such as spectral acceleration correlation coefficients, which can vary based on the seismicity of the specific region under consideration, are not available for Eastern Canada, there is also no study on computation of CMS for the east using the currently available constituents such as the WNA-based correlation coefficients. Furthermore, ground motion prediction equations (GMPEs) are also required to compute CMS. There are several GMPEs developed for Eastern North America based on different assumptions and model functions. Whether selection of the underlying GMPE to compute the CMS affects the outcome in an Eastern Canadian context, has not been addressed in the literature so far.

Elastic spectral amplitudes associated with damping levels higher than the conventional 5% critical damping are important in seismic design and evaluation of structures equipped with energy dissipating and seismic isolation systems. They are widely used in simplified structural seismic design and evaluation methods proposed by several design codes and guidelines (e.g. CHBDC 2014, NBCC 2015) and can be obtained either by computing the spectral amplitudes at the desired damping level or applying damping reduction factors to the available 5%-damped amplitudes. The former approach is commonly done through GMPEs. GMPEs providing spectral amplitudes at higher damping levels are not currently available for Eastern Canada. The latter approach is usually taken by design codes due to their simple application. The damping reduction factors provided by the Canadian codes are mainly based on ground motions from regions with high seismicity such as Western North America (WNA). There are very few studies on damping reduction factors in ENA, e.g. Atkinson and Pierre (2004) and Cameron and Green (2007), however, GMPEs predicting high damping spectral amplitudes for ENA have not been developed so far. These GMPEs can provide a wide range of spectral amplitudes corresponding to different ground motion parameters (e.g.

magnitude and distance) at different damping levels which can be used to develop equations for prediction of damping reduction factors. Furthermore, these GMPEs can be adopted in PSHA to determine seismic hazard maps, UHS and CMS at various damping levels. Although damping reduction factors prescribed by design codes and guidelines are based on studies on the seismic hazard in WNA, an important consideration is that the majority of the previous studies have focused upon ground motions for shallow crustal earthquakes, whereas ground motions for subduction earthquakes (including deep inslab and mega-thrust interface events) have not been much investigated. The large magnitudes of mega-thrust subduction earthquakes, and the potentially-high stress drops for deep inslab earthquakes, are important factors that control the duration and frequency content of ground motions - which are relevant properties for damped structural responses. It is therefore expected that the differing characteristics of ground motions for different earthquake types that contribute to hazard have major influence on the damping reduction factors.

1.2 Objectives

1.2.1 General objective

The main objective of this research is to investigate the applicability of state-of-the art tools to seismic design and evaluation of structures in ENA, particularly Eastern Canada, considering the currently available seismographic data. Subsequently, the underlying ingredients for such tools which are specific to seismic hazard in Eastern Canada or ENA are developed.

1.2.2 Specific Objectives

To achieve the general objective of this research, the following specific objectives were set:

- Compute CMS for an Eastern Canadian location, e.g. Montreal, to illustrate a step-by-step procedure to construct CMS using the region-specific ingredients such as ground motion prediction equations (GMPEs) consistent with the code-prescribed UHS;
- Perform a more in-depth investigation of the effect of variations in the main ingredients on the resulting CMS;
- Determine ENA-specific correlation coefficients for spectral amplitudes to supplement the commonly used WNA-based coefficients;

– Develop equations to predict spectral displacements at different damping levels for Eastern North America to facilitate determination of damping reduction factors as well as displacement-based probabilistic seismic hazard analysis (PSHA) in this region;
– Investigate damping reduction factors specific to the three ground motion types dominating the seismic hazard in Western Canada and developing a single functional form for prediction of such damping reduction factors.

Section 1.3 provides more detailed explanations on the intended methodology to achieve the abovementioned objectives.

1.3 Methodology

1.3.1 Step-by-Step Computation of CMS for Eastern Canada

Although the general methodology to compute CMS is available in the literature, computation of CMS using parameters specific to Eastern Canada has not been investigated. CMS is first computed for an Eastern Canadian location using the currently available seismic data in the literature. To this end, the underlying GMPE for the UHS prescribed in National Building Code of Canada for Montreal is selected to compute the CMS. The deaggregation results for Montreal are used with the GMPE to generate spectral amplitudes and determine the input parameters for computation of CMS. The step-by-step procedure to obtain a CMS for a location in Eastern Canada is then provided.

Finally, the computed CMS is used in response spectrum analysis of a building in Montreal and the results are compared to those obtained from a similar analysis on the same building using the code prescribed UHS.

1.3.2 Conducting a more in-depth investigation on computation of CMS in Eastern Canada

At this stage the procedure to compute a CMS in Eastern Canada has been presented. However, the obtained CMS was computed using a GMPE which was developed in 1995. In addition, the spectral correlation factors are determined from ground motion records specific to regions of high seismicity. As Eastern Canada is a region of moderate seismicity, we investigate the feasibility of

computing CMS with correlation coefficients obtained from ground motions specific to this region. For this purpose we first study the effect of selection of the underlying GMPE on the resulting CMS by selecting a number of GMPEs already proposed in the literature for Eastern Canada or ENA. Next, a database of ground motion records from ENA is compiled and by means of the state-of-the-art GMPE for Eastern Canada spectral correlation coefficients at different periods of vibration are developed for this region. The effect of using the determined coefficients on the obtained CMS is investigated.

1.3.3 Prediction of high-damping spectral amplitudes

Damping reduction factors for displacements are gaining more attention in alternative seismic design methods such as DBD and also by being incorporated in various design codes, particularly to obtain the final displacement of seismically isolated structures. These factors can be obtained directly by studying the ground motion spectra at different damping levels or by using the high damping spectral amplitudes predicted by ground motion prediction equations. The latter approach is taken in this thesis as, with the increasing attention being given to displacements, there is a lack of GMPEs predicting displacement amplitudes in ENA. Furthermore the developed GMPEs can also contribute to determination of seismic hazard maps in terms of displacements at various damping levels for Eastern Canada.

To develop equations to predict high-damping spectral displacements, a database of hybrid ground motion records is adopted and the records are spectrally matched to the predictions of the state-of-the-art GMPE developed for Eastern Canada. This also ensures that the final results are in accordance with the most recent approaches and tools taken by the Geological Survey of Canada (GSC). Next, the spectral displacements from the matched records are used to develop a functional form for prediction of 5%-damped spectral displacements in ENA. Subsequently, spectral displacements at higher damping levels are computed from the matched records. The same functional form is used to develop equations for the high damping spectral amplitudes in ENA.

1.3.4 Prediction of damping reduction factors considering different ground motion types in Western Canada

A large majority of the equations proposed for prediction of damping reduction factors are developed considering shallow crustal ground motion records of active tectonic regions such as

WNA. The results of some of these studies are used in design codes and regulations. However, for a region such as Western Canada, crustal ground motions are only one of the contributing sources to seismic hazard. Ground motions from the Cascadia subduction zone, i.e. inslab and interface event types, also contribute to the seismic hazard in this region. As a result, we select Vancouver as a location associated with high seismic risk and develop equations predicting damping reduction factors with consideration of the three types of contributing events. To this end, a large database of crustal, inslab and interface ground motions from active tectonic regions is compiled. Using the deaggregation results for Vancouver, records are selected based on their magnitude and distance and the corresponding displacement spectra at different damping levels are generated. Damping reduction factors are then determined from the obtained spectra. Next, a functional form is proposed and through regression analyses equations are developed to predict damping reduction factors for each event type considering the seismic hazard in Vancouver.

1.4 Scope and original contributions

This thesis makes multiple original contributions.

The preliminary investigation of CMS in Eastern Canada presents an original study to assess the feasibility of application of CMS to structural analysis in Eastern Canada. A step-by-step procedure that takes account of seismic hazard in Eastern Canada is provided which can be adopted by the structural engineering community in the region.

Through a parametric study on the ingredients of CMS in Eastern Canada, it was shown that the selected GMPE can considerably affect the spectral amplitudes of the CMS mainly at shorter periods. This might have an impact on the seismic analysis or evaluation of structures with relatively short fundamental periods and also those for which higher mode effects are significant.

The first study of spectral correlation coefficients in Eastern Canada was conducted and these coefficients were determined through historical records from ENA. The study of the applicability to Eastern Canada of spectral correlation models developed based on WNA ground motions, suggests higher spectral correlations in Eastern Canada than predicted by a WNA-based model.

The dependency of the determined correlation coefficients for Eastern Canada on magnitude was found to be generally pronounced as one of the two periods, between which the correlation is considered, is shifted towards the longer period range. On the contrary, distance-dependency of the

determined correlation coefficients for Eastern Canada was found to be less significant for distances of interest in structural engineering applications.

It was also shown that the effects of magnitude- or distance-based correlation coefficients on the CMS developed for three eastern cities of Toronto, Montreal, and Quebec are (1) generally negligible at long periods and (2) significant at shorter periods particularly when the conditioning period T^* to compute the CMS is less than approximately 0.5 s.

Through a spectral matching of a set of hybrid empirical records to the state-of-the-art Canadian GMPE, a new data set of hybrid records, of various damping levels, which are in accordance with the NBCC 2015 prescriptions is formed.

Conducting regression analyses on records matched to the state-of-the-art Canadian GMPE at different damping levels, equations capable of predicting high damping spectral amplitudes for Eastern Canada are proposed. These equations, being the first equations considering high damping spectral amplitudes, can contribute to further assessment of the seismic hazard in Eastern Canada.

Damping reduction factors for ENA are obtained from predicted spectral displacements and shown to be period dependent. This observation reiterates the greater uncertainty in the analysis results when period independent damping reduction factors from other regions are used. Thus the obtained period dependent damping reduction factors are shown to be better representatives of damping trends in Eastern Canada.

To investigate damping reduction factors in Western Canada, a large data set records from all the three event types contributing to the seismic hazard in Western Canada is compiled. This data set can be used in further assessment of seismic risk and hazard in WNA.

Damping reduction factors for different ground motion types in Western Canada are studied and characterized. This is the first study to address such factors for inslab and interface events specific to Vancouver. Furthermore, equations are proposed to predict damping reduction factors for Vancouver which can be readily applied to the current design and evaluation procedures.

1.5 Organization of the thesis

Following this Introduction chapter, a literature review of the topics discussed in this thesis is presented in Chapter 2. Chapters 3 to 6 contain the comparative and parametric studies,

characterizations of damping reduction factors in Eastern and Western Canada, and the developed equations predicting high damping spectral amplitudes and damping reduction factors in both regions. These chapters correspond to the four articles published or accepted in peer reviewed journals. Chapter 7 contains brief examples of application of the developed equations and the determined coefficients in the analysis of structures in Canada. Chapter 8 briefly discusses the findings in this thesis and the conclusions. Further recommendations are included in Chapter 9.

CHAPTER 2 LITERATURE REVIEW

2.1 Introduction

This chapter contains a brief review of literature on the subjects included in this research work. It starts with an overview of seismicity and ground motions in Canada followed by the evolution of seismic design provisions in national building and bridge design codes of Canada. Conditional mean spectrum, ground motion prediction equations, and damping reduction factors are also discussed.

2.2 Seismicity and ground motions in Canada

2.2.1 Brief review of the nature of earthquakes and basic terminology

The majority of natural earthquakes occur in the top layer (crust) of the earth. The deformations of crustal sections result in an accumulation of elastic energy in the rocks (Bolt 1989). This energy is released due to rupture along a pre-existing fault zone and as a result seismic waves are transmitted radially from the zone of rupture causing ground shaking. The damage associated with an earthquake can be related to either the fault movement or the ground shaking. The latter would generally cause most structural damage since structures are often built far from the faults. The theory of plate tectonics, proposed in the 1960s, is the most commonly accepted theory to explain the reasons behind the occurrence of earthquakes (Condie 2003). It states that the crust consists of a number of small and large plates floating on a viscous medium. The plates move at a relatively small rate (up to approximately 15 cm) each year (Filliatrault 2002). Their interaction can be in form of a transform, diverge or subduction motion (Miao and Langston 2008). According to plate tectonics theory, when the resistance of the rock is exceeded, earthquakes occur at the boundary of adjacent plates thus creating a rupture (Turcotte and Schubert 2002). According to Reid's elastic rebound theory, the movement in the fault happens when strain is accumulated in the rock on either side due to the gradual shift by the crust (Scholz 1972). As the resistance of the rock is exceeded, the crust reacts by snapping back and releasing the energy propagating waves that travel in every direction resulting in earthquakes. The fault mechanisms are categorized into three types: the strike-

slip fault caused by transform motion, the normal fault caused by the diverge motion and the underthrust fault caused by the subduction motion of the plates (Bolt 1989).

Different kinds of waves are generated during earthquakes. Waves travelling within the solid earth are called the body waves and the waves near the ground surface are called the surface waves (Filiatrault 2002). There are two kinds of body waves: primary waves which are horizontal tension and compression waves travelling in the direction of the wave front and the secondary waves which are shear waves travelling perpendicularly to the wave front (Bolt 1982). There are also two kinds of waves associated with surface waves: Rayleigh waves which are vertical waves and Love waves which are horizontal waves both travelling along the ground surface (Bozorgnia and Bertero 2004). Primary waves are generally characterized by their high frequency and are the first to reach a site. The secondary waves are of lower frequency (Bozorgnia and Bertero 2004). Yet they are known as the most destructive to the structure due to their greater amplitude. In general, the amplitude of body waves decrease with distance from the hypocenter. This relation for the surface waves is the reciprocal of the square root of the same distance. Thus surface waves travel over a greater distance (Filiatrault 2002).

"Magnitude" is used to describe the size of an earthquake. This was introduced by Richter in 1930 by defining a standard event and giving the magnitude of a given earthquake, M_{L} (Local Magnitude), by calculating the difference between the amplitudes of the two events (Lee et al. 1972). To date, by modifying Richter's work, a variety of magnitude scales have been introduced depending on different wave types. Therefore, the values are not absolute. In addition to local magnitude a number of other magnitude scales are used: surface wave magnitude (M_{S}), body wave magnitude (m_{b}), moment magnitude (M_{W}) and Nuttli's magnitude (M_{N}). Moment magnitude (M_{W}) is one of the more recent magnitude scales and is determined considering the energy released by the causative fault. M_{W} is now commonly used in estimation of earthquake magnitudes and in ground motion prediction equations. Nevertheless, M_{W} is not very reliable to estimate low magnitudes (Filiatrault et al. 2013). Instead, other magnitude scales such as M_{N} are used to obtain more reliable magnitudes for smaller earthquakes (Atkinson and Boore 2011).

2.2.2 Seismicity in Canada

Figure 2-1 shows the map of historical earthquakes in Canada up to 2012 (Natural Resources Canada 2015). It is seen that the eastern and the western regions of Canada are more earthquake-

prone than the central and the northern regions. In addition, most of the Canadian population lives in eastern and western Canada, usually concentrated in major cities or along corridors such as the St. Lawrence River. This implies a higher seismic risk in these two regions, to be linked to various structural vulnerability indexes corresponding to a diversified built environment. For instance, although seismic hazard in western Canada is greater (Adams and Atkinson 2003), larger cities in the east are also at risk owing to the presence of many unreinforced masonry buildings which generally behave poorly during earthquakes (Filiatrault 2002).

There are three zones in Eastern Canada were significant seismic activity is observed: western Quebec, the Charlevoix region and the lower St. Lawrence region (Lamontagne 1987, Lamontagne et al. 2003). In the west, three distinct tectonic regions can be identified: the Queen Charlotte region, the offshore region of the west coast and the continental region (Milne et al. 1978). Due to the relative lack of seismic activity in Canada, particularly in the east, the seismicity of this region is usually studied by considering the global seismicity of North America. A number of differences between earthquakes occurring in the east and the west were reported in the literature. First, seismic waves in Eastern Canada have a lower attenuation rate than their western counterparts (Atkinson and Boore 2011). Therefore, they can be felt in longer distances from the epicentre. For instance, the Saguenay earthquake of 1988 was felt in Washington D.C., in the south and in Thunder Bay, Ontario in the west (Filiatrault 2002). In contrast, western earthquakes usually attenuate quickly within 100 km from the epicentre. One other difference in the seismicity of these regions is the fault systems. The fault systems in WNA extend to the surface, while there is no evidence so far of surface faulting in ENA. Surface faulting generally results in more reliable seismic hazard evaluation in the west, while intra-plate seismicity such as in Quebec leaves seismologists with lots of unknowns. Furthermore, higher frequency content is associated with the ground motions recorded in ENA (Atkinson and Beresnev 1998). This can easily be seen from the acceleration time-histories from these regions as illustrated in Figure 2-2. Finally, shallow crustal earthquakes are not the only type of ground motions contributing to the seismic hazard in the west. Cascadia subduction zone deep inslab and mega-thrust interface earthquakes play a considerable role in the seismicity of this region. The large magnitude of interface events has greatly contributed to the relatively long duration of such events, and the potentially high stress drops for inslab earthquakes have contributed to the high frequency nature of these event types. In the east, contrary to the west, shallow crustal ground motions are the only contributors to the seismic hazard.

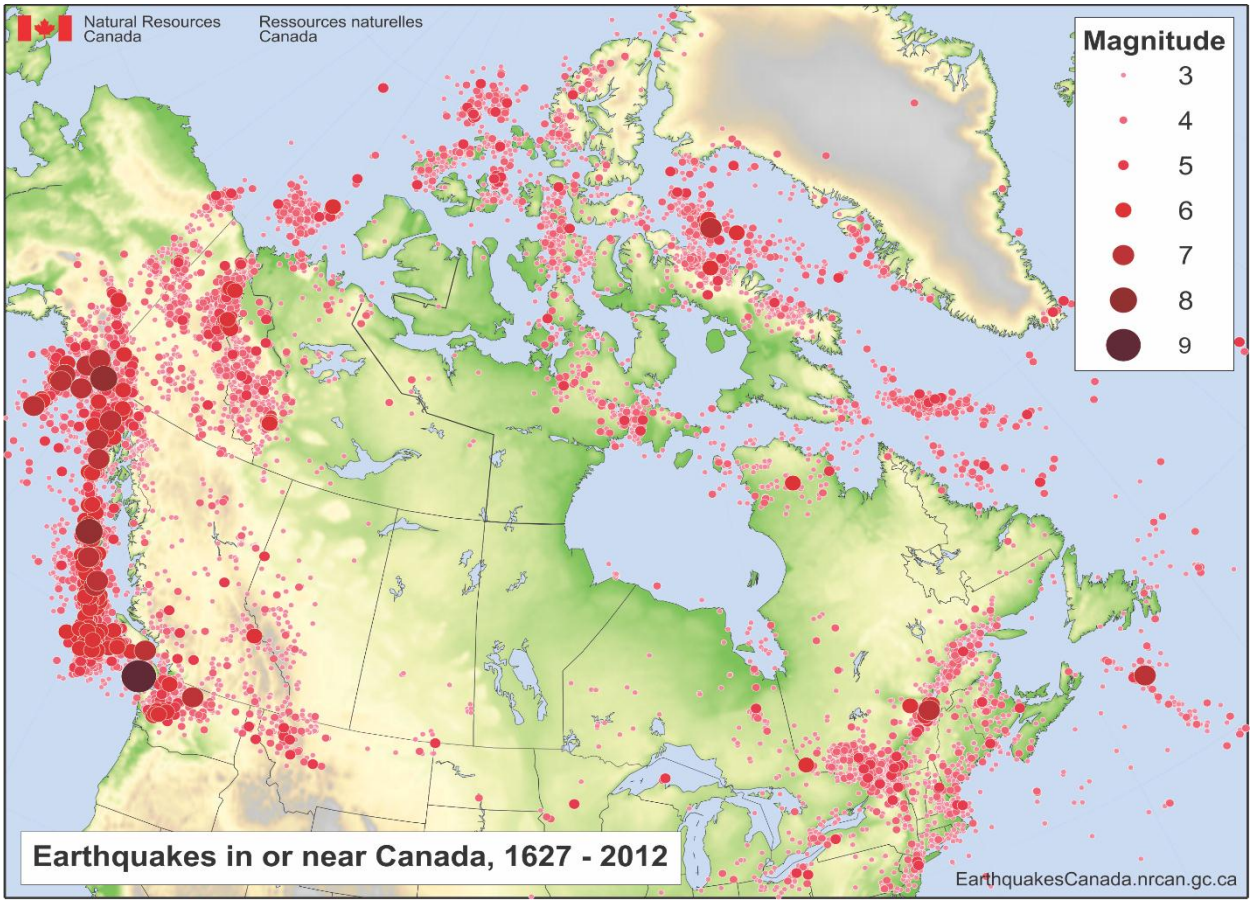

Figure 2-1: Historical earthquakes in or near Canada (GSC 2015)

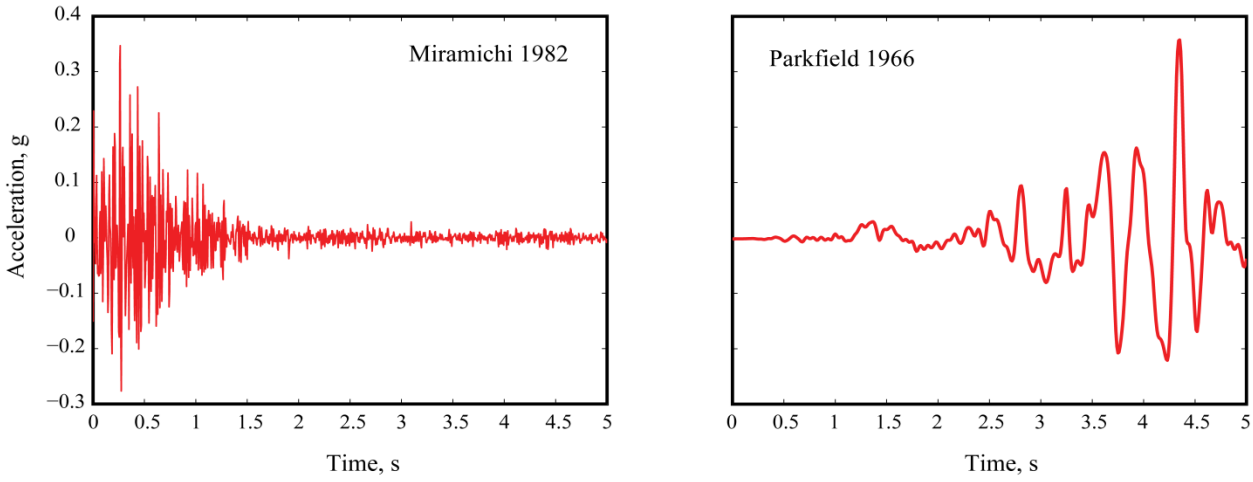

Figure 2-2: Ground motion records from Eastern and Western North America

Eastern and western shallow crustal earthquakes have similar focal depths of approximately between surface and 30 km (Natural Resources Canada 2013a, 2013b). This excludes the Cascadia subduction zone in the west where much deeper focal points can be produced.

Ground-motion prediction equations (GMPEs), also known as attenuation relationships, are usually simple equations developed to predict ground-motion-related parameters such as spectral accelerations, peak ground accelerations (PGA) and spectral displacements in a specific region. Data obtained from previously experienced events are used either directly as input to develop GMPEs or for calibration of the parameters needed to develop GMPEs. The most basic GMPEs give the intensity of the ground-motion as a function of magnitude and distance whereas more sophisticated ones consider other parameters such as site class and fault type. An example of GMPEs is the one developed in 2008 for WNA, the details of which can be found in Boore and Atkinson (2008). Exceedance rates of ground-motion parameters such as PGA can be calculated for different ground motion scenarios in a given location using GMPEs and probabilistic calculations. Assuming Poissonian distribution, the probability of exceedance of the desired parameter can be calculated for the desired recurrence interval (e.g. 50 years) and the corresponding hazard curve is then formed. Reducing the hazard curve to a single probability of exceedance (e.g. 2% in 50 years) and repeating the procedure for different periods of vibration, leads to a curve with values for ground-motion parameters (e.g. spectral acceleration) with the same probability of exceedance. This curve is called a Uniform Hazard Spectrum (UHS) (Field 2011). Uniform hazard acceleration spectra corresponding to different localities in Canada have been provided by National building Code of Canada (NBCC 2005, 2010, 2015). Figure 2-3 illustrates NBCC 2010 UHS for Montreal and Vancouver. UHS are mainly used to obtain site-specific spectral accelerations required to determine design base shear. UHS-compatible time-histories are also useful for time-history analyses. In this case, historical records that match a section of the UHS should be selected and, if required, modified using various available frequency-domain (Carballo and Cornell 2000), time-domain (Naeim et al. 2004) or conditional mean spectral matching techniques (Baker 2011). The selected records should be typically in the same magnitude-distance range and tectonic environment that is causing the hazard (Atkinson and Beresnev 1998). These conditions are however hard to satisfy due to the scarcity of historical records in low to moderate seismic environments such as in Quebec. This concern is circumvented by generating simulated physically realizable records which reproduce the repeatable features of past events while preserving

randomness, an important feature of ground-motions (Atkinson and Beresnev 1998, Atkinson 2009).

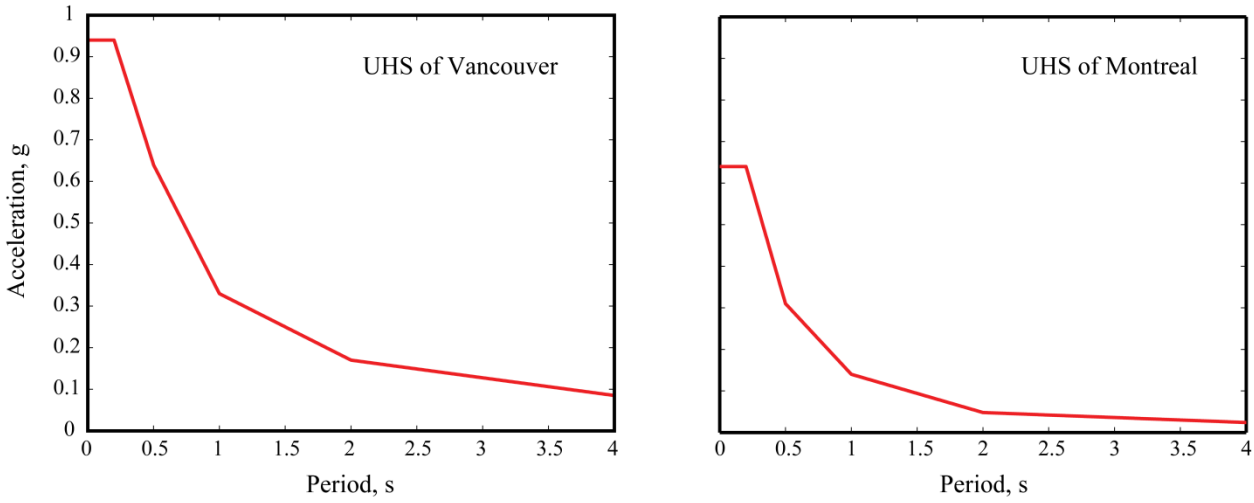

Figure 2-3: Uniform hazard spectra for Vancouver and Montreal as prescribed by NBCC 2010

2.3 Evolution of National Building Code of Canada

Earthquake engineering in Canada is tightly linked to the implementation of the seismic provisions of the National Building Code of Canada (Filiatrault 2002, Mitchell et al. 2010). Although the present research proposal is mainly concerned with the seismic design and evaluation of bridge structures, the major historical milestones of the NBCC seismic provisions are briefly reviewed next (Filiatrault 2002, Mitchell et al. 2010):

- The publication of the NBCC started in 1941. The first Canadian seismic provisions, included in the code's appendices, were influenced by the 1937 edition of the Uniform Building Code (UBC) of the United States. The static method included a uniform lateral load based on a seismic coefficient depending on soil-bearing capacity.
- In the 1953 and 1960 NBCC editions, modified seismic design provisions were included in the main body of the code. Four seismic intensity zoning maps of Canada were considered as well as taking account of structural flexibility in the calculation of the seismic coefficient.

- In the 1965 NBCC edition, a design base shear formula proportional to the weight of each floor, varying along the height of the building and including the effects of structural ductility was introduced for the first time in Canada. Furthermore, torsional couples also appeared in this edition of NBCC. Finally the NBCC 1965 recognized dynamic analysis as an alternative to static procedure with the condition of being performed by a "competent authority".
- The 1970 NBCC edition introduced a seismic zoning map for Canada including contours of peak horizontal acceleration based on a 100 year return period for the entire country. The 100 year acceleration values, however, were not included in the base shear formula. The code also stipulated that a portion of the lateral static load be applied to the roof to account for higher modes effects and it also allowed the reduction of the overturning moment at the base of the structure.
- The 1975 NBCC edition modified the base shear formula to directly include the 100-year acceleration values in the lateral load calculation. Moreover, the steps to perform the dynamic analysis of a "complex or irregular" structure, based on an elastic design response spectrum, were included in the commentary of the code.
- The 1978 and 1980 NBCC editions required the shear force calculated by dynamic analysis to be at least 90% of the one resulted from the static analysis. No major changes were included in these editions in comparison to the 1975 one.
- The 1985 NBCC edition included seismic zoning maps with peak horizontal acceleration and velocities having a uniform return period of 475 years for the entire country.
- The 1990 edition's base shear equation emphasized the role of ductility on reducing the lateral design forces. The strength-reduction factor R was introduced in this edition.
- The major changes made in the 1995 NBCC edition were an additional force modification factor, new expressions for building periods of vibration and new torsional eccentricity expressions. It also required that the base shear resulting from the dynamic analysis not to be less than 80% of the static value.
- NBCC 2005 contained a number of major changes including site-specific UHS with a probability of exceedence of 2% in 50 years, i.e. a 2500 year return period. Moreover, the dynamic analysis was chosen as the preferred method of analysis and had to be used for structures with certain irregularities. A new equation for base shear calculation was provided with an additional equation to limit the lateral force to a minimum value. A coefficient

accounting for higher modes effects was introduced. Two different reduction factors were also provided to account for ductility and overstrength. The 5%-damped design spectral values for specific periods were given (T = 0.2, 0.5, 1.0, 2.0 and T ≥ 4). Finally, the load factor for earthquake effect was taken as 1.0 due to the low probability of exceedance corresponding to the UHS.

– In NBCC 2010, the UHS for all the regions except western Canada are recalculated. This was done as a result of a decrease in the short-period hazard in low seismicity zones and an increase in the corresponding long-period hazard. Modifications were also made to the lower limit of the lateral seismic force and therefore the values of M_v (accounting for higher modes effect) were also modified. Moreover, additional force modification factors were introduced as well as supplementary restrictions for post-disaster buildings.

– In the most recent NBCC edition (2015), the underlying model for calculation of seismic hazard across Canada and generation of seismic hazard maps has been replaced with a more recent model proposed by Atkinson and Adams (2013). The UHS for all the regions are recalculated. This was done as the previous model was based on studies dating back almost two decades. Furthermore, due to the increasing interest in spectral amplitudes at longer periods, the UHS amplitudes in NBCC 2015 are provided up to 10 s. Figure 2-4 illustrates the 2005 and 2010 NBCC UHS for Montreal.

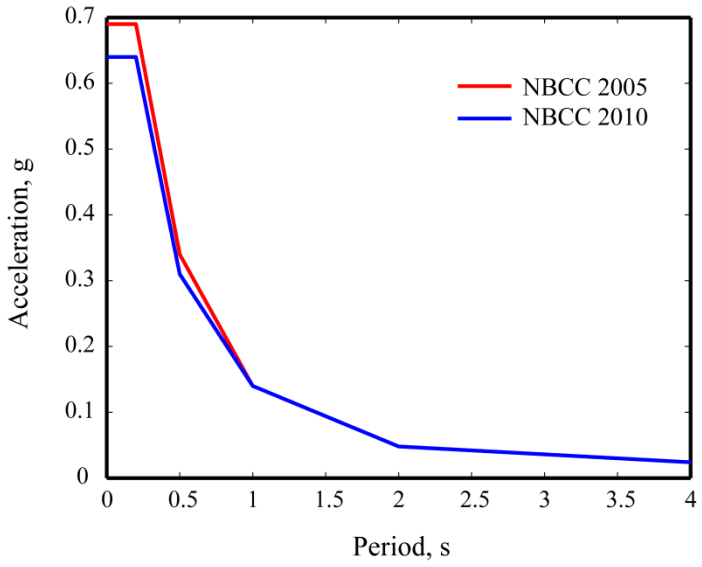

Figure 2-4: Uniform hazard spectra for Montreal as prescribed by NBCC 2005 and 2010

2.4 Evolution of Canadian Highway Bridge Design Codes

Minimum consideration of the seismic design of bridges was introduced in the 1966 edition of the Canadian Highway Bridge Design Code (CHBDC), but it was only in the 1988 edition of the code that significant details on earthquake loads were given. The evolution of these provisions is briefly summarized as follows (Dion 2010, Massicotte 2011):

- Section 5.1.19 of CSA 1966 stipulated that the static equivalent lateral load applied by an earthquake at the center of gravity of the structure, regardless of the horizontal direction, is taken as a percentage of the dead weight of the structure as follows:
  - 2% when the structure is on a soil with a bearing capacity of at least 4 ton/ft^2
  - 4% when the structure is on a soil with a bearing capacity of less than 4 ton/ft^2
  - 6% when the structure is on a pile foundation
- CSA 1974 did not specify any values for design earthquake loads. However, article 5.1.22 mentioned the necessity of taking the earthquake load into consideration in areas where earthquakes are expected.
- Article 5.1.21 of CSA 1978 prescribed that the earthquake load should be considered as an equivalent static load applied in one horizontal direction to the center of gravity of the structure. This load was calculated using the dead weight of the structure, a response coefficient C ($0.0 < C < 0.8$) depending on the seismic zone where the structure is located, and a factor F ($0.8 < F < 1.0$) taking account of the support condition of the structure. For more complex structures, it was prescribed to use a spectral method where the value of the response factor C was defined by response spectra varying with the depth of the rock under the foundation and the maximum acceleration in rock type A. It was stated that the given response spectra were based on those from California, and were therefore potentially conservative for Canada. It also mentioned the need to conduct dynamic analysis in special cases, such as structures with natural period of vibration over 3.0 seconds, or in areas with unusual geological conditions. Finally, the code briefly mentioned the minimum expected resisting force in restraint or energy dissipating systems.
- CSA 1988 (CSA-S6-M88) also had the same approach as the previous edition. However, the calculation of the static equivalent force had been modified by introducing a risk coefficient I (I=1 or I=1.3), a foundation factor F ($1.0 < F < 1.5$), a coefficient c_v varying with the zonal

seismic acceleration Z_a and the zonal seismic velocity V_z. A velocity ratio v was also introduced, with values to be taken from the National Building Code of Canada 1985. This edition of the bridge code did not provide more information on spectral methods or dynamic analysis; however, it recommended using the American codes for seismic design.

– CHBDC 2000, CHBDC 2006, and the most recent CHBDC 2014 have allotted their fourth chapters to seismic design. In CHBDC 2014, Chapter 4 prescribes applying an equivalent static method including "Uniform-load method" or "Single-mode spectral method" method, for seismic design of bridges. However, they only apply to regular bridges of normal importance or emergency bridges located in low to moderate seismic zones. The codes describe elastic dynamic methods including "Multi-mode elastic response spectral analysis" and "Elastic time-history analysis" applicable to the majority of other cases. They also prescribe the use of the "Non-linear time history analysis method" for emergency bridges located in moderate to high seismic zones. "Inelastic static push-over analysis" is also prescribed for major irregular route bridges and emergency bridges.

  Performance-based design approaches are also introduced in the latest version of CHBDC and are required for all emergency bridges and irregular major route bridges. In addition, CHBDC 2014 has adopted a UHS similar to that of NBCC 2015 and provides spectral acceleration and displacement amplitudes for different site classes. CHBDC 2014 also prescribes using the equivalent static method to design of seismically isolated bridges. However, there are limitations to applicability of this method to such bridges. Provisions about damping systems are not yet given.

It should be noted that the prescribed seismic loads have generally increased in recent decades, due to the higher seismic hazard level considered, and thus prescriptions for obtaining a ductile seismic behavior have been introduced. Older bridges which are still in use today may not meet the current standards on ductility and resistance to seismic loads and require strengthening and rehabilitation. The use of advanced seismic protection such as seismic isolation and added damping constitute efficient solutions that are applicable to both the seismic rehabilitation of existing bridges and building new bridges.

2.5 Conditional mean spectrum

Dynamic time-history analysis has become a popular method to determine structural response to ground motions. For this purpose, ground motion records are commonly selected and often scaled to match a uniform hazard spectrum (UHS) with a given probability of exceedance (or non exceedance), e.g., 2 % in 50 years. The spectral amplitudes provided by the UHS at all considered periods are those associated with the defined probability of exceedance, and therefore, the UHS does not represent each individual spectrum. For this reason and the inherent conservatism associated with the UHS, the appropriateness of using this spectrum as a target for ground motion selection has been criticized (e.g. Baker 2011). As an alternative, the Conditional Mean Spectrum (CMS) was proposed (Baker and Cornell 2006, Baker 2011). A CMS is a mean response spectrum computed based on the condition that the spectral acceleration matches a target amplitude at a given period. The difference between the target spectral acceleration and that predicted by a GMPE at the same period is evaluated as a number of standard deviations associated with this GMPE. This difference, denoted by ε, plays a significant role in the construction of CMS. Determination of ε values has been widely addressed in the literature (McGuire 1995, Harmsen 2001, Baker and Cornell 2005, Baker and Jayaram 2008, Burks and Baker 2012). Harmsen (2001) provided contour maps of modal and mean ε values for central and Eastern United States (CEUS) and Western United States (WUS) based on probabilistic seismic hazard analysis (PSHA). Burks and Baker (2012) investigated the occurrence of negative ε values at short periods particularly in Eastern North America (ENA). The correlation between ε values at different periods shapes the CMS in the period range of interest. A step-by-step procedure to construct CMS is included in Chapter 3 and a flowchart summarizing these steps is provided in Chapter 4. The procedure starts with the determination of a target spectral acceleration S_{a} at the desired period T^*. Provided that the target spectral amplitude is obtained from a probabilistic seismic hazard analysis (PSHA), the mean (or modal) values of magnitude M, epicentral distance R, and epsilon $\varepsilon(T^*)$ can be taken from the corresponding seismic hazard deaggregation. ε is defined as the difference, measured as the number of standard deviations, between the predicted and the target spectral accelerations associated with a specific magnitude M, distance R, and period T . Next, a GMPE is selected. In the case where a PSHA is used, the same GMPE that produced the mean (modal) values in the previous step can generally be adopted. The spectral predictions of the GMPE are determined for the selected magnitude M and distance R combination in the desired period range. The reported

sigma values for the GMPEs at each period are also considered. If a PSHA is not available or the ε value is not provided in the deaggregation results, the ε value at T^* can be calculated for a specific magnitude M, distance R, and spectral acceleration S_{a} at this period as (Baker 2011)

$$\varepsilon(T^*) = \frac{\ln S_{\mathrm{a}}(T^*) - \mu_{\ln\, S_{\mathrm{a}}}(M, R, T^*)}{\sigma_{\ln\, S_{\mathrm{a}}}(T^*)} \tag{2.1}$$

where $S_{\mathrm{a}}(T^*)$ is the spectral amplitude from the target spectrum, $\mu_{\ln\, S_{\mathrm{a}}}(M, R, T)$ represents the predictions of the GMPE, and $\sigma_{\ln\, S_{\mathrm{a}}}(T^*)$ is the standard deviation in logarithmic units provided by the GMPE. Suitable correlation coefficients $\rho(T, T^*)$ are then used to calculate the value of ε at other periods T as $\varepsilon(T^*) = \rho(T, T^*)\, \varepsilon(T^*)$. The CMS $\mu^{(\mathrm{CMS})}_{\ln S_{\mathrm{a}}(T)}$ and the associated conditional standard deviation $\sigma^{(\mathrm{CMS})}_{\ln S_{\mathrm{a}}(T)}$ are obtained as

$$\mu^{(\mathrm{CMS})}_{\ln S_{\mathrm{a}}(T)} = \mu_{\ln\, S_{\mathrm{a}}}(M, R, T) + \varepsilon(T)\, \sigma_{\ln S_{\mathrm{a}}}(T) = \mu_{\ln\, S_{\mathrm{a}}}(M, R, T) + \rho(T, T^*)\, \varepsilon(T^*) \sigma_{\ln S_{\mathrm{a}}}(T) \tag{2.2}$$

and

$$\sigma^{(\mathrm{CMS})}_{\ln S_{\mathrm{a}}(T)} = \sigma_{\ln S_{\mathrm{a}}}(T) \sqrt{1 - \rho^2(T, T^*)} \tag{2.3}$$

Lin et al. (2013) discussed four approaches, three approximate and one exact to determine the CMS. The proposed methods vary based on the number of considered GMPEs, their corresponding weights in a PSHA-related logic tree and deaggregation, as well as multiple earthquake scenarios contributing to seismic hazard. “Method 1” uses the mean values of the required parameters, e.g., M and R combinations, from deaggregation, and substitutes them into a single GMPE. Equation 2.2 is then used to compute CMS. “Method 2”, a refined version of “Method 1”, considers all the GMPEs used to conduct PSHA and their logic tree weights. The same procedure as “Method 1” is used to compute CMS for each GMPE. The final CMS is obtained by summing up the computed CMS considering their logic tree weights. “Method 3” considers GMPE deaggregations, if available, to determine the mean value of the required parameters to be used with each individual GMPE, e.g., M and R combinations, and next, similar to “Method 1”, the CMS corresponding to

each GMPE is computed. "Method 3" also takes, from GMPE deaggregation, the probability that each GMPE predicted exceedance (or occurrence) of $S_a(T)$. The final CMS is computed as the sum of the obtained CMS considering the mentioned probabilities. "Method 4", the exact method, follows the steps of "Method 3" with the difference that the individual CMS is computed for each set of parameters, e.g., M and R combinations, obtained from PSHA deaggregation results and not only for the mean values of such parameters. The contribution of each of such parameter combinations to exceedance (or occurrence) of $S_a(T)$ is considered in computation of the final CMS similar to "Method 3".

The above introduction to CMS and the details provided in Chapter 3 and Chapter 4 reiterate the role of GMPEs in computation of CMS. A number of commonly used GMPEs in North America are introduced next.

2.5.1 Ground motion prediction equations

Ground motion prediction equations (GMPEs) are vital ingredients for calculation of seismic hazard and spectral demands in a region. They provide the median spectral amplitudes corresponding to a set of parameters including magnitude and source to site distance. GMPEs depend largely on the assumed parameters representing seismic characteristics of the region of interest such as stress drop and fault types. These assumed parameters and also the database of studied records vary from one GMPE to another. Thus the predictions of such equations are not necessarily identical. The majority of GMPEs developed for North America so far provide pseudo spectral accelerations at 5%-damping ratio. GMPEs predicting high damping spectral amplitudes particularly displacements have rarely been addressed. Below, a short description of a few GMPEs developed for North America, Eastern North America in particular, is presented.

Atkinson and Boore (1995) used a stochastic model based on observations from 91 earthquakes in Eastern United States and Canada to predict ground motions in ENA with magnitudes M_W from 4 to 7.25 and hypocentral distances R_h ranging from 10 to 500 km. They simulated a set of ground motions covering the entire distance range for higher magnitudes (M_W > 6.5) and only close distances ($R_{RUP} \leq 25$ km) for smaller magnitudes. A regression analysis was then conducted to obtain the 5%-damped median pseudo-spectral accelerations for bedrock sites. For deep soil sites, Atkinson and Boore (1995) suggest multiplying the amplitudes at bedrock by period-dependent soil amplification factors.

Silva et al. (2002) proposed a GMPE with different coefficients accounting for single and double corner frequency models with constant and variable stress drops and magnitude saturation. Regression analyses were performed on the data from 13,500 simulations. The proposed GMPE covers a Joyner–Boore distance of $1 \leq R_{jb} \leq 400$ km and a moment magnitude (M_W) range of $M_W = 4.5$ to $M_W = 8.5$ for CEUS and ENA hard rock sites. The single corner frequency model with variable stress drop and the double corner frequency model with magnitude saturation have been used for seismic hazard analysis in Canada (e.g. Atkinson and Goda 2011, Atkinson and Adams 2013).

Campbell (2003) proposed a set of *hybrid empirical* ENA GMPEs obtained using four empirical WNA GMPEs proposed by Abrahamson and Silva (1997), Campbell (1997), Sadigh et al. (1997) and Campbell and Bozorgnia (2003). The idea behind the proposed methodology is to adjust predictions from GMPEs of earthquake-rich regions to estimate ground motions in a region having a paucity of significant ground motions. The estimates of the selected GMPEs were adjusted by factors calculated as the ratio of the stochastic ground motion estimates in ENA to the predictions of the western GMPEs. This resulted in an expression predicting the geometrical mean of 5%-damped pseudo-spectral accelerations along two horizontal components on hard rock sites for magnitudes $5 \leq M_W \leq 8.2$ and rupture distances $0 \leq R_{RUP} \leq 1000$ km.

Atkinson and Boore (2006) developed a set of relationships to predict ENA ground motions using a stochastic finite fault model (Hanks and McGuire 1981, Boore 1983). A data set of 38,400 simulated ground motions having magnitudes between $M_W = 3.5$ and $M_W = 8$ and fault distances ranging from 1 to 1000 km was compiled. The simulated ground motions corresponded to 24 stations located along 8 lines spreading out from the center of the top of the fault in equal azimuths. Equations to predict the median amplitudes of 5 %-damped pseudo-spectral accelerations (PSA) for ENA ground motions were developed through regression analyses of the simulated records. Modifications due to new seismographic data were made to these equations as provided in Atkinson and Boore (2011).

To predict ENA ground motions, Atkinson (2008) adopted a *referenced empirical* approach which combines available data from ENA to that from an active tectonic and better-instrumented reference region, in this case WNA. Based on the same database of ground motions used by Atkinson and Boore (2006), Atkinson (2008) proposed a GMPE corresponding to ground motion

characteristics in ENA while having an overall magnitude scaling behavior of observations in WNA (Atkinson 2008). The database included ENA records with a magnitude range of M_W = 4.3 to M_W = 7.6. The reference WNA GMPE used is the Boore and Atkinson (2008) relations, modified later by Atkinson and Boore (2011) based on new seismographic data. Prediction of ground motions for ENA using Boore and Atkinson (2008) GMPEs requires application of an adjustment factor which depends only on period and distance (Atkinson and Boore 2011) and is determined based on the ratio of the observed ENA ground motions to the predictions of BA08. Average horizontal component pseudo-accelerations are then generated for a desired magnitude, distance, period, fault mechanism, National Earthquake Hazard Reduction Program (NEHRP) B/C soil condition, i.e. V_{S30} = 760 m/s, and Joyner-Boore distance range of $1 \leq R_{jb} \leq 1000$ km. It is worth mentioning that the main difference between this referenced empirical approach and the hybrid empirical method proposed by Campbell (2003) is that it directly employs observational ENA ground motion data instead of using a stochastic model.

The Boore and Atkinson (2008) relationships are one of the five sets of equations developed under the Next Generation Attenuation Relationships for Western USA (NGA West) program coordinated by Pacific Earthquake Engineering Research Center (PEER). These relationships were based on results from regression analyses on records from shallow crustal ground motions in active tectonic regions compiled in the PEER-NGA West data set. The equations were developed for a magnitude range of M_W = 5.0 to M_W = 8.0, closest horizontal distance to the surface projection of the fault plane (R_{jb}) of up to 200 km and a time-averaged shear-wave velocity in the top 30m (V_{S30}) of $180 \leq V_{S30} \leq 1300$ m/s. Modifications due to new seismographic data were made to these equations as provided in Atkinson and Boore (2011).

Pezeshk et al. (2011) proposed a new GMPE for ENA based on a hybrid empirical method adopting five WNA GMPEs provided by PEER. The GMPEs were developed by Abrahamson and Silva (2008), Boore and Atkinson (2008), Campbell and Bozorgnia (2008), Chiou and Youngs (2008) and Idriss (2008). The ratio of the stochastic ground motion simulations in ENA to the predictions of the GMPEs of WNA is used as an adjustment factor to predict ground motions in ENA. By considering the seismological characteristics of each region, the adjustment factors represent the regional differences in source, path and site (Pezeshk et al. 2011). The new GMPE covers a magnitude range of M_W = 5 to M_W = 8 and closest distances to the fault rupture (R_{RUP}) of $1 \leq R_{RUP}$

≤ 1000 km and is used to generate median 5 %-damped pseudo-accelerations in ENA for given magnitude and distance considering hard rock sites, i.e., V_{S30} ≥ 2000 m/s.

Atkinson and Adams (2013) proposed a new set of GMPEs consisting of a representative or central GMPE and upper and lower GMPEs to account for epistemic uncertainty about the central one. The central GMPE is determined by calculating the geometric mean of five peer reviewed GMPEs. The geometric mean ± its standard deviation is considered as the upper/lower GMPE. The five GMPEs are those developed by Silva et al. (2002), Atkinson and Boore (2006), Atkinson (2008), and Pezeshk et al. (2011). The final predictions are provided in terms of moment magnitudes and epicentral distances for B/C, i.e., V_{S30} = 760 m/s site condition.

2.6 Damping reduction factors

Elastic displacement spectra associated with damping levels higher than the conventional 5% critical damping are important in the seismic design and evaluation of structures equipped with energy dissipating and seismic isolation systems. High-damping displacement spectra are also required for displacement-based design and evaluation techniques, such as the Direct Displacement-Based Design method (Priestley and Kowalsky 2000, Priestley et al. 2007). One method to determine high damping spectral amplitudes is using ground motion prediction equations (GMPEs) developed specifically for damping levels higher than 5%. A number of GMPEs predicting spectral amplitudes at various damping levels have been proposed for different regions, e.g. Chen and Yu (2008) for Western North America (WNA), and Akkar and Bommer (2007) and Cauzzi and Faccioli (2008) for Europe. These are useful in conducting probabilistic seismic hazard analysis to assess seismic hazard values for higher damping ratios. It is noted that GMPEs predicting high damping spectral amplitudes are not yet developed for Eastern North America.

The second approach is through damping reduction factors, denoted hereafter by η, which are commonly used to evaluate the effect of damping on seismic demands and are defined as the ratio between the 5%-damped displacement $S_{\mathrm{d}}(T, 5\%)$ or pseudo acceleration spectrum $S_{\mathrm{a}}(T, 5\%)$, and displacement spectra $S_{\mathrm{d}}(T, \xi)$ or pseudo-acceleration spectra $S_{\mathrm{a}}(T, \xi)$ for higher damping levels at a period T

$$\eta(T,\xi) = \frac{S_{\mathrm{d}}(T,\xi)}{S_{\mathrm{d}}(T,5\%)} = \frac{S_{\mathrm{a}}(T,\xi)}{S_{\mathrm{a}}(T,5\%)} \tag{2.1}$$

Most guidelines and building codes adopt the approach of damping reduction factors (e.g. UBC-97, EC8 2004, ATC 2010, AASHTO 2010, ASCE7-10 and CHBDC 2014). An advantage of the latter approach is that these damping reduction factors can be applied directly to code-prescribed spectral amplitudes to evaluate damping effects.

Several equations have been proposed in the literature to approximate damping reduction factors considering seismic hazard in different regions. Newmark and Hall (1973, 1982) used the horizontal and vertical components of 14 pre-1973 California ground motions to propose damping reduction factors corresponding to damping levels lower than 20%. Bommer et al. (2000) studied the damped displacement spectra of 183 ground motion components from 43 shallow earthquakes recorded on rock, stiff and soft soil sites in Europe and the Middle East. They proposed an equation which was implemented in Eurocode 8 (2004). The Chinese guidelines for seismically isolated structures include a period-independent equation for damping reduction factors (Zhou et al. 2003). Lin and Chang (2004) studied 1037 accelerograms recorded in the United States to propose period-dependent damping reduction factors for periods between 0.1 s and 6 s and damping ratios between 2% and 50%. Atkinson and Pierre (2004) extended the simulations performed to generate a dataset of synthetic records which was used in developing the GMPE of Atkinson and Boore (1995) for ENA and for scenarios between M_{W} = 4.0 and M_{W} = 7.25 at hypocentral distances of 10 km to 500 km. The 1%, 2% 3%, 5%, 7%, 10%, and 15%-damped response spectra were computed and finally a magnitude-distance independent set of η factors was proposed for periods between 0.05 s and 2 s, magnitudes greater than 5, and distances shorter than 150 km. Cameron and Green (2007) proposed a set of damping modification factors for damping levels between 1% and 50% for magnitude-binned ground motion records from shallow crustal events. Ground motion duration was shown to be highly influential on damping reduction factors, whereas source-to-site distance was found to have negligible effect for damping levels of 2% and above. They also showed that site conditions have minor influence on damping modification factors for shallow crustal events in active tectonic regions. AASHTO (2010) includes a simplified equation to obtain damping reduction factors for damping levels up to 50%, while suggesting caution regarding its use for damping ratios greater than 30%. Rezaeian et al. (2014) studied a database of 2250 records from shallow crustal ground motions and developed a magnitude- and distance-based model to predict

damping modification factors for the average horizontal component of ground motion and damping levels of between 0.5% and 30%. They observed the period dependency of the damping modification factors and also reported a strong dependency of these factors on ground motion duration. The abovementioned factors and equations are all period-independent, except for those proposed by Atkinson and Pierre (2004), Lin and Chang (2004), Cameron and Green (2007) and Rezaeian et al. (2014). A recent investigation of several period-dependent and period-independent damping reduction factors by Cardone et al. (2009) showed that period-dependent models provide the most accurate predictions of computed displacement spectra. Furthermore, Bradley (2014) reiterates the period- and duration-dependency of damping reduction factors while questioning the accuracy of a number of proposed equations, namely the one prescribed by Eurocode 8 (2004) where response amplification is characterized in terms of source- and site-specific effects. It should be noted that some older equations are based on studies that may lack adequate record processing of the used accelerograms (i.e. such as filtering and zero-padding) and therefore might not be suitable for long period ranges.

An important consideration is that the majority of the previous studies have focused upon ground motions for shallow crustal earthquakes, whereas ground motions for subduction earthquakes (including deep inslab and mega-thrust interface events) have not been much investigated. The large magnitudes of mega-thrust subduction earthquakes, and the potentially-high stress drops for deep inslab earthquakes, are important factors that control the duration and frequency content of ground motions - which are relevant properties for damped structural responses. It is therefore expected that the differing characteristics of ground motions for different earthquake types that contribute to hazard have major influence on the damping reduction factors.

CHAPTER 3 ARTICLE 1: APPLICATION OF CONDITIONAL MEAN SPECTRA FOR EVALUATION OF A BUILDING'S SEISMIC RESPONSE IN EASTERN CANADA

Poulad Daneshvar, Najib Bouaanani, and Pierre Léger

Paper published in *Canadian Journal of Civil Engineering*, Volume 41,
Pages 769-773 DOI:dx.doi.org/10.1139/cjce-2013-0241

Submitted 23 May 2013. Accepted 29 May 2014.

An existing eight-storey reinforced concrete shear wall building located in Montreal is studied to evaluate the impact of applying a conditional mean spectrum (CMS) in lieu of the conventional uniform hazard spectrum (UHS) to the seismic evaluation of such structures. The construction of the CMS is reviewed and adapted to take account of seismic hazard in Montreal. The developed CMS and their envelopes were used to conduct modal response spectrum analyses of the building and the results are compared to those obtained from the NBCC 2005 UHS. Justifications of similarities or differences between CMS and UHS-based results are illustrated throughout the paper.

Nomenclature

Abbreviations

AB95	Ground motion prediction equation developed by Atkinson and Boore (1995)
GMPE	Ground motion prediction equation
ENA	Eastern North America
GSC	Geological Survey of Canada
NBCC	National Building Code of Canada

UHS	Uniform hazard spectrum
USGS	United States Geological Survey
WNA	Western North America

Symbols

M	Moment magnitude
M_{bLg}	Nuttli's magnitude
R	Hypocentral distance
R_{RUP}	Rupture distance
S_{a}	Spectral acceleration
$\bar{S}_a(T)$	CMS spectral acceleration amplitude at period T
T	Period of vibration
T^*	Period at which the CMS is anchored to the UHS
$\varepsilon(T)$	The difference between the spectral amplitudes of the UHS and the predicted accelerations measured at a period T as the number of standard deviations
$\mu_{\log S_{\mathrm{a}}(T)}$	Mean spectral accelerations given by the GMPE
$\sigma_{\log\ S_{\mathrm{a}}(T)}$	Standard deviation in logarithmic units provided by the GMPE
$\rho(T, T^*)$	Spectral acceleration correlation coefficient

3.1 Introduction

The NBCC (2005, 2010) prescribes uniform hazard spectrum (UHS) with a probability of exceedence of 2% in 50 years. The prescribed UHS accelerations are specific to each site of interest and correspond to a given probability of exceedance and do not represent an individual seismic event. The appropriateness of the UHS as a target for seismic safety assessment is debatable because of its inherent conservatism. As an alternative, the conditional mean spectrum (CMS) has been proposed (Baker 2011). A CMS is a mean response spectrum computed based on the condition that spectral acceleration matches a target amplitude at a given period. The U.S. geological survey (USGS 2010) provides online tools to compute CMS for both eastern and western regions of the United States. However, these are based on ground motion models adopted for the seismic hazard in the United States, while development and application of CMS in eastern Canada have not yet been explored. This work addresses (i) the construction of the CMS considering seismic hazard in Montreal, (ii) the application of this CMS for seismic evaluation of an existing 8-storey reinforced concrete shear wall building located in Montreal, and (iii) comparison of the results to those obtained using conventional UHS. As addressed in Hong et al. (2006) and Hong and Goda (2006), nonnormal distribution of the probabilistic seismic hazard analysis results, to determine the UHS, does not provide very uniform spectral amplitudes in terms of probability of exceedance when the median of the results are considered rather than the mean. Nevertheless, this is the approach taken by the GSC to determine the UHS amplitudes provided in the NBCC (2005, 2010). The main objective of this note is to shed light on the usage of CMS in eastern Canada with the currently available tools such as the UHS prescribed in the NBCC, which is the only tool that the engineering community is provided with and is regarded as a representative of the 2% in 50 year probability of exceedance at all periods.

3.2 Building analyzed

An eight-storey reinforced concrete residential building adapted from Panneton et al. (2006) has been selected for this study. The building is located in Montreal and has a total height of 23.2 m from the ground level. The lateral load resisting system of the building includes four individual shear walls and three cores corresponding to stairway or elevator shafts as illustrated in Figure 3-1. The building was initially designed using NBCC 1995 and CSAA23.3-94 (CSA 1994). It was then re-evaluated according to NBCC 2005 and CSA-A23.3-04 (CSA 2002) requirements to assess the

effects of various modeling assumptions as described by Panneton et al. (2006). In this work, the seismic response of the building is studied in the transverse North-South direction. The fundamental period of the structure along this direction is 1.53 s. The irregular shape of the building, as illustrated in Figure 3-1, suggests significant torsional effects upon being excited and thus the first mode of the building is mainly governed by torsion. However, the first mode is not purely torsional and the building mass is also excited and displaced in longitudinal and transverse directions. The reader is referred to Panneton et al. (2006) for more details on the irregularity of the building and the associated torsional effects.

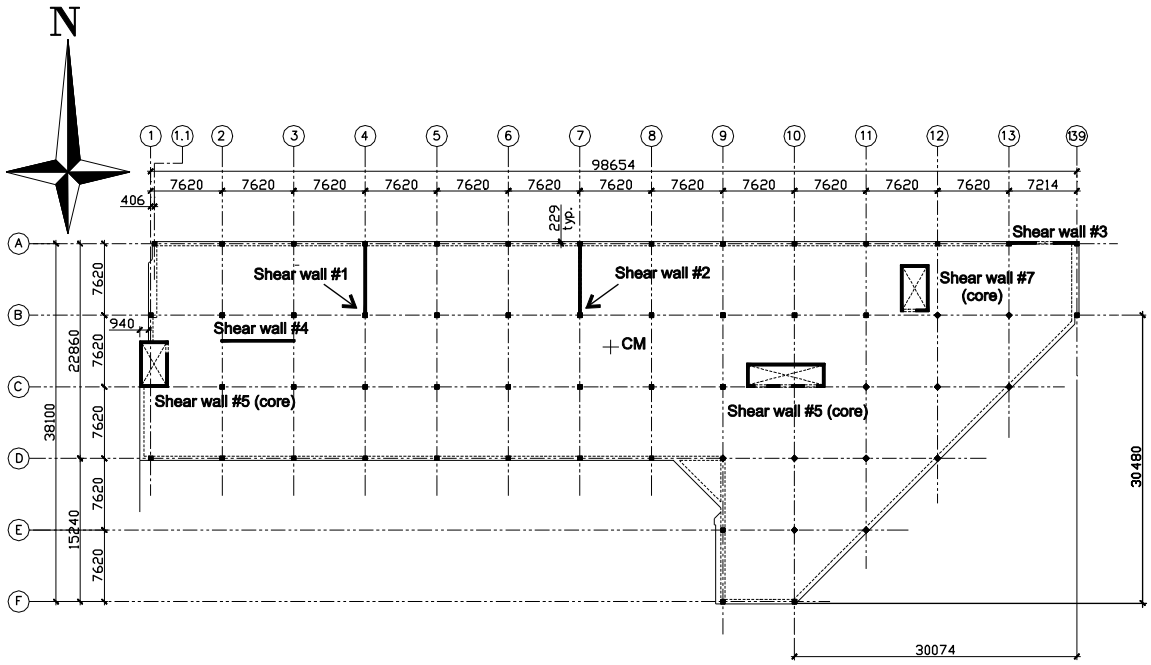

Figure 3-1: Typical plan view of the analyzed reinforced concrete building (from Panneton et al. 2006).

3.3 Computation of CMS

The general step by step procedure provided by Baker (2011) is adapted hereafter to construct a CMS used later for the seismic analysis of the building described above. The NBCC 2005 UHS is adopted here due to the availability of the corresponding deaggregation data and the underlying AB95 ground motion prediction equations (GMPE) (Atkinson and Boore 1995). The choice of NBCC 2005 UHS is also consistent with the re-evaluation of the building mentioned in the previous section and provides the readers with a convenient reference to Panneton et al. (2006) for the

building's details and the corresponding modelling assumptions. It is important to note that if a different GMPE model (i.e., other than AB95) or a UHS (i.e., other than the one prescribed in 2005 NBCC) are selected, the methodology described below is still applicable as long as both the GMPE model and UHS (target spectrum) are updated.

Step one: Determine $S_a(T^*)$

The CMS has to be anchored to a target spectral acceleration $S_a(T^*)$ at a specific period T^* commonly taken as the fundamental period of the structure. In this study, T^* = 1.53 s and the target spectral acceleration $S_a(T^*)$ is that of the NBCC 2005 UHS for Montreal at T^* = 1.53 s. The mean magnitude and distance associated with $S_a(T^*)$ are determined next using seismic deaggregation provided by GSC for Montreal upon request. The provided deaggregation is practically similar to those presented in Halchuk et al. (2007). Such information is available only at specific periods not necessarily equal to the period of interest T^* = 1.53 s. It is suggested here to use linear interpolation of deaggregation data corresponding to bracketing periods of 1 s and 2 s which is the same approach adopted in the guidelines provided by NIST (2011). For example, Figure 3-2(a) shows the seismic hazard deaggregation corresponding to the UHS at a period of 1 s as well as the mean and modal Nuttli magnitudes M_{bLg}, and hypocentral distances R. To minimize uncertainty in predicting short period amplitudes and to obtain more reliable magnitudes representing the small to moderate events in eastern North America, the magnitude-recurrence relations and the GMPEs in the seismic hazard analysis are suggested to be based on Nuttli magnitude (Atkinson and Boore 2011, Filliatrault et al. 2013, GSC 2013). Thus the deaggregation data obtained from GSC, similar to that presented in Halchuk et al. (2007), was originally expressed in terms of Nuttli magnitude M_{bLg} which is then converted to the moment magnitude M implemented in AB95 GMPE using the relationships proposed by Atkinson (1993) and Boore and Atkinson (1987)

$$M = 0.98M_{bLg} - 0.39 \qquad M_{bLg} \leq 5.5 \qquad [3.1]$$

$$M = 2.715 - 0.277M_{bLg} + 0.127M_{bLg}^2 \qquad M_{bLg} > 5.5 \qquad [3.2]$$

The resulting converted mean magnitude-distance pairs at 1 s and 2 s are (M = 6.835, R = 64 km) and (M = 6.895, R = 79 km), respectively. Linear interpolation yields the mean values of M = 6.867 and R = 72 km at T^* = 1.53 s.

Step 2: Determine $\varepsilon(T^*)$

GSC has adopted the AB95 GMPE proposed by Atkinson and Boore (1995) to determine the NBCC 2005 UHS. The same GMPE is used hereafter for consistency. The additional coefficient included in an updated AB95 GMPE is considered to predict spectral accelerations corresponding to Soil type C (Atkinson 1995, Adams et al. 2003). The mean values of M = 6.867 and R = 72 km corresponding to T^* = 1.53 s are used as an input for the AB95 GMPE to generate the median spectral accelerations illustrated in Figure 3-2(b). The NBCC 2005 UHS for Montreal is also shown in Figure 3-2(b). The difference between the spectral amplitudes of the UHS and the AB95 predicted accelerations can be measured at a period T as the number $\varepsilon(T)$ of standard deviations (Baker 2011)

$$\varepsilon(T) = \frac{\log\ S_a(T) - \mu_{\log\ S_a}(M, R, T)}{\sigma_{\log\ S_a}(T)} \qquad [3.3]$$

where $\mu_{\log\ S_a}$ is the mean spectral acceleration predicted by AB95, and $\sigma_{\log\ S_a}$ is the standard deviation associated with the predictions of AB95. The regression analyses for determining the coefficients for GMPEs are usually performed on the logarithm of observed or simulated spectral values and thus the corresponding standard deviation is automatically given in logarithmic scale. The standard deviation for AB95 predictions is given as 0.3 in logarithmic units (Atkinson 1995, Adams et al. 2003). Epsilon values at T = 0.4 s, T = 1 s and T^* = 1.53 s are shown in Figure 3-2(b) for illustration purposes.

Step 3: Determine $\varepsilon(T)$

The CMS is anchored to the UHS only at the selected period T^*. Therefore, $\varepsilon(T)$ values have to be modified through multiplication of $\varepsilon(T^*)$ by a coefficient $\rho(T, T^*)$ that takes account of correlations of ground motion spectral accelerations across periods in the range of interest. Such correlations can be evaluated statistically considering a large number of ground motions, which is

very difficult to achieve in eastern North America (ENA) due to the scarcity of recorded earthquake events. In the absence of ENA site specific information, we assume that the correlation coefficient proposed by Baker and Jayaram (2008) can be applied to ENA as well. Baker and Jayaram's (2008) correlation coefficients are mostly based on western North America (WNA) data from shallow crustal events which are similar to the type of ground motions observed in ENA.

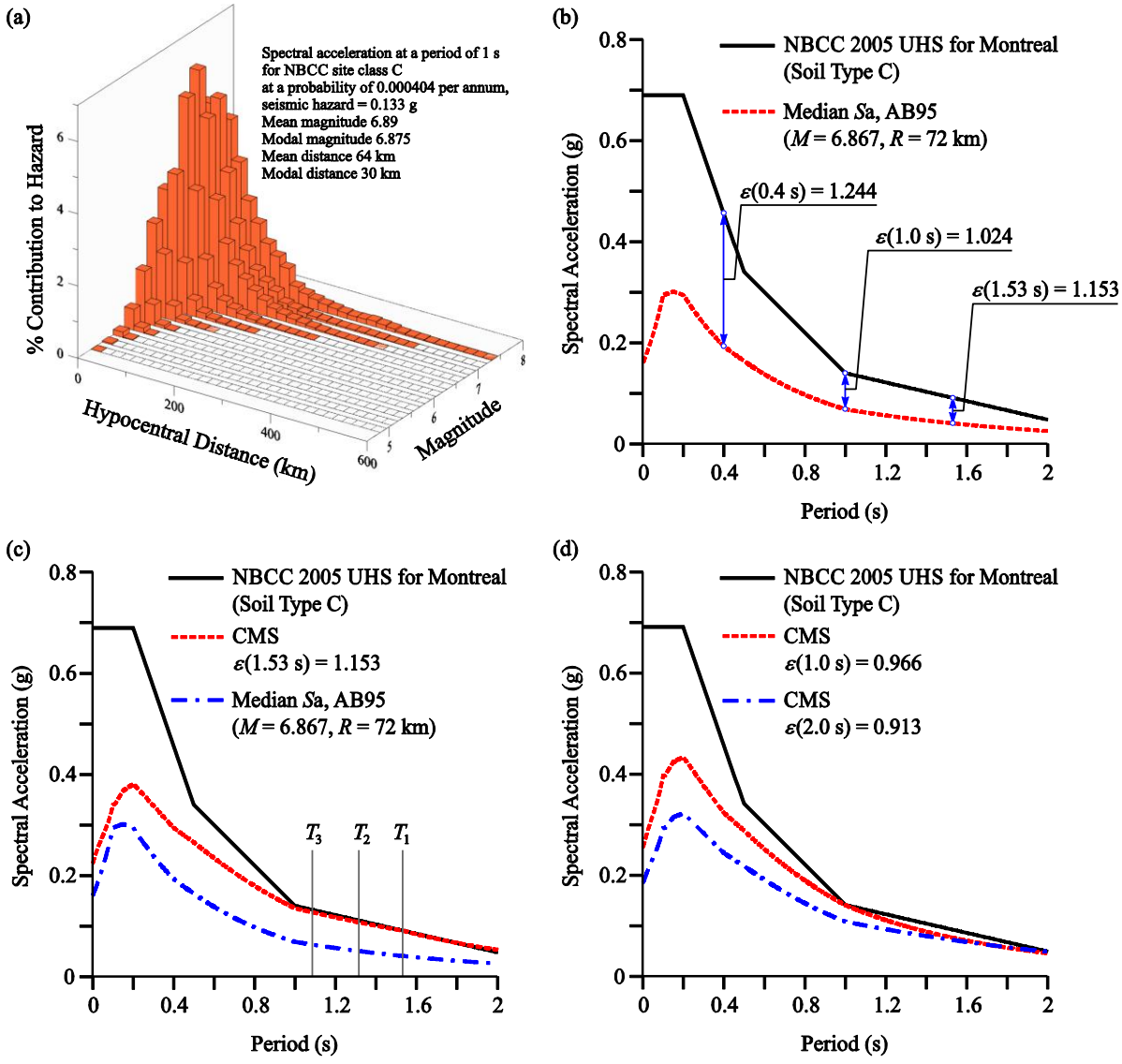

Figure 3-2: (a) seismic hazard deaggregation for Montreal at 1 s from GSC, (b) NBCC 2005 UHS for Montreal and the median acceleration amplitudes predicted by AB95, (c) NBCC 2005 UHS for Montreal and the CMS anchored at T^* = 1.53 s and (d) T^* = 1 s and 2 s.

Lin et al. (2013) also report that the online tool provided by USGS to construct CMS for locations within the United States uses the same correlation model (i.e. Baker and Jayaram 2008) for eastern United States which similar to eastern Canada is a stable continental seismic zone.

Step 4: Compute CMS

The CMS spectral acceleration amplitudes $\bar{S}_a(T)$ at period T are conditioned on $\varepsilon(T^*)$ and are obtained as (Baker 2011)

$$\log \bar{S}_a(T) = \mu_{\log\, S_a}(M, R, T) + \rho(T, T^*)\, \varepsilon(T^*)\, \sigma_{\log\, S_a}(T) \qquad [3.4]$$

Figure 3-2(c) illustrates the resulting CMS of Montreal for T^* = 1.53 s, as well as the NBCC 2005 UHS, and the predictions of AB95 considering mean magnitude M = 6.867 and distance R = 72 km. The first three structural vibration periods T_1, T_2 and T_3 are also shown in Figure 3-2(c). Figure 3-2(d) presents the CMS for mean magnitude-distance pairs (M = 6.835, R = 64 km) and (M = 6.895, R = 79 km) corresponding to bracketing periods of 1 s and 2 s, respectively. These results confirm that the CMS tends to reduce the over conservatism associated with the UHS at periods other than the anchoring period T^*.

3.4 Application of the computed CMS

A 3D finite element model of the building is constructed in SAP2000 (CSI 2011) as described by Panneton et al. (2006). Response spectrum analyses of the structure are performed in the transverse direction considering the NBCC 2005 UHS and the CMS obtained previously. The resulting building's elastic base shears along the transverse (North-South) direction are illustrated in Figure 3-3(a) as well as the non-negligible base shears obtained along the orthogonal longitudinal (East-West) direction due to plan irregularity (Figure 3-1). Figure 3-2(a) includes base shears computed using CMS at 1.53 s, 1 s and 2 s, as well as the envelope. The results show that in comparison to the UHS-based analyses, a decrease between 31% and 45% in the building's base shear is observed, in the transverse direction, when the CMS is anchored between 1 s and 2 s, respectively. This decrease reaches 33% when the CMS is anchored to the UHS at the building's fundamental period while the envelope of the three CMS causes a 28% decrease in the base shear. The relative decrease in the base shear in the longitudinal direction remains roughly the same for the four CMS. Such

decrease is obtained because spectral acceleration values given by the CMS are equal to those of the UHS only at one specific period, i.e. 1 s, 1.53 s or 2 s, and are lower elsewhere. Therefore, the contribution of higher modes of vibration to the base shear is reduced when the CMS is adopted as spectral accelerations at lower periods are not associated with the same probability of exceedence as in the UHS. The envelope of the three CMS matches the UHS at more periods, thus leading to the highest CMS-based base shears although they remain below the UHS-based values as shown in Figure 3-2(a).

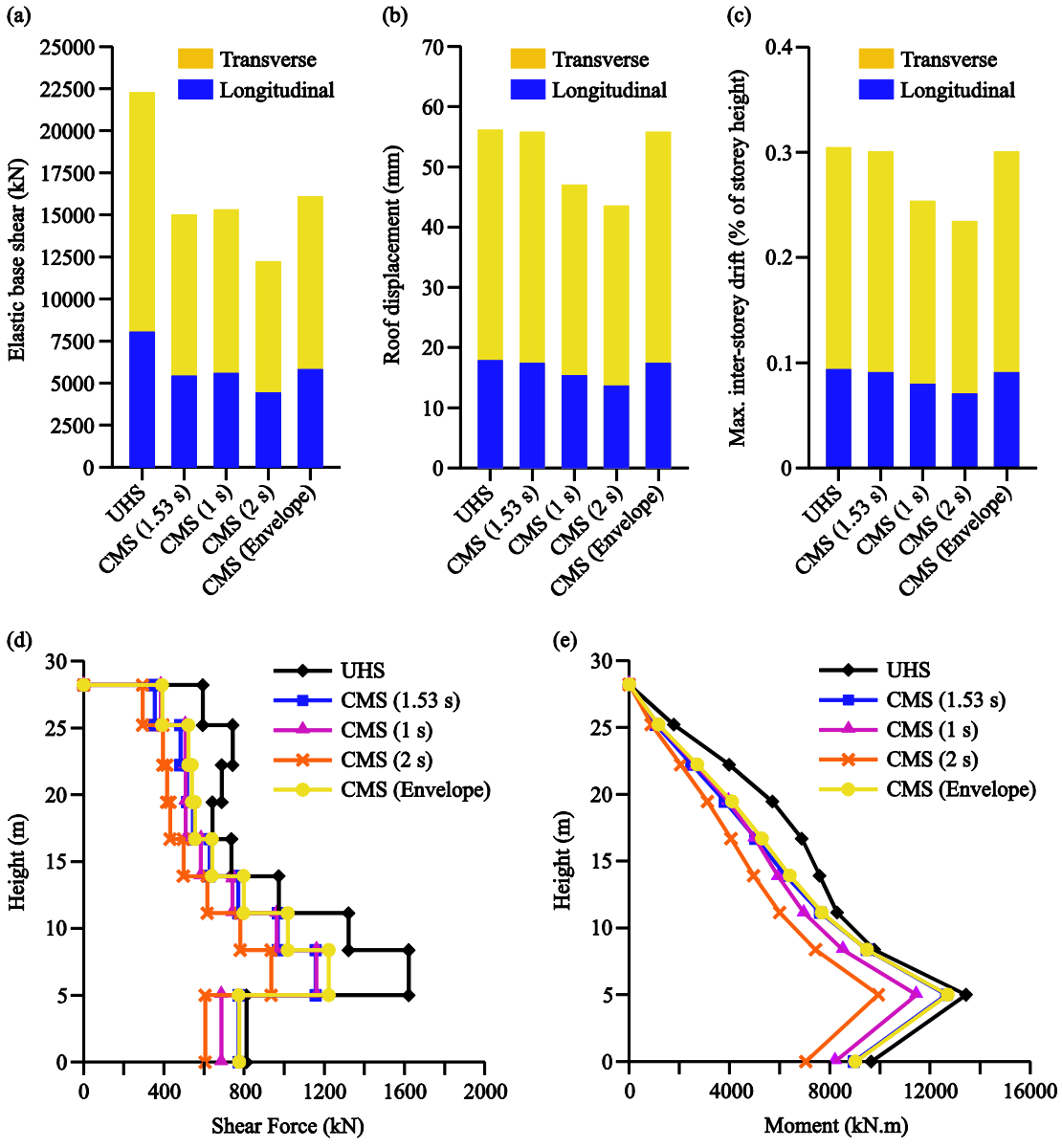

Figure 3-3: Comparison of UHS- and CMS-based response spectrum analysis results.

Figure 3-3(b) also shows that the obtained CMS- and UHS-based roof displacements are practically similar. The same observation applies to maximum inter-storey drifts computed using CMS and UHS as shown in Figure 3-3(c). These response indicators are indeed dominated by the fundamental mode response of the studied building and the CMS is anchored to the UHS at the fundamental period. The distributions of shear forces and bending moments in shear wall no. 4 (Figure 3-1) are illustrated in Figure 3-3(d) and (e). The three CMS-based shear force distributions are of lower amplitudes than the UHS-based ones, with maximum differences observed at the first and second floors. The distributions corresponding to CMS at 1.53 s and 1 s are close, while that corresponding to CMS at 2 s is distinctly lower. CMS-based moment distributions are also lower than UHS-based over the height of the building. Maximum differences between the two types are however concentrated from the 4^{th} to the 6^{th} floors, while bending moments near the base are closer.

3.5 Conclusions

This work presented an original study to assess the application of CMS to conduct response spectrum analyses of an existing 8-storey reinforced concrete shear wall building located in eastern Canada (Montreal). The construction of the CMS was reviewed and adapted to take account of seismic hazard in Montreal. The developed CMS and their envelope were used to conduct modal response spectrum analyses of the building and the results were compared to those obtained from the NBCC 2005 UHS. For the building studied, CMS-based shear forces and bending moments were found generally smaller than those corresponding to the UHS, while CMS- and UHS-based roof displacements and maximum inter-storey drifts were found to be practically the same. Justifications of similarities or differences between CMS- and UHS-based results were given throughout the paper. Elastic base shear values were adopted in this study and the factors suggested by NBCC to account for inelastic behavior were not applied. Inter-period correlation coefficients developed based on WNA ground motions were also adopted in the absence of ENA-based specific information.

Acknowledgements

The authors would like to acknowledge the financial support of the Natural Sciences and Engineering Research Council of Canada (NSERC) and the Canadian Seismic Research Network (CSRN).

References

Adams, J., and Halchuk, S. 2003. Fourth generation seismic hazard maps of Canada: Values for over 650 Canadian localities intended for the 2005 National Building Code of Canada. Geological Survey of Canada Open File 4459.

Adams, J., Halchuk, S., 2004. Fourth-generation seismic hazard maps for the 2005 National Building Code of Canada. 13th World Conference on Earthquake Engineering (13WCEE), Vancouver, Paper No. 2502.

Atkinson, G.M. 1993. Source spectra for earthquakes in eastern North America. Bulletin of Seismological Society of America, **83**: 1778-1798.

Atkinson, G.M. 1995. Ground motion relations for use in eastern hazard analyses. In Proceedings, 7th Canadian Conference on Earthquake Engineering, Montreal, June 1995, 1001-1008.

Atkinson, G.M., and Boore, D.M. 1995. Ground-motion relations for Eastern North America. Bulletin of the Seismological Society of America, **85**(1): 17-30.

Atkinson, G.M., and Boore, D.M., 2011. Modifications to existing ground-motion prediction equations in light of new data. Bulletin of the Seismological Society of America, **101**(3): 1121-1135.

Baker, J.W. 2011. Conditional mean spectrum: Tool for ground-motion selection. Journal of Structural Engineering, **137**(3): 322-331.

Baker, J.W., and Jayaram, N. 2008. Correlation of spectral acceleration values from NGA ground motion models. Earthquake Spectra, **24**(1): 299-317.

Boore, D., and Atkinson, G.M. 1987. Stochastic prediction of ground motion and spectral response parameters at hard-rock sites in eastern North America, Bulletin of the Seismological Society of America. **77**: 440-467.

CSA. 1994. Design of Concrete Structures. Standard CAN/CSA A23.3-94, Canadian Standards Association, Rexdale, Ont.

CSA. 2002. Design of Concrete Structures, Draft 4 (December 2002). Standard CAN/CSA A23.3-04, Canadian Standards Association, Rexdale, Ont.

CSI. 2011. SAP2000. Version 15.0.0. [Computer Program]. Computers and Structures, Inc, Berkeley, Ca.

Filliatrault, A., Trremblay, R., Christopoulos, C., Folz, B. and Pettinga, D., 2013. Elements of earthquake engineering and structural dynamics. Presses internationales Polytechnique, Canada.

Geological Survey of Canada (GSC). 2013. http://www.earthquakescanada.nrcan.gc.ca/info-gen/faq-eng.php#ml_and_mn. Accessed 24 January 2014.

Hong, H.P., and Goda, K., 2006. A comparison of seismic-hazard and risk deaggregation. Bulletin of the Seismological Society of America, **96**(6): 2021-2039.

Hong, H.P., Goda, K., and Davenport, A.G., 2006. Seismic hazard analysis: A comparative study. Canadian Journal of Civil Engineering, **33**: 1156-1171.

Halchuk, S., Adams, J., and Anglin, F., 2007. Revised deaggregation of seismic hazard for selected Canadian cities. 9th Canadian Conference on Earthquake Engineering (9CCEE), Ottawa, Paper No. 1188.

Lin, T., Harmsen, S.C., Baker, J.W., and Luco, N., 2013. Conditional spectrum incorporating multiple causal earthquakes and ground motion prediction models. Bulletin of Seismological Society of America, **103**(2A): 1103-1116.

NBCC. 1995. National Building Code of Canada, Associate Committee on the National Building Code, National Research Council of Canada, Ottawa, ON.

NBCC. 2005. National Building Code of Canada, Associate Committee on the National Building Code, National Research Council of Canada, Ottawa, ON.

NBCC. 2010. National Building Code of Canada, Associate Committee on the National Building Code, National Research Council of Canada, Ottawa, ON.

NIST, National Institute of Standards and Technology, 2011. Selecting and scaling earthquake ground motions for performing response-history analyses. NIST GCR 11-917-15. Prepared by the NEHRP Consultants Joint Venture for the National Institute of Standards and Technology, Gaithersburg, Maryland.

USGS. 2010. United States Geological Survey. Available from https://geohazards.usgs.gov/deaggint/2008/

Panneton, M., Léger, P., and Tremblay, R. (2006). Inelastic analysis of a reinforced concrete shear wall building according to the National Building Code of Canada 2005. Canadian Journal of Civil Engineering, **33**(7): 854-871.

CHAPTER 4 ARTICLE 2: ON COMPUTATION OF CONDITIONAL MEAN SPECTRUM IN EASTERN CANADA

Poulad Daneshvar, Najib Bouaanani, and Audrey Godia

Paper published in *Journal of Seismology*, Volume 19,
Pages 443-467 DOI: 10.1007/s10950-014-9476-6

Submitted 26 September 2014. Accepted 22 December 2014.

This paper investigates the main ingredients required to compute Conditional Mean Spectra (CMS) in Eastern Canada and assesses their effects on the obtained CMS. We particularly address the influence of ground motion prediction equations (GMPEs) and correlations between spectral accelerations. CMS are computed using two approximate methods, and the results are illustrated for three locations with different seismic hazard and risk levels. It is found that selection of GMPEs considerably influences the CMS, particularly at shorter periods. A database of historical records from Eastern Canada is studied to obtain correlation coefficients. The results suggest higher spectral correlations than predicted by a model based on ground motions from Western North America (WNA). The sensitivity of correlation coefficients to magnitude and epicentral distance is also verified, revealing that magnitude has a more significant effect on these coefficients than distance. We also show that the effect of magnitude- or distance-based correlation coefficients on the CMS is (1) generally negligible at long periods and (2) significant at shorter periods particularly when the conditioning period is less than approximately 0.5 s. This work is the first study addressing in detail the ingredients and construction of CMS in Eastern Canada. The methodology and results discussed are expected to enhance the application of CMS in this region.

Nomenclature

Abbreviations

A08	Ground motion prediction equation developed by Atkinson (2008)

AA13	Ground motion prediction equation developed by Atkinson and Adams (2013)
AB06	Ground motion prediction equation developed by Atkinson and Boore (2006)
BA08	Ground motion prediction equation developed by Atkinson and Boore (2008)
BJ08	Spectral acceleration correlation coefficients proposed by Baker and Jayaram (2008)
PZT11	Ground motion prediction equation developed by Pezeshk et al. (2011)
SGD02	Ground motion prediction equation developed by Silva et al. (2002)
CEUS	Central and Eastern United States
CMS	Conditional mean spectrum
ENA	Eastern North America
GMPE	Ground motion prediction equation
GSC	Geological Survey of Canada
NBCC	National Building Code of Canada
NGA West	Next Generation Attenuation Relationships for Western USA
PEER	Pacific Earthquake Engineering Research Center
PGA	Peak ground acceleration
PSHA	Probabilistic seismic hazard analysis
UHS	Uniform hazard spectrum
USGS	United States Geological Survey
WNA	Western North America
WUS	Western United States

Symbols

i	Number of GMPEs
M	Magnitude
M_{W}	Magnitude

P_{i}	The weight assigned to the i th GMPE
R	Distance; Epicentral distance
R_{jb}	Joyner-Boore distance
R_{RUP}	Closest distance to the fault rupture
S_{a}	Spectral acceleration from the target spectrum
T	Period of vibration
T^*	Period at which the CMS is anchored to the UHS
$T^{*'}$	Modified T^* to account for the high frequency content of the database of records
$T_{\mathrm{amp1.5}}$	The shortest period at which $S_{\mathrm{a}}(T^*)$reaches 1.5 times the PGA
T_{new}	Modified T to account for the high frequency content of the database of records
V_{S30}	Time-averaged shear-wave velocity in the top 30m
$\varepsilon(T)$	The difference between the spectral amplitudes of the UHS and the predicted accelerations measured at a period T as the number of standard deviations
$\mu_{\ln S_{\mathrm{a}}(T)}^{(\mathrm{CMS})}$	Spectral accelerations given by CMS at period T
$\sigma_{\ln\ S_{\mathrm{a}}(T)}$	Standard deviation in logarithmic units provided by the GMPE
$\sigma_{\ln S_{\mathrm{a}}(T)}^{(\mathrm{CMS})}$	Standard deviation in logarithmic units associated with CMS
$\rho(T, T^*)$	Spectral acceleration correlation coefficient

4.1 Introduction

Dynamic time-history analysis has become a popular method to determine structural response to ground motions. For this purpose, ground motion records are commonly selected and often scaled to match a uniform hazard spectrum (UHS) with a given probability of exceedance (or non exceedance), e.g., 2 % in 50 years. The spectral amplitudes provided by the UHS at all considered periods are those associated with the defined probability of non exceedance, and therefore, the UHS does not represent each individual spectrum. For this reason and the inherent conservatism associated with the UHS, the appropriateness of using this spectrum as a target for ground motion selection has been criticized. As an alternative, the Conditional Mean Spectrum (CMS) was proposed (Baker and Cornell 2006; Baker 2011). A CMS is a mean response spectrum computed based on the condition that the spectral acceleration matches a target amplitude at a given period. The difference between the target spectral acceleration and that predicted by a ground motion prediction equation (GMPE) at the same period is evaluated as a number of standard deviations associated with this GMPE. This difference, denoted by ε, plays a significant role in the construction of CMS. Determination of ε values has been widely addressed in the literature (McGuire 1995; Harmsen 2001; Baker and Cornell 2005; Baker and Jayaram 2008; Burks and Baker 2012). Harmsen (2001) provided contour maps of modal and mean ε values for Central and Eastern United States (CEUS) and Western United States (WUS) based on probabilistic seismic hazard analysis (PSHA). Burks and Baker (2012) investigated the occurrence of negative ε values at short periods particularly in Eastern North America (ENA). The correlation between ε values at different periods shapes the CMS in the period range of interest. A number of prediction equations have been proposed to determine the inter-period correlation coefficients based on the period on which the CMS is conditioned (Inoue and Cornell 1990; Baker and Cornell 2006; Baker and Jayaram 2008). The concept of CMS is also gaining attention in ENA which is a region with low to moderate seismic activity. However, the majority of the studies concerning ε and CMS have been conducted considering the seismicity of Western North America (WNA). USGS (http://earthquake.usgs.gov/hazards/apps, last accessed July 2014) provides PSHA-based CMS and ε for both eastern and western regions of the USA. These results are, however, based on ground motion models adopted to define seismic hazard in the USA. In the absence of correlation models specific to ENA, and Eastern Canada in particular, those developed for regions with higher seismic

activity such as WNA have been used instead (Daneshvar et al. 2014). However, the applicability of such models to ENA and mainly Eastern Canada has not been fully addressed.

This work focuses on the ingredients required to construct CMS in Eastern Canada and investigates the effects of their variations on the constructed CMS. The paper is organized as follows. First, a review of the general steps to construct the CMS is presented in Section 2. In Section 3, we investigate the sensitivity of CMS and ε to six different GMPEs including a newly proposed GMPE that accounts for up-to-date seismological characteristics of ENA. In Section 4, correlation coefficients for spectral accelerations specific to Eastern Canada are determined based on historical records, compared to a commonly used WNA correlation model and then their effects on the CMS evaluated. This section also demonstrates the effects of magnitude and epicentral distance on correlation coefficients for Eastern Canada and the resulting CMS. The findings are illustrated for three locations with low and moderate seismic hazard and risk, i.e., Toronto, Montreal, and Quebec.

4.2 Review of the general steps to construct CMS

A general step by step procedure for CMS computation was proposed by Baker (2011). To facilitate appraisal of the different steps of this procedure and its programming, we propose the flowchart illustrated in Figure 4-1. The procedure starts with the determination of a target spectral acceleration S_a at the desired period T^*. Provided that the target spectral amplitude is obtained from a probabilistic seismic hazard analysis (PSHA), the mean (or modal) values of magnitude M, epicentral distance R, and epsilon $\varepsilon(T^*)$ can be taken from the corresponding seismic hazard deaggregation. ε is defined as the difference, measured as the number of standard deviations, between the predicted and the target spectral accelerations associated with a specific magnitude M, distance R, and period T . Next, a GMPE has to be selected. In the case where a PSHA is used, the same GMPE that produced the mean (modal) values in the previous step can generally be adopted. The spectral predictions of the GMPE are determined for the selected magnitude M and distance R combination in the desired period range. The reported sigma values for the GMPEs at each period are also considered. If a PSHA is not available or the ε value is not provided in the deaggregation results, the ε value at T^* can be calculated for a specific magnitude M, distance R, and spectral acceleration S_a at this period as (Baker 2011)

$$\varepsilon(T^*) = \frac{\ln S_a(T^*) - \mu_{\ln\, S_a}(M, R, T^*)}{\sigma_{\ln\, S_a}(T^*)} \tag{4.1}$$

where $S_a(T^*)$ is the spectral amplitude from the target spectrum, $\mu_{\ln\, S_a}(M, R, T)$ represents the predictions of the GMPE, and $\sigma_{\ln\, S_a}(T^*)$ is the standard deviation in logarithmic units provided by the GMPE. Suitable correlation coefficients $\rho(T, T^*)$, such as the ones suggested by Baker and Jayaram (2008), referred to as BJ08 hereafter, are then used to calculate the value of ε at other periods T as $\varepsilon(T^*) = \rho(T, T^*)\ \varepsilon(T^*)$. We note that the determination of correlation coefficients for Eastern Canada and also applicability of BJ08 to this region is discussed later in Section 4.4. The CMS $\mu^{(\mathrm{CMS})}_{\ln S_a(T)}$ and the associated conditional standard deviation $\sigma^{(\mathrm{CMS})}_{\ln S_a(T)}$ are obtained as

$$\mu^{(\mathrm{CMS})}_{\ln S_a(T)} = \mu_{\ln\, S_a}(M, R, T) + \varepsilon(T)\ \sigma_{\ln S_a}(T) = \mu_{\ln\, S_a}(M, R, T) + \rho(T, T^*)\ \varepsilon(T^*)\sigma_{\ln S_a}(T) \tag{4.2}$$

and

$$\sigma^{(\mathrm{CMS})}_{\ln S_a(T)} = \sigma_{\ln S_a}(T)\sqrt{1 - \rho^2(T, T^*)} \tag{4.3}$$

Lin et al. (2013) discussed four approaches, three approximate and one exact to determine CMS. The proposed methods vary based on the number of considered GMPEs, their corresponding weights in a PSHA-related logic tree and deaggregation, as well as multiple earthquake scenarios contributing to seismic hazard. “Method 1” uses the mean values of the required parameters, e.g., M and R combinations, from deaggregation, and substitutes them into a single GMPE. Equation 2 is then used to compute CMS. “Method 2”, a refined version of “Method 1”, considers all the GMPEs used to conduct PSHA and their logic tree weights. The same procedure as “Method 1” is used to compute CMS for each GMPE. The final CMS is obtained by summing up the computed CMS considering their logic tree weights. “Method 3” considers GMPE deaggregations, if available, to determine the mean value of the required parameters to be used with each individual GMPE, e.g., M and R combinations, and next, similar to “Method 1”, the CMS corresponding to each GMPE is computed. “Method 3” also takes, from GMPE deaggregation, the probability that each GMPE predicted exceedance (or occurrence) of $S_a(T)$. The final CMS is computed as the sum

of the obtained CMS considering the mentioned probabilities. “Method 4”, the exact method, follows the steps of “Method 3” with the difference that the individual CMS is computed for each set of parameters, e.g., *M* and *R* combinations, obtained from PSHA deaggregation results and not only for the mean values of such parameters. The contribution of each of such parameter

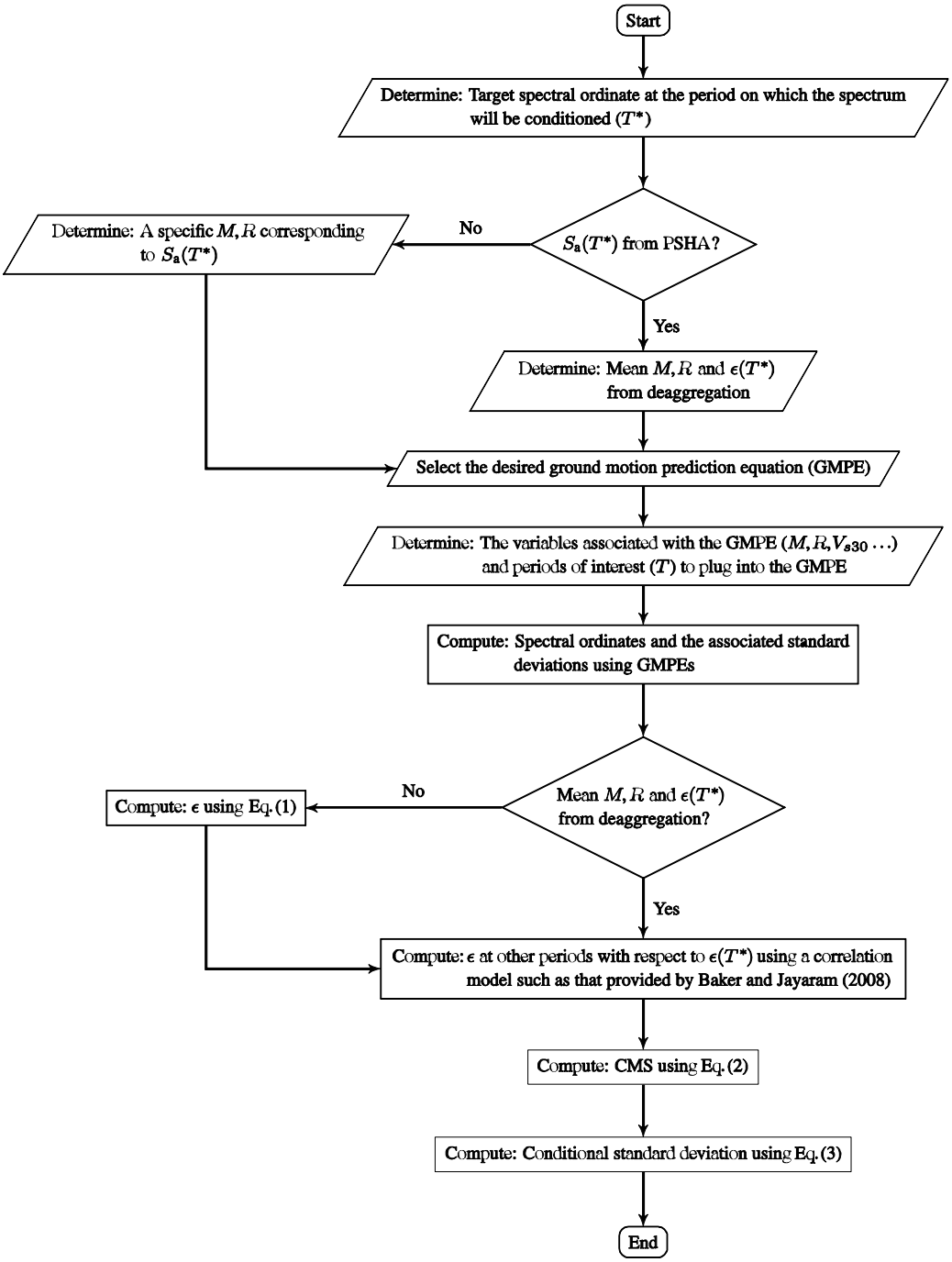

Figure 4-1: Flowchart illustrating the procedure to compute CMS.

combinations to exceedance (or occurrence) of $S_a(T)$ is considered in computation of the final CMS similar to "Method 3". The reader is referred to Lin et al. (2013) for a detailed explanation of the considered parameters and approaches and to Daneshvar et al. (2014) for a step by step construction of CMS to analyze an eight-storey building in Montreal.

4.3 Construction of CMS for Eastern Canada

Figure 4-1 and Section 2 clearly confirm that GMPEs are one of the fundamental ingredients needed to calculate CMS. The effect of varying GMPEs on the resulting CMS and ε values is studied in Section 4.3.2. Such a study requires adoption of "Method 1" in Lin et al. (2013). This method is indeed the only one of the four proposed by Lin et al. (2013) that considers a single GMPE which is not necessarily the one used for PSHA or construction of the target UHS. Accordingly, a comparison of the effects of different GMPEs on the resulting CMS considering the same UHS can be carried out. Section 4.3.1 introduces the GMPEs used in this study.

4.3.1 Ground motion prediction equations

A variety of GMPEs have been proposed in the literature to predict spectral amplitudes in ENA. The main parameters of some of the GMPEs selected for this study are summarized in **Error! eference source not found.** and are briefly described next. Silva et al. (2002) proposed a GMPE with different coefficients accounting for single and double corner frequency models with constant and variable stress drops and magnitude saturation. The single corner frequency model with variable stress drop, referred to as SGD02S hereafter, and the double corner frequency model with magnitude saturation, referred to as SGD02D hereafter, are selected for this study. Regression analyses were performed on the data from 13,500 simulations. The proposed GMPE covers a Joyner–Boore distance of $1 \leq R_{jb} \leq 400$ km and a moment magnitude (M_W) range of $M_W = 4.5$ to $M_W = 8.5$ for CEUS and ENA hard rock sites. Atkinson and Boore (2006) developed a set of relationships, referred to as AB06 hereafter, to predict ENA ground motions using a stochastic finite fault model (Hanks and McGuire 1981; Boore 1983). A data set of 38,400 simulated ground motions having magnitudes between $M_W = 3.5$ and $M_W = 8$ and fault distances ranging from 1 to 1000 km was compiled. Equations to predict the median amplitudes of 5 %-damped pseudo-spectral accelerations (PSA) for ENA ground motions were developed through regression analyses of the simulated records. Modifications due to new seismographic data were made to AB06

equations as provided in Atkinson and Boore (2011). The modified version of AB06 is used in this study.

To predict ENA ground motions, Atkinson (2008) adopted a *referenced empirical* approach which combines available data from ENA to that from an active tectonic and better-instrumented reference region, in this case WNA. Based on the same database of ground motions used by Atkinson and Boore (2006), Atkinson (2008) proposed a GMPE, referred to as A08 hereafter, corresponding to ground motion characteristics in ENA while having an overall magnitude scaling behavior of observations in WNA (Atkinson 2008). The database included ENA records with a magnitude range of M_{W} = 4.3 to M_{W} = 7.6. The reference WNA GMPE used is the Boore and Atkinson (2008) relations, modified later by Atkinson and Boore (2011) based on new seismographic data. The Boore and Atkinson (2008) relationships are one of the five sets of equations developed under the Next Generation Attenuation Relationships for Western USA (NGAWest) program coordinated by Pacific Earthquake Engineering Research Center (PEER). These relationships were based on results from regression analyses on records from shallow crustal ground motions in active tectonic regions compiled in the PEER-NGA West data set. The equations were developed for a magnitude range of M_{W} = 5.0 to M_{W} = 8.0, closest horizontal distance to the surface projection of the fault plane (Rjb) of up to 200 km and a time-averaged shear-wave velocity in the top 30m (V_{S30}) of 180 ≤ V_{S30} ≤ 1300 m/s. The A08 GMPE covers a Joyner–Boore distance range of 1 ≤ R_{jb} ≤ 1000 km. It is worth mentioning that the main difference between this referenced empirical approach and the hybrid empirical method proposed by Campbell (2003) is that it directly employs observational ENA ground motion data instead of using a stochastic model. The modified version of A08 (Atkinson and Boore 2011) is used in this study.

Pezeshk et al. (2011) proposed a new GMPE for ENA, referred to as PZT11 hereafter, based on a hybrid empirical method adopting five WNA GMPEs provided by PEER. The GMPEs were developed by Abrahamson and Silva (2008), Boore and Atkinson (2008), Campbell and Bozorgnia (2008), Chiou and Youngs (2008) and Idriss (2008). The new GMPE covers a magnitude range of M_{W} = 5 to M_{W} = 8 and closest distances to the fault rupture (R_{RUP}) of 1 ≤ R_{RUP} ≤ 1000 km and is used to generate median 5 %-damped pseudo-accelerations in ENA for given magnitude and distance considering hard rock sites, i.e., V_{S30} ≥ 2000 m/s.

Table 4.1 Characteristics of the ground motion prediction equations used in this study

GMPEs	Mag. Scale/Range	Dist. metric/Range	Period range	Response variable	Damping values
Silva et al. (2002) – SGD02	M_W/4.5 – 8.5	R_{jb}/1 – 400 km	0 - 10 s	PSA	5%
Atkinson and Boore (2006) – A06	M_W/3.5 – 8.0	R_{RUP}/1 – 1000 km	0 – 5 s	PSA	5%
Atkinson (2008) – A08	M_W/4.3 – 7.6	R_{jb}/1 – 1000 km	0 – 5 s	PSA	5%
Pezeshk et al. (2011) – PZT11	M_W/5.0 – 8.0	R_{RUP}/1 – 1000 km	0 - 10 s	PSA	5%
Atkinson and Adams (2013)–AA13	M_W/4.5 – 8.0	R_{EPI}/1 – 800 km	0 - 10 s	PSA	5%

The above-mentioned GMPEs use different distance measures to predict ground motions. To compare the predictions on a uniform distance basis, the equations suggested by Atkinson and Adams (2013) were adopted to convert all distance measures to hypocentral distance, which is the measure used by the Geological Survey of Canada (GSC) for deaggregation results.

4.3.2 Sensitivity of CMS-shape and ε to GMPEs

"Method 1" was introduced by Lin et al. (2013) as one of the approximate methods to compute CMS. It assumes that the target spectrum can be used with a GMPE other than its original underlying GMPE(s). The "Method 1" procedure is similar to that illustrated in Figure 4-1. Hence, the UHS prescribed by the National Building Code of Canada (NBCC 2010) considering a return period of 2 % in 50 years for three major Eastern Canadian cities, Toronto, Montreal, and Quebec, are used as the target spectra in this section. For each location, the underlying deaggregation results provided by GSC, upon request, are consulted to extract the M and R combination corresponding to $S_{\mathrm{a}}(T^*)$ taken fromthe UHS. These M and R sets are presented in Table 4.2. Considering structures with fundamental periods of T^* = 0.2 s, T^* = 0.5 s, T^* = 1 s, and T^* = 2 s, Eqs. 4.1, 4.2, and 4.3 are used to obtain $\varepsilon(T^*)$, $\varepsilon(T)$, and the CMS corresponding to each GMPE and T^*. It is noted that the GSC deaggregation is provided for NBCC 2010 site class C and thus the GMPE predictions are modified using the coefficients given in Atkinson and Boore (2011) to correspond to this site class. Furthermore, deaggregation results provided by GSC do not include mean $\varepsilon(T)$ values and thus, as mentioned in Section 4.2, Eq. 4.1 is used to obtain $\varepsilon(T^*)$ and $\varepsilon(T)$. Figure 4-2, Figure 4-3, and Figure 4-4 illustrate the CMS computed using each of the adopted GMPEs and UHS. The level of conservatism included in the UHS in comparison to CMS, as mentioned in Section 4.1, is clearly observed. We can see that in the cases where the CMS is anchored to the UHS at a short period, i.e., T^* = 0.2 s, the accelerations corresponding to the resulting CMS can exceed those of the UHS depending on which GMPE is used. Such an observation is expected as the NBCC 2010 UHS are capped at T = 0.2 s, i.e., the spectral accelerations at periods shorter than T = 0.2 s are equal to that at T = 0.2 s whereas originally the UHS can have a peak at the period range shorter than T = 0.2 s. Figure 4-2 to Figure 4-4 also show the variation in CMS amplitudes as a result of changes in the underlying GMPE. The dispersion of CMS amplitudes is more dramatic at the shorter period range where there is larger difference between the predictions of the GMPEs. The broadness of this range depends on the selected T^*. We note that the amplifications observed

in the CMS corresponding to Silva et al. (2002) at shorter periods root from the particular spectral shape predicted by SGD02 combined with the correlation coefficients. The epsilon values reported in Figure 4-2 to Figure 4-4 shed more light on the reason behind the variation in CMS amplitudes.

Table 4.2 Mean magnitude and distance scenarios for Toronto, Montreal, and Quebec at different periods extracted from deaggregation results obtained from GSC in 2010

Location	T(s)	M_W	R (km)
Toronto	0.2	5.6	99
	0.5	6.5	217
	1.0	6.7	234
	2.0	6.8	282
Montreal	0.2	6.1	36
	0.5	6.6	51
	1.0	6.8	64
	2.0	6.9	79
Quebec	0.2	6.0	41
	0.5	6.6	68
	1.0	6.8	81
	2.0	6.8	95

It is shown in Eqs. 4.1 and 4.2, that the standard deviation and consequently the epsilon corresponding to each GMPE greatly affect CMS amplitudes. The difference between CMS amplitudes and those from the UHS at longer periods partly depends on how far the GMPE predictions are from the UHS. As can be seen in Figure 4-2 to Figure 4-4, the CMS computed using SGD02S can result in overconservative amplitudes when anchored to the UHS at longer periods. This is mainly due to the fact that SGD02S produces conservative spectral amplitudes in comparison to the other GMPEs studied (Atkinson and Adams 2013). As the correlation coefficients for all the illustrated CMS are calculated using BJ08, the only influential factors are the predicted spectral amplitudes and the $\varepsilon(T^*)$.

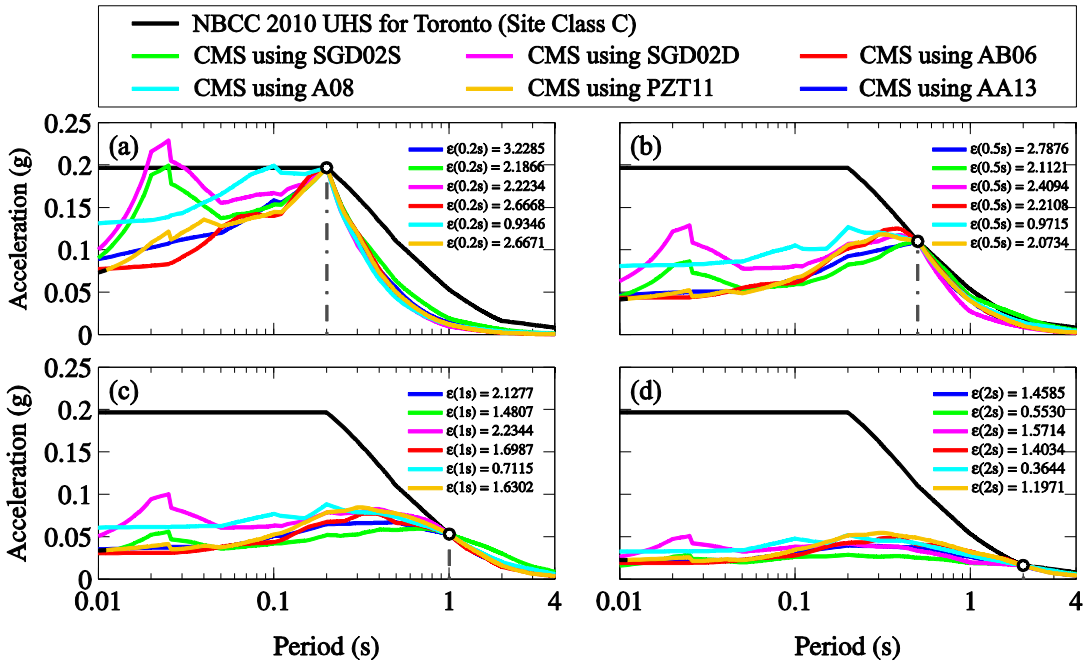

Figure 4-2: GMPE-based variation of CMS computed by matching to NBCC 2010 prescribed UHS for Toronto at (a) T^* = 0.2 s, (b) T^* = 0.5 s, (c) T^* = 1 s, and (d) T^* = 2 s.

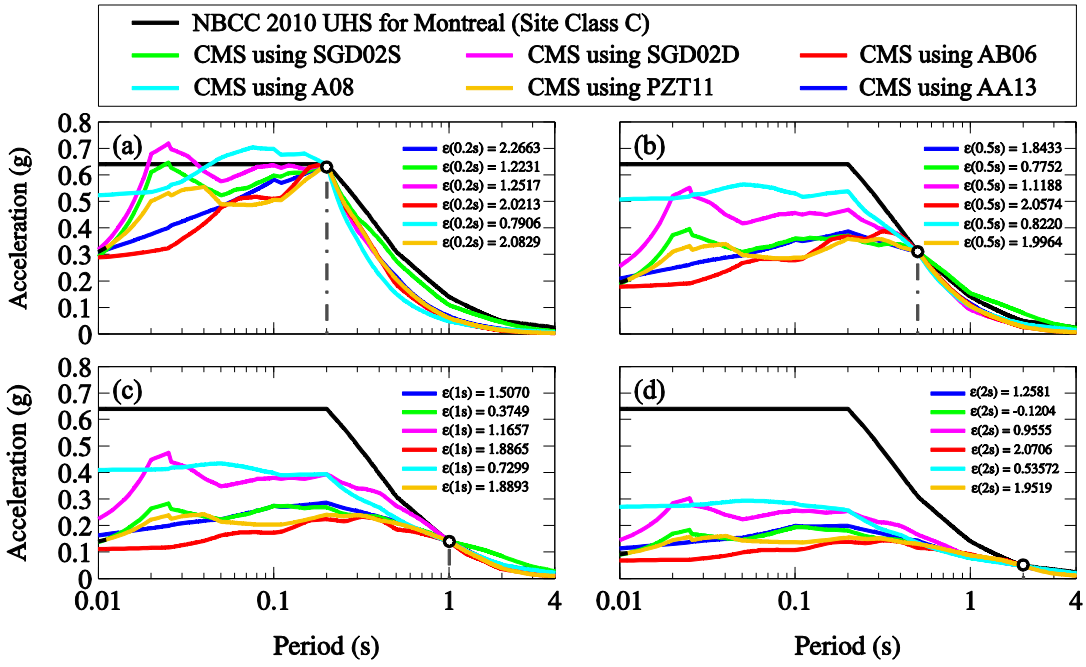

Figure 4-3: GMPE-based variation of CMS computed by matching to NBCC 2010 prescribed UHS for Montreal at (a) T^* = 0.2 s, (b) T^* = 0.5 s, (c) T^* = 1 s, and (d) T^* = 2 s.

The presented results reiterate the approximative nature of "Method 1" and confirm that a certain bias can be introduced when GMPEs other than the one(s) underlying a given UHS are used to

generate the CMS. This emphasizes the importance of appropriately selecting GMPEs to construct CMS, especially for structures with relatively short fundamental periods and also those for which higher mode effects are significant.

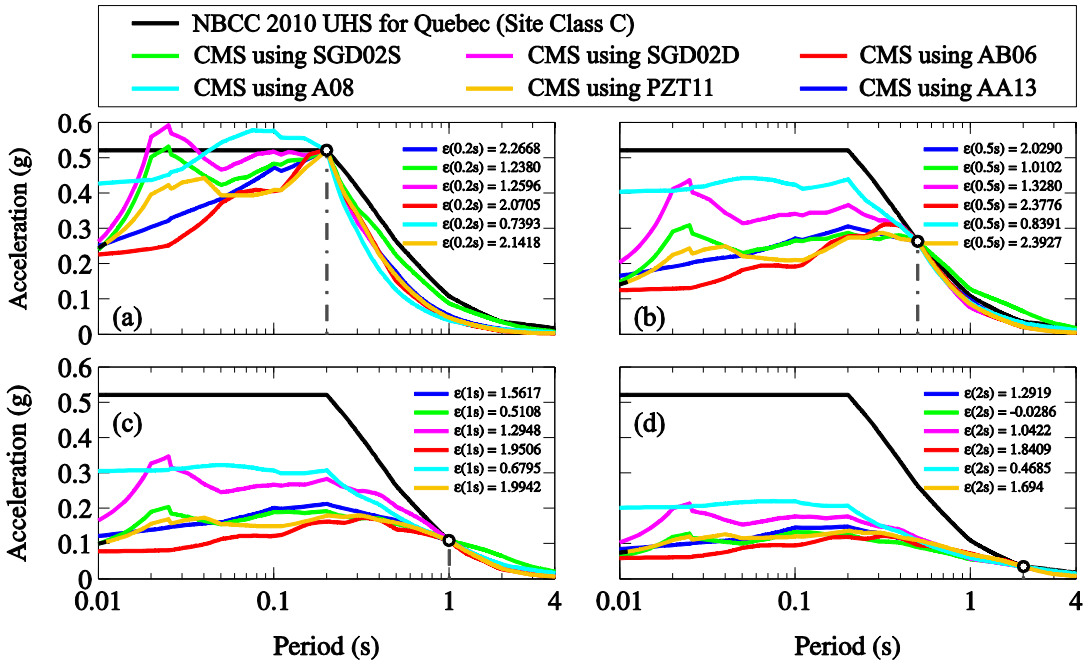

Figure 4-4: GMPE-based variation of CMS computed by matching to NBCC 2010 prescribed UHS for Quebec at (a) T^* = 0.2 s, (b) T^* = 0.5 s, (c) T^* = 1 s, and (d) T^* = 2 s.

4.3.3 Consideration of multiple GMPEs

Lin et al. (2013) suggest "Method 2" as another approximate approach to compute CMS. "Method 2" is a refined version of "Method 1" in the sense that all the GMPEs used in the PSHA are considered and their corresponding weights in the PSHA logic tree are accounted for. Equations 4.4 and 4.5 are suggested to obtain the CMS and the conditional standard deviations

$$\mu_{\ln S_a(T)}^{(\mathrm{CMS})} = \sum_i P_i \, \mu_{\ln S_a(T),i}^{(\mathrm{CMS})} \tag{4.4}$$

and

$$\sigma_{\ln S_a(T)}^{(CMS)} = \sqrt{\sum_i P_i \left\{ \left[\sigma_{\ln S_a(T),i}^{(CMS)} \right]^2 + \left[\mu_{\ln S_a(T),i}^{(CMS)} - \mu_{\ln S_a(T)}^{(CMS)} \right]^2 \right\}} \quad (4.5)$$

where i is the number of GMPEs and P_i is the weight assigned to the i th GMPE in the PSHA logic tree. To investigate the application of "Method 2" to generate CMS in Eastern Canada, the prescribed NBCC 2010 UHS with 2 % in 50 years return period for Toronto, Montreal, and Quebec are selected as the target spectra and the ENA GMPE model proposed by Atkinson and Adams (2013) is used to construct CMS. This GMPE, referred to as AA13 hereafter, consists of a representative or central GMPE and upper and lower GMPEs to account for epistemic uncertainty about the central one. The central GMPE is determined by calculating the geometric mean of five peer reviewed GMPEs. The geometric mean ± its standard deviation is considered as the upper/lower GMPE. The five GMPEs are SGD02S, SGD02D, AB06, A08, and PZT11. The final predictions are provided in terms of moment magnitudes and epicentral distances for B/C, i.e., V_{S30} = 760 m/s site condition. The reader is referred to Atkinson and Adams (2013) for more details about the determination of the central, upper, and lower GMPEs, the distance metric conversions, and also the conversion factors used to modify the predictions corresponding to different site conditions to represent those of B/C site condition. The CMS computed using the AA13 central GMPE is also included in Figure 4-2 to Figure 4-4 for comparison purposes. The weights assigned to the central, upper, and lower GMPEs in PSHA are period-based and are given, respectively, as follows: 0.5, 0.25, and 0.25 for $T \geq 1$ s; 0.4, 0.4, and 0.2 for $T \leq 0.2$ s; and a transition of weights is considered between $T > 0.2$ s and $T < 1.0$ s, e.g., 0.4, 0.35, and 0.25 for $T = 0.5$ s (Atkinson and Adams 2013). The spectral amplitudes corresponding to B/C, i.e., V_{S30} = 760 m/s site condition are not provided by GSC for the NBCC 2010 UHS while the GMPEs provide spectral accelerations for B/C site condition. Thus, in order to maintain consistency, period-dependent factors (Atkinson and Boore 2011) are applied to the predictions of the GMPEs to represent NBCC 2010 site class C. The three GMPEs and their corresponding weights are used along with Eqs. 4.4 and 4.5 to compute the CMS using "Method 2". Figure 4-5, Figure 4-6, and Figure 4-7 show the obtained CMS conditioned on spectral accelerations at T^* = 0.2 s, T^* = 0.5 s, T^* = 1 s, and T^* = 2 s. Figure 4-5 to Figure 4-7 also compare the CMS computed using "Method 2" to those computed considering "Method 1" using the AA13 central GMPE and the upper and lower GMPEs, individually. It can be seen that the CMS computed considering the central GMPE using "Method

1" and "Method 2" are very similar. In fact, this similarity is expected as both methods are supposed to produce approximate spectral amplitudes for a particular exact CMS. Slight differences between the CMS obtained from the two methods are observed for short periods. This roots from the weighting scheme of AA13 at this period range.

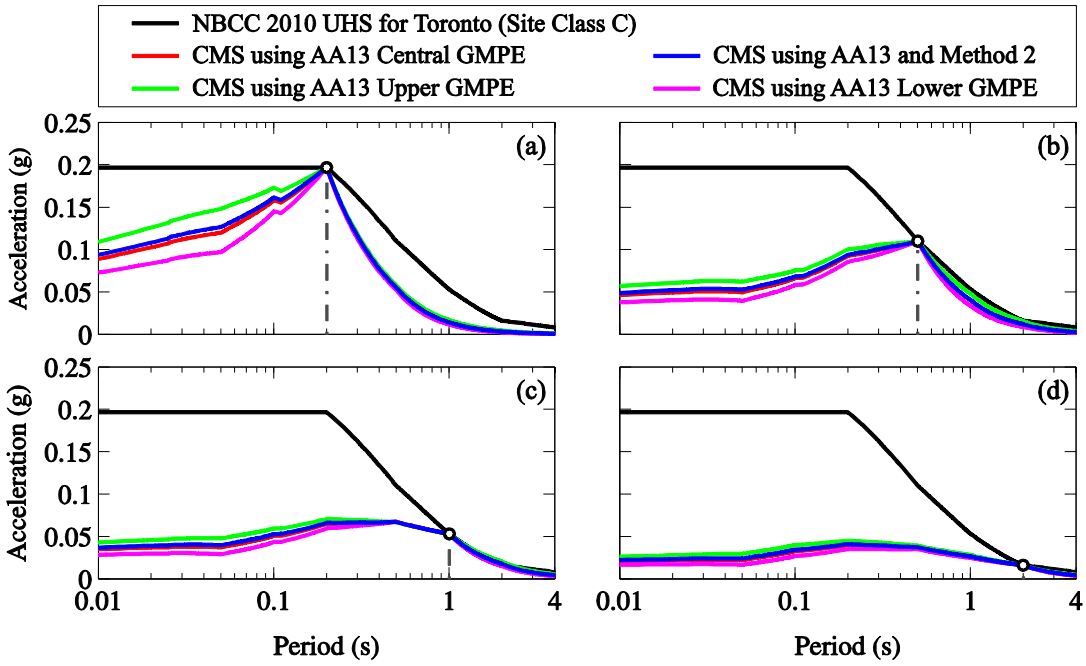

Figure 4-5: CMS computed using Method 2 (Lin et al. 2013) and by matching to NBCC 2010 prescribed UHS for Toronto at (a) T^* = 0.2 s, (b) T^* = 0.5 s, (c) T^* = 1 s, and (d) T^* = 2 s compared to CMS computed using a single GMPE.

In general, as the outcome of the two methods is fairly similar, "Method 1", due to its simplicity, is suggested to be used with AA13 central GMPEs to compute CMS for Eastern Canada. Nevertheless, for structures with very short fundamental periods, using "Method 2" results in more refined CMS as the logic tree weights, are also considered in the computations. Indeed, relatively larger differences, through the entire period range considered, could be observed if the upper and lower GMPEs are replaced with those that are not related to the central GMPE. However, the UHS prescribed by NBCC 2010 for Eastern Canada are determined based on the same approach adopted in this study, i.e., central, upper, and lower GMPEs.

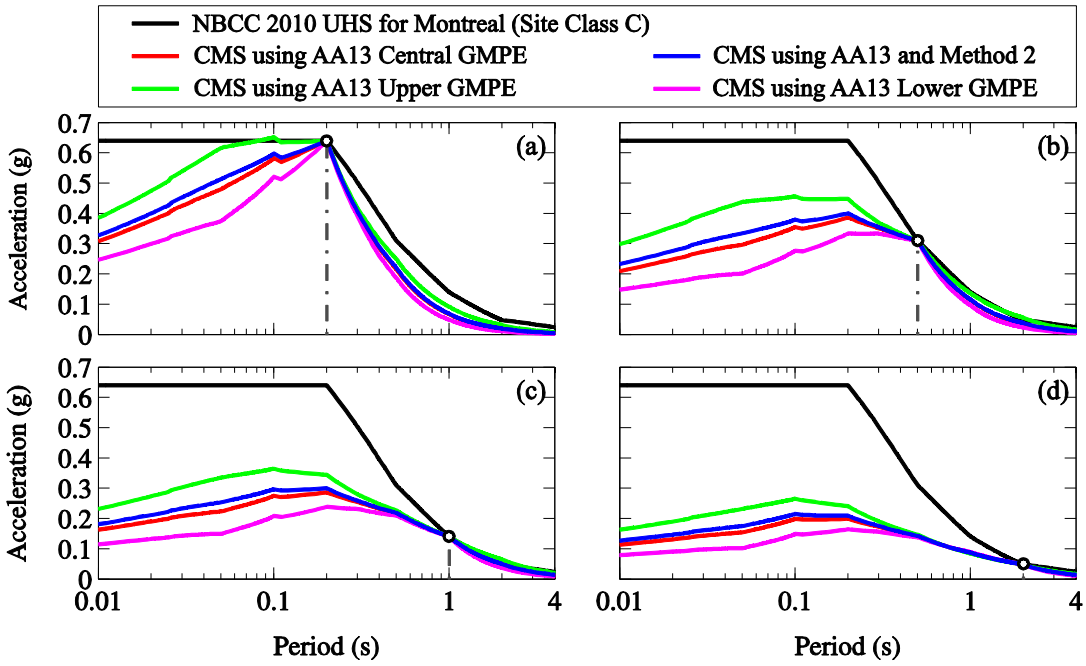

Figure 4-6: CMS computed using Method 2 (Lin et al. 2013) and by matching to NBCC 2010 prescribed UHS for Montreal at (a) T^* = 0.2 s, (b) T^* = 0.5 s, (c) T^* = 1 s, and (d) T^* = 2 s compared to CMS computed using a single GMPE.

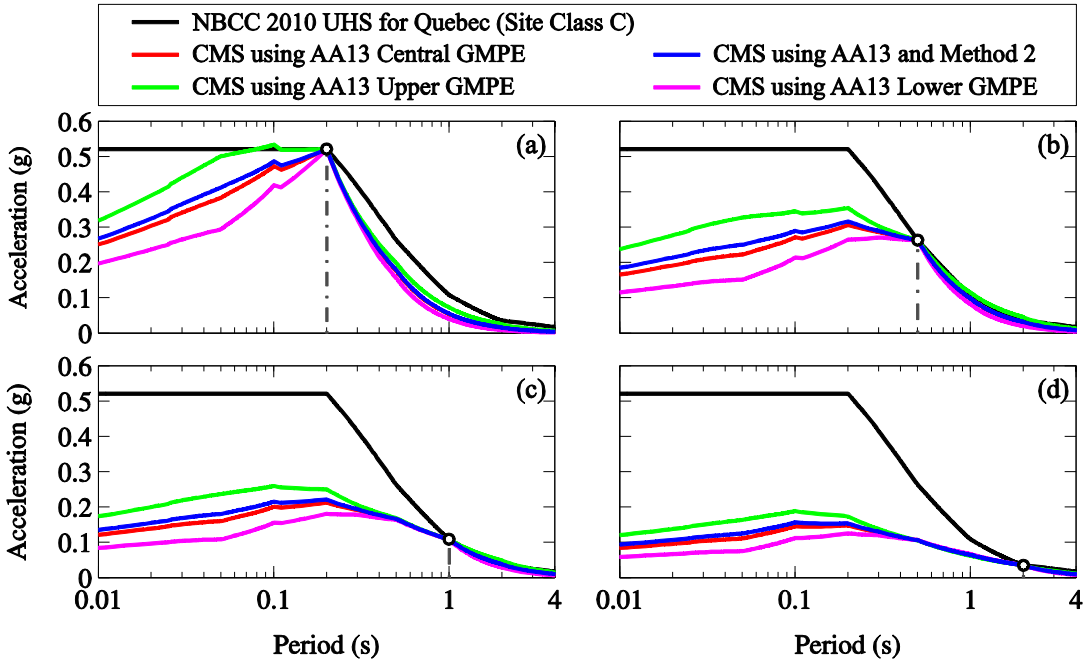

Figure 4-7: CMS computed using Method 2 (Lin et al. 2013) and by matching to NBCC 2010 prescribed UHS for Quebec at (a) T^* = 0.2 s, (b) T^* = 0.5 s, (c) T^* = 1 s, and (d) T^* = 2 s compared to CMS computed using a single GMPE.

4.4 Correlation model for spectral accelerations

4.4.1 Correlation coefficients in Eastern Canada

The CMS calculated and presented in Section 4.3 require the application of a correlation model, as pointed out in Section 4.2. One of the most commonly used correlation models is the one proposed by Baker and Jayaram (2008) which is developed using four different NGA West GMPEs and considering shallow crustal ground motion records from NGA West ground motion library (http://peer.berkeley.edu/nga, last accessed July 2014). The applicability of BJ08 to regions other than WNA was confirmed by Jayaram et al. (2011) who studied Japanese records from a subduction zone and concluded that the BJ08 model, which was developed using shallow crustal earthquakes, can represent the correlations in this region up to an acceptable extent. Lin et al. (2013), although pointing out the lack of data to confirm or reject the applicability of BJ08 model to stable continental sources, conclude that ground motion prediction equations, earthquake magnitude, distance, and rupture mechanisms have almost insignificant effects on the correlation models. Lin et al. (2013) also report that the online tool provided by USGS to construct CMS for locations within the USA uses BJ08 model for the Eastern part which is a stable continental seismic zone that can be assumed similar to Eastern Canada. Based on the above discussion, we decided to use BJ08 model to construct the CMS for Toronto, Montreal, and Quebec in Section 4.3.

To the authors' knowledge, there is no available study on correlation coefficients specific to Eastern Canada and their agreement with the proposed BJ08 model. A major obstacle against the full assessment of ε values and the derivation of prediction equations for correlation coefficients in Eastern Canada is the very limited number of records of interest for the engineering community in terms of magnitude and distance. For this reason, model BJ08, developed using WNA records, has been commonly used in the absence of ENA-specific correlation models. The applicability of this model is investigated further herein by comparing its predictions to available observations from Eastern Canada. For this purpose, we compiled a database of 108 horizontal accelerograms from eight earthquakes with magnitudes M_{W} from 4.5 to 6.9 and epicentral distances R from 6.8 to 640 km. All selected ground motions were recorded on hard rock sites, i.e., NBCC 2010 site class A: $V_{S30} \geq 1500$ m/s. A list of the corresponding earthquake events is provided in Table 4.3. The ground motion accelerograms are obtained from publications of the Geological Survey of Canada (Weichert et al. 1986; Munro and Weichert 1989; GSC 2006; Lin and Adams 2010) and

the database of time-series from Southeastern Canada earthquakes available at http://www.seismotoolbox.ca (last accessed July 2014). The AA13 central GMPE is selected as the reference GMPE to determine correlation coefficients in Eastern Canada. The difference between the 5 %-damped acceleration spectra of the accelerograms considered and those predicted by AA13, i.e., ε, is then calculated at periods of between T = 0.01 s and T = 5 s. This definition of epsilon results in the same correlation coefficients as those obtained from the ε defined in Eq. 4.1 as also pointed out by Baker and Jayaram (2008). This definition will also introduce less bias in the results caused by the type of 5%-damped acceleration spectrum considered, e.g., geometric mean, individual component, or rotation-independent geometric mean. The mean amplitudes for each type of 5 %-damped acceleration spectrum are indeed very similar whereas this is not necessarily the case for corresponding standard deviations. As suggested by Baker and Jayaram (2008), the Pearson product-moment correlation coefficient is used to estimate the correlation coefficient between $\varepsilon(T_1)$ and $\varepsilon(T_2)$, i.e., $\rho(T_1, T_2)$:

$$\rho(T_1, T_2) = \frac{\sum_{i=1}^{n}\left[\varepsilon_i(T_1) - \overline{\varepsilon(T_1)}\right]\left[\varepsilon_i(T_2) - \overline{\varepsilon(T_2)}\right]}{\sqrt{\sum_{i=1}^{n}\left[\varepsilon_i(T_1) - \overline{\varepsilon(T_1)}\right]^2 \sum_{i=1}^{n}\left[\varepsilon_i(T_2) - \overline{\varepsilon(T_2)}\right]^2}} \tag{4.6}$$

where n is the number of observations, i.e., records, $\varepsilon_i(T_1)$ and $\varepsilon_i(T_2)$ are the i th observations of $\varepsilon(T_1)$ and $\varepsilon(T_2)$, respectively, and $\overline{\varepsilon(T_1)}$ and $\overline{\varepsilon(T_2)}$ are their means, respectively. Figure 4-8a and b show examples of calculated $\varepsilon(T_1)$ and $\varepsilon(T_2)$ values and the resulting $\rho(T_1, T_2)$, i.e., the slopes of the illustrated lines. It can be seen that the $\rho(T_1, T_2)$ values, i.e., the slopes, for Eastern Canada are larger than those given by BJ08. This is confirmed through contour graphs for the $\rho(T_1, T_2)$ values corresponding to the majority of the period pairs obtained from Eq. 4.6 as illustrated in Figure 4-9a and b. Although similar trends are observed in the obtained $\rho(T, T^*)$ from Eastern Canadian records and predictions of BJ08 model, the values are not identical. It seems that there is a higher correlation between spectral accelerations at different periods in Eastern Canada than predicted by BJ08 model. Carlton and Abrahamson (2014) suggest that correlation coefficients are sensitive to the high frequency content of ground motion records, e.g., those recorded on hard rock sites. Therefore, the application of correlation models such as BJ08 needs consideration of this characteristic of ground motions. Accordingly, Carlton and Abrahamson (2014) propose $T_{\text{amp1.5}}$,

the shortest period at which $S_a(T^*)$ reaches 1.5 times the PGA, as a measure to determine the period at which the high frequency content influence the response spectrum. Carlton and Abrahamson (2014) reported that the database of ground motions used to develop BJ08 has a $T_{\text{amp1.5}}$ of 0.1 s. They also reported that $\rho(T, T^*)$ values obtained from other data sets containing records from high seismicity regions and having $T_{\text{amp1.5}}$ close to that of BJ08 are very similar to predictions of BJ08.

Table 4.3 Historical ENA ground motions studied

Event	M_W	Number of records	Site class
Nahanni (11/1985)	4.6	2	A
Nahanni (12/1985)	6.9	4	A
Saguenay (1988)	5.8	18	A
Cap-Rouge (1997)	4.7	16	A
Pymatuning (1998)	5.0	2	A
Côte-Nord (1999)	4.7	18	A
Au-Sable-Forks (2002)	5.1	26	A
Rivière-du-Loup (2005)	5.0	16	A
Val-des-Bois (2010)	5.0	6	A

Carlton and Abrahamson (2014) also propose that when BJ08 correlation coefficients are used to compute CMS from a controlling scenario (e.g., M and R scenarios) representing a response spectrum that has a $T_{\text{amp1.5}}$ value different from 0.1 s, the following modifications be applied to obtain suitable BJ08 results: (1) determine $T^{*\prime} = 0.1 \times T^*/T_{\text{amp1.5}}$; (2) determine $\rho(T^{*\prime}, T)$ using BJ08 model; and (3) calculate $T_{\text{new}} = T \times T_{\text{amp1.5}}/0.1$. To investigate the applicability of the modified BJ08 correlation coefficients to Eastern Canada, first the $T_{\text{amp1.5}}$ of the records in the database of this study is calculated and found to be $T_{\text{amp1.5}}$ = 0.045 s. This $T_{\text{amp1.5}}$ = 0.045 s reveals the very high-frequency characteristic of the Eastern Canadian records in comparison to those used to develop BJ08 model. The correlation coefficients from the database are then compared to those given by BJ08 model at different $T_{\text{amp1.5}}$ values. Both sets of coefficients, from Eastern Canada and from BJ08, are modified according to the procedure suggested by Carlton and Abrahamson (2014) where necessary. Figure 4-10 and Figure 4-11 illustrate the modified correlation coefficients, i.e., "Eastern Canada Modified" and "BJ08 Modified", for T^* = 0.2 s, T^* = 0.5 s, T^* = 1 s, and T^* = 2 s. It can be seen that even after considering the effect of high-frequency content

of ground motions, the correlation coefficients obtained for Eastern Canada are higher than those predicted by BJ08 model. The observed shifts in the period ranges for the modified correlation coefficients result from conversion of their corresponding periods T to T_{new} which are not identical. It should be noted that the $\rho(T_1, T_2)$ values obtained from the historical records in Eastern Canada could be affected by the limitations associated with record selection in the region. We also note that the accelerograms included in the database compiled in this study were not used to develop AA13 GMPE. This is contrary to the approach adopted to develop BJ08 model.

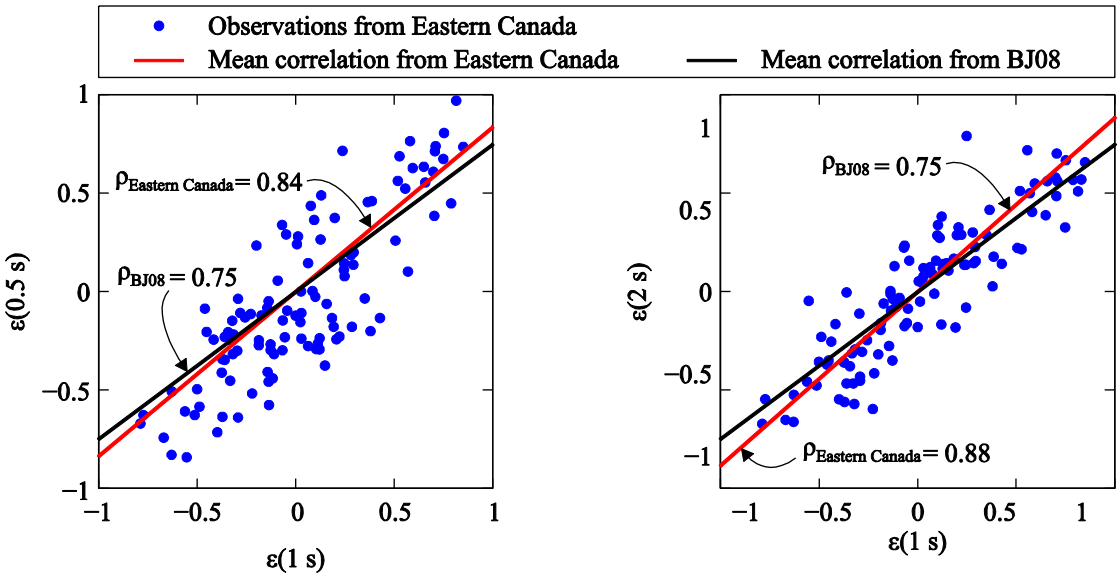

Figure 4-8: Observed $\varepsilon(T)$ and the corresponding correlation coefficients defined as the slope of each line: (a) between T = 0.5 s and T = 1 s, and (b) between T = 1 s and T = 2 s.

Table 4.4 Magnitude-based classification of the records in the studied database of ground motions

Bin	Event	M	Number of records
M1	Nahanni (11/1985)	4.6	2
	Cap-Rouge (1997)	4.7	16
	Côte-Nord (1999)	4.7	18
M2	Nahanni (12/1985)	6.9	4
	Saguenay (1988)	5.8	18
	Pymatuning (1998)	5.0	2
	Au-Sable-Forks (2002)	5.1	26
	Rivière-du-Loup (2005)	5.0	16
	Val-des-Bois (2010)	5.0	6

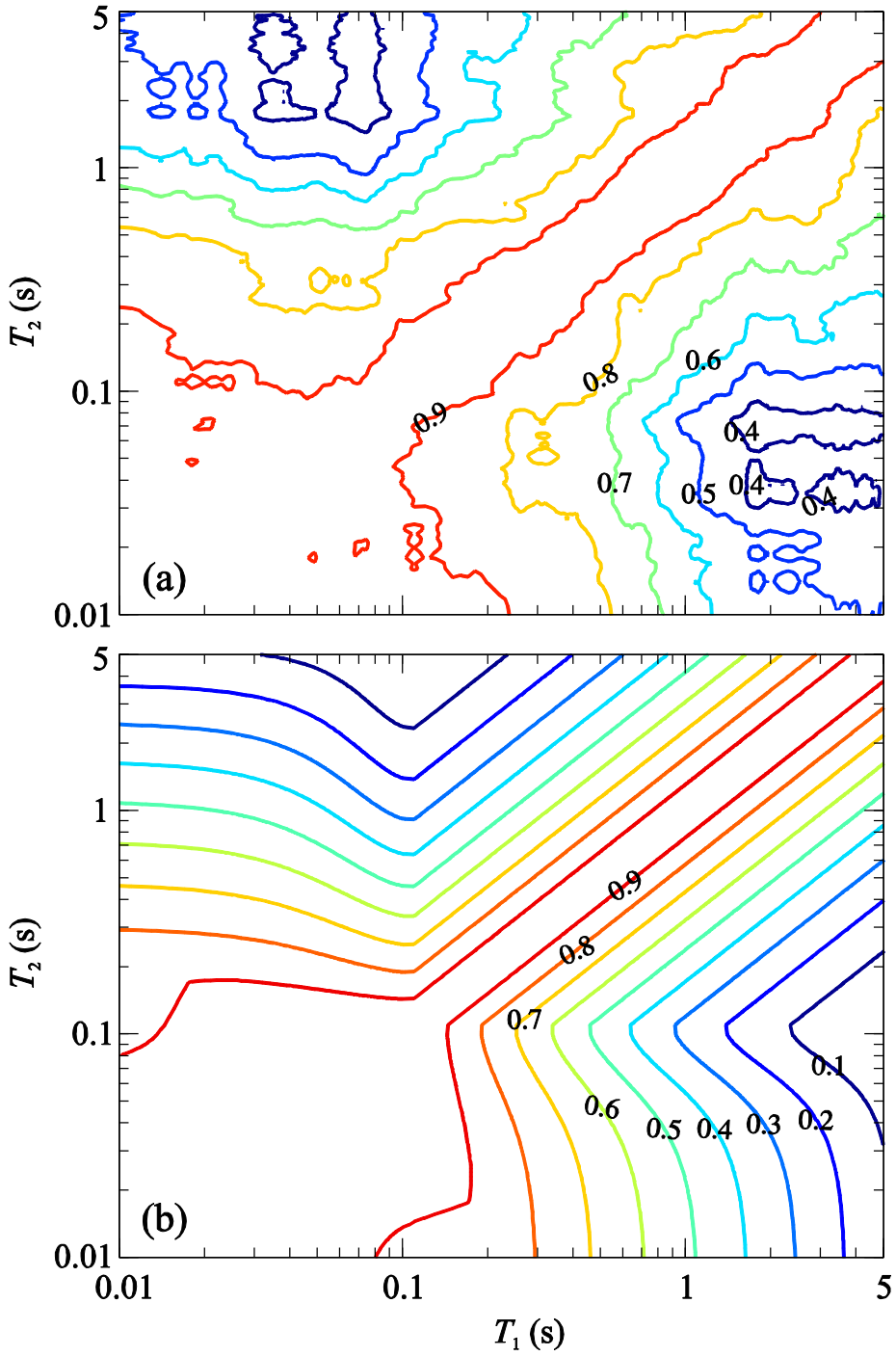

Figure 4-9: Correlation coefficients obtained from (a) ground motions in Eastern Canada and (b) Baker and Jayaram (2008). The *numbers over the contour lines* represent the corresponding correlation coefficients.

Based on the results presented in Figure 4-10 and Figure 4-11, there appears to be a need to further investigate the spectral correlations in this region in light of data recorded in the future.

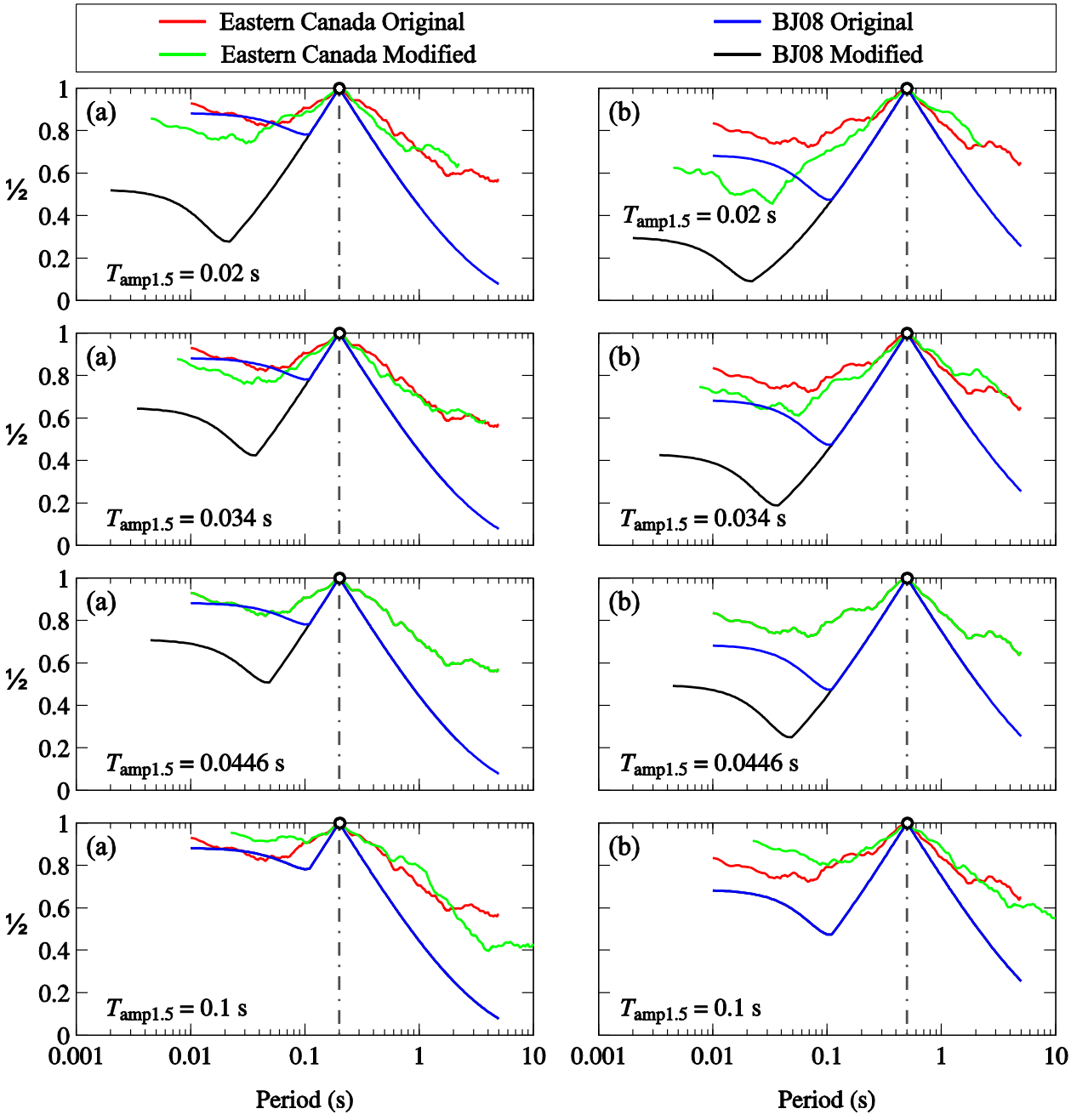

Figure 4-10: Comparison between obtained correlation coefficients for Eastern Canada and those from BJ08 model at different $T_{amp1.5}$ values for (a) T^* = 0.2 s and (b) T^* = 0.5 s.

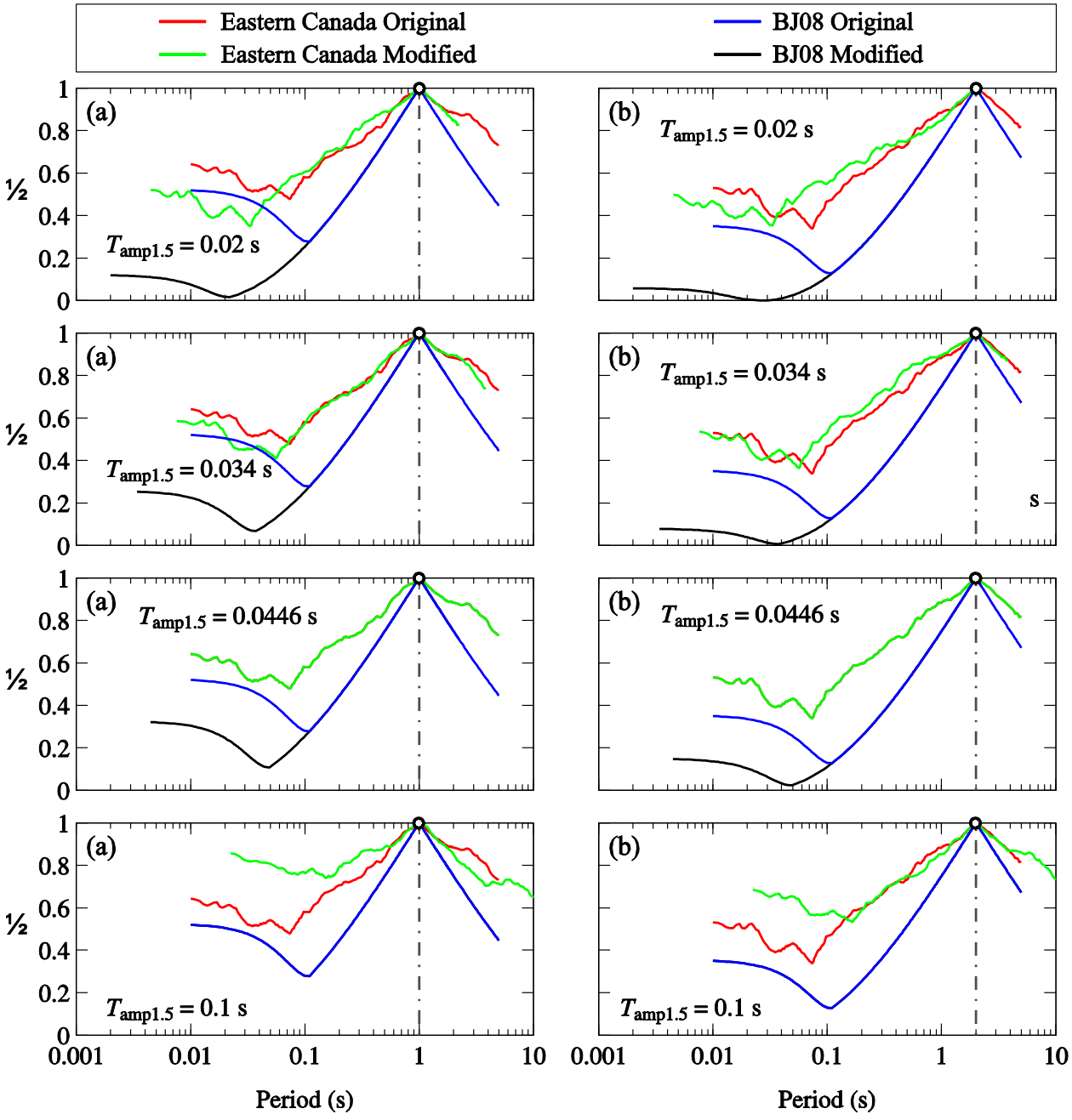

Figure 4-11: Comparison between obtained correlation coefficients for Eastern Canada and those from BJ08 model at different $T_{amp1.5}$ values for (a) T^* = 1 s and (b) T^* = 2 s.

4.4.2 Magnitude and distance dependence of correlation coefficients

Correlation coefficients from BJ08 model and those specific to Eastern Canada determined in this study both consider ρ to be independent from magnitude and distance of the ground motions. This is mainly based on the observations reported by Baker and Cornell (2005). To investigate the

applicability of this assumption to ground motions in Eastern Canada, the accelerograms in the database are classified once based on the corresponding magnitude and then based on epicentral distance. Ground motions of magnitudes $M_W < 5$, which are more frequent in Eastern Canada (www.seismotoolbox.ca), are generally of lower importance for structural engineering purposes. Thus, records with magnitudes $M_W \geq 5$ and $M_W < 5$ are grouped together into bins M1 and M2, respectively, as indicated in Table 4.4. In addition, the accelerograms in the original database are divided into four bins based on epicentral distance R: (R1) $R \leq 100$ km, (R2) 100 km $< R \leq 200$ km, (R3) 200 km $< R \leq 400$ km, and (R4) $R \geq 400$ km. Ground motions with epicentral distances shorter than 100 km are generally more interesting for structural engineering applications.

Table 4.5 Distance-based classification of the records in the studied database of ground motions

Event	M_W	R1	R2	R3	R4
Nahanni (11/1985)	4.6	2	-	-	-
Nahanni (12/1985)	6.9	4	-	-	-
Saguenay (1988)	5.8	8	10	-	-
Cap-Rouge (1997)	4.7	-	12	2	2
Pymatuning (1998)	5.0	-	-	2	-
Côte-Nord (1999)	4.7	-	-	14	4
Au-Sable-Forks (2002)	5.1	-	4	2	20
Rivière-du-Loup (2005)	5.0	14	-	2	-
Val-des-Bois (2010)	5.0	6	-	-	-

Therefore, records with distances in this range are grouped together in one bin, i.e., R1. Events with 100 km $< R \leq 200$ km can still have considerable effect on structures. As a result, the distance interval is kept at 100 km for the next bin, i.e., R2. This interval is increased to 200 km to form a bin from accelerograms recorded at longer distances less than 400 km, i.e., R3. As a number of GMPEs extend predictions to epicentral distances over 400 km (e.g., Atkinson and Adams 2013), ground motions recorded at such distances are also included and grouped together, i.e., R4. The proposed distance-based classification of the accelerograms studied is presented in Table 4.5.

The correlation coefficients for each bin were next computed using AA13 central GMPE taking the same approach as in Section 4.4.1. The high frequency content of the records was also addressed

by considering the $T_{\text{amp1.5}}$ corresponding to each bin and following the procedure suggested by Carlton and Abrahamson (2014). The values for $T_{\text{amp1.5}}$ corresponding to Bins M1 and M2 and Bins R1 to R4 were found to be 0.040, 0.047, 0.028, 0.042, 0.053, and 0.063 s, respectively. Figure 4-12 and Figure 4-13 compare the obtained correlation coefficients to those determined regardless of magnitude and distance effects in Section 4.4.1 at T^* = 0.2 s, T^* = 0.5 s, T^* = 1 s, and T^* = 2 s. Figure 4-12 and Figure 4-13 clearly show that the period range through which the magnitude-dependency of correlation coefficients is pronounced, moves from longer periods to shorter periods as T^* increases. It is also illustrated that, in general, there is a higher correlation among the lower magnitude records in Eastern Canada, i.e., Bin M1. The correlation coefficients associated with the records from higher magnitudes, i.e., Bin M2, show a close agreement with those obtained from the entire database although the two sets tend to deviate at period ranges with high magnitude-dependency. This agreement can partly be related to the number of records in Bin M2 which contains approximately 2/3 of the records in the entire database. Figure 4-14 and Figure 4-15 reveal the distance-dependency of the correlation coefficients in Eastern Canada. It can be seen that the obtained distance-based correlation coefficients for Eastern Canada do not vary dramatically with epicentral distances up to 400 km, i.e., Bins R1, R2, and R3. Nevertheless, correlation coefficients of ground motions at very long distances, i.e., Bin R4, demonstrate poor correlation in the entire period range considered for almost all the values of T^*. In general, the difference between the coefficients from Bins R1, R2, and R3 and those from the entire database is mainly due to very low coefficients from Bin R4 which are considered in the determination of correlation coefficients for the entire database.

We next investigate whether the magnitude- and distance-based classifications of correlation coefficients computed for Eastern Canada will considerably affect the resulting CMS. To this end, the AA13 central GMPE is selected as the underlying model. The NBCC 2010 UHS for Toronto, Montreal, and Quebec corresponding to NBCC 2010 site class A are adopted as the target spectra as all the ground motions studied were recorded on hard rock sites. The predictions of AA13 are modified to represent ground motions for site class A as already mentioned in Section 4.3.3. Modified correlation coefficients including the effects of high frequencies, i.e., $T_{\text{amp1.5}}$, are taken from the appropriate bins which are based on mean M and R from deaggregation and are used to compute CMS. Figure 4-16, Figure 4-17, Figure 4-18, Figure 4-19, Figure 4-20, and Figure 4-21 present the computed CMS using the magnitude- and distance-based correlation coefficients along

with the CMS computed using BJ08 correlation coefficients and those from the entire database of this study. It can be seen that, for all the three locations, magnitude-based coefficients do not have a considerable effect on the CMS when anchored at longer periods, i.e., T = 1 s and T = 2 s. However, when the CMS is anchored at shorter periods, i.e., T = 0.2 s and T = 0.5 s, higher spectral

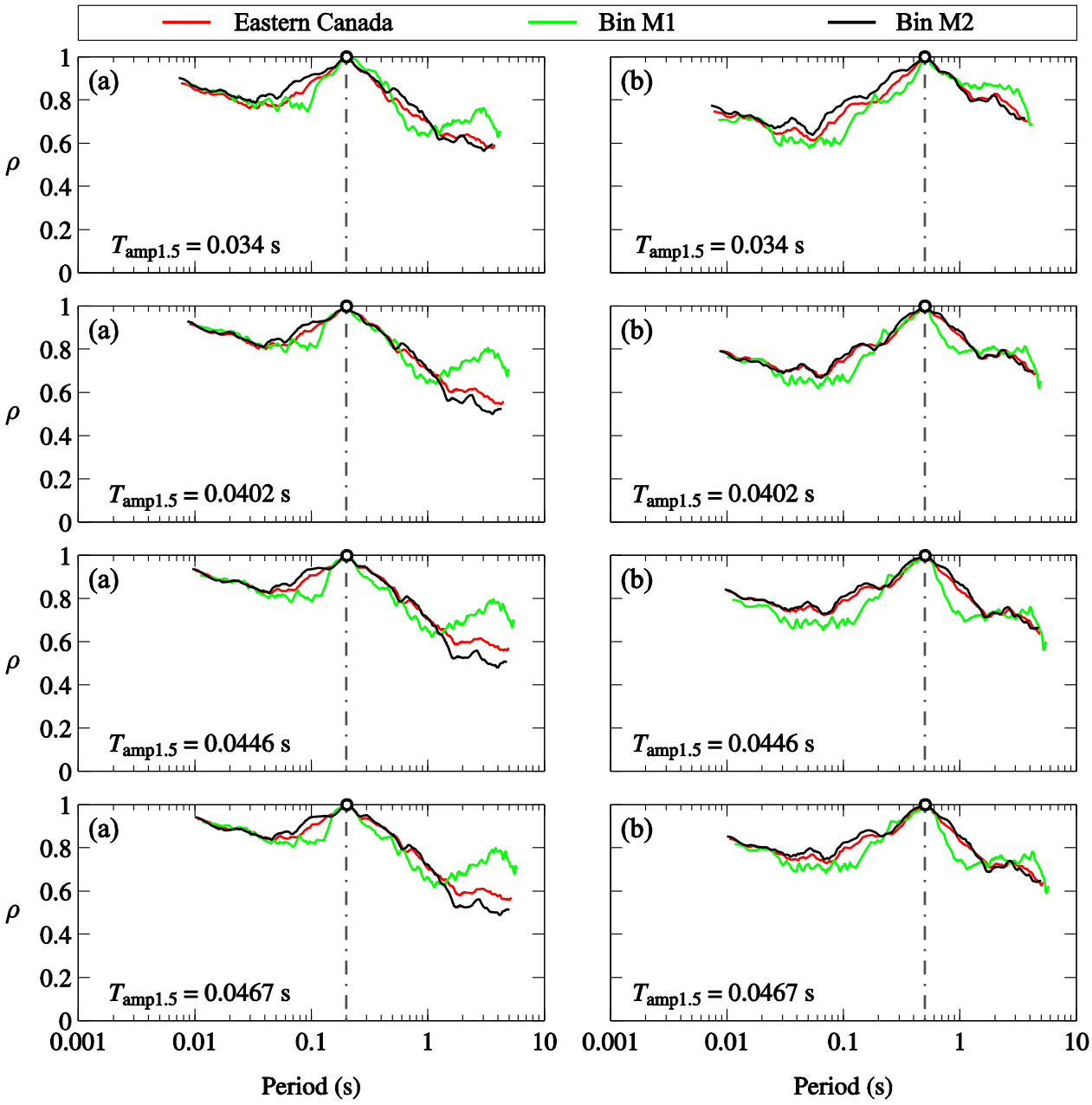

Figure 4-12: Comparison between obtained correlation coefficients for Eastern Canada from magnitude-based bins and those from the entire records database at different $T_{amp1.5}$ values for (a) T^* = 0.2 s and (b) T^* = 0.5 s.

amplitudes are obtained using the magnitude-dependent coefficients.

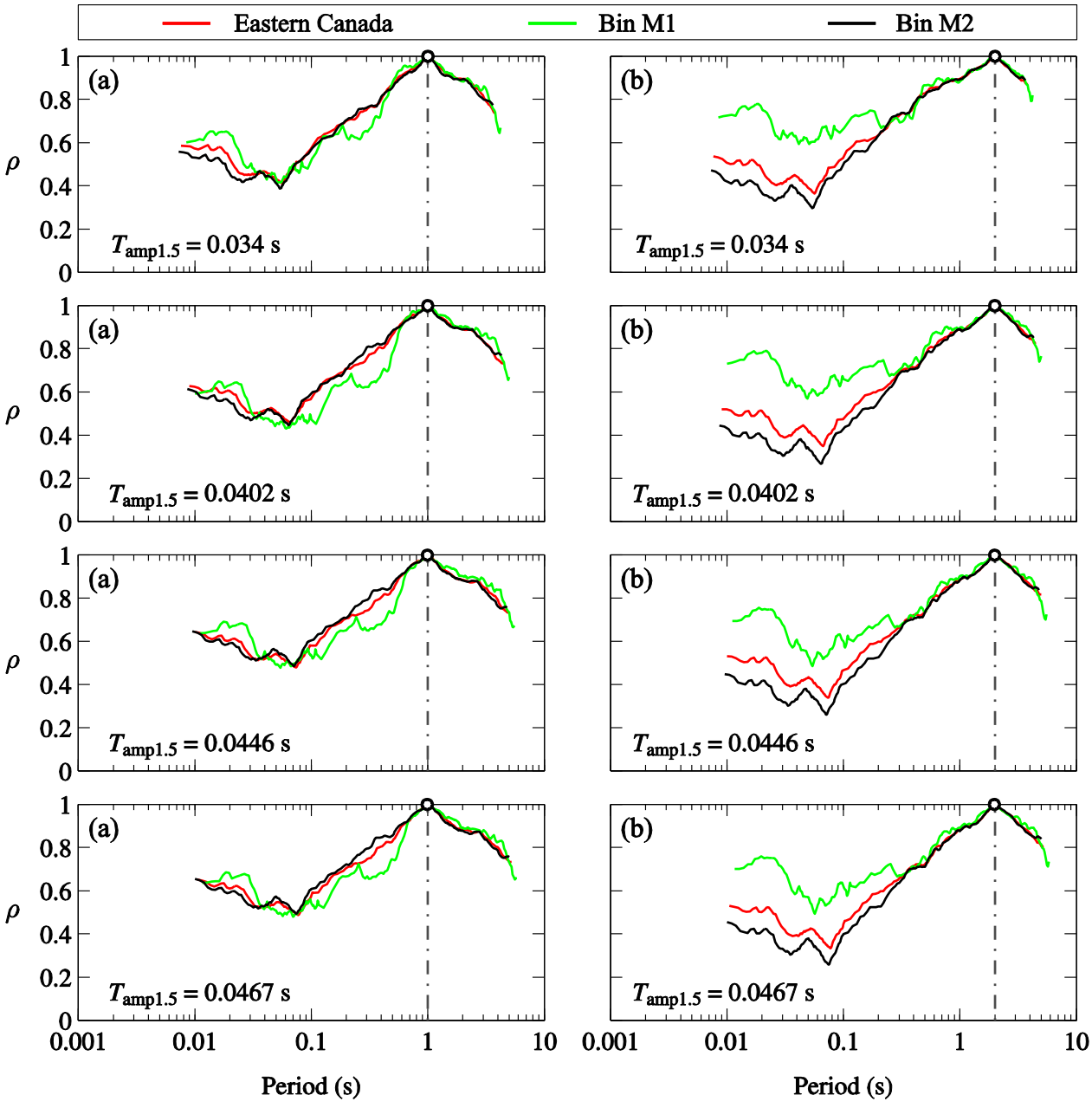

Figure 4-13: Comparison between obtained correlation coefficients for Eastern Canada from magnitude-based bins and those from the entire records database at different $T_{amp1.5}$ values for (a) T^* = 1 s and (b) T^* = 2 s.

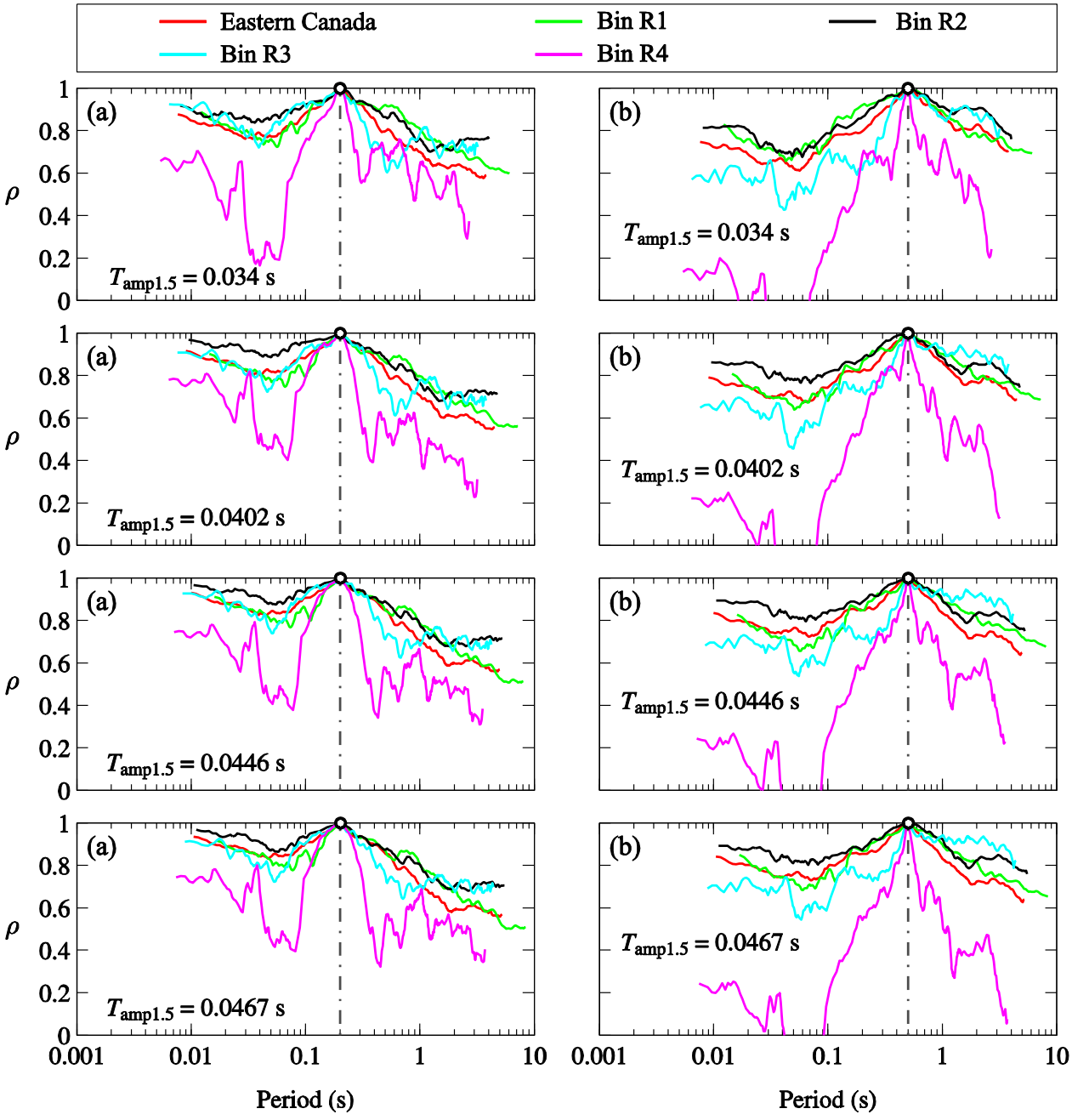

Figure 4-14: Comparison between obtained correlation coefficients for Eastern Canada from distance-based bins and those from the entire records database at different $T_{amp1.5}$ values for (a) T^* = 0.2 s and (b) T^* = 0.5 s.

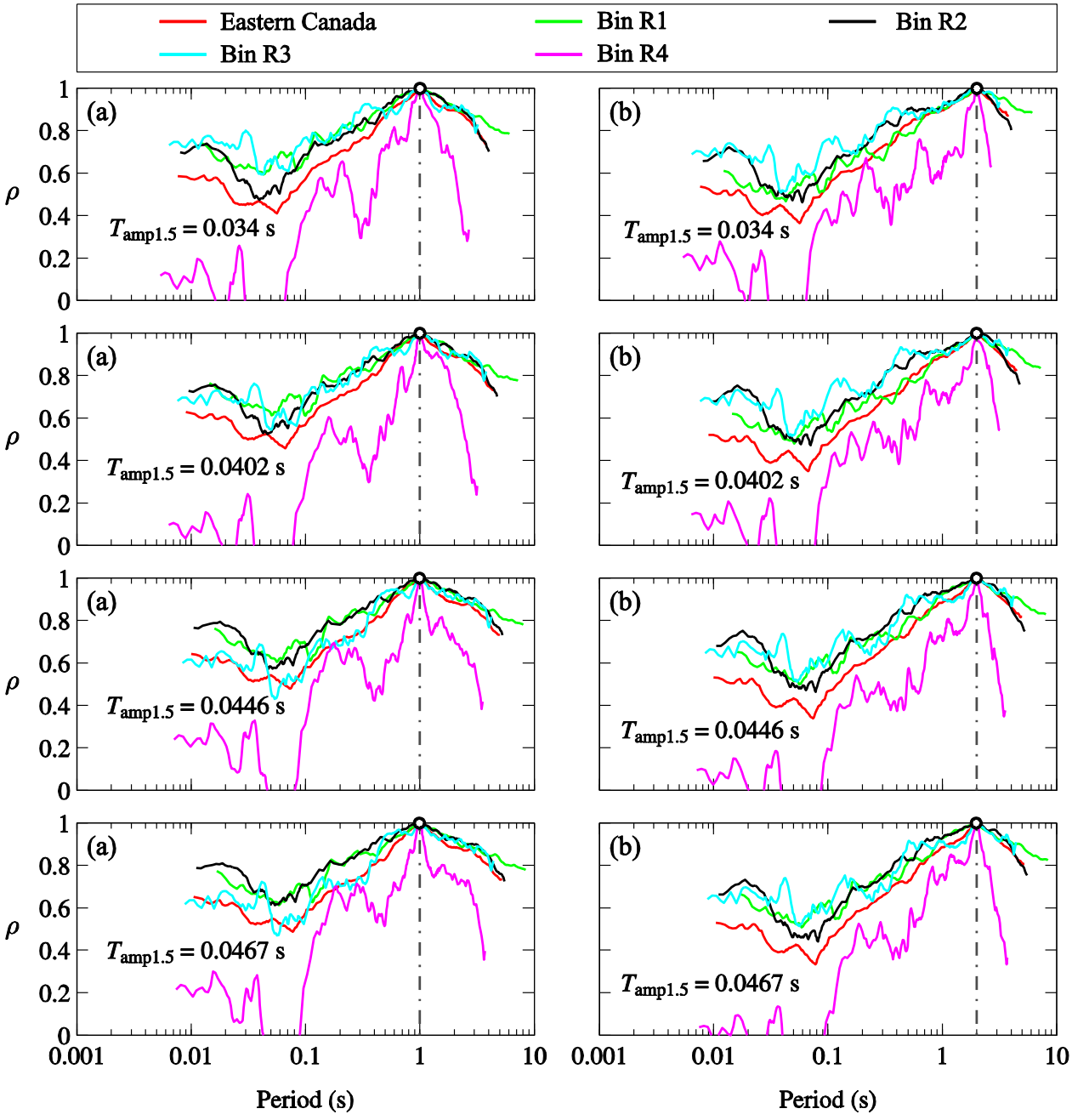

Figure 4-15: Comparison between obtained correlation coefficients for Eastern Canada from distance-based bins and those from the entire records database at different $T_{amp1.5}$ values for (a) T^* = 1 s and (b) T^* = 2 s.

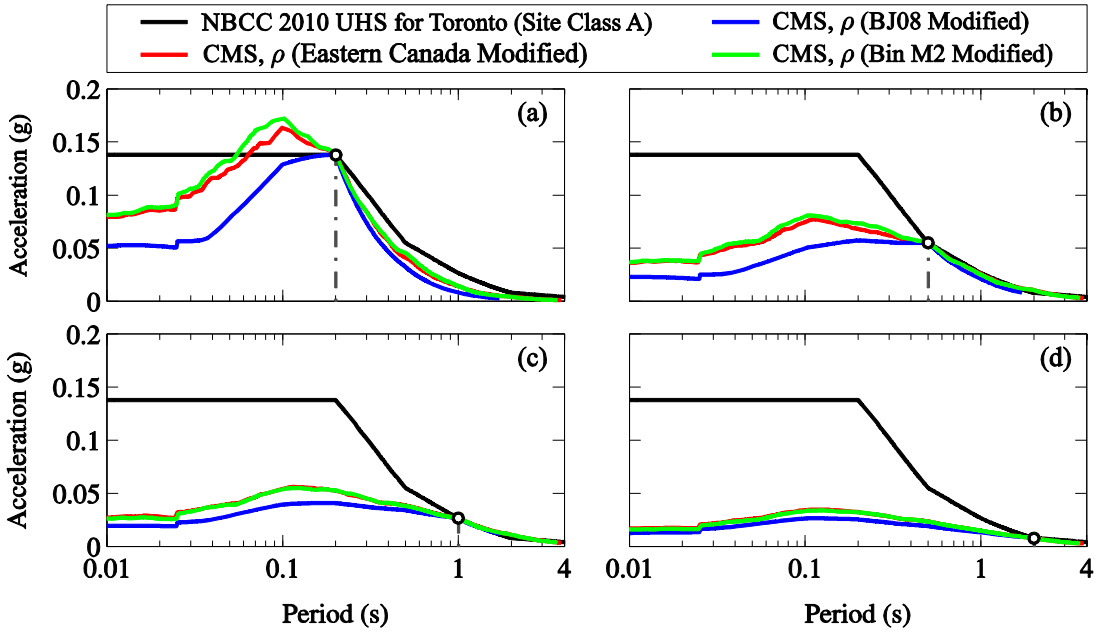

Figure 4-16: CMS computed using the magnitude-based ρ s for Eastern Canada and by matching to NBCC 2010 prescribed UHS for Toronto at (a) T^* = 0.2 s, (b) T^* = 0.5 s, (c) T^* = 1 s, and (d) T^* = 2 s.

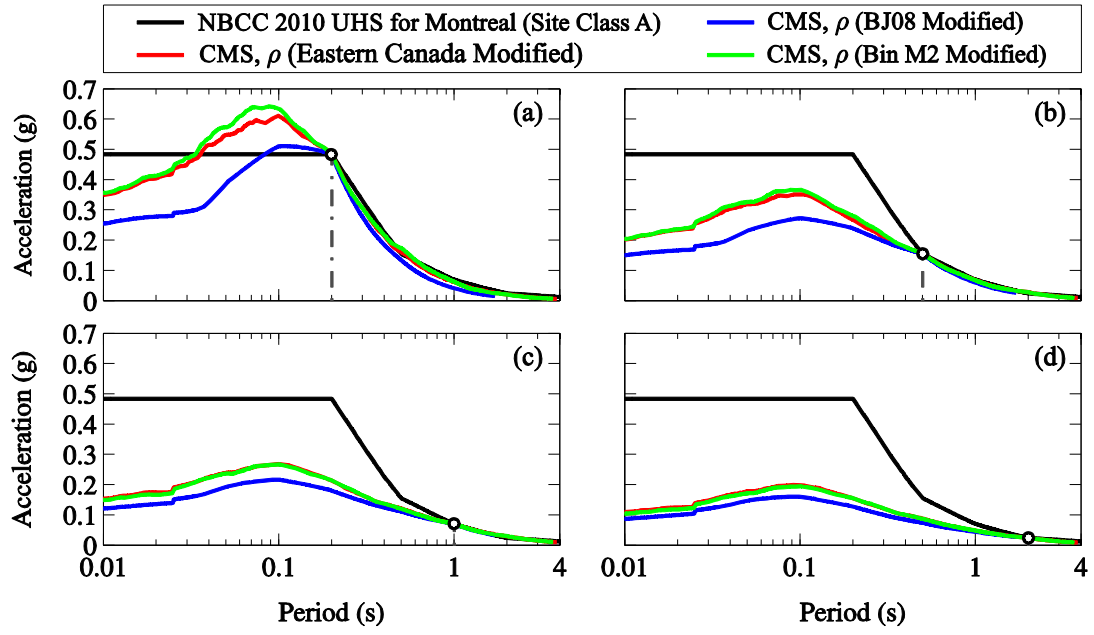

Figure 4-17: CMS computed using the magnitude-based ρ s for Eastern Canada and by matching to NBCC 2010 prescribed UHS for Montreal at (a) T^* = 0.2 s, (b) T^* = 0.5 s, (c) T^* = 1 s, and (d) T^* = 2 s.

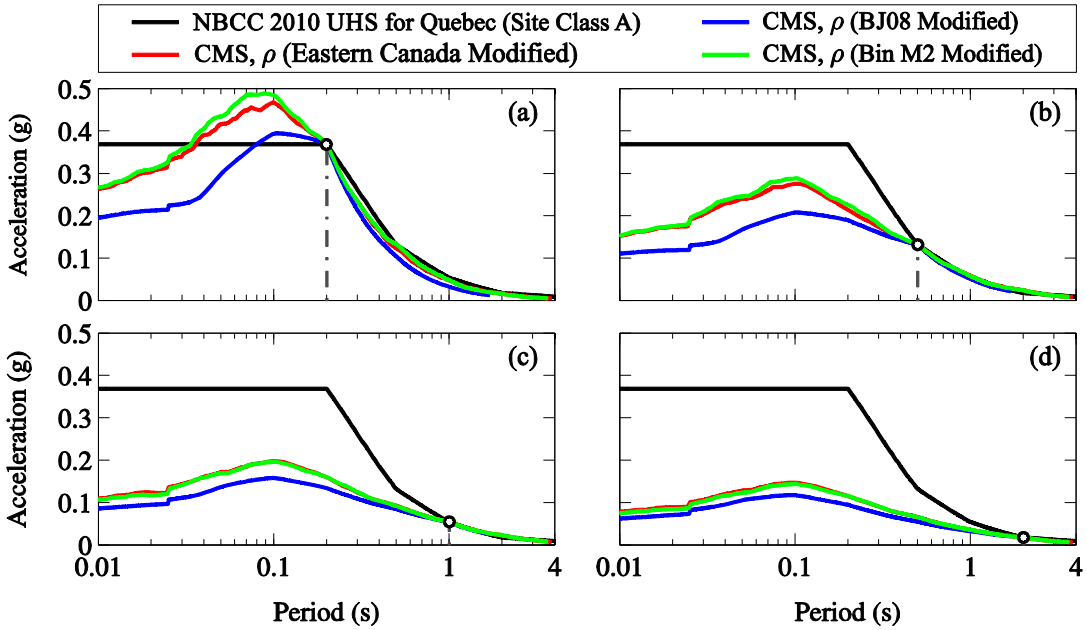

Figure 4-18: CMS computed using the magnitude-based ρ s for Eastern Canada and by matching to NBCC 2010 prescribed UHS for Quebec at (a) T^* = 0.2 s, (b) T^* = 0.5 s, (c) T^* = 1 s, and (d) T^* = 2 s.

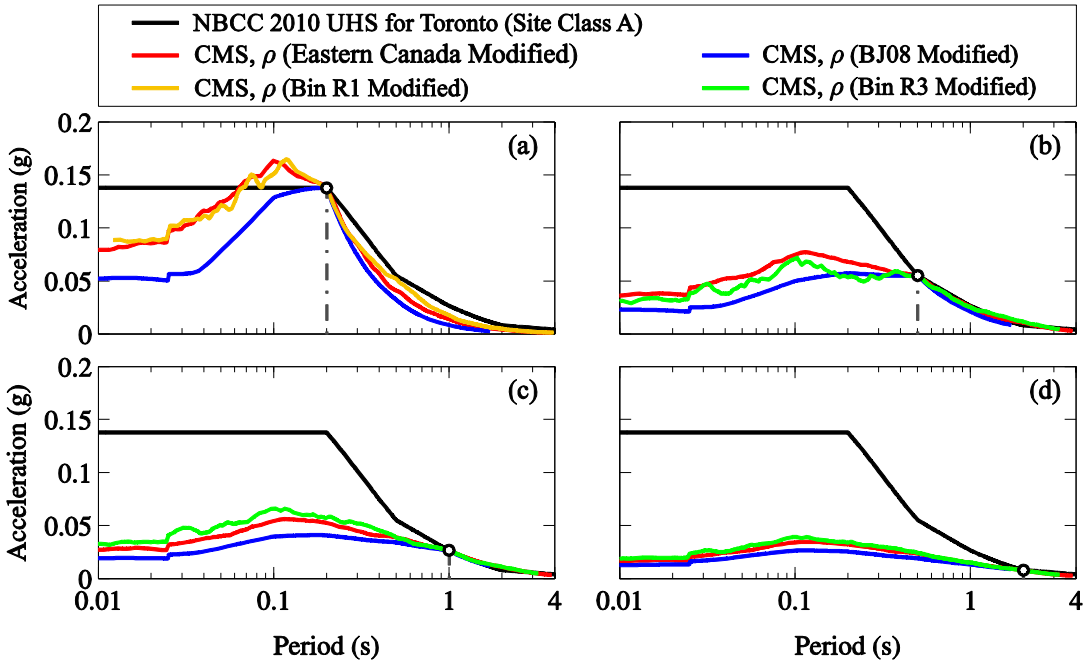

Figure 4-19: CMS computed using the distance-based ρ s for Eastern Canada and by matching to NBCC 2010 prescribed UHS for Toronto at (a) T^* = 0.2 s, (b) T^* = 0.5 s, (c) T^* = 1 s, and (d) T^* = 2 s.

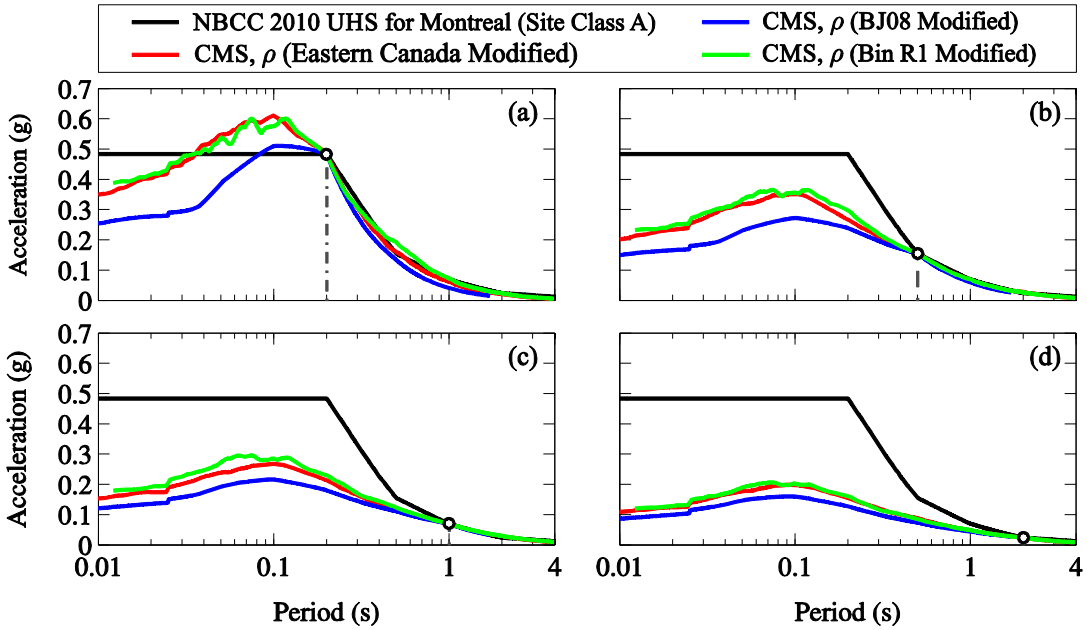

Figure 4-20: CMS computed using the distance-based ρ s for Eastern Canada and by matching to NBCC 2010 prescribed UHS for Montreal at (a) T^* = 0.2 s, (b) T^* = 0.5 s, (c) T^* = 1 s, and (d) T^* = 2 s.

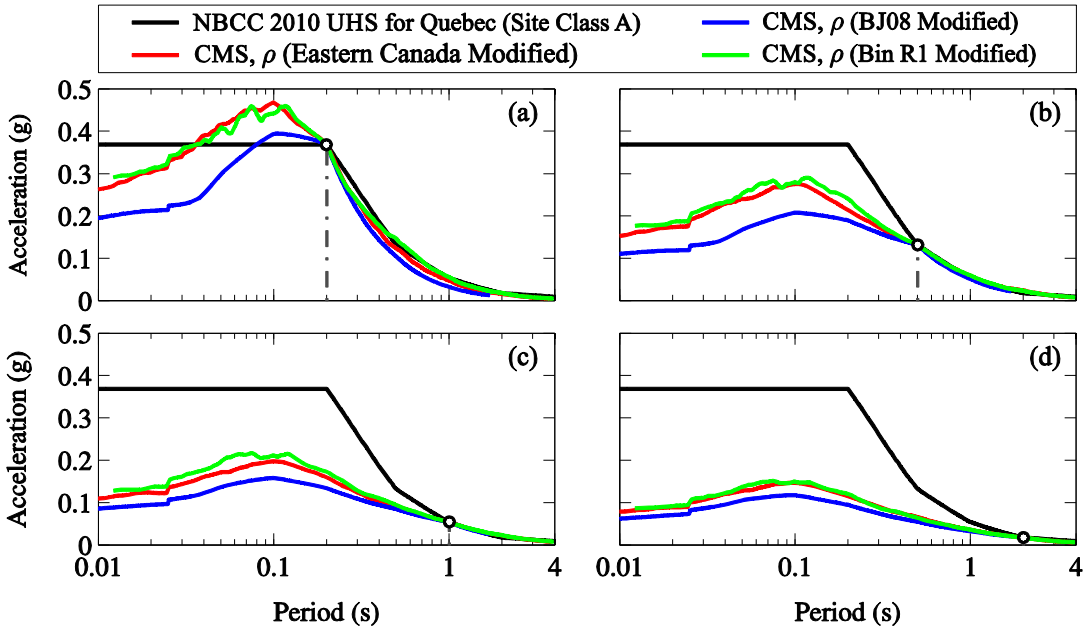

Figure 4-21: CMS computed using the distance-based ρ s for Eastern Canada and by matching to NBCC 2010 prescribed UHS for Quebec at (a) T^* = 0.2 s, (b) T^* = 0.5 s, (c) T^* = 1 s, and (d) T^* = 2 s.

As expected from the correlation coefficients illustrated in Figure 4-10 and Figure 4-11, adopting BJ08 model yields to lower CMS in comparison to those using correlation coefficients obtained from the studied database of Eastern Canada records. Similar observations are made for the CMS constructed using distance-based coefficients. However, in this case, the effect of distance is more pronounced when the CMS is anchored at longer periods. Generally, in comparison to the CMS computed using BJ08 model, it is seen that the obtained correlation coefficients result in higher spectral amplitudes at shorter period ranges.

We also observe that, due to the modification made for the high frequency content of the records (Carlton and Abrahamson 2014), the period ranges through which the correlation coefficients are determined are modified based on the $T_{\mathrm{amp1.5}}$ associated with each data base of records. Hence, as can be seen in Figure 4-16 to Figure 4-21, the CMS obtained using BJ08 model and considering the $T_{\mathrm{amp1.5}}$ for the controlling event, from deaggregation results, extends only up to T = 1.7 s. This is clearly seen in Figure 4-10 and Figure 4-11 when the coefficients are calculated for different values of $T_{\mathrm{amp1.5}}$. This observation reiterates the necessity of further research to determine correlation models specific to Eastern Canada and underlines the possible underestimation when using BJ08 model to compute CMS in this region.

4.5 Conclusions

This work assessed the main ingredients required to construct CMS in Eastern Canada and investigated the effect of their variations on the obtained CMS. The construction of CMS was reviewed and adapted to take account of the seismic hazard in three different Eastern Canadian cities: Toronto, Montreal, and Quebec. The effect of variation in $\varepsilon(T^*)$ on the computed CMS as a function of the underlying GMPE was investigated. It was shown that the selected GMPE can considerably affect the spectral amplitudes of the CMS mainly at shorter periods. This might have an impact on the seismic analysis or evaluation of structures with relatively short fundamental periods and also those for which higher mode effects are significant. The CMS computed using two approximate methods, i.e., “Methods 1 and 2” were found to be moderately different only at short period ranges. This is mainly due to the weights associated with the GMPEs for Eastern Canada. While “Method 1” could be used to compute CMS in Eastern Canada due to its simplicity, refined computations including logic tree weights are recommended for short-period structures or those significantly influenced by higher mode effects. We also investigated the applicability to

Eastern Canada of spectral correlation models developed based on WNA ground motions. To this end, a database of ground motions recorded in Eastern Canada was compiled and correlation coefficients were determined using an up-to-date GMPE developed for ENA. The effects of higher frequency content of ground motions on correlation coefficients were also considered. The results suggest higher spectral correlations than predicted by a WNA-based model. We note, however, that this trend is based on currently available ground motions recorded in Eastern Canada and that it needs to be validated in light of future observations. Finally, we studied the dependency of correlation coefficients in Eastern Canada on magnitude and epicentral distance, two of the key characteristics of ground motions and their predictions. Records of lower magnitude demonstrated higher correlations at short periods for longer conditioning periods T^*. We found that the dependency of obtained correlation coefficients $\rho(T_1, T_2)$ on magnitude is generally pronounced as one of the two periods T_1 or T_2 is shifted towards the longer period range. Distance-dependency was found to be less significant for distances of interest in structural engineering applications. We also showed that the effects of magnitude- or distance-based correlation coefficients on the CMS developed for the three cities are (1) generally negligible at long periods and (2) significant at shorter periods particularly when the conditioning period T^* is less than approximately 0.5 s. This work is the first study addressing in detail the ingredients and construction of CMS in Eastern Canada. The methodology and results discussed are expected to enhance the application of CMS in this region.

Acknowledgements

The authors would like to acknowledge the financial support of the Natural Sciences and Engineering Research Council of Canada (NSERC), the Canadian Seismic Research Network (CSRN), and the Quebec Fund for Research on Nature and Technology (FRQNT).

References

Abrahamson NA, Silva WJ (2008) Summary of the Abrahamson & Silva NGA ground motion relations. Earthquake Spectra 24:67–97

Atkinson GM (2008) Ground-motion prediction equations for Eastern North America from a referenced empirical approach: implications for epistemic uncertainty. Bull Seismol Soc Am 98(3):1304–1318

Atkinson GM, Adams J (2013) Ground motion prediction equations for application to the 2015 Canadian national seismic hazard maps. Can J Civ Eng 40:988–998

Atkinson GM, Boore DM (2006) Earthquake ground-motion prediction equations for Eastern North America. Bull Seismol Soc Am 96(6):2181–2205

Atkinson GM, Boore DM (2011) Modifications to existing ground-motion prediction equations in light of new data. Bull Seismol Soc Am 101(3):1121–1135

Baker JW (2011) Conditional mean spectrum: Tool for ground motion selection. J Struct Eng 137(3):322–331

Baker JW, Cornell CA (2005) Vector-valued ground motion intensity measure for probabilistic seismic demand analysis. John A. Blume Earthqukae Engineering Center, Report No. 150, Stanford, California

Baker JW, Cornell CA (2006) Correlation of response spectral values for multi-component ground motions. Bull Seismol Soc Am 96(1):215–227

Baker JW, Jayaram N (2008) Correlation of spectral acceleration values from NGA ground motion models. Earthquake Spectra 24(1):299–317

Boore DM (1983) Stochastic simulation of high-frequency ground motions based on seismological models of the radiated spectra 73:1865–1894

Boore DM, Atkinson GM (2008) Ground-motion prediction equations for the average horizontal component of PGA, PGV, and 5 %-damped PSA at spectral periods between 0.01 s and 10.0 s. Earthquake Spectra 24(1):99–138

Burks LS, Baker JW (2012) Occurrence of negative epsilon in seismic hazard analysis deaggregation, and its impact on target spectra computation. Earthq Eng Struct Dyn 41(8):1241–1256

Campbell KW (2003) Prediction of strong motion using the hybrid empirical method and its use in the development of ground-motion (attenuation) relations in Eastern North America. Bull Seismol Soc Am 93(3): 1012–1033

Campbell KW, Bozorgnia Y (2008) NGA ground motion model for the geometric mean horizontal component of PGA, PGV, PGD and 5 % damped linear elastic response spectra for periods ranging from 0.01 to 10 s. Earthquake Spectra 24:139–171

Carlton B, Abrahamson N (2014) Issues and approaches for implementing conditional mean spectra in practice. Bull Seismol Soc Am 104(1):503–512

Chiou BSJ, Youngs RR (2008) An NGA model for the average horizontal component of peak ground motion and response spectra. Earthquake Spectra 24(3):173–215

Daneshvar P, Bouaanani N, Leger P (2014) Application of conditional mean spectra for evaluation of a building's seismic response in Eastern Canada. Can J Civil Eng 41(8):769–773

Geological Survey of Canada (GSC) (2006) http://www.earthquakescanada.nrcan.gc.ca. Accessed 27 Sept 2006

Hanks T, McGuire RK (1981) The character of high-frequency strong ground motion. Bull Seismol Soc Am 71:2071–2095

Harmsen SC (2001) Mean and modal epsilon in the deaggregation of probabilistic ground motion. Bull Seismol Soc Am 91(6):1537–1552

Idriss IM (2008) An NGA empirical model for estimating the horizontal spectral values generated by shallow crustal earthquakes. Earthquake Spectra 24:217–242

Inoue T, Cornell CA (1990) Seismic hazard analysis of multidegree-of-freedom structures. Reliability of marine structures, RMS-8, Stanford, CA, 70 p

Jayaram N, Baker JW, Okano H, Ishida H, McCann MW, Mihara Y (2011) Correlation of response spectral values in Japanese ground motions. Earthquakes and Structures 2(4):357–376

Lin L, Adams J (2010) Strong motion records of the Valdes-Bois, Qubec, Earthquake of June 23, 2010. Canadian Hazard Information Service Internal Report 2010-1.1, Geological Survey of Canada

Lin T, Harmsen SC, Baker JW, Luco N (2013) Conditional spectrum computation incorporating multiple causal earthquakes and ground motion prediction models. Bull Seismol Soc Am 103(2A):1103–1116

McGuire RK (1995) Probabilistic seismic hazard analysis and design earthquakes: closing the loop. Bull Seismol Soc Am 85(5):1275–1284

Munro PS, Weichert D (1989) The Saguenay earthquake of November 25, 1988, processed strong motion records. Geological Survey of Canada, Open File 1996

NBCC (2010) National Building Code of Canada, Associate Committee on the National Building Code, National Research Council of Canada, Ottawa, Ont

Pezeshk S, Zandieh A, Tavakoli B (2011) Hybrid empirical ground-motion prediction equations for Eastern North America using NGA models and updated seismological parameters. Bull Seismol Soc Am 101(4): 1859–1870

Silva W, Gregor N, Darragh R (2002) Development of regional hard rock attenuation relations for Central and Eastern North America. Technical Report, Pacific Engineering and Analysis, El Cerrito, California

Weichert DH, Wetmiller RJ, Horner RB, Munro PS, Mork PN (1986) StrongMotion Records from the 23 December 1985, Ms 6.9 Nahanni, NWT, and some Associated Earthquakes. Geological Survey of Canada, Pacific Geoscience Centre, Open File Report 1330

CHAPTER 5 ARTICLE 3: PREDICTION OF HIGH-DAMPING SEISMIC DEMANDS IN EASTERN NORTH AMERICA

Poulad Daneshvar and Najib Bouaanani

Paper published in *Journal of Earthquake Engineering*,

DOI:10.1080/13632469.2014.990654

Submitted 3 March 2014. Accepted 17 November 2014.

This paper investigates high-damping seismic demands and associated damping reduction factors in Eastern North America (ENA). A database of hybrid empirical records with moment magnitudes $M \geq 6.0$ is first studied to evaluate 5%- to 30%-damped seismic demands. A new magnitude- and distance-based equation is proposed to predict ENA spectral displacements and then used to characterize their sensitivity to variations in period, magnitude, epicentral distance and site conditions. The proposed equation is also used to assess damping reduction factors in ENA. The results contribute to improved assessment of seismic demands in ENA while accounting for added-damping in structural seismic design.

Nomenclature

Abbreviations

CEUS	Central and Eastern United States
CSA	Canadian Standard Association
DBD	Displacement-based design
ENA	Eastern North America
GMPE	Ground motion prediction equation
GSC	Geological Survey of Canada

NBCC	National Building Code of Canada
NEHRP	National Earthquake Hazard Reduction Program
PEER	Pacific Earthquake Engineering Research Center
PSA	Pseudo spectral acceleration
USGS	United States Geological Survey
WNA	Western North America
WUS	Western United States

Symbols

a_{i}	Regression coefficient
M	Moment magnitude
R	Epicentral distance
S_{a}	Spectral acceleration
$S_{\mathrm{a}}(T,\xi)$	Spectral acceleration at a period T and an equivalent damping ratio of ξ
S_{d}	Spectral displacement
$S_{\mathrm{d}}(T,\xi)$	Spectral displacement at a period T and an equivalent damping ratio of ξ
T	Period of vibration
ξ	Equivalent damping ratio
η	Damping reduction factor
V_{S30}	Time-averaged shear-wave velocity in the top 30m

5.1 Introduction

Damage and loss caused by Loma Prieta (1989) and Northridge (1994) earthquakes promoted the application of energy dissipation systems to various structures (Ramirez et al. 2002) either as a retrofit strategy or as a measure to prevent or diminish damage to structural members. Utilization of simplified seismic design or evaluation methodologies incorporating added-damping effects of such systems requires the determination of spectral amplitudes associated with damping levels higher than the common 5% of critical. For example, high-damping displacement spectra are needed to determine the displacements across seismic isolation devices in bridge structures according to the simplified design methods prescribed in the Canadian Highway Bridge Design Code (CAN/CSA S6). High-damping seismic demands and damping modification factors corresponding to ground motions in various regions have been investigated by several researchers such as Newmark and Hall (1973, 1982), Tolis and Faccioli (1999), Borzi et al. (2001), Atkinson and Pierre (2004), Faccioli et al. (2004), Karakostas et al. (2007), and Faccioli and Villani (2009). Studies of seismic demands in Europe also resulted in ground motion prediction equations (GMPE) for displacements (Bommer and Elnashai 1999, Akkar and Bommer 2007, Cauzzi and Faccioli 2008).

Most of the research characterizing seismic hazard in Eastern North America (ENA), a zone with moderate to low seismic activity, has focused on the prediction of earthquake-induced pseudo-accelerations for a 5% critical damping level (Atkinson and Boore 1995, Somerville et al. 2001, Silva et al. 2002, Campbell 2003, Atkinson and Boore 2006, Campbell 2007, Atkinson 2008, Pezeshk et al. 2011). Some of these results have led to seismic hazard maps, site-specific uniform hazard pseudo-acceleration spectra and corresponding disaggregation data (NRCC 2005, NRCC 2010, ASCE7-10, USGS, Atkinson and Beresnev 1998, Hwang et al. 2001, Adams and Atkinson 2003, Adams and Halchuk 2004, Atkinson 2009, Shahjouei and Pezeshk 2013). Despite the increasing application of energy dissipating and seismic isolation devices to different types of structures, and the emergence of seismic design and evaluation methods which require spectral amplitudes at damping levels above 5% critical, little attention has been devoted to predicting seismic demands corresponding to high-damping levels in ENA. Furthermore, damping reduction factors corresponding to seismic hazard in this region have been rarely addressed. The main objective of this paper is to contribute to filling this gap by characterizing high-damping spectral

displacements induced by ENA-type ground motions and developing magnitude- and distance-based equations to predict these seismic demands.

5.2 Records used

ENA records of significant magnitude are sparse and most of the available ground motions are of low magnitude or were recorded at relatively long distances. A large number of ENA records have been complied as part of the NGA-East project (Goulet et al. 2013). However, most of these records are from events of moment magnitudes M lower than 5.5 and far field epicentral distances *R* higher than 50 km (Goulet et al. 2013), which implies fairly low seismic amplitudes. One of the objectives of the present work is to characterize high-damping seismic demands and corresponding damping reduction factors for events with moment magnitudes larger than M = 6.0, which are of more interest to structural engineering applications. For this purpose, we investigate seismic demands corresponding to a set of hybrid empirical ground motions originally proposed by McGuire et al. (2001) to conduct seismic analyses in Central and Eastern United States (CEUS) or ENA.

The original data set covers a wide range of magnitudes and distances to compensate for the limited number of recorded ground motions in these regions. McGuire et al. (2001) generated this data set by applying a scaling process to ground motions recorded in seismically active regions including California, Montana, Italy, Uzbekistan, Mexico, Georgia, Taiwan, Turkey, Japan and Iran. The data set also includes records from Saguenay (1988) and Nahanni (1985) events which are typical of ENA seismic hazard. A single corner frequency point source model was adopted by McGuire et al. (2001) to determine transfer functions relating ground motions from seismically active regions to ENA ground motions of the same magnitude, distance and site condition. The resulting hybrid empirical records maintain realistic inter-component phase, amplitude relationships and frequency to frequency variability (McGuire et al. 2001). A total of 552 horizontal hybrid records provided for rock and soil sites are selected from this database for the purpose of the present work. The distinction between the site conditions is made through $V_{s30,}$ the average shear-wave velocity in the uppermost 30 m, based on the NEHRP site classification. Records having a $V_{s30} \geq 360$ m/s are categorized as rock sites, i.e. NEHRP site classes A, B, and C, and those with a $V_{s30} < 360$ m/s are categorized as deep soil sites, i.e. NEHRP site classes D and E. The selected records cover a moment magnitude range of M = 6.0 to M = 7.6 and epicentral distances *R* from 1 to 250 km. Figure 5-1 shows the M-*R* distributions of the selected records.

As widely known, computation of reliable displacement time-histories and spectra from recorded ground motions is usually associated with difficulties related to their processing such as base-line correction, filtering issues (more pronounced effects on displacement spectra), long-period drift, and analog-to-digital conversion for data recorded decades ago using analog instruments (Bommer and Elnashai 1999, Boore 2005, Paolucci et al. 2008, Akkar and Boore 2009). Although detailed information about the processing of the above-described hybrid records was not provided by McGuire et al. (2001), it is assumed, according to an example given in the same reference, that casual four-pole Butterworth high-pass and low-pass filters were applied except for near source short duration records where acasual Butterworth filters were used. As high-pass filters can significantly affect the spectral displacements resulting from the processed records at long period ranges, the displacement spectrum corresponding to each record is not considered beyond the period at which the record is filtered. Figure 5-2 illustrates the range of applied high-pass filters for the selected records. Results are shown next for a period range up to 2.0 s to reinforce confidence in the predicted spectral amplitudes.

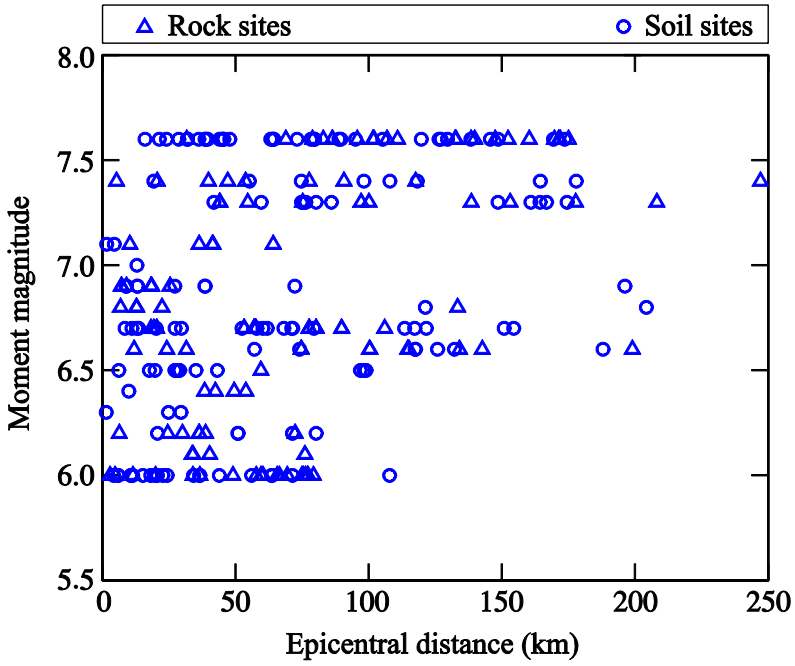

Figure 5-1: Magnitude and distance distributions of the records used in this study for rock and soil sites

5.3 Target spectral pseudo-accelerations and spectral matching

The hybrid empirical records were originally developed to conduct seismic analyses after being scaled or matched to target spectral pseudo-accelerations of interest (McGuire et al. 2001). The aim of this work is to characterize seismic demands that are consistent with seismic hazard in ENA. Accordingly, we generate target spectral pseudo-accelerations using the new model underlying seismic hazard maps and uniform hazard spectra of the 2015 editions of the National Building Code of Canada (NBCC) and the Canadian Highway Bridge Design Code (CAN/CSA-S6). This model, developed by Atkinson and Adams (2013) and referred to as AA13 hereafter, consists of a central GMPE and upper and lower GMPEs to account for epistemic uncertainty about the central one. The central GMPE is determined by calculating the geometric mean of five peer reviewed mean GMPEs available in the literature. The geometric mean plus/minus (±) its standard deviation is considered as the upper/lower GMPE. The five GMPEs are SGD02SC (Silva, Gregor and Darragh 2002, the single corner model with variable stress), SGD02DC (Silva, Gregor and Darragh 2002, the double corner model with magnitude saturation), AB06 (Atkinson and Boore 2006, 2011), A08 (Atkinson 2008) and PZT11 (Pezeshk, Zandieh and Tavakoli 2011). The final predictions are provided in terms of moment magnitudes and epicentral distances for B/C site condition. The reader is referred to Atkinson and Adams (2013) for more details about the determination of the central, upper and lower GMPEs, distance metric conversions, and also conversion factors used to modify the predictions corresponding to different site conditions to represent those of B/C site condition. The spectral pseudo-accelerations provided by the central GMPE of the AA13 model for different moment magnitudes and epicentral distances are selected as target spectra for the purpose of the present study. To maintain compatibility between site conditions, conversion factors proposed by Atkinson and Adams (2013) and Atkinson and Boore (2011) are adopted to account for ground motions on rock, i.e. site class A (rock sites), and deep soil sites, i.e. site class D (soil sites). To be consistent with distance metrics used in the table of predictions provided by Atkinson and Adams (2013), the epicentral distances corresponding to the hybrid empirical record are taken from PEER Ground Motion Database (http://peer.berkeley.edu/nga). The computer program RSPMatch2005 (Abrahamson 1992, Hancock et al. 2006) is used to match the 5%-damped pseudo-acceleration response spectrum of each hybrid empirical record with a given moment magnitude M ($6.0 \leq M \leq 7.6$) and epicentral

distance R ($1 \leq R \leq 250$ km) to the AA13 target spectral pseudo-accelerations corresponding to the same M and R.

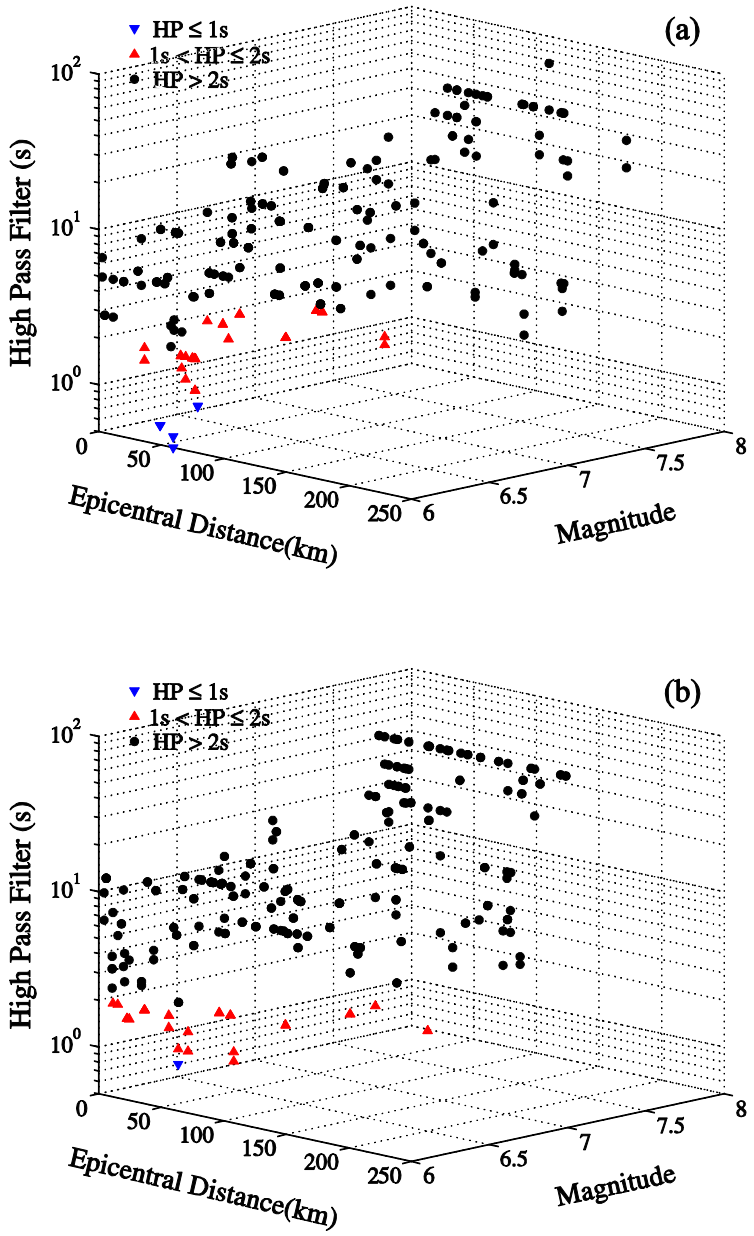

Figure 5-2: Distribution of the records used in this study based on the applied high pass filter (HP): (a) rock sites; (b) soil sites.

Spectral matching is carried out over a period range up to 2.0 s using two passes considering a tolerance of 5%. This matching process resulted in a total of 523 acceptably matched hybrid

records corresponding to rock and soil sites. The final selection consists of 244 records on rock sites, and 279 on soil sites.

5.4 5%-damped seismic demands

The 5%-damped displacement spectra of the matched hybrid records described above are computed for periods up to T = 2.0 s and epicentral distances up to R = 250 km. The computed spectra are divided into two bins based on the corresponding site condition, i.e. rock or soil sites. Regression analyses using the least square approach are performed on the obtained 5%-damped spectral displacement ordinates of the records from each bin. To investigate the trends in each bin, we first propose a simple functional form which is linear in logarithmic scale with a minimum number of coefficients

$$\log_{10} S_{\mathrm{d}}(T) = a_1 + a_2 \mathrm{M} + a_3 \log_{10} R + a_4 R + a_5 S_{\mathrm{S}} \tag{5.1}$$

where $S_{\mathrm{d}}(T)$ is the spectral displacement (m) at a period T of a random horizontal component of a ground motion of moment magnitude M and epicentral distance R (km) and where a_1, a_2, a_3, a_4, and a_5 are coefficients determined by regression analyses. S_{S} in Eq. (5.1) is a dummy variable that takes a value of 0 when predicting displacements for rock sites and a value of 1 for soil sites. The adopted functional form satisfies the relationship between the logarithm of spectral ordinates and magnitude. It also takes account of inelastic and seismic wave geometric attenuation as a function of the distance from the source (Boore and Joyner 1982).

Comparisons between the predictions of Eq. (5.1) and the records in the database at different periods are illustrated in Figure 5-3(a) and (b). A very good agreement is observed between the predictions of the proposed equation and the spectral displacements from the matched hybrid records. The equation tends to slightly over predict a number of displacement amplitudes at very short distances. However, predictions improve as the distance increases. Figure 5-3(a) and (b) also illustrate the combined effect of magnitude and distance on displacements. The predicted displacements decrease with a steep slope towards longer distances, which illustrates the pronounced attenuating effect of increasing epicentral distance at intermediate and high magnitudes.

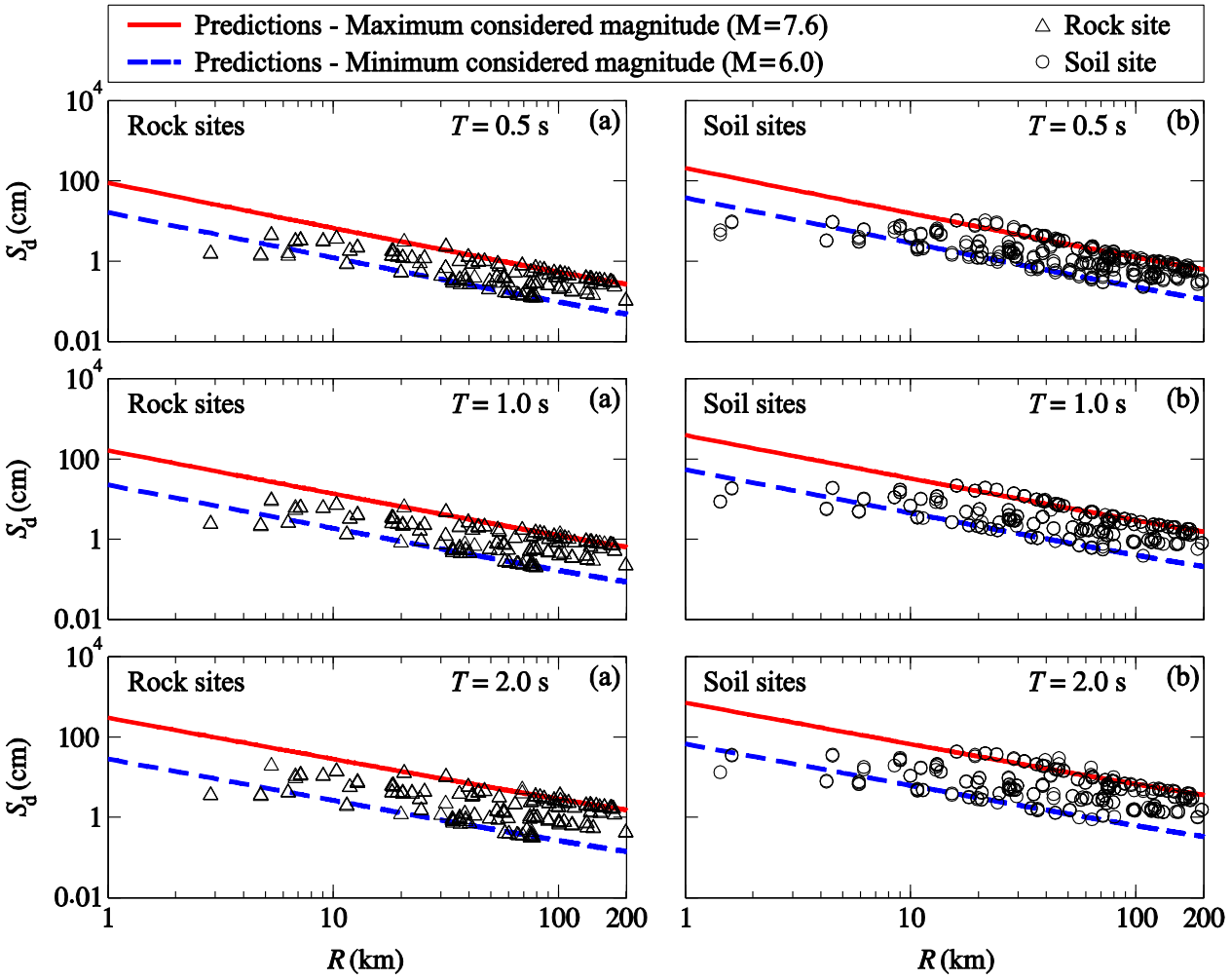

Figure 5-3: Comparison between 5%-damped spectral displacements predicted using Eq. (5.1) developed in this study and those computed from the data set of hybrid empirical records for magnitudes between M = 6.0 and M = 7.6 and periods of 0.5, 1.0, and 2.0 s: (a) rock sites; and (b) soil sites.

It can be observed from Figure 5-3(a) and (b) that the difference between predictions corresponding to minimum and maximum considered magnitudes at a given period increases as the period lengthens. Figure 5-3(a) and (b) also clearly show that regardless of spectral displacement amplitudes, the studied seismic demands follow similar magnitude- and distance-based trends on both rock and soil sites.

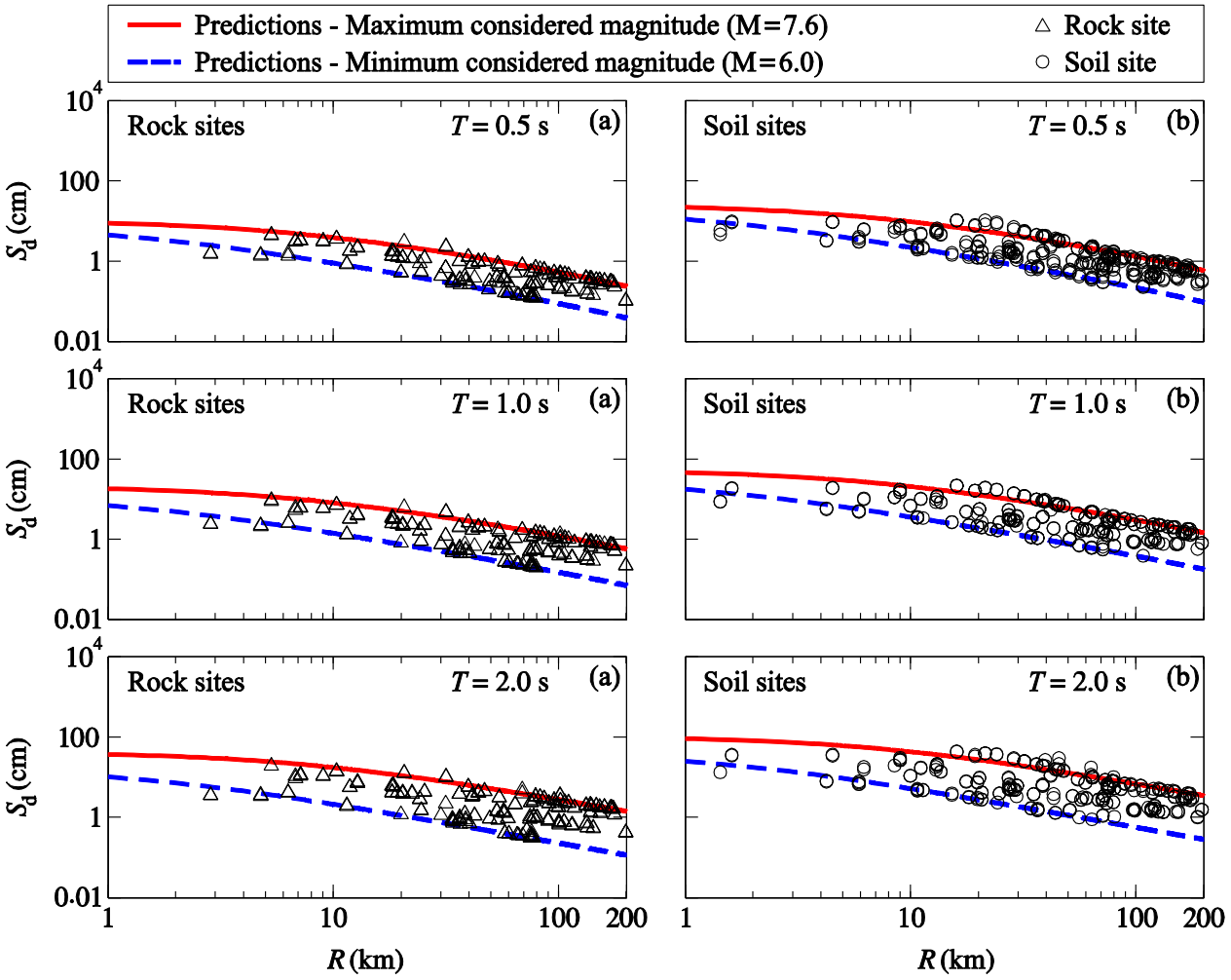

Figure 5-4: Comparison between 5%-damped spectral displacements predicted using Eq. (5.2) developed in this study and those computed from the data set of hybrid empirical records for magnitudes between M = 6.0 and M = 7.6 and periods of 0.5, 1.0, and 2.0 s: (a) rock sites; and (b) soil sites.

The proposed functional form of Eq. (5.1) does not consider saturation effects, i.e. Spectral amplitudes from large earthquakes are relatively independent from magnitude (magnitude saturation) and/or distance (distance saturation) in the near field. These effects are however clearly seen in Figure 5-3(a) and 3(b). Therefore, a second functional form is proposed to consider such effects which generally result in more realistic predictions at shorter distances (Campbell 1981, Silva et al. 2002, Campbell and Bozorgnia 2008, Pezeshk et al. 2011)

$$\log_{10} S_{\mathrm{d}}(T) = a_1 + a_2 \mathrm{M} + a_3 (\mathrm{M}-6)^2 + a_4 \log_{10}\left(R + a_5 \exp(\mathrm{M}-6)\right) + a_6 \left(R + a_5 \exp(\mathrm{M}-6)\right) + a_7 S_{\mathrm{S}} \quad (5.2)$$

The saturation term in Eq. (5.2), i.e. $a_5 \exp(\mathrm{M}-6)$, is adapted from the one originally proposed by Campbell (1981), i.e. $c_1 \exp(c_2 \mathrm{M})$. The added saturation term makes Eq. (5.2) a nonlinear model function and thus coefficients a_1, a_2, a_3, a_4, a_5, a_6 and a_7 are determined through nonlinear regression analyses.

Comparisons between the predictions of Eq. (5.2) and the records in the database at different periods are illustrated in Figure 5-4(a) and (b). Similar to Eq. (5.1), a very good agreement is observed between the predictions of Eq. (5.2) and the spectral displacements from the matched hybrid records. However, the effect of the added saturation term is now clearly seen. Both magnitude and distance saturations are observed in the predictions of Eq. (5.2) which are in agreement with the trends in the computed displacements from the records in the database. The pronounced attenuating effect corresponding to the increase in epicentral distance at intermediate and high magnitudes is also captured by the proposed equation. Observations of the relation between the considered maximum and minimum magnitudes and the studied period are akin to those of Eq. (5.1).

Figure 5-5 and Figure 5-6 compare the 5%-damped predicted spectral pseudo-accelerations S_{a} from Eqs. (5.1) and (5.2), i.e. multiplication of S_{d} by $(4\pi^2)/T^2$ to obtain S_{a} at a given period T, to those obtained from the central and individual GMPEs of the AA13 model. These results clearly show that the 5%-damped spectral pseudo-accelerations and displacements provided by the proposed equations based on the selected hybrid records are in very good agreement with the predictions of the AA13 model for the considered rock and soil sites. However, Eq. (5.2) tends to under predict spectral pseudo-accelerations corresponding to magnitudes higher than M = 7.0 and distances up to approximately R = 30 km. This roots from the lack of records at these magnitude and distance ranges combined with the magnitude and distance saturation term introduced in the equation. Eq. (5.1) provides a better prediction at the same M-R combinations due to the linear continuous increase in the predictions towards shorter distances as a result of the absence of a magnitude and distance saturation term. This term is however to be included considering generally

observed trends from other records (Campbell 1981, Silva et al. 2002, Campbell and Bozorgnia 2008, Pezeshk et al. 2011).

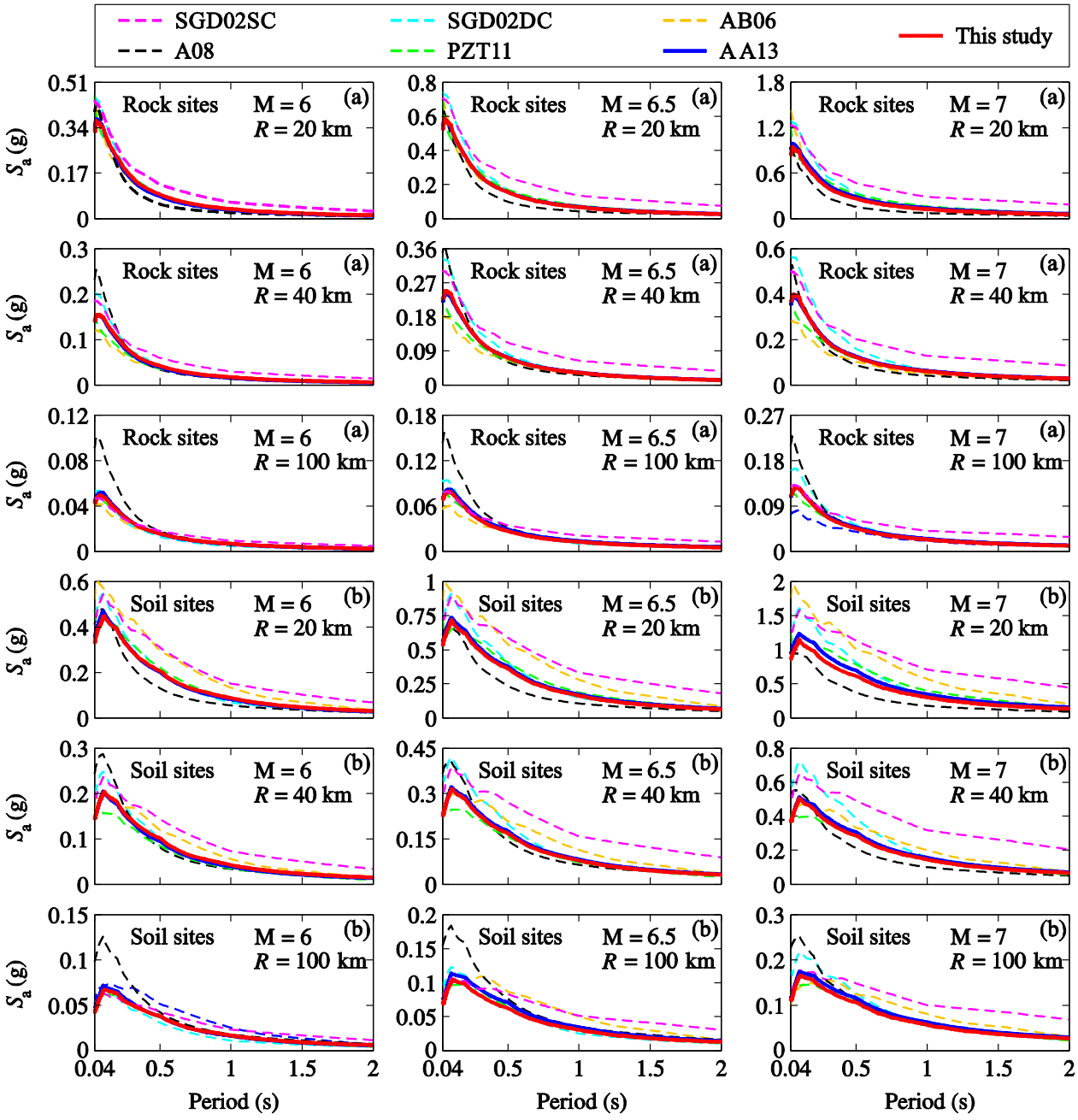

Figure 5-5: Comparison between 5%-damped spectral pseudo-acceleration predictions of the central GMPE proposed by Atkinson and Adams (2013) and those from Eq. (5.1) developed in this study: (a) rock sites; and (b) soil sites.

For this reason, only Eq. (5.2) will be used next to determine higher damping seismic demands and associated damping reduction factors. The coefficients and mean logarithmic residuals corresponding to Eq. (5.2) are provided in Table 5.1. We note that the spectral displacements predicted by Eq. (5.2) are the mean expected displacement amplitudes for the region as the underlying spectra have been spectrally matched to the central AA13 GMPE and thus are not intended to be modified with their standard deviation values. As a result, and to prevent any possible confusion, the standard deviations are not provided. Instead, to represent the goodness of the fit for the predicted values, mean residuals at each period are given for both site classes. As the spectra have been matched to AA13 central GMPE in the period range of study, the same standard deviations used in determination of AA13 upper and lower GMPEs (Atkinson and Adams 2013) apply to proposed Eq. (5.2). Validation of the predictions of Eq. (5.2) against computed higher damping spectral displacements of the hybrid records will be presented in the next section.

5.5 High-damping seismic demands

The 10%-, 15%-, 20%-, 25%- and 30%-damped displacement response spectra of the hybrid records described previously are first computed. For each damping level, nonlinear regression analyses using the least square approach are performed on the obtained damped spectral ordinates. To maintain uniformity, the same functional form as in Eq. (5.2) is adopted for damping levels higher than 5%. Table 5.2 to Table 5.6 list the coefficients and standard deviations resulting from regression analyses. Figure 5-7 and Figure 5-8 show the comparison between the computed spectral displacements and the predictions corresponding to damping levels of 15% and 30% at different periods. Trends similar to those observed for the 5%-damped predicted and computed spectral displacements are seen at higher damping levels for ground motions for both rock and soil sites.

Figure 5-9 and Figure 5-10 show the spectral displacements generated using the functional form of Eq. (5.2) and the coefficients provided in Table 5.1 to Table 5.6, corresponding to a number of magnitude-distance combinations at different damping levels. Figure 5-9 and Figure 5-10 clearly demonstrate the expected effect of magnitude and distance on displacement demands through the studied period range, i.e. larger displacements correspond to higher magnitudes whereas an increase in epicentral distance has an opposite effect on seismic demands. It is also observed that the decline in the increasing branch of displacement demands disappears with increasing

magnitude, a behavior that affects the definition of the control periods of displacement design spectra.

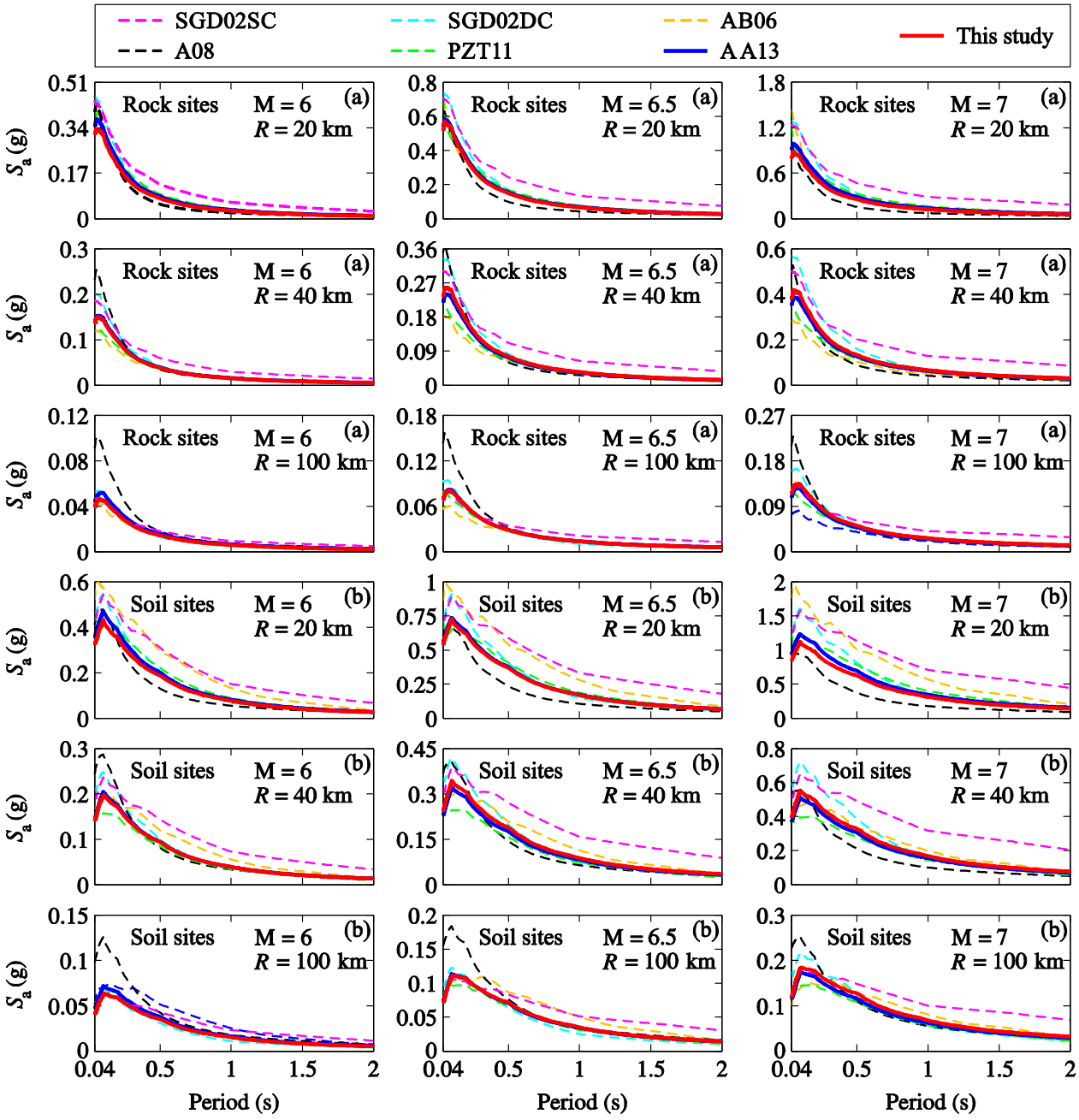

Figure 5-6: Comparison between 5%-damped spectral pseudo-acceleration predictions of the central GMPE proposed by Atkinson and Adams (2013) and those from Eq. (5.2) developed in this study: (a) rock sites; and (b) soil sites.

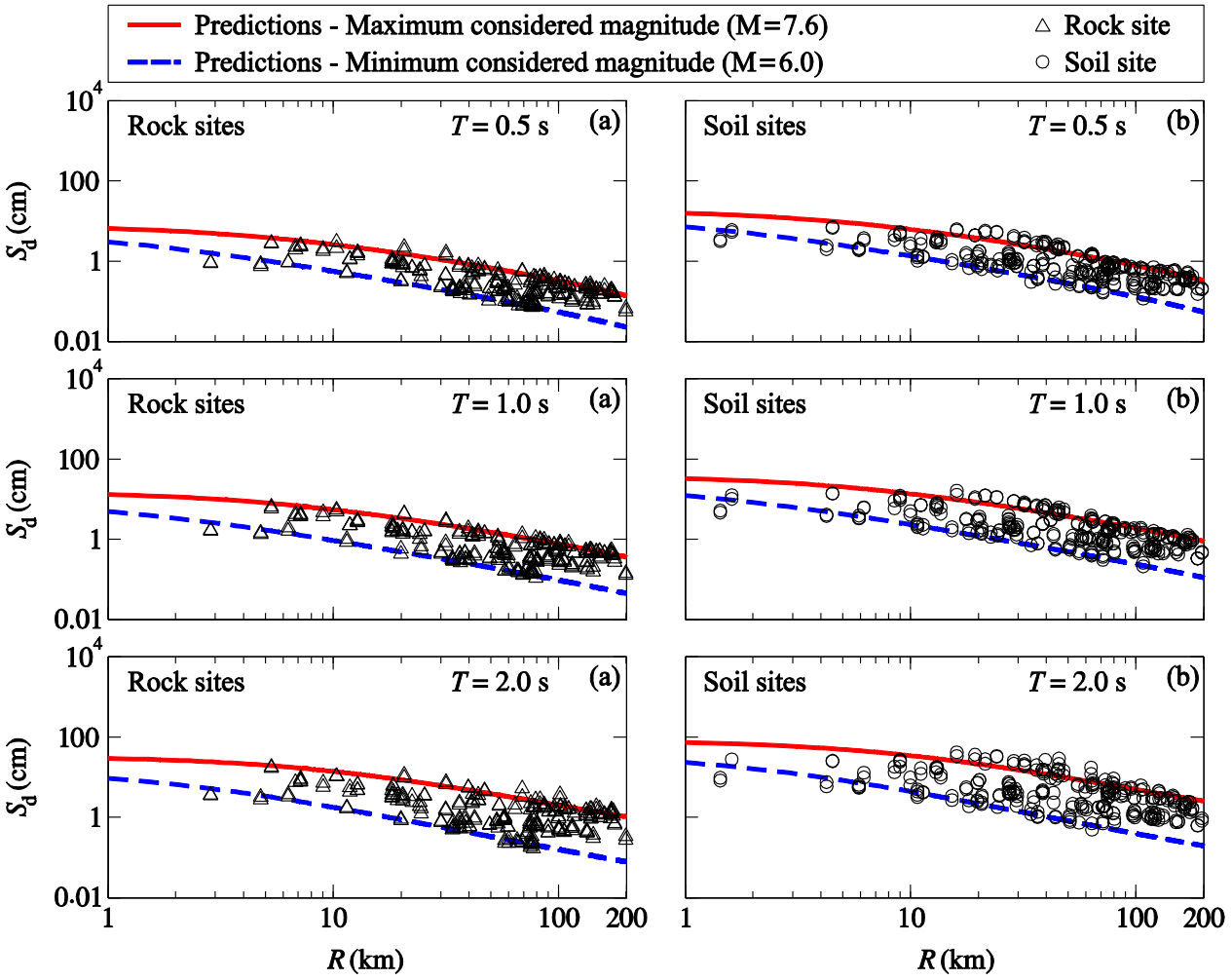

Figure 5-7: Comparison between 15%-damped spectral displacements predicted using Eq. (5.2) developed in this study and those computed from the data set of hybrid empirical records for magnitudes between M = 6.0 and M = 7.6 and periods of 0.5, 1.0, and 2.0 s: (a) rock sites; and (b) soil sites.

Figure 5-9 and Figure 5-10 also show that displacement spectral shapes tend to become smoother at higher damping ratios. This effect is more pronounced at lower magnitudes and shorter distances in particular, as the 5%-damped displacement spectra for rock and soil sites are smoother at higher magnitudes. As mentioned previously, it is suggested that the provided equation and coefficients corresponding to higher magnitudes, i.e. M > 7 and shorter distances, i.e. approximately R < 30 km, be used with caution due to the small number of near field hybrid records in the database.

Finally, we note that the high damping spectral pseudo-accelerations at a given period T can be obtained from Eq. (2) and Table 5.2 to Table 5.6 through multiplication of S_d by $(4\pi^2)/T^2$.

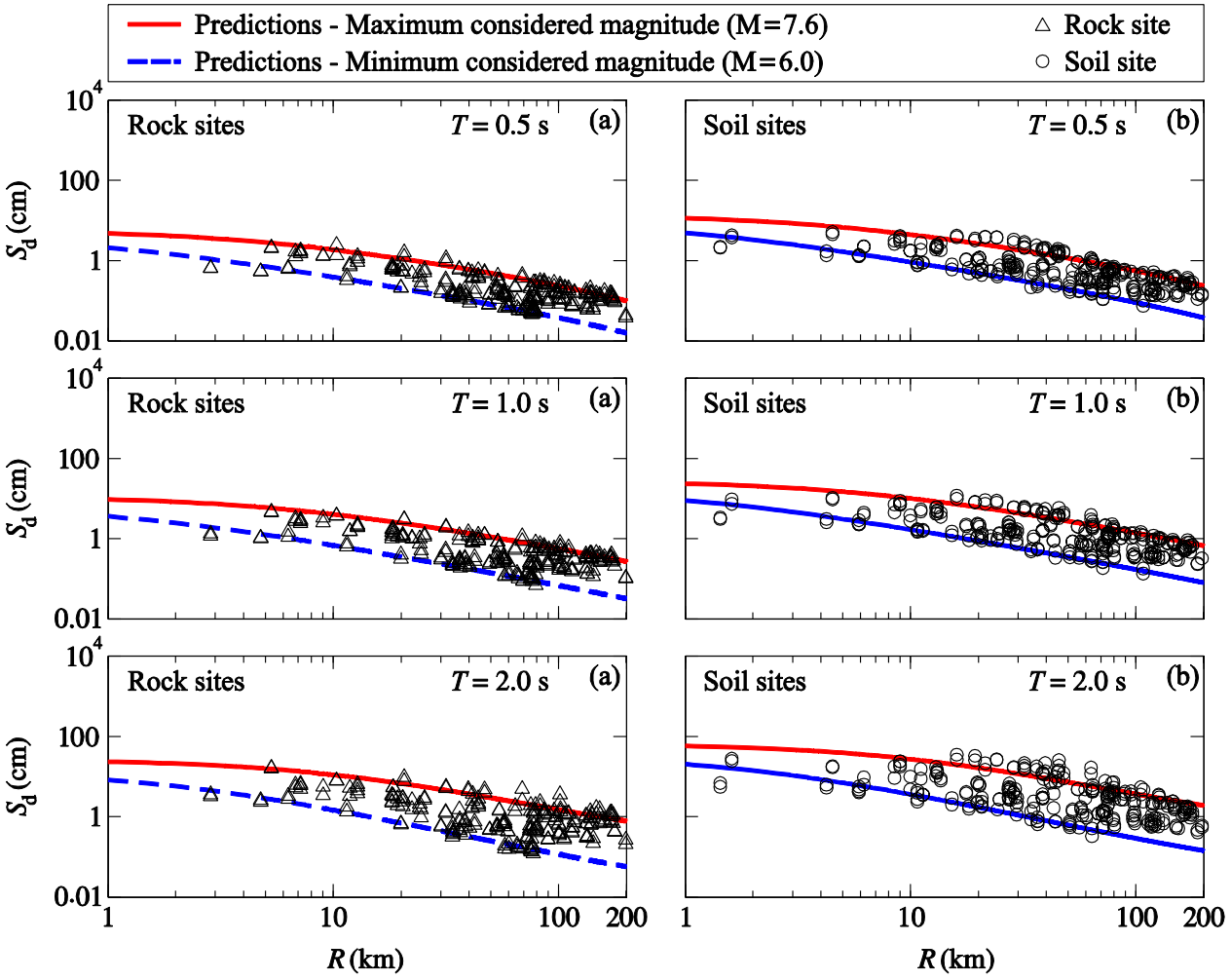

Figure 5-8: Comparison between 30%-damped spectral displacements predicted using Eq. (5.2) developed in this study and those computed from the data set of hybrid empirical records for magnitudes between M = 6.0 and M = 7.6 and periods of 0.5, 1.0, and 2.0 s: (a) rock sites; and (b) soil sites.

Table 5.1 Coefficients and mean values of the logarithm of residuals of Eq. (5.2) for 5% damping corresponding to horizontal motions on rock and soil sites

	Coefficients for Eq. (2) at 5% damping								
T (s)	a_1	a_2	a_3	a_4	a_5	a_6	a_7	Mean log. Residuals	
								Rock	Soil
0.040	-5.36409	0.51781	-0.02660	-1.20615	1.94522	-0.00121	0.01313	0.0033	0.0058
0.045	-5.42371	0.55313	-0.04709	-1.23885	2.10822	-0.00100	0.01815	0.0031	0.0059
0.050	-5.33824	0.54642	-0.04266	-1.18596	2.06082	-0.00140	0.01230	0.0026	0.0057
0.055	-5.28286	0.54342	-0.04673	-1.15881	1.84157	-0.00135	0.02520	0.0027	0.0058
0.060	-5.16751	0.52369	-0.03867	-1.10224	1.66305	-0.00159	0.04167	0.0023	0.0058
0.065	-5.08995	0.53142	-0.04033	-1.13928	1.99686	-0.00133	0.05548	0.0025	0.0059
0.070	-4.97158	0.51830	-0.03842	-1.12501	1.80661	-0.00130	0.07043	0.0030	0.0060
0.075	-4.99378	0.53163	-0.04731	-1.12641	1.81361	-0.00124	0.07912	0.0028	0.0062
0.080	-4.86016	0.51973	-0.03521	-1.13054	1.89214	-0.00125	0.08949	0.0028	0.0059
0.085	-4.88796	0.53059	-0.04180	-1.12555	1.88596	-0.00122	0.10247	0.0031	0.0062
0.090	-4.82748	0.53252	-0.04173	-1.14367	1.95553	-0.00109	0.11395	0.0031	0.0062
0.095	-4.88984	0.54414	-0.05079	-1.12032	1.91291	-0.00117	0.12638	0.0030	0.0061
0.100	-4.79011	0.53591	-0.04589	-1.12276	2.01155	-0.00118	0.13958	0.0031	0.0055
0.150	-4.72314	0.53814	-0.05641	-1.01085	1.33508	-0.00136	0.19303	0.0020	0.0050
0.200	-4.71125	0.56477	-0.07425	-1.01799	1.35031	-0.00111	0.24687	0.0019	0.0057
0.250	-4.73268	0.58048	-0.07845	-1.00088	1.28405	-0.00106	0.27791	0.0019	0.0059
0.300	-4.78418	0.60175	-0.08827	-1.00164	1.23008	-0.00092	0.31029	0.0020	0.0060
0.350	-4.85896	0.62287	-0.09375	-0.99904	1.23666	-0.00084	0.33681	0.0020	0.0060
0.400	-4.95961	0.64505	-0.10178	-0.98650	1.21224	-0.00082	0.35758	0.0020	0.0061
0.450	-5.00303	0.66312	-0.10666	-1.00062	1.26732	-0.00066	0.37279	0.0019	0.0066
0.500	-5.09159	0.68340	-0.11474	-0.99696	1.25255	-0.00059	0.39196	0.0020	0.0068
0.550	-5.09255	0.68860	-0.11181	-0.99826	1.24029	-0.00055	0.39540	0.0020	0.0065
0.600	-5.18577	0.70700	-0.11662	-0.99302	1.28346	-0.00056	0.39928	0.0019	0.0062
0.650	-5.23595	0.72093	-0.11951	-1.00186	1.30524	-0.00046	0.39672	0.0018	0.0062
0.700	-5.29120	0.73113	-0.12133	-0.99054	1.24791	-0.00048	0.39915	0.0018	0.0066
0.750	-5.32340	0.74316	-0.12322	-1.00360	1.32564	-0.00039	0.39993	0.0018	0.0069
0.800	-5.38102	0.75159	-0.12480	-0.98950	1.21633	-0.00040	0.40252	0.0019	0.0067
0.850	-5.41599	0.76176	-0.12733	-0.99280	1.28919	-0.00036	0.40417	0.0019	0.0063
0.900	-5.46825	0.77352	-0.12997	-0.99558	1.30281	-0.00032	0.40819	0.0019	0.0062
0.950	-5.54587	0.78384	-0.13369	-0.97408	1.21684	-0.00039	0.40753	0.0019	0.0057
1.000	-5.50090	0.78238	-0.12970	-0.98660	1.26435	-0.00031	0.40351	0.0019	0.0049
1.100	-5.58107	0.80263	-0.13285	-1.00070	1.33763	-0.00022	0.40118	0.0018	0.0047
1.200	-5.67449	0.81982	-0.13291	-0.99445	1.40916	-0.00024	0.40101	0.0018	0.0048
1.300	-5.81050	0.84640	-0.14105	-1.00010	1.44695	-0.00019	0.39926	0.0019	0.0046
1.400	-5.81590	0.85126	-0.13818	-1.00346	1.41810	-0.00015	0.39704	0.0018	0.0047
1.500	-5.88750	0.86567	-0.14122	-1.00596	1.42432	-0.00008	0.39808	0.0018	0.0048
1.600	-5.97837	0.88280	-0.14421	-1.00522	1.46054	-0.00006	0.39785	0.0020	0.0050
1.700	-6.07042	0.89791	-0.14751	-0.99618	1.40383	-0.00009	0.39653	0.0020	0.0050
1.800	-6.05388	0.89796	-0.14191	-0.99756	1.41574	-0.00006	0.39542	0.0019	0.0055
1.900	-6.09457	0.91018	-0.14246	-1.00899	1.52445	-0.00004	0.39470	0.0019	0.0055
2.000	-6.00353	0.90184	-0.13388	-1.02178	1.47770	0.00005	0.39183	0.0020	0.0060

Table 5.2 Coefficients and mean values of the logarithm of residuals of Eq. (5.2) for 10% damping corresponding to horizontal motions on rock and soil sites

	Coefficients for Eq. (2) at 10% damping								
T (s)	a_1	a_2	a_3	a_4	a_5	a_6	a_7	Mean log. Residuals	
								Rock	Soil
0.040	-5.56486	0.53818	-0.04010	-1.21183	1.98772	-0.00126	0.02677	0.0049	0.0087
0.045	-5.53269	0.54962	-0.04266	-1.21172	2.17812	-0.00131	0.04040	0.0043	0.0069
0.050	-5.52004	0.57044	-0.04990	-1.24616	2.33246	-0.00109	0.04322	0.0046	0.0071
0.055	-5.24699	0.51772	-0.02924	-1.15273	1.71609	-0.00148	0.05358	0.0041	0.0068
0.060	-5.24915	0.52740	-0.04035	-1.14854	1.61865	-0.00129	0.06567	0.0048	0.0072
0.065	-5.20871	0.52879	-0.04356	-1.13179	1.68188	-0.00137	0.08147	0.0045	0.0072
0.070	-5.10274	0.53017	-0.04128	-1.16590	1.93074	-0.00117	0.09179	0.0045	0.0075
0.075	-5.01567	0.52373	-0.03713	-1.15622	1.93405	-0.00118	0.09683	0.0042	0.0072
0.080	-4.96694	0.52469	-0.03386	-1.15756	1.99910	-0.00120	0.10665	0.0044	0.0070
0.085	-5.12303	0.55709	-0.05335	-1.15619	1.98023	-0.00115	0.11465	0.0044	0.0072
0.090	-5.04161	0.55064	-0.05280	-1.15030	1.94404	-0.00119	0.12526	0.0041	0.0076
0.095	-5.00430	0.54789	-0.05206	-1.13810	1.88925	-0.00121	0.13821	0.0043	0.0073
0.100	-4.96123	0.54190	-0.05403	-1.11763	1.82023	-0.00123	0.14857	0.0043	0.0071
0.150	-4.78224	0.53497	-0.04464	-1.04120	1.52143	-0.00145	0.20171	0.0038	0.0064
0.200	-4.60368	0.53339	-0.05388	-1.04310	1.46014	-0.00111	0.24767	0.0038	0.0070
0.250	-4.71279	0.55474	-0.06203	-0.99079	1.16301	-0.00119	0.27564	0.0031	0.0074
0.300	-4.69187	0.56608	-0.06786	-0.99118	1.19800	-0.00110	0.30716	0.0033	0.0072
0.350	-4.83819	0.59646	-0.08441	-0.98253	1.09643	-0.00093	0.33537	0.0036	0.0071
0.400	-4.88727	0.61126	-0.08508	-0.97265	1.09569	-0.00094	0.35383	0.0034	0.0073
0.450	-5.03447	0.64964	-0.10127	-0.99986	1.19852	-0.00074	0.36733	0.0033	0.0076
0.500	-5.17844	0.67513	-0.11230	-0.98384	1.07042	-0.00077	0.38333	0.0038	0.0076
0.550	-5.36829	0.71281	-0.12859	-0.99449	1.12811	-0.00064	0.39040	0.0037	0.0079
0.600	-5.27946	0.70810	-0.11883	-1.01564	1.25097	-0.00049	0.39362	0.0034	0.0075
0.650	-5.38741	0.73105	-0.12763	-1.01697	1.31240	-0.00048	0.39219	0.0032	0.0072
0.700	-5.38383	0.73206	-0.12361	-1.00727	1.27830	-0.00047	0.39363	0.0033	0.0074
0.750	-5.41883	0.74157	-0.12063	-1.00374	1.44286	-0.00056	0.39627	0.0035	0.0073
0.800	-5.49441	0.75608	-0.12606	-1.00227	1.32213	-0.00048	0.39507	0.0038	0.0075
0.850	-5.60347	0.77212	-0.13405	-0.98356	1.17878	-0.00050	0.39468	0.0038	0.0076
0.900	-5.63486	0.77934	-0.13612	-0.98073	1.10627	-0.00045	0.39581	0.0033	0.0073
0.950	-5.68186	0.78777	-0.13988	-0.97336	1.06271	-0.00041	0.39754	0.0031	0.0073
1.000	-5.66207	0.79198	-0.13677	-0.99196	1.21440	-0.00034	0.39776	0.0031	0.0068
1.100	-5.70892	0.81173	-0.13878	-1.02373	1.43229	-0.00022	0.39953	0.0030	0.0065
1.200	-5.76802	0.82145	-0.13684	-1.01092	1.39909	-0.00022	0.40079	0.0030	0.0063
1.300	-5.89832	0.84233	-0.14248	-0.99777	1.31651	-0.00025	0.39948	0.0031	0.0064
1.400	-5.81453	0.83731	-0.13088	-1.01972	1.29801	-0.00011	0.39569	0.0029	0.0065
1.500	-5.85804	0.84912	-0.13045	-1.02890	1.32973	-0.00001	0.39823	0.0030	0.0067
1.600	-5.92241	0.86538	-0.13240	-1.03799	1.44684	0.00000	0.39858	0.0035	0.0072
1.700	-5.93928	0.87038	-0.12882	-1.03341	1.39103	-0.00002	0.39418	0.0035	0.0072
1.800	-5.91084	0.87118	-0.12182	-1.04327	1.41387	0.00001	0.39306	0.0034	0.0079
1.900	-5.83344	0.86746	-0.11493	-1.06411	1.47658	0.00013	0.39155	0.0038	0.0092
2.000	-5.80885	0.87464	-0.11250	-1.09224	1.55209	0.00025	0.39158	0.0050	0.0116

Table 5.3 Coefficients and mean values of the logarithm of residuals of Eq. (5.2) for 15% damping corresponding to horizontal motions on rock and soil sites

	Coefficients for Eq. (2) at 15% damping								
T (s)	a_1	a_2	a_3	a_4	a_5	a_6	a_7	Mean log. Residuals	
								Rock	Soil
0.040	-5.53092	0.51247	-0.03590	-1.15720	1.78766	-0.00147	0.03143	0.0064	0.0095
0.045	-5.67836	0.56397	-0.05444	-1.22023	2.05964	-0.00114	0.05891	0.0056	0.0082
0.050	-5.37282	0.52612	-0.03762	-1.20899	1.89025	-0.00103	0.06199	0.0062	0.0084
0.055	-5.42431	0.54137	-0.04699	-1.18436	1.73824	-0.00113	0.06794	0.0058	0.0082
0.060	-5.27918	0.53489	-0.03663	-1.20305	1.91677	-0.00114	0.08371	0.0061	0.0080
0.065	-5.20262	0.52933	-0.04057	-1.18759	1.86023	-0.00109	0.09539	0.0060	0.0085
0.070	-5.15385	0.52993	-0.04119	-1.18078	1.91366	-0.00107	0.10329	0.0055	0.0087
0.075	-5.07409	0.53003	-0.03608	-1.19395	2.08176	-0.00106	0.11159	0.0055	0.0085
0.080	-5.10417	0.53845	-0.03891	-1.17159	2.02567	-0.00123	0.11987	0.0056	0.0082
0.085	-5.18997	0.55444	-0.05308	-1.15063	1.89390	-0.00121	0.12715	0.0055	0.0082
0.090	-5.15803	0.55519	-0.05336	-1.14357	1.88956	-0.00128	0.13667	0.0052	0.0082
0.095	-5.16017	0.55766	-0.06152	-1.13165	1.72084	-0.00118	0.14712	0.0054	0.0086
0.100	-5.09674	0.54861	-0.05875	-1.11135	1.67031	-0.00127	0.15629	0.0054	0.0082
0.150	-4.86042	0.53523	-0.04413	-1.04259	1.51841	-0.00150	0.20877	0.0050	0.0076
0.200	-4.63856	0.52423	-0.04541	-1.03636	1.46987	-0.00120	0.24836	0.0049	0.0083
0.250	-4.74970	0.54656	-0.05542	-0.98385	1.12542	-0.00131	0.27926	0.0039	0.0084
0.300	-4.64445	0.54672	-0.05600	-0.99617	1.19673	-0.00111	0.30993	0.0045	0.0083
0.350	-4.84676	0.58181	-0.07702	-0.96841	0.98882	-0.00102	0.33464	0.0048	0.0084
0.400	-4.92342	0.59909	-0.07869	-0.95228	0.95379	-0.00104	0.35415	0.0046	0.0085
0.450	-5.11198	0.64787	-0.09929	-0.99247	1.16901	-0.00084	0.36632	0.0047	0.0085
0.500	-5.27754	0.67556	-0.11134	-0.97291	0.98782	-0.00086	0.37866	0.0053	0.0083
0.550	-5.44621	0.70924	-0.12582	-0.98119	0.99268	-0.00071	0.38587	0.0051	0.0087
0.600	-5.41528	0.71857	-0.12277	-1.02198	1.23359	-0.00048	0.39117	0.0047	0.0084
0.650	-5.43323	0.72821	-0.12354	-1.02776	1.35300	-0.00044	0.39198	0.0046	0.0081
0.700	-5.46552	0.73580	-0.12470	-1.01751	1.37829	-0.00046	0.39305	0.0043	0.0082
0.750	-5.48663	0.74190	-0.12192	-1.01129	1.42332	-0.00051	0.39463	0.0047	0.0084
0.800	-5.53757	0.75122	-0.12465	-1.00371	1.30073	-0.00046	0.39361	0.0050	0.0085
0.850	-5.64526	0.76937	-0.13232	-0.99633	1.18824	-0.00042	0.39301	0.0050	0.0088
0.900	-5.70040	0.77989	-0.13571	-0.98978	1.11562	-0.00042	0.39357	0.0044	0.0088
0.950	-5.72828	0.78582	-0.13791	-0.98281	1.05580	-0.00040	0.39220	0.0040	0.0089
1.000	-5.73636	0.79261	-0.13827	-0.99570	1.11617	-0.00033	0.39509	0.0041	0.0087
1.100	-5.73450	0.80722	-0.13480	-1.03681	1.46522	-0.00019	0.39941	0.0041	0.0080
1.200	-5.70938	0.80303	-0.12632	-1.02222	1.31787	-0.00020	0.40090	0.0041	0.0081
1.300	-5.79810	0.82032	-0.12820	-1.01989	1.30181	-0.00018	0.39879	0.0040	0.0080
1.400	-5.79206	0.82665	-0.12281	-1.03933	1.28655	-0.00001	0.39763	0.0040	0.0082
1.500	-5.79483	0.83310	-0.12030	-1.05100	1.29875	0.00009	0.39845	0.0044	0.0087
1.600	-5.82471	0.84487	-0.11743	-1.06277	1.42981	0.00008	0.39791	0.0051	0.0093
1.700	-5.84413	0.85237	-0.11545	-1.06253	1.41542	0.00003	0.39286	0.0053	0.0100
1.800	-5.77520	0.84941	-0.10700	-1.07797	1.49784	0.00006	0.39065	0.0056	0.0110
1.900	-5.68546	0.84414	-0.09816	-1.09966	1.53857	0.00017	0.38935	0.0064	0.0133
2.000	-5.66296	0.85807	-0.09653	-1.15608	1.76974	0.00041	0.39261	0.0085	0.0167

Table 5.4 Coefficients and mean values of the logarithm of residuals of Eq. (5.2) for 20% damping corresponding to horizontal motions on rock and soil sites

	Coefficients for Eq. (2) at 20% damping								
T (s)	a_1	a_2	a_3	a_4	a_5	a_6	a_7	Mean log. Residuals	
								Rock	Soil
0.040	-5.65323	0.51530	-0.04781	-1.12139	1.47411	-0.00145	0.04377	0.0082	0.0106
0.045	-5.52186	0.52959	-0.03796	-1.21404	1.91973	-0.00104	0.06529	0.0070	0.0093
0.050	-5.42090	0.52876	-0.02981	-1.21523	2.05088	-0.00116	0.07587	0.0071	0.0091
0.055	-5.43668	0.53711	-0.04375	-1.18963	1.81154	-0.00113	0.08450	0.0069	0.0086
0.060	-5.33418	0.53186	-0.03912	-1.18646	1.85577	-0.00116	0.09529	0.0066	0.0089
0.065	-5.10337	0.50540	-0.02189	-1.18322	1.94614	-0.00121	0.10364	0.0064	0.0089
0.070	-5.13923	0.52296	-0.03199	-1.19513	2.01827	-0.00108	0.11447	0.0068	0.0093
0.075	-5.15033	0.52892	-0.04023	-1.17663	1.90758	-0.00108	0.12198	0.0065	0.0094
0.080	-5.17183	0.53729	-0.04443	-1.16078	1.89563	-0.00118	0.13075	0.0064	0.0090
0.085	-5.22729	0.54898	-0.05151	-1.14067	1.83840	-0.00129	0.13977	0.0064	0.0088
0.090	-5.25491	0.55857	-0.06113	-1.13691	1.75755	-0.00119	0.14692	0.0063	0.0092
0.095	-5.17386	0.54645	-0.05690	-1.11396	1.63430	-0.00129	0.15444	0.0062	0.0091
0.100	-5.11482	0.54360	-0.05564	-1.11730	1.69424	-0.00126	0.16265	0.0062	0.0089
0.150	-4.96640	0.54269	-0.04811	-1.04109	1.55637	-0.00155	0.21462	0.0058	0.0082
0.200	-4.73040	0.52842	-0.04468	-1.03586	1.43347	-0.00125	0.25227	0.0056	0.0091
0.250	-4.76928	0.54113	-0.04931	-0.98951	1.15096	-0.00133	0.28498	0.0046	0.0089
0.300	-4.67209	0.53992	-0.05089	-0.99321	1.12781	-0.00111	0.31313	0.0051	0.0092
0.350	-4.82818	0.56771	-0.06777	-0.96396	0.93782	-0.00104	0.33547	0.0055	0.0093
0.400	-4.98186	0.59601	-0.07712	-0.94198	0.86443	-0.00108	0.35378	0.0055	0.0093
0.450	-5.18299	0.64734	-0.09713	-0.98504	1.13130	-0.00089	0.36605	0.0056	0.0090
0.500	-5.34403	0.67526	-0.10908	-0.96942	0.96884	-0.00089	0.37743	0.0062	0.0088
0.550	-5.42796	0.69694	-0.11671	-0.98244	0.99155	-0.00074	0.38421	0.0060	0.0089
0.600	-5.50732	0.72495	-0.12354	-1.02770	1.25279	-0.00046	0.38863	0.0055	0.0090
0.650	-5.49757	0.73007	-0.12257	-1.03447	1.38100	-0.00038	0.39088	0.0054	0.0089
0.700	-5.52219	0.73697	-0.12423	-1.02544	1.42525	-0.00040	0.39228	0.0053	0.0092
0.750	-5.55657	0.74236	-0.12360	-1.00848	1.35005	-0.00046	0.39336	0.0054	0.0094
0.800	-5.59020	0.75003	-0.12428	-1.00511	1.25267	-0.00041	0.39303	0.0055	0.0096
0.850	-5.67483	0.76674	-0.13002	-1.00650	1.19707	-0.00035	0.39344	0.0054	0.0098
0.900	-5.73103	0.77680	-0.13335	-0.99665	1.10526	-0.00037	0.39229	0.0048	0.0099
0.950	-5.76376	0.78405	-0.13590	-0.99142	1.05329	-0.00037	0.39228	0.0046	0.0100
1.000	-5.77756	0.79141	-0.13568	-1.00177	1.11689	-0.00032	0.39343	0.0046	0.0100
1.100	-5.79287	0.80695	-0.13205	-1.03615	1.40650	-0.00019	0.39813	0.0048	0.0094
1.200	-5.73590	0.80039	-0.12137	-1.03106	1.30655	-0.00018	0.39984	0.0050	0.0095
1.300	-5.78209	0.81452	-0.12095	-1.04507	1.31437	-0.00005	0.39880	0.0048	0.0095
1.400	-5.77589	0.81987	-0.11638	-1.05743	1.30760	0.00006	0.39792	0.0050	0.0098
1.500	-5.78338	0.82784	-0.11489	-1.07073	1.32809	0.00015	0.39737	0.0057	0.0107
1.600	-5.80082	0.83905	-0.11135	-1.08759	1.44882	0.00016	0.39569	0.0065	0.0113
1.700	-5.80075	0.84523	-0.10926	-1.09355	1.46758	0.00015	0.39115	0.0071	0.0125
1.800	-5.74528	0.84463	-0.10185	-1.10856	1.52692	0.00017	0.38900	0.0078	0.0142
1.900	-5.65656	0.84336	-0.09336	-1.14528	1.67288	0.00032	0.38980	0.0092	0.0170
2.000	-5.64087	0.85701	-0.09304	-1.19525	1.86684	0.00052	0.39254	0.0116	0.0209

Table 5.5 Coefficients and mean values of the logarithm of residuals of Eq. (5.2) for 25% damping corresponding to horizontal motions on rock and soil sites

	Coefficients for Eq. (2) at 25% damping								
T (s)	a_1	a_2	a_3	a_4	a_5	a_6	a_7	Mean log. Residuals	
								Rock	Soil
0.040	-5.63047	0.50972	-0.03979	-1.12797	1.62898	-0.00157	0.05601	0.0084	0.0104
0.045	-5.52618	0.52720	-0.04265	-1.22626	1.93124	-0.00081	0.07746	0.0074	0.0103
0.050	-5.37031	0.50278	-0.02369	-1.15922	1.82860	-0.00143	0.08742	0.0073	0.0098
0.055	-5.51924	0.54363	-0.04826	-1.18517	1.87722	-0.00113	0.09716	0.0077	0.0093
0.060	-5.27149	0.51702	-0.03318	-1.19410	1.89067	-0.00103	0.10537	0.0074	0.0097
0.065	-5.23833	0.52217	-0.03133	-1.19434	1.99253	-0.00106	0.11487	0.0072	0.0093
0.070	-5.22494	0.52580	-0.03682	-1.18146	1.91514	-0.00103	0.12254	0.0075	0.0098
0.075	-5.13661	0.52232	-0.03266	-1.18539	2.02607	-0.00111	0.13269	0.0071	0.0095
0.080	-5.19611	0.52960	-0.04261	-1.14328	1.81366	-0.00124	0.14123	0.0070	0.0094
0.085	-5.28379	0.54975	-0.05660	-1.14159	1.76942	-0.00115	0.14843	0.0071	0.0096
0.090	-5.26868	0.54951	-0.05533	-1.11795	1.74981	-0.00136	0.15586	0.0066	0.0094
0.095	-5.21841	0.54893	-0.05835	-1.12668	1.72065	-0.00121	0.16248	0.0067	0.0095
0.100	-5.17007	0.54399	-0.05334	-1.11179	1.73394	-0.00136	0.16948	0.0065	0.0093
0.150	-5.04338	0.54643	-0.05110	-1.03643	1.55822	-0.00159	0.21999	0.0063	0.0087
0.200	-4.85396	0.53615	-0.04710	-1.02135	1.33106	-0.00132	0.25662	0.0060	0.0092
0.250	-4.80014	0.53942	-0.04637	-0.99489	1.19616	-0.00134	0.28932	0.0050	0.0092
0.300	-4.69647	0.53613	-0.04780	-0.99584	1.08458	-0.00109	0.31415	0.0054	0.0099
0.350	-4.87336	0.56663	-0.06578	-0.96403	0.89473	-0.00104	0.33653	0.0059	0.0100
0.400	-5.04583	0.59815	-0.07666	-0.94128	0.87324	-0.00110	0.35369	0.0061	0.0099
0.450	-5.26194	0.64889	-0.09706	-0.97343	1.06300	-0.00094	0.36599	0.0062	0.0094
0.500	-5.40316	0.67525	-0.10749	-0.96452	0.94281	-0.00091	0.37675	0.0067	0.0092
0.550	-5.45721	0.69315	-0.11317	-0.98113	0.98469	-0.00073	0.38305	0.0065	0.0093
0.600	-5.54561	0.72079	-0.12073	-1.01787	1.19742	-0.00049	0.38678	0.0060	0.0094
0.650	-5.54250	0.72769	-0.12042	-1.02804	1.32548	-0.00040	0.38944	0.0060	0.0095
0.700	-5.57717	0.73740	-0.12400	-1.02593	1.37141	-0.00036	0.39167	0.0059	0.0099
0.750	-5.60287	0.74222	-0.12303	-1.01181	1.31911	-0.00039	0.39173	0.0058	0.0102
0.800	-5.65072	0.75216	-0.12499	-1.00711	1.22651	-0.00037	0.39199	0.0057	0.0104
0.850	-5.72137	0.76690	-0.12886	-1.00895	1.19666	-0.00032	0.39280	0.0056	0.0106
0.900	-5.75742	0.77492	-0.13100	-1.00382	1.13231	-0.00033	0.39248	0.0051	0.0107
0.950	-5.79007	0.78303	-0.13346	-1.00240	1.09699	-0.00031	0.39221	0.0050	0.0109
1.000	-5.79364	0.78859	-0.13112	-1.01161	1.15658	-0.00027	0.39236	0.0049	0.0109
1.100	-5.81882	0.80348	-0.12796	-1.03719	1.34490	-0.00017	0.39747	0.0054	0.0107
1.200	-5.76901	0.80260	-0.11962	-1.05134	1.32861	-0.00005	0.40002	0.0057	0.0108
1.300	-5.79086	0.81258	-0.11661	-1.06177	1.31710	0.00003	0.39812	0.0056	0.0110
1.400	-5.77811	0.81612	-0.11169	-1.06909	1.30204	0.00010	0.39648	0.0061	0.0115
1.500	-5.78378	0.82507	-0.11022	-1.08604	1.34980	0.00018	0.39598	0.0069	0.0124
1.600	-5.81541	0.84023	-0.11044	-1.10929	1.47082	0.00024	0.39425	0.0079	0.0134
1.700	-5.77805	0.84196	-0.10584	-1.12166	1.50151	0.00027	0.39034	0.0089	0.0152
1.800	-5.73002	0.84371	-0.09922	-1.14140	1.58721	0.00032	0.38837	0.0099	0.0173
1.900	-5.68069	0.84971	-0.09356	-1.18048	1.78511	0.00043	0.39044	0.0116	0.0201
2.000	-5.69845	0.86601	-0.09679	-1.21887	1.90194	0.00059	0.39050	0.0142	0.0242

Table 5.6 Coefficients and mean values of the logarithm of residuals of Eq. (5.2) for 30% damping corresponding to horizontal motions on rock and soil sites

	Coefficients for Eq. (2) at 30% damping								
T (s)	a_1	a_2	a_3	a_4	a_5	a_6	a_7	Mean log. Residuals	
								Rock	Soil
0.04	-5.52826	0.49986	-0.02515	-1.17712	1.88581	-0.00137	0.06894	0.0097	0.0105
0.05	-5.71865	0.55398	-0.05582	-1.22526	2.02947	-0.00090	0.08901	0.0087	0.0106
0.05	-5.49173	0.51813	-0.03413	-1.16255	1.89913	-0.00132	0.09776	0.0073	0.0101
0.06	-5.47982	0.54043	-0.03659	-1.21296	2.22508	-0.00115	0.10635	0.0079	0.0094
0.06	-5.32630	0.51624	-0.03298	-1.16982	1.93811	-0.00120	0.11362	0.0075	0.0097
0.07	-5.30184	0.52219	-0.03437	-1.17175	1.94976	-0.00119	0.12562	0.0075	0.0100
0.07	-5.20463	0.51429	-0.02994	-1.16541	1.95422	-0.00118	0.13108	0.0075	0.0097
0.08	-5.18559	0.51269	-0.03504	-1.13457	1.80773	-0.00129	0.14027	0.0075	0.0096
0.08	-5.22197	0.52672	-0.04067	-1.13734	1.85731	-0.00129	0.14895	0.0074	0.0095
0.09	-5.23440	0.53302	-0.04771	-1.12815	1.75310	-0.00127	0.15671	0.0074	0.0096
0.09	-5.23311	0.53851	-0.05144	-1.12256	1.77533	-0.00128	0.16239	0.0070	0.0097
0.10	-5.27215	0.55062	-0.05679	-1.12178	1.80136	-0.00130	0.16988	0.0068	0.0095
0.10	-5.24532	0.54884	-0.05819	-1.10812	1.74323	-0.00135	0.17643	0.0067	0.0096
0.15	-5.12707	0.55226	-0.05628	-1.03377	1.51668	-0.00156	0.22503	0.0065	0.0089
0.20	-4.97954	0.54691	-0.05078	-1.01168	1.27626	-0.00140	0.26139	0.0063	0.0092
0.25	-4.87547	0.54679	-0.05002	-1.00511	1.22219	-0.00127	0.29205	0.0053	0.0095
0.30	-4.78704	0.54371	-0.05202	-0.99619	1.06027	-0.00107	0.31572	0.0055	0.0103
0.35	-4.91450	0.56612	-0.06358	-0.96309	0.87703	-0.00104	0.33621	0.0061	0.0104
0.40	-5.11853	0.60363	-0.07711	-0.94311	0.91676	-0.00111	0.35294	0.0066	0.0102
0.45	-5.31225	0.64687	-0.09555	-0.96076	0.97647	-0.00099	0.36539	0.0065	0.0097
0.50	-5.46663	0.67744	-0.10795	-0.95954	0.92801	-0.00092	0.37483	0.0068	0.0096
0.55	-5.49023	0.69116	-0.11036	-0.97905	0.99798	-0.00074	0.38173	0.0067	0.0096
0.60	-5.55976	0.71359	-0.11631	-1.00670	1.13920	-0.00053	0.38492	0.0064	0.0098
0.65	-5.56359	0.72233	-0.11745	-1.02054	1.25553	-0.00040	0.38750	0.0064	0.0101
0.70	-5.61287	0.73529	-0.12163	-1.02225	1.32565	-0.00036	0.39033	0.0063	0.0104
0.75	-5.65927	0.74625	-0.12305	-1.01924	1.33267	-0.00035	0.39024	0.0059	0.0107
0.80	-5.70357	0.75545	-0.12493	-1.01417	1.23385	-0.00032	0.39062	0.0058	0.0110
0.85	-5.73434	0.76407	-0.12517	-1.01528	1.21861	-0.00031	0.39202	0.0057	0.0111
0.90	-5.74357	0.76842	-0.12499	-1.01288	1.17365	-0.00030	0.39235	0.0054	0.0112
0.95	-5.77636	0.77634	-0.12624	-1.01115	1.14910	-0.00028	0.39233	0.0053	0.0113
1.00	-5.78343	0.78269	-0.12494	-1.02180	1.20504	-0.00022	0.39370	0.0054	0.0116
1.10	-5.81676	0.79767	-0.12335	-1.04302	1.29565	-0.00011	0.39749	0.0060	0.0118
1.20	-5.80140	0.80444	-0.11753	-1.06565	1.32062	0.00003	0.40018	0.0063	0.0120
1.30	-5.81801	0.81409	-0.11424	-1.07653	1.33578	0.00009	0.39874	0.0065	0.0123
1.40	-5.80183	0.81781	-0.11021	-1.08416	1.33504	0.00014	0.39576	0.0071	0.0131
1.50	-5.81130	0.82846	-0.10907	-1.10334	1.40209	0.00021	0.39428	0.0081	0.0140
1.60	-5.85601	0.84517	-0.11119	-1.12484	1.48494	0.00028	0.39277	0.0093	0.0156
1.70	-5.80101	0.84679	-0.10574	-1.14823	1.57704	0.00036	0.38971	0.0105	0.0177
1.80	-5.75548	0.84987	-0.09997	-1.17170	1.67444	0.00042	0.38819	0.0118	0.0200
1.90	-5.72278	0.85715	-0.09649	-1.20542	1.81429	0.00052	0.38939	0.0138	0.0229
2.00	-5.72096	0.86962	-0.09837	-1.23996	1.93500	0.00064	0.38962	0.0163	0.0269

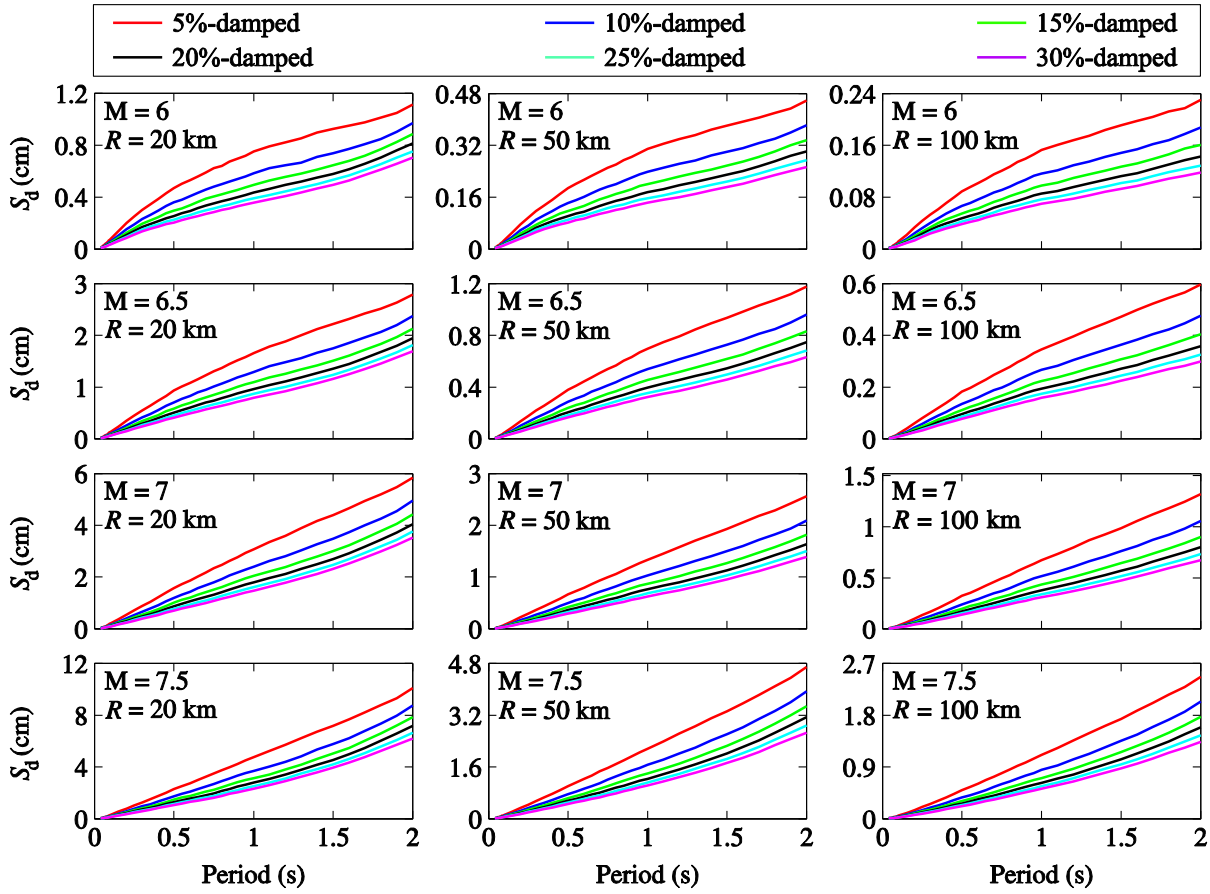

Figure 5-9: Displacement spectra at different damping levels for selected magnitudes and distances computed using Eq. (5.2) developed in this study for rock sites.

5.6 Application to assessment of damping reduction factors in ENA

Damping reduction factors, denoted hereafter as η, are commonly used to evaluate the effect of damping on seismic demands and are defined as the ratio between the 5%-damped displacement spectrum $S_{\mathrm{d}}(T,5\%)$, respectively pseudo-acceleration $S_{\mathrm{a}}(T,5\%)$, and displacement spectra $S_{\mathrm{d}}(T,\xi)$, resp. pseudo-acceleration $S_{\mathrm{a}}(T,\xi)$, for higher damping levels ξ at a period T

$$\eta(T,\xi)=\frac{S_{\mathrm{d}}(T,\xi)}{S_{\mathrm{d}}(T,5\%)}=\frac{S_{\mathrm{a}}(T,\xi)}{S_{\mathrm{a}}(T,5\%)} \tag{5.3}$$

To investigate the effects of moment magnitude and distance on η factors, the studied records are first classified into 8 bins for each site condition, i.e. rock or soil, as indicated in Table 5.7.

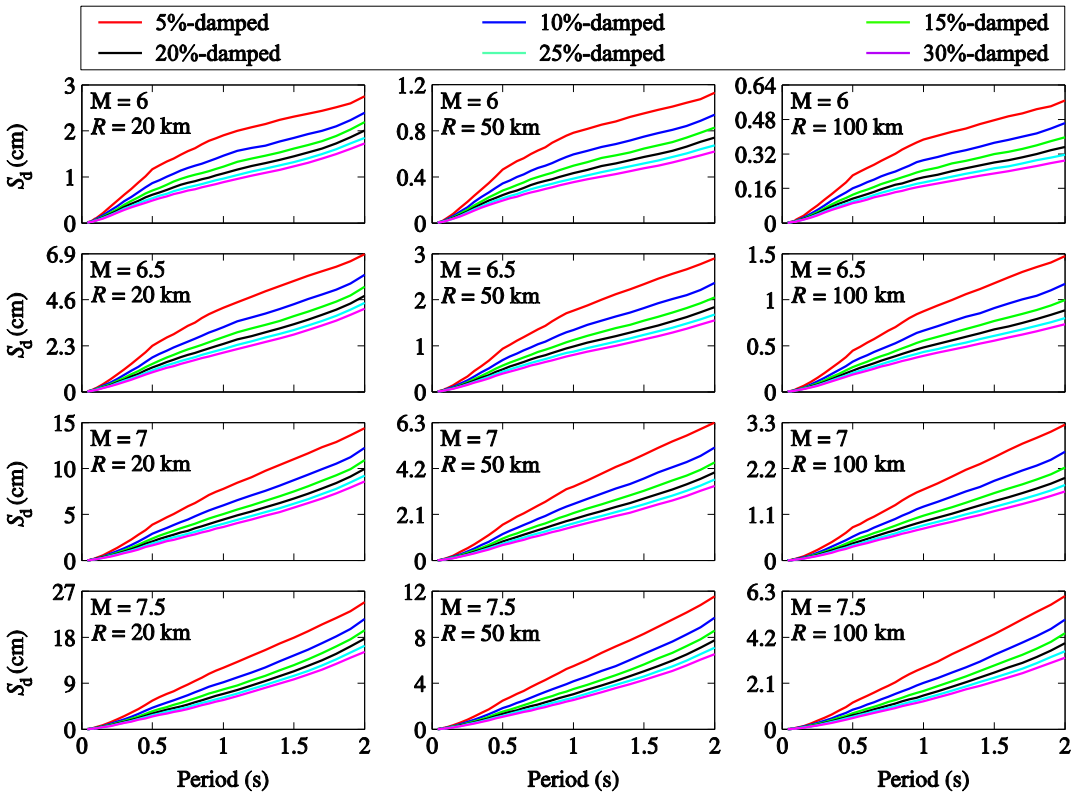

Figure 5-10: Displacement spectra at different damping levels for selected magnitudes and distances computed using Eq. (5.2) developed in this study for soil sites.

The η factors corresponding to damping levels of 10%, 15%, 20%, 25% and 30% for each record of the 8 bins are then computed for periods up to 2.0 s. Figures 11 and 12 show the means of the η factors obtained for each bin. We note that the jagged curves of η factors from Bin IV for rock sites are due to the small number of records in this bin. The pronounced period dependency of computed η factors particularly at shorter distances, i.e. Bin I, mainly roots from the high frequency content of the ground motions in ENA. High-frequency ground motions expose a structure having a short vibration period to more cycles in comparison to a structure vibrating at a longer period and thus the effect of damping is more significant on short-period structures (Naeim and Kircher 2001). This results in relatively lower η factors in the short period range. High magnitude ground motions with epicenters at relatively longer distances have more pronounced

effects on long-period structures. This explains the greater effect of damping at longer periods and thus observation of slightly lower η factors at longer periods for motions from farther distances. This trend can be observed in Figure 5-11 and Figure 5-12 where the effect of distance on η factors for rock and soil sites is generally not significant at short periods, while it is more pronounced towards longer periods. At higher damping levels, this effect increases the difference between the η factors at longer periods as the ground motions in Bin I are not expected to significantly affect structures with vibration periods in this range and hence the larger corresponding η factors. Romero and Rix (2005) and Darragh and Shakal (1991) report ground motion amplifications on soil sites at longer periods which explains the observed effect of damping for soil sites even at longer periods, e.g. Figure 5-11(b). However, as magnitude increases, nonlinear soil behavior results in more predominant damping effects at short periods while they decrease as period lengthens (Romero and Rix 2005), i.e. Figure 5-12(b). Figure 5-11 and Figure 5-12 reveal that, for rock sites, magnitude has generally less significant effects on η factors than distance in the period range of study. Similar to magnitude, distance influences the η factors from soil sites more noticeably than those from rock sites for periods up to 2.0 s.

Table 5.7 Magnitude-distance classification of the records in the database

Bin	Moment Magnitude M	Epicentral Distance R (km)	No. of Records	
			Rock Sites	Soil Sites
I	$6.0 \leq M < 7.0$	$1 \leq R \leq 50$	74	90
II	$6.0 \leq M < 7.0$	$50 < R \leq 100$	60	44
III	$6.0 \leq M < 7.0$	$100 < R \leq 150$	16	18
IV	$6.0 \leq M < 7.0$	$150 < R \leq 250$	2	9
V	$M \geq 7.0$	$1 \leq R \leq 50$	22	40
VI	$M \geq 7.0$	$50 < R \leq 100$	26	41
VII	$M \geq 7.0$	$100 < R \leq 150$	24	21
VIII	$M \geq 7.0$	$150 < R \leq 250$	20	16

Several equations have been proposed in the literature to approximate η factors considering seismic hazard in different regions. Newmark and Hall (1973, 1982) [NH1973, NH1982], used the horizontal and vertical components of 14 pre-1973 California ground motions to determine

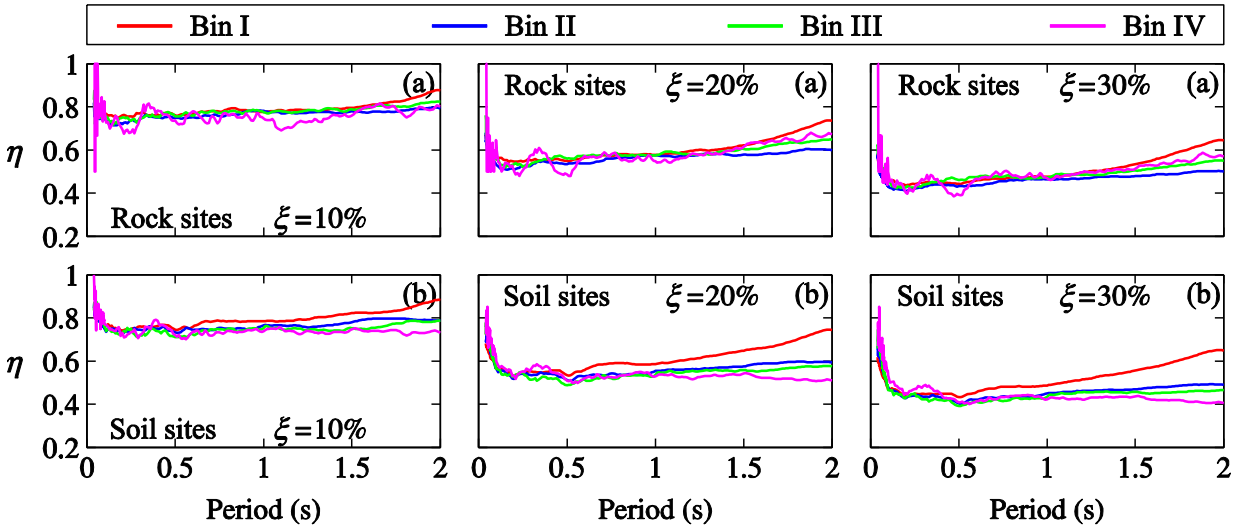

Figure 5-11: Damping reduction factors computed for ground motions in Bins I– IV: (a) rock sites; and (b) soil sites.

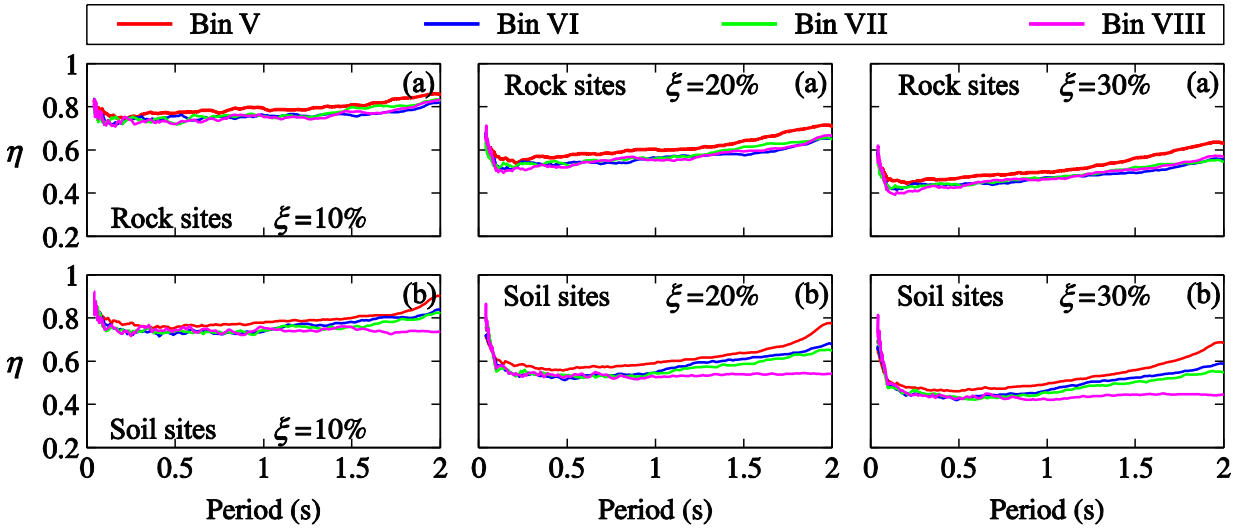

Figure 5-12: Damping reduction factors computed for ground motions in Bins V– VIII: (a) rock sites; and (b) soil sites.

maximum spectral amplitudes corresponding to damping levels lower than 20%. Considering the median values of the damped peak amplitudes, equations were proposed for displacement reduction factors. Bommer et al. (2000) [BEW2000], studied the damped displacement spectra of ground motion components from 43 shallow earthquakes recorded on rock, stiff soil and soft soil sites in Europe and the Middle East. They proposed an equation which was implemented in Eurocode 8 (2004). The Chinese guidelines for seismically isolated structures (Zhou et al. 2003) [ZWX2003], propose a period independent equation. Lin and Chang (2004) [LC2004], proposed an equation for damping reduction factors based on the displacement responses of SDOF systems for periods between 0.1 and 6 s and damping ratios between 2% and 50%. The database of the studied records consisted of 1037 accelerograms recorded in the United States. Atkinson and Pierre (2004) [AP2004], extended the simulations performed to develop the GMPE of Atkinson and Boore (1995) for moment magnitudes between 4 and 7.25 at hypocentral distances of 10 to 500 km. The 1%, 2% 3%, 5%, 7%, 10% and 15%-damped response spectra were computed and finally a magnitude and distance independent set of η factors were proposed for periods between 0.05 and 2.0 s, magnitudes greater than 5 and distances shorter than 150 km. AASHTO (2010) includes a simplified equation to obtain the damping reduction factor for damping levels up to 50%, while recommending caution with factors for damping ratios greater than 30% corresponding to hysteretically-damped isolation systems. The same η factors are prescribed by ASCE7-10 for isolated structures. ASCE7-10 also prescribes a set of damping modification factors for structural response which is slightly different from those prescribed for isolated systems particularly at higher damping levels.

Figure 5-13 compares the damping reduction factors determined using the proposed functional form of Eq. (2) and the coefficients provided in Table 5.1 to Table 5.6 to predictions of the above-mentioned equations for records on rock and soil sites at damping levels of 10%, 20% and 30%. The results show that period-independent equations fail to appropriately predict variations of damping reduction factors particularly at longer periods where a constant increase in the η factors is observed. It is also seen that period-dependent damping reduction factors by Lin and Chang (2004) are not in good agreement with the computed η factors as they: (i) over-estimate η factors for periods up to between 1.5 and 1.7 s for both rock and soil sites, and (ii) under-estimate η factors for soil sites after these periods. We note that it is somehow expected that the above

described period-independent equations as well as the period-dependent relationship proposed by Lin and Chang (2004) do not fully match η factors in ENA since they were developed using record databases mainly from other regions. Predictions by Atkinson and Pierre (2004) show relatively better agreement with the observed variation in η factors within their range of application, i.e. $\xi \leq 10\%$.

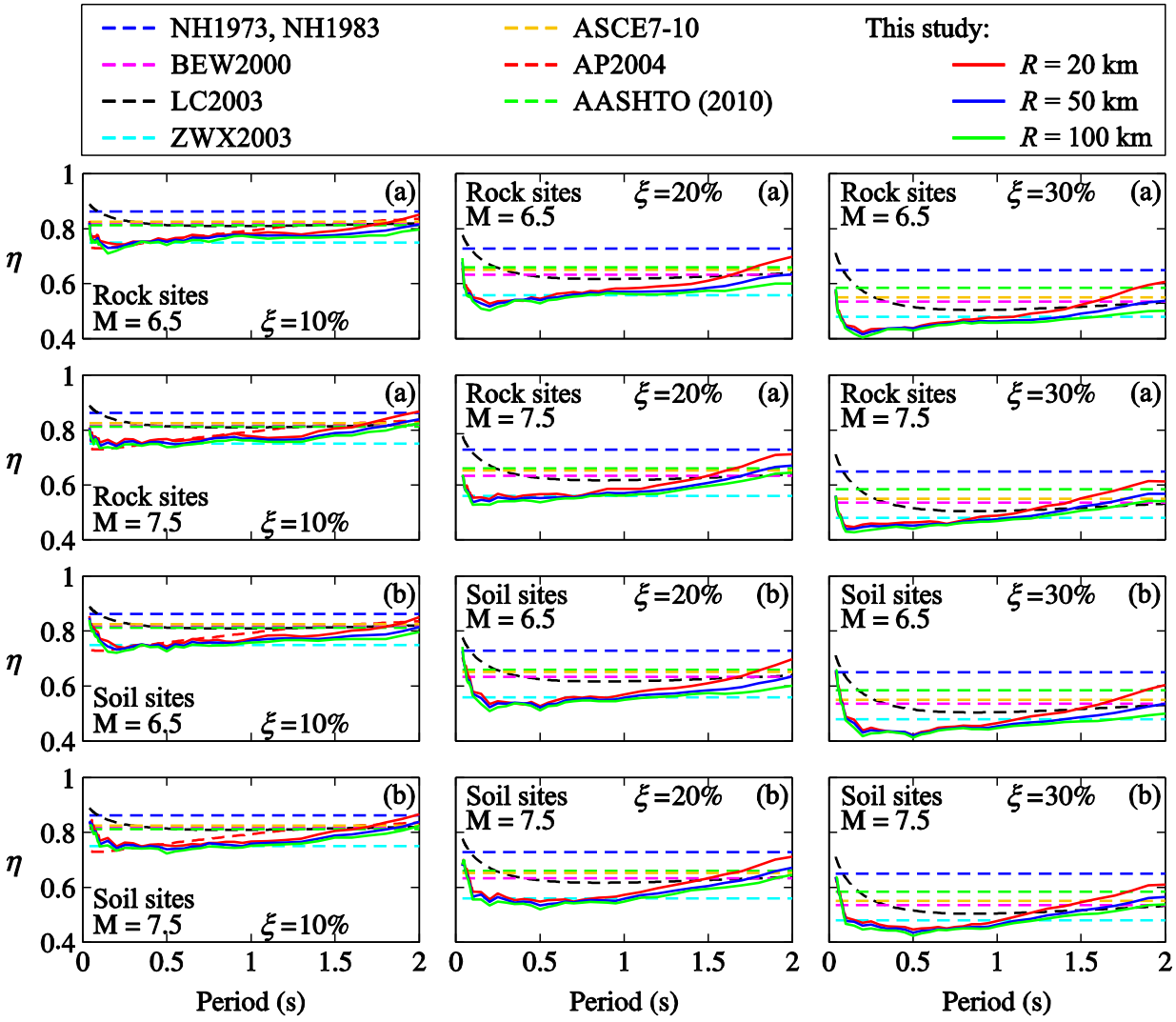

Figure 5-13: Comparison between damping reduction factors computed using Eq. (5.2) developed in this study and predictions of relationships available in the literature: (a) rock sites; and (b) soil sites.

Figure 5-13 also shows that the η factors predicted using the proposed functional form in Eq. (5.2) and the coefficients provided in Table 5.1 to Table 5.6 are in good agreement with the computed η factors illustrated in Figure 5-11 and Figure 5-12. These results verify the applicability of the proposed equation for different damping levels for horizontal motions on both rock and soil sites.

5.7 Summary and conclusions

This work aimed at assessing seismic demands and associated damping reduction factors corresponding to ENA horizontal ground motions with moment magnitudes larger than M = 6.0, which are of more interest to structural engineering applications. For this purpose, a database of 552 horizontal hybrid empirical records was first compiled to cover appropriate magnitude and epicentral distance ranges. Each selected record with a given moment magnitude M, with $6.0 \leq M \leq 7.6$, and epicentral distance R, with $1 \leq R \leq 250$ km, was then spectrally matched to the 5%-damped spectral pseudo-accelerations provided for the same M and R combination by GMPEs accounting for recent developments related to ENA seismic hazard. The matched records were used to compute 5%-, 10%-, 15%-, 20%-, 25%- and 30%-damped spectral displacements on which nonlinear regression analyses were conducted to obtain a magnitude- and distance-based prediction equation for periods up to 2.0 s. The majority of predicted displacement spectra followed a similar trend showing a shift in peak displacement amplitudes towards longer periods as moment magnitude increases. The results also confirmed the expected direct (respectively reciprocal) relation between displacement demands and magnitude (resp. distance). The proposed equation was also used to characterize damping reduction factors considering the effects of moment magnitude, epicentral distance and site condition. The period dependency of damping reduction factors, particularly at higher damping levels, was illustrated and discussed. The effect of distance and magnitude on damping reduction factors was found to be less significant than the effect of period particularly at shorter periods. We also observed that the effect of distance on damping reduction factors is more pronounced for soil sites as well as the effect of moment magnitude. The results of this work will contribute to an improved assessment of seismic demands considering the particularities of seismic hazard in ENA while accounting for added-damping in the design of structures equipped with energy dissipation systems. We finally mention that the results presented in this work focused on a period range up to 2.0 s and that further research is needed to assess ENA seismic demands at longer periods.

Acknowledgements

The authors would like to acknowledge the financial support of the Natural Sciences and Engineering Research Council of Canada (NSERC) and the Canadian Seismic Research Network (CSRN).

References

AASHTO, American Association of State Highway and Transportation Officials, 2010. *AASHTO LRFD Bridge Design Specifications*, Washington, D.C.

Abrahamson, N. A., 1992. Non-stationary spectral matching, *Seismological Research Letters* **63**, 30.

Adams, J., and Atkinson, G. M., 2003. Development of seismic hazard maps for the proposed 2005 edition of the National Building Code of Canada, *Canadian Journal of Civil Engineering* **30**, 255-271.

Adams, J., and Halchuk, S., 2004. Fourth-generation seismic hazard maps for the 2005 National Building Code of Canada, in *Proceedings, 13th World Conference of Earthquake Engineering*, paper 2502, Vancouver.

Akkar, S., and Bommer, J. J., 2007. Prediction of elastic displacement response spectra in Europe and the Middle East, *Earthquake Engineering and Structural Dynamics* **36**, 1275-1301.

Akkar, S., and Boore, D., 2009. On baseline corrections and uncertainty in response spectra for baseline variations commonly encountered in digital accelerograph records, *Bulletin of the Seismological Society of America* **99**, 1671-1690.

ASCE7-10, American Society of Civil Engineers, 2010. *ASCE7-10 Minimum design loads for buildings and other structures*, Reston, Virginia.

Atkinson, G. M., 2008. Ground-motion prediction equations for Eastern North America from a referenced empirical approach: Implications for epistemic uncertainty, *Bulletin of the Seismological Society of America* **98**, 1304-1318.

Atkinson, G. M., 2009. Earthquake time histories compatible with the 2005 National building code of Canada uniform hazard spectrum, *Canadian Journal of Civil Engineering* **36**, 991-1000.

Atkinson, G. M., and Adams, J., 2013. Ground motion prediction equations for application to the 2015 Canadian national seismic hazard maps, *Canadian Journal of Civil Engineering* **40**, 988-998.

Atkinson, G. M., and Beresnev, A., 1998. Compatible ground-motion time histories for new national seismic hazard maps, *Canadian Journal of Civil Engineering* **25**, 305-318.

Atkinson, G. M., and Boore, D. M., 1995. Ground-motion relations for Eastern North America, *Bulletin of the Seismological Society of America* **85,** 17-30.

Atkinson, G. M., and Boore, D. M., 2006. Earthquake ground-motion prediction equations for Eastern North America, *Bulletin of the Seismological Society of America* **96**, 2181-2205.

Atkinson, G. M., and Boore, D. M., 2007. Earthquake ground-motion prediction equations for Eastern North America, *Bulletin of the Seismological Society of America* **97**, 1032.

Atkinson, G. M., and Boore, D. M., 2011. Modifications to existing ground-motion prediction equations in light of new data, *Bulletin of the Seismological Society of America* **101**, 1121-1135.

Atkinson, G. M., and Pierre, J. R., 2004. Ground-motion response spectra in eastern North America for different critical damping values, *Seismological Research Letters* **75**, 541-545.

Bommer, J. J., and Elnashai, A. S., 1999. Displacement spectra for seismic design, *Journal of Earthquake Engineering* **3**, 1-32.

Bommer, J. J., Elnashai, A. S., and Weir, A. G., 2000. Compatible acceleration and displacement spectra for seismic design codes. *Proceedings of the 12th World Conference on Earthquake Engineering*, Auckland, New Zealand, Paper No. 0207.

Boore, D. M., 2005. On pads and filters: Processing strong-motion data, *Bulletin of the Seismological Society of America* **95**, 745-750.

Boore, D. M., and Joyner, W. B., 1982. The empirical prediction of ground motion, *Bulletin of the Seismological Society of America* **72**, S43-S60.

Borzi, B., Calvi, G. M., Elnashai, A. S., Faccioli, E., and Bommer, J. J., 2001. Inelastic spectra for displacement-based seismic design, *Soil Dynamics and Earthquake Engineering* **21**, 47-61.

Campbell, k. W., 1981. Near-source attenuation of peak horizontal acceleration, *Bulletin of the Seismological Society of America* **71**, 2039-2070.

Campbell, K. W., 2003. Prediction of strong motion using the hybrid empirical method and its use in the development of ground-motion (attenuation) relations in Eastern North America, *Bulletin of the Seismological Society of America* **93**, 1012-1033.

Campbell, K. W., 2004. Correction: Prediction of strong motion using the hybrid empirical method and its use in the development of ground-motion (attenuation) relations in Eastern North America, *Bulletin of the Seismological Society of America* **94**, 2418.

Campbell, K. W., 2007. Validation and update of hybrid empirical ground motion (attenuation) relations for the CEUS, U.S. Geological Survey, Award 05HQGR0032.

Campbell, K. W., and Bozorgnia, Y., 2008. NGA groung motion model for the geometric mean horizontal component of PGA, PGV, PGD and 5% damped linear elastic response spectra for periods ranging from 0.01 to 10 s, *Earthquake Spectra*, **24**, 139-171.

CAN/CSA-S6, Canadian Standards Association, 2006. *Canadian Highway Bridge Design Code*, Mississauga, Canada.

Cauzzi, C., and Faccioli, E., 2008. Broadband (0.05 to 20 s) prediction of displacement response spectra based on worldwide digital records, *Journal of Seismology* **12**, 453-475.

Darragh, R. B., and Shakal, A. F., 1991, The site response of two rock and soil station pairs to strong and weak ground motions, *Bulletin of the Seismological Society of America*, **81**, 1885-1899.

EC8, European Committee for Standardization, 2004. *Eurocode 8: Design of Structures for Earthquake Resistance - Part1: General Rules, Seismic Actions and Rules for Buildings, EN 1998-1, CEN*, Brussels, Belgium.

Faccioli, E., Paolucci, R., and Rey, J., 2004. Displacement spectra for long periods, *Earthquake Specrta* **20**, 347-376.

Faccioli, E., and Villani, M., 2009. Seismic hazard mapping for Italy in terms of broadband displacement response spectra, *Earthquake Spectra* **25**, 515-539.

Goulet, C. A., Kishida, T., Cramer, C. H., Darragh, R. B., and Silva, W. J., 2013. The NGA-East database: Development, challenges and prooducts, *Presentation in 85th Annual Meeting of the Eastern Section of the Seismological Society of America,* La Malbaie, Québec, Canada.

Hancock et al., 2006. An improved method of matching response spectra of recorded earthquake ground motion using wavelets, *Journal of Earthquake Engineering* **10**, 67-89.

Hwang, H., Pezeshk, S., Lin, Y. W., He, J., and Chiu, J. M., 2001. *Generation of synthetic ground motion*, Report MAAEC RR-2 Project, Mid-America Earthquake Center, Illinois.

Karakostas, C. Z., Athanassiadou, C. J., Kappos, A. J., and Lekidis, V. A., 2007. Site-dependent design spectra and strength modification factors, based on records from Greece. *Soil Dynamics and Earthquake Engineering* **27**, 1012-1027.

Lin, Y. Y., and Chang, K. C., 2004. Effects of site classes on damping reduction factors. *Journal of Structural Engineering*, **130**, 1667-1675.

McGuire, R. K., Silva, W. J., and Costantino, C. J., 2001. *Technical basis for revision of regulatory guidance on design ground motions: hazard-and-risk-consistent ground motion spectra guidelines*, Report NUREG/CR-6728, U.S. Nuclear Regulatory Commission Office of Nuclear Regulatory Research, Washington, DC.

National Research Council of Canada (NRCC), 2005. *National Building Code of Canada, NBCC 2005*, National Research Council of Canada, Ottawa, ON.

National Research Council of Canada (NRCC), 2010. *National Building Code of Canada, NBCC 2010*, National Research Council of Canada, Ottawa, ON.

Newmark, N. M., and Hall, W. J., 1973. *Seismic design criteria for nuclear reactor facilities*. Report No. 46, Building Practices for Disaster Mitigation, National Bureau of Standards, US Department of Commerce.

Newmark, N. M., and Hall, W. J., 1982. Earthquake spectra and design EERI monograph series. Earthquake Engineering Research Institute, Oakland, CA.

Paolucci, R., Rovelli, A., Faccioli, E., Cauzzi, C., Finazzi, D., Vanini, M., Di Alessandro, C., and Calderoni, G., 2008. On the reliability of long-period response spectral ordinates from digital accelerograms, Earthquake Engineering & *Structural Dynamics*, **37**, 697-710.

Pezeshk, S., Zandieh, A., and Tavakoli, B., 2011. Hybrid empirical ground-motion prediction equations for Eastern North America using NGA models and updated seismological parameters, *Bulletin of the Seismological Society of America*, **101**, 1859-1870.

Priestley, M. J. N., Calvi, G. M., and Kowalsky, M. J., 2007. *Displacement-Based Seismic Design of Structures*. IUSS Press, Pavia, Italy.

Ramirez, O. M., Constantinou, M. C., Whittaker, A. S., Kircher, C. A., and Chrysostomou, C. Z., 2002. Elastic and inelastic seismic response of buildings with damping systems, *Earthquake Spectra*, **18**, 531-547.

Romero, S. M., and Rix, G. J., 2005. *Ground motion amplification of soils in the upper Mississippi Embayment.* Report 05-01, Mid-America Earthquake Center, University of Illinois at Urbana-Champaign.

Shahjouei, A., and Pezeshk, S., 2013. Producing broadband synthetic time histories for central and eastern North America, in *Proceedings, Structures Congress 2013*, Pittsburgh, 1767-1776.

Silva, W. J., Gregor, N. J., and Darragh, R., 2002. *Development of regional hard rock attenuation relations for Central and Eastern North America*, Technical Report, Pacific Engineering and Analysis, El Cerrito, CA.

Somerville, P., Collins, N., Abrahamson, N., Graves, R., and Saikia, C., 2001. Ground motion attenuation relations for the Central and Eastern United States, U.S. Geological Survey, Award 99HQGR0098.

Tolis, S. V., and Faccioli, E., 1999. Displacement design spectra, *Journal of Earthquake Engineering* **3**, 107-125.

United States Geological Survey (USGS). Earthquake Hazards Program, earthquake.usgs.gov. last accessed 07 October 2014.

Zhou, F., Wenguang, L., and Xu, Z., 2003. State of the art on applications, R & D and design rules for seismic isolation in China. *Proceedings of the 8th World Seminar on Seismic Isolation, Energy Dissipation and Active Vibration Control of Structures*, Yerevan, Armenia.

CHAPTER 6 ARTICLE 4: DAMPING REDUCTION FACTORS FOR CRUSTAL, INSALB, AND INTERFACE EARTHQUAKES CHARACTERIZING SEISMIC HAZARD IN SOUTH-WESTERN BRITISH COLUMBIA, CANADA

Poulad Daneshvar, M.EERI, Najib Bouaanani, M.EERI,
Katsuichiro Goda, M.EERI and Gail M. Atkinson, M.EERI

Paper published in *Earthquake Spectra*,

DOI:http://dx.doi.org/10.1193/061414EQS086M

Submitted 25 June 2014. Accepted 23 January 2015.

High-damping displacement spectra and corresponding damping reduction factors (η) are important ingredients for seismic design and analysis of structures equipped with seismic protection systems, as well as for displacement-based design methodologies. In this paper, we investigate η factors for three types of earthquakes characterizing seismic hazard in south-western British Columbia, Canada: (i) shallow crustal, (ii) deep inslab, and (iii) interface subduction earthquakes. We use a large and comprehensive database including records from recent relevant earthquakes, such as the 2011 Tohoku event. Our key observations are: (i) there is negligible dependence of η on soil class; (ii) there is significant dependence of η on the frequency content and duration of ground motions that characterize the different record types and (iii) η is dependent on period, particularly for inslab events. Period-dependent equations are proposed to predict η for damping ratios between 5% and 30% corresponding to the three event types.

Nomenclature

Abbreviations

CEUS	Central and Eastern United States

CSA	Canadian Standard Association
DBD	Displacement-based design
ENA	Eastern North America
GMPE	Ground motion prediction equation
GSC	Geological Survey of Canada
JMA	Japan Meteorological Agency
K-NET	Japanese database of ground motions
KiK-net	Japanese database of ground motions
SK-net	Japanese database of ground motions
NBCC	National Building Code of Canada
NEHRP	National Earthquake Hazard Reduction Program
PEER	Pacific Earthquake Engineering Research Center
PSA	Pseudo spectral acceleration
PSHA	Probabilistic Seismic Hazard Analysis
USGS	United States Geological Survey
WNA	Western North America
WUS	Western United States

Symbols

a_{i}	Regression coefficient
C_{i}	The Fourier amplitude coefficient
f_{i}	The discrete fast Fourier transform (FFT) frequencies between 0.25 and 20 Hz
Δf	The frequency intervals used in FFT
M	Moment magnitude

R_{RUP}	Rupture distance
S_{a}	Spectral acceleration
$S_{\mathrm{a}}(T,\xi)$	Spectral acceleration at a period T and an equivalent damping ratio of ξ
S_{d}	Spectral displacement
$_{\mathrm{d}}(T,\xi)$	Spectral displacement at a period T and an equivalent damping ratio of ξ
T	Period of vibration
T^{*}	Period at which PSHA is performed
T_{m}	Mean period of an accelerogram
ξ	Equivalent damping ratio
η	Damping reduction factor
V_{S30}	Time-averaged shear-wave velocity in the top 30m

6.1 Introduction

Elastic displacement spectra associated with damping levels higher than the conventional 5% critical damping are important in the seismic design and evaluation of structures equipped with energy dissipating and seismic isolation systems. High-damping displacement spectra are also required for displacement-based design and evaluation techniques, such as the Direct Displacement-Based Design method (Priestley and Kowalsky 2000; Priestley et al. 2007). Such displacement spectra can be determined using: (i) ground motion prediction equations (GMPEs) developed specifically for damping levels higher than 5%, or (ii) damping reduction factors, denoted hereafter by η, which are defined as the ratio between the 5%-damped displacement spectrum $S_d(T,5\%)$ and displacement spectra $S_d(T,\xi)$ for higher damping levels ξ at a period T

$$\eta(T,\xi) = \frac{S_d(T,\xi)}{S_d(T,5\%)} \tag{6.1}$$

A number of GMPEs predicting spectral amplitudes at various damping levels have been proposed for different regions, e.g. Chen and Yu (2008) for western North America (WNA), and Akkar and Bommer (2007) and Cauzzi and Faccioli (2008) for Europe. These are useful in conducting probabilistic seismic hazard analysis to assess seismic hazard values for higher damping ratios. On the other hand, most guidelines and building codes adopt the approach of damping reduction factors (e.g. UBC-97, Eurocode8 2004, CHBDC 2006, ATC 2010, AASHTO 2010, and ASCE7-10). An advantage of the latter approach is that these damping reduction factors can be applied directly to code-prescribed spectral amplitudes to evaluate damping effects.

The main objectives of this work are: (i) to determine and characterize damping reduction factors corresponding to three event types contributing to seismic hazard in south-western British Columbia (BC), i.e. crustal, inslab, and interface events, and (ii) to propose model equations for the median of these damping reduction factors as a function of damping ratio, period, and soil class. The adopted procedure for developing such damping reduction factors for Vancouver is based on the evaluation of the damping reduction factors using various sets of ground motion records that are selected based on seismic deaggregation (i.e. dominant scenarios). The parameterization of the prediction models for η is guided by the current seismic provisions in Canada (NBCC 2010). This

provides a practical means to extend the usability of the current seismic design requirements in place. Vancouver is selected to conduct probabilistic seismic hazard analysis (PSHA); site conditions corresponding to soft rock and soft soil sites, which characterize the Greater Vancouver region, are considered.

Various equations have been proposed in the literature to approximate damping reduction factors considering seismic hazard in different regions. Newmark and Hall (1973, 1982) used the horizontal and vertical components of 14 pre-1973 California ground motions to propose damping reduction factors corresponding to damping levels lower than 20%. Bommer et al. (2000) studied the damped displacement spectra of 183 ground motion components from 43 shallow earthquakes recorded on rock, stiff and soft soil sites in Europe and the Middle East. They proposed an equation which was implemented in Eurocode 8 (2004). The Chinese guidelines for seismically isolated structures include a period-independent equation for damping reduction factors (Zhou et al. 2003). Lin and Chang (2004) studied 1037 accelerograms recorded in the United States to propose period-dependent damping reduction factors for periods between 0.1 s and 6 s and damping ratios between 2% and 50%. Atkinson and Pierre (2004) extended the simulations performed to generate a dataset of synthetic records which was used in developing the GMPE of Atkinson and Boore (1995) for scenarios between **M**4.0 and **M**7.25 at hypocentral distances of 10 km to 500 km. The 1%, 2% 3%, 5%, 7%, 10%, and 15%-damped response spectra were computed and finally a magnitude-distance independent set of η factors was proposed for periods between 0.05 s and 2 s, magnitudes greater than 5, and distances shorter than 150 km. Cameron and Green (2007) proposed a set of damping modification factors for damping levels between 1% and 50% for magnitude-binned ground motion records from shallow crustal events. Ground motion duration was shown to be highly influential on damping reduction factors, whereas source-to-site distance was found to have negligible effect for damping levels of 2% and above. They also showed that site conditions have minor influence on damping modification factors for shallow crustal events in active tectonic regions. AASHTO (2010) includes a simplified equation to obtain damping reduction factors for damping levels up to 50%, while suggesting caution regarding its use for damping ratios greater than 30%. Rezaeian et al. (2014) studied a database of 2250 records from shallow crustal ground motions and developed a magnitude- and distance-based model to predict damping modification factors for the average horizontal component of ground motion and damping levels of between 0.5% and 30%. They observed the period dependency of the damping modification factors and also reported a strong

dependency of these factors on ground motion duration. The abovementioned factors and equations are all period-independent, except for those proposed by Atkinson and Pierre (2004), Lin and Chang (2004), Cameron and Green (2007) and Rezaeian et al. (2014). A recent investigation of several period-dependent and period-independent damping reduction factors by Cardone et al. (2009) showed that period-dependent models provide the most accurate predictions of computed displacement spectra. Furthermore, Bradley (2014) reiterates the period- and duration-dependency of damping reduction factors while questioning the accuracy of a number of proposed equations, namely the one prescribed by Eurocode 8 (2004) where response amplification is characterized in terms of source- and site-specific effects. It should be noted that some older equations are based on studies that may lack adequate record processing of the used accelerograms (i.e. such as filtering and zero-padding) and therefore might not be suitable for long period ranges.

An important consideration is that the majority of the previous studies have focused upon ground motions for shallow crustal earthquakes, whereas ground motions for subduction earthquakes (including deep inslab and mega-thrust interface events) have not been much investigated. The large magnitudes of mega-thrust subduction earthquakes, and the potentially-high stress drops for deep inslab earthquakes, are important factors that control the duration and frequency content of ground motions - which are relevant properties for damped structural responses. It is therefore expected that the differing characteristics of ground motions for different earthquake types that contribute to hazard have major influence on the damping reduction factors. This is a research gap in the current literature that warrants further investigations, and is the focus of this study.

Southwestern BC is a seismically-active region with three distinct event types that contribute to seismic hazard: (i) shallow crustal, (ii) deep inslab, and (iii) interface Cascadia subduction earthquakes. Ground motions recorded in environments similar to these three tectonic settings have been shown to have distinctive characteristics in terms of frequency content and duration (Pina 2010; Jayaram et al. 2011; Tehrani et al. 2014). It is not known whether damping reduction factors corresponding to the three event types would be different, as there are no recent studies that address these effects. This is the novelty of this study. There are several highly-populated urban centers in BC, such as the Greater Vancouver region, where major infrastructure was constructed prior to the adoption of modern seismic provisions in the mid-1970s. The rehabilitation of this infrastructure using seismic isolation or added damping requires the availability of appropriate damping reduction factors. Such damping reduction factors are also required for displacement-based design

of new infrastructure in the region. To the authors' knowledge however, there is no published work that investigated and compared damping reduction factors corresponding to crustal, inslab, and interface earthquakes characterizing seismic hazard in south-western BC or a similar tectonic setting.

6.2 Preliminary selection of ground motion records

The records used in this study are selected from two sources: (i) the PEER-NGA database to represent worldwide shallow crustal events, and (ii) K-NET, KiK-net and SK-net databases to represent inslab and interface events. The record characteristics of the PEER-NGA database can be found at http://peer.berkeley.edu/nga/index.html, while those of K-NET, KiK-net and SK-net databases are available at www.k-net.bosai.go.jp, www.kik.bosai.go.jp and www.sknet.eri.u-tokyo.ac.jp, respectively. Further information about the Japanese databases can be found in Goda and Atkinson (2009) and Goda and Atkinson (2010).

The following selection criteria were applied to form a preliminary combined dataset of K-NET, KiK-net and SK-net records enriched with earthquakes that occurred up to 2012: (1) maximum depth is 500 km; (2) minimum Japan Meteorological Agency (JMA) magnitude is 3.0; (3) maximum hypocentral distance is 1500 km; (4) minimum horizontal peak ground acceleration (PGA, geometric mean) is 1.0 cm/s^2; and (5) at least 10 records are available for each seismic event satisfying the preceding four conditions. This preliminary selection led to a combined set of 555,750 records from 6261 earthquakes. To emphasize important characteristics of damaging ground motions in terms of amplitudes, spectral content, and duration, we further refined the PEER-NGA and the combined K-NET/KiK-net/SK-net dataset by applying additional selection criteria: (i) only horizontal components recorded on ground surface are considered; (ii) magnitude-distance cut-off limits considered by Goda and Atkinson (2009) are applied with the minimum moment magnitude **M** equal to 6.0; (iii) average shear-wave velocity in the uppermost 30 m V_{s30} between 180 m/s and 760 m/s representing soil classes C and D; and (iv) geometric means of the PGA and PGV of the two horizontal components greater than 100 cm/s^2 and 10 cm/s, respectively. These refined selection criteria resulted in a total of 2302 earthquake horizontal accelerograms. The number of accelerograms for crustal earthquakes is 1098 (716 components are from the NGA database while 382 components are from the combined Japanese database); the number of accelerograms for inslab earthquakes is 622; and the number of accelerograms for interface

earthquakes is 582. The interface records are either from the **M**8.3 2003 Tokachi-oki or the **M**9.0 2011 Tohoku earthquakes to capture the record properties related to large magnitudes of the Cascadia subduction events.

6.3 Record selection based on probabilistic seismic hazard analysis

The seismic hazard model developed by Atkinson and Goda (2011) for western Canada is adopted herein to conduct PSHA for Vancouver. This PSHA is based on simulated seismic activities spanning 5 million years, and an annual non-exceedance probability of 0.9996, i.e. a return period of 2500 years. It is carried out at different periods T^* = 0.2 s, 0.5 s, 1.0 s, 2.0 s, and 3.0 s to investigate the effect on high-damping spectral amplitudes. The deaggregation analysis is based on an "approximately equal criterion" as discussed by Hong and Goda (2006). Deaggregation results are shown in Table 1 in terms of mean moment magnitude **M** and mean rupture distance R_{rup} at each period T^* for each event type and soil class, in accordance with standard deaggregation practice. The identified scenarios are not overly sensitive to the choice of mean versus mode. Each of the three sets contains the deaggregation results for soil classes C and D. It can be seen that for crustal and inslab event types, deaggregation results are affected by the choice of T^* while they are almost insensitive to the changes in soil class. The deaggregation results for interface events are shown to be independent of both soil class and period $T^* \leq 3$ s. The results in Table 1 suggest that

Table 6.1 Magnitude-distance criteria for the selected records based on deaggregation results

		T^* = 0.2 s		T^* = 0.5 s		T^* = 1.0 s		T^* = 2.0 s		T^* = 3.0 s	
Event Type	Soil Class	**M**	R_{rup}	**M**	R_{rup}	**M**	R_{rup}	**M**	R_{rup}	**M**	R_{rup}
Crustal	C	6.5	11	6.7	13	6.8	15	7.0	15	7.1	15
	D	6.5	14	6.7	14	6.8	18	7.0	15	7.1	17
Inslab	C	6.8	62	7.0	55	7.0	54	7.1	54	7.2	58
	D	6.9	61	7.0	56	7.0	52	7.1	51	7.2	53
Interface	C	8.6	141	8.6	141	8.6	142	8.6	142	8.6	141
	D	8.6	142	8.7	142	8.6	141	8.6	141	8.6	141

a final selection of ground motions taking account of appropriate scenarios for each earthquake type should be conducted.

6.4 Final selected records

The final step in the scenario-based record selection is to identify a set of records representing each event type and the corresponding mean **M** and mean R_{rup} obtained from deaggregation. For this purpose, a **M**-R_{rup} trade off of 40 km, 60 km, and 60 km is adopted for crustal, inslab, and interface events, respectively. This suggests that, for example, a crustal record having a magnitude of one unit lower than the mean **M** obtained from deaggregation, will be selected provided that it has a R_{rup} of 40 km shorter than the mean R_{rup} obtained from deaggregation (Baker and Cornell 2006). For inslab and interface records, a slightly longer trade-off distance of 60 km than crustal records is considered to account for a wider distance range of these records. For the inslab and interface datasets considered, the **M**-R_{rup} trade-off distance has a negligible effect on the selected records.

The final selection consists of 60 horizontal accelerograms for each combination of event type and soil class. In other words, 360 horizontal components are used for evaluating the η factors for a given deaggregation period T^*; the selected records for different T^* values are not identical as the target magnitude-distance criteria for the record selection depend on T^* (see Table 6.1). Figure 6-1 illustrates the magnitude-distance distribution of the selected records for soil classes C and D. Figure 6-2 shows the 5%-damped displacement spectra and the corresponding mean and standard deviation from the selected records based on $T^* = 0.2$ s.

6.5 Damping reduction factors

To investigate the correlation between the η factors and damping ratios in each bin and in the considered period range, we first compute the ratio between the obtained displacement amplitudes at damping levels ξ = 10%, 15%, 20%, 25%, and 30%, and those at ξ = 5% for each set of the selected records corresponding to each T^*. Figure 6-3 and Figure 6-4 show the computed median η factors for the considered damping levels, event types, and soil classes. The choice of median as a representative statistical metric for the central tendency is motivated by the fact that the η factors can be approximated by the log-normal distribution. The effect of damping ratio on η factors is

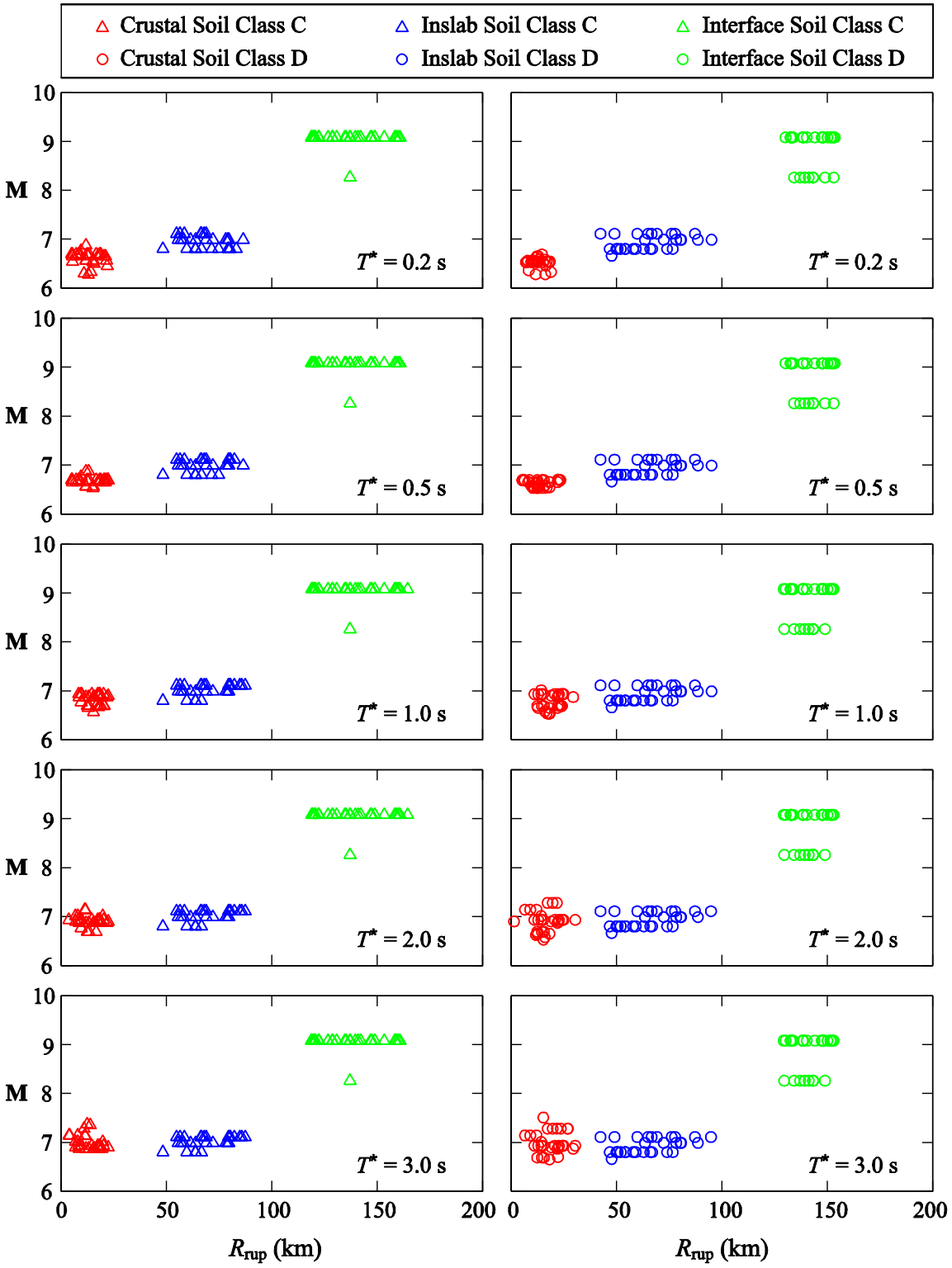

Figure 6-1: Magnitude-distance distribution of the selected records for soil classes C and D at different periods T*.

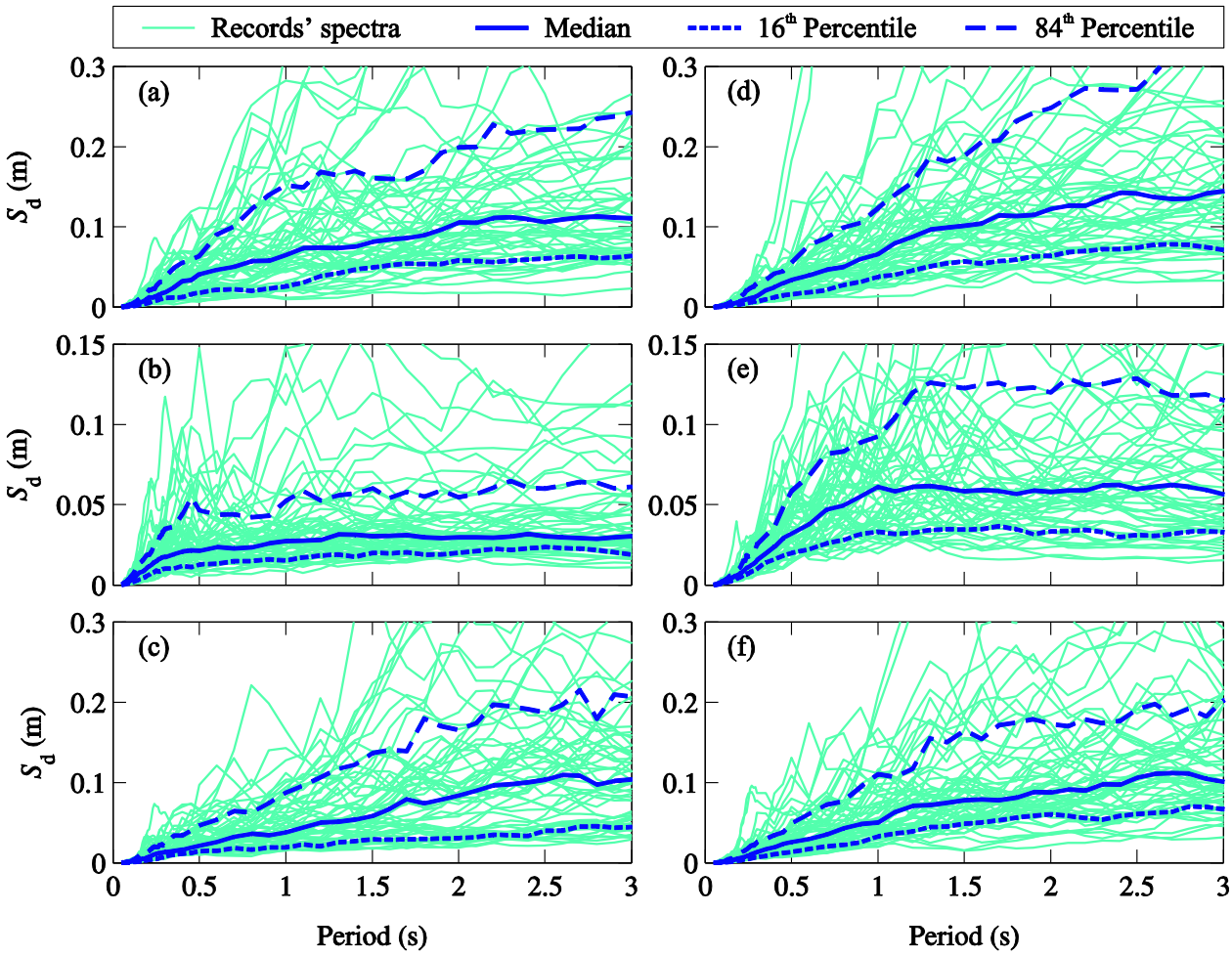

Figure 6-2: Selected records and corresponding medians of 5%-damped spectral displacements and 16th and 84th percentiles at T^* = 0.2 s: (a) and (d) Crustal events; (b) and (e) Inslab events, and (c) and (f) Interface events; (a) to (c) Soil class C and (d) to (f) Soil class D.

clearly illustrated in these figures. As expected, smaller damping reduction factors are associated with higher damping levels. This is mainly due to the influence of damping ratio on the number of loading cycles, in a ground motion wave packet, required to reach a steady state for displacement (Bradley 2014). In comparison to low damping levels, the steady state is reached after fewer cycles at higher damping levels, resulting in considerably smaller spectral displacements, hence the smaller η factors. Figure 6-3 and Figure 6-4 also show the dependency of computed η factors on the period T at which spectral displacements are determined.

We note that for all the three event types the significant period dependency of η factors at very short periods, i.e. shorter than approximately 0.15 s to 0.2 s is attributed to the facts that all the

spectra at different damping levels approach a displacement amplitude of 0 towards $T = 0$ and gradually diverge as the period lengthens and the difference between the spectral displacements at

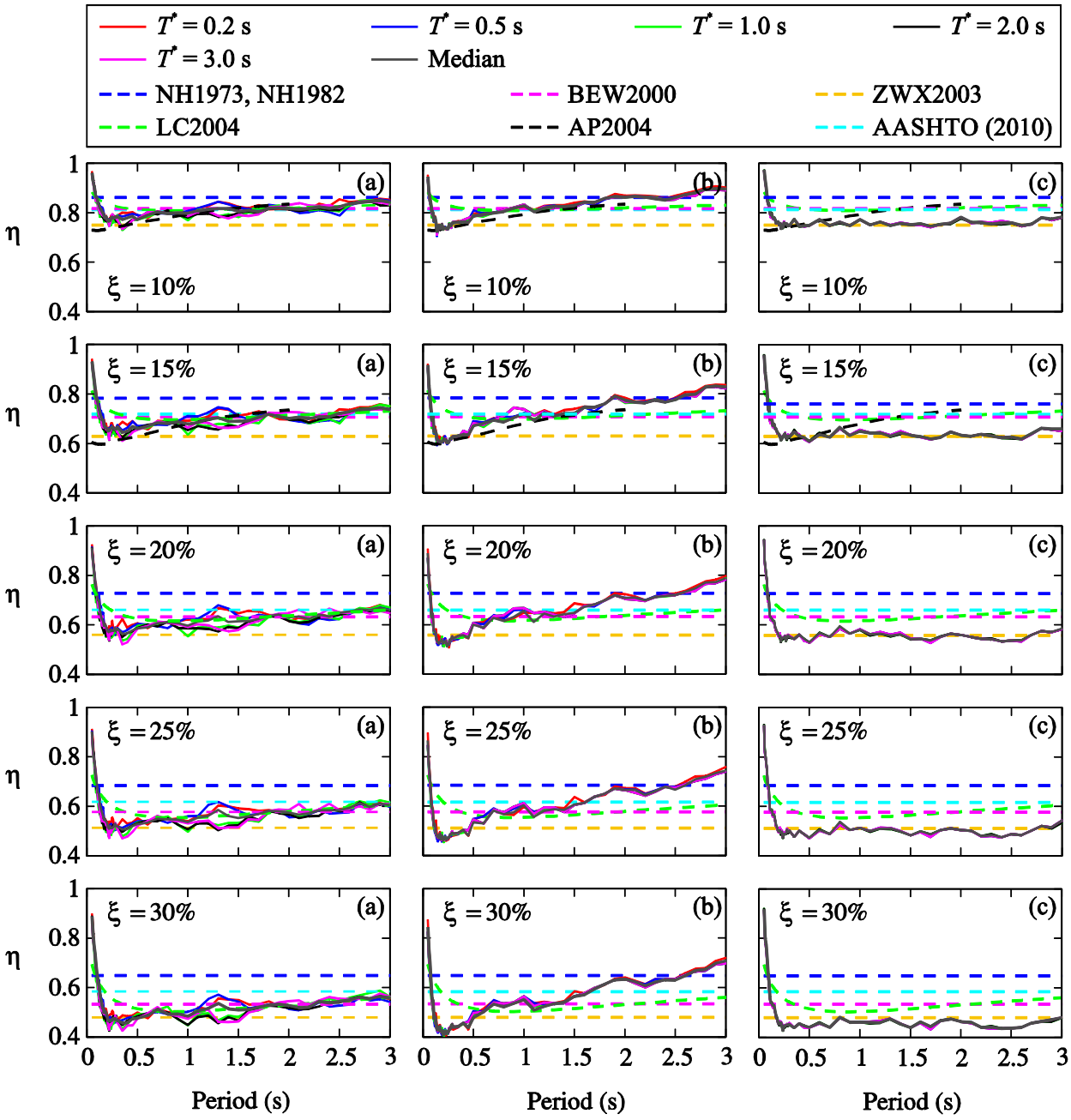

Figure 6-3: Damping reduction factors computed from the displacement spectra of the studied (a) Crustal, (b) Inslab and (c) Interface records for soil class C and predictions of some available equations.

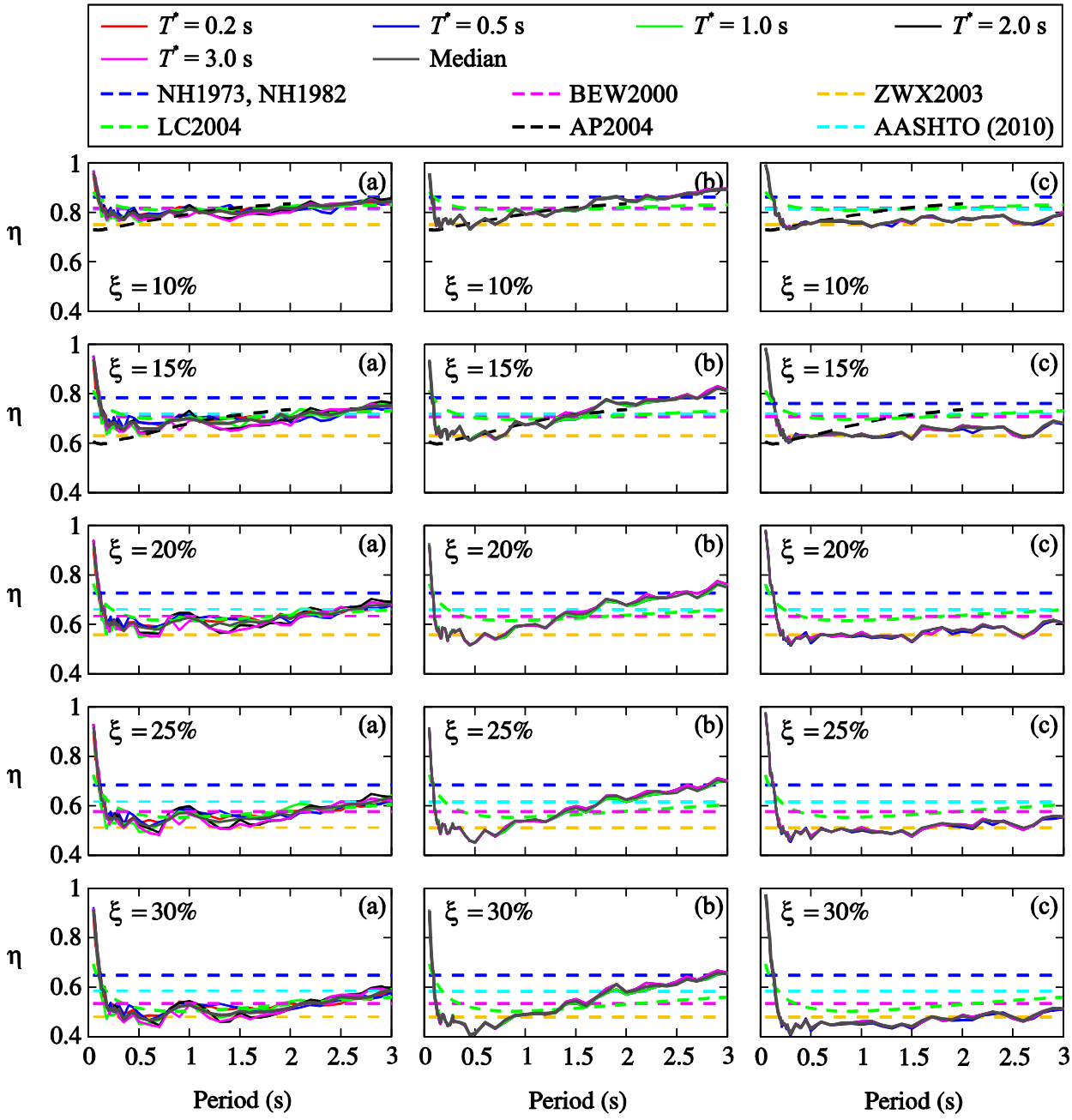

Figure 6-4: Damping reduction factors computed from the displacement spectra of the studied (a) Crustal, (b) Inslab and (c) Interface records for soil class D and predictions of some available equations.

various damping levels increases. In what follows we characterize the period dependency of the η factors beyond periods of 0.15 s to 0.2 s. The period dependency of the η factors is particularly noticeable for inslab records over the whole studied period range $0 \leq T \leq 3$ s.

Slight dependency on period is observed for crustal events as η increases moderately towards longer periods. The damping reduction factors of interface records show no significant period dependency, although minor influence of period can be observed at very short periods, i.e. $T \leq 0.5$ s, and long periods, i.e. 2.5 s $\leq T \leq 3$ s. These local decreases in the η factors are attributed to the existence of wave packets, in specific segments of ground motion records, having a narrow bandwidth of frequencies. This creates local spectral peaks in low damping spectra, i.e. ξ = 5%, resulting in relatively smaller η factors at higher damping levels for which the wider bandwidth of frequencies produces smoother spectra (Bradley 2014). Damping reduction factors for inslab events are more evidently period dependent in comparison to the other two event types.

To obtain further insights about the event-type dependency of the η factors, the selected records are studied based on their frequency content and significant duration of ground motions. The significant duration is defined as the time interval of the Arias intensity between 5% and 95% (Trifunac and Brady 1975). The portion of each selected accelerogram corresponding to this duration measure is extracted. Rathje et al. (1998, 2004) suggested the mean period, T_{m}, as a robust measure of the frequency content of a ground motion, which can be computed using the following equation

$$T_{\mathrm{m}} = \frac{\sum_i C_i^2 / f_i}{\sum_i C_i^2} \tag{6.2}$$

where C_i represents the Fourier amplitude coefficients and f_{i} the discrete fast Fourier transform (FFT) frequencies between 0.25 and 20 Hz with Δf, the frequency intervals used in FFT computation, not greater than 0.05 Hz. The T_{m} values corresponding to each of the selected accelerograms are computed using Equation (6.2) and the results for the three event types are compared in Figure 6-5 for the two soil classes. Figure 6-5(a) shows that lower T_{m} values are associated with inslab events consistently, i.e. inslab events are of higher frequency content (attributed to high stress drop source parameters). This feature of inslab events is also mentioned by Chen et al. (2013). Considering a high-frequency record, a structure having a lower period of vibration undergoes more cycles in comparison to a structure having a longer period and thus the

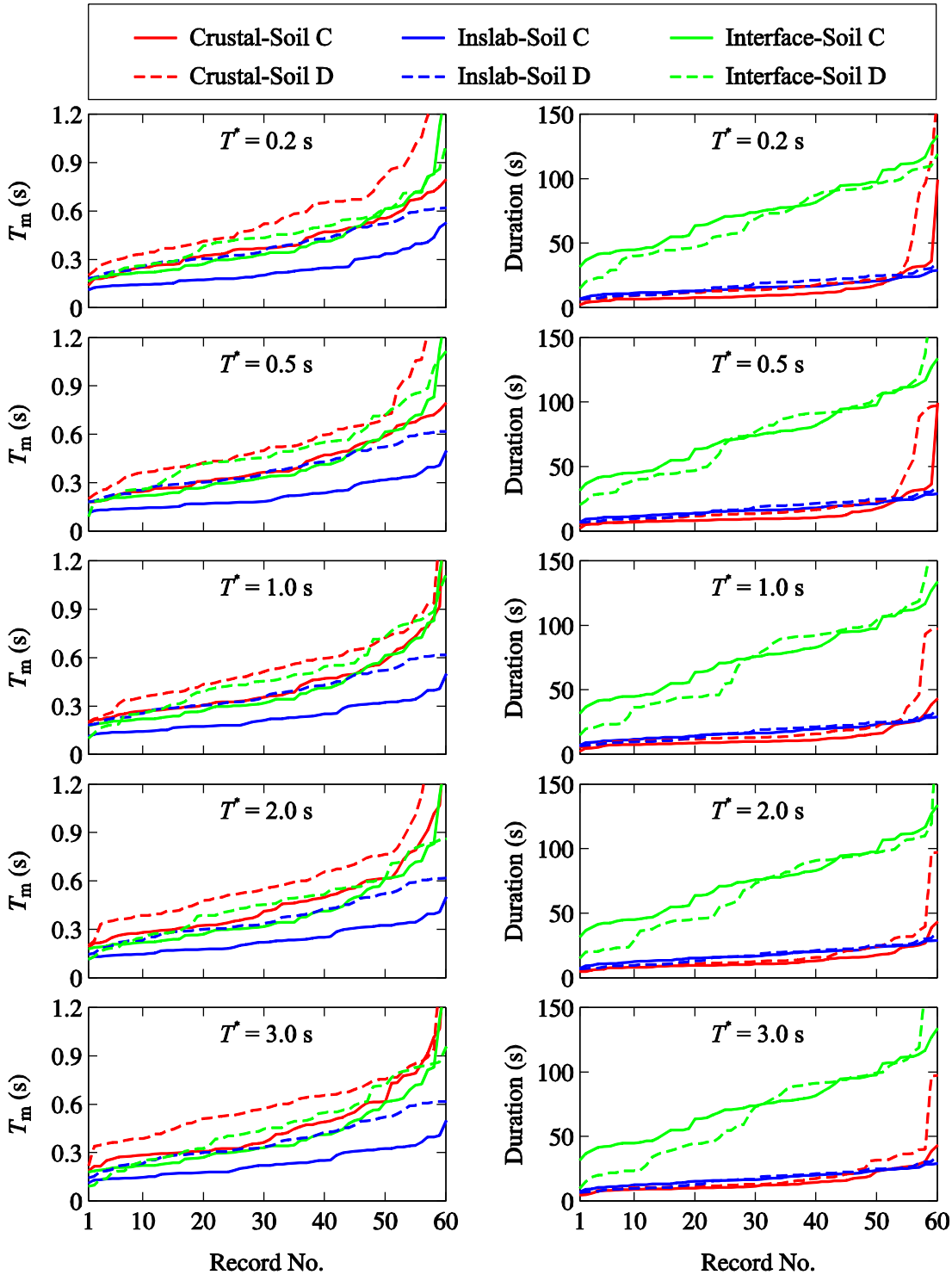

Figure 6-5: (a) Mean period and (b) duration for the 5%-95% Arias intensity interval of the selected records from the three event types at T* = 0.2 s, 0.5 s, 1.0 s, 2.0 s and 3.0 s for soil classes C and D.

effect of damping is more significant for the former (Naeim and Kircher 2001). This explains the smaller damping reduction factors at shorter periods for inslab events, which have richer high frequency content. Figure 6-5(b) compares the duration of the selected records based on their event types. As expected, records from the selected interface events have considerably longer durations than those of the crustal and inslab events, due to the inclusion of very large events, i.e. **M**9 2011 Tohoku event. Bommer and Mendis (2005) and Zhou et al. (2014) reported a decrease in damping reduction factors with an increase in duration of records. The obtained damping reduction factors for interface events are smaller than those from other events and thus are in accordance with the observations of Bommer and Mendis (2005) and Zhou et al. (2014). Based on a study of harmonic excitation of single-degree-of-freedom systems, Zhou et al. (2014) also reported that the maximum displacement reaches a plateau and does not increase further when the system is subjected to a higher number of cycles, resulting in almost constant damping reduction factors at each damping level. The near-constant damping reduction factors for interface events that we obtain are in accord with these previous studies, and point to the importance of duration effects on damping when considering the engineering implications of great subduction earthquakes.

Figure 6-3 and Figure 6-4 also compare the η factors from sets of records corresponding to each T^* at which PSHA is conducted. It is seen that the damping reduction factors for inslab and interface records are not influenced by the selected T^*. This is expected for interface events as the deaggregation results shown in Table 1 suggest that the same set of records is selected irrespective of the selected T^*. Moderate differences are observed for crustal events as a result of changes in T^*. Such differences are more noticeable at periods T approximately between 1 s and 1.7 s, where η factors from sets of records corresponding to $T^* \geq 1$ s demonstrate a less T^*-dependent behavior. Figure 6-5 also reveals a negligible effect of T^* on the general trends in frequency content and duration of the selected records. The minor changes in the scenarios, i.e. mean **M** and mean R_{rup}, for crustal and inslab events (Table 1) lead to the majority of the selected records for each T^* being similar, which explains the minor or even negligible effect of T^* on the η factors and the trends in the frequency content and duration of the selected records.

A comparison of the results in terms of soil class (i.e. Figure 6-3 and Figure 6-4) reveals that the two soil classes, i.e. soil classes C and D, present broadly similar η factors. The negligible differences between the deaggregation results for soil classes C and D are the reason for such

observations. The minor effect of site conditions on η factors from shallow crustal earthquakes has previously been reported in the literature (e.g. Lin and Chang 2004; Rezaeian et al. 2014).

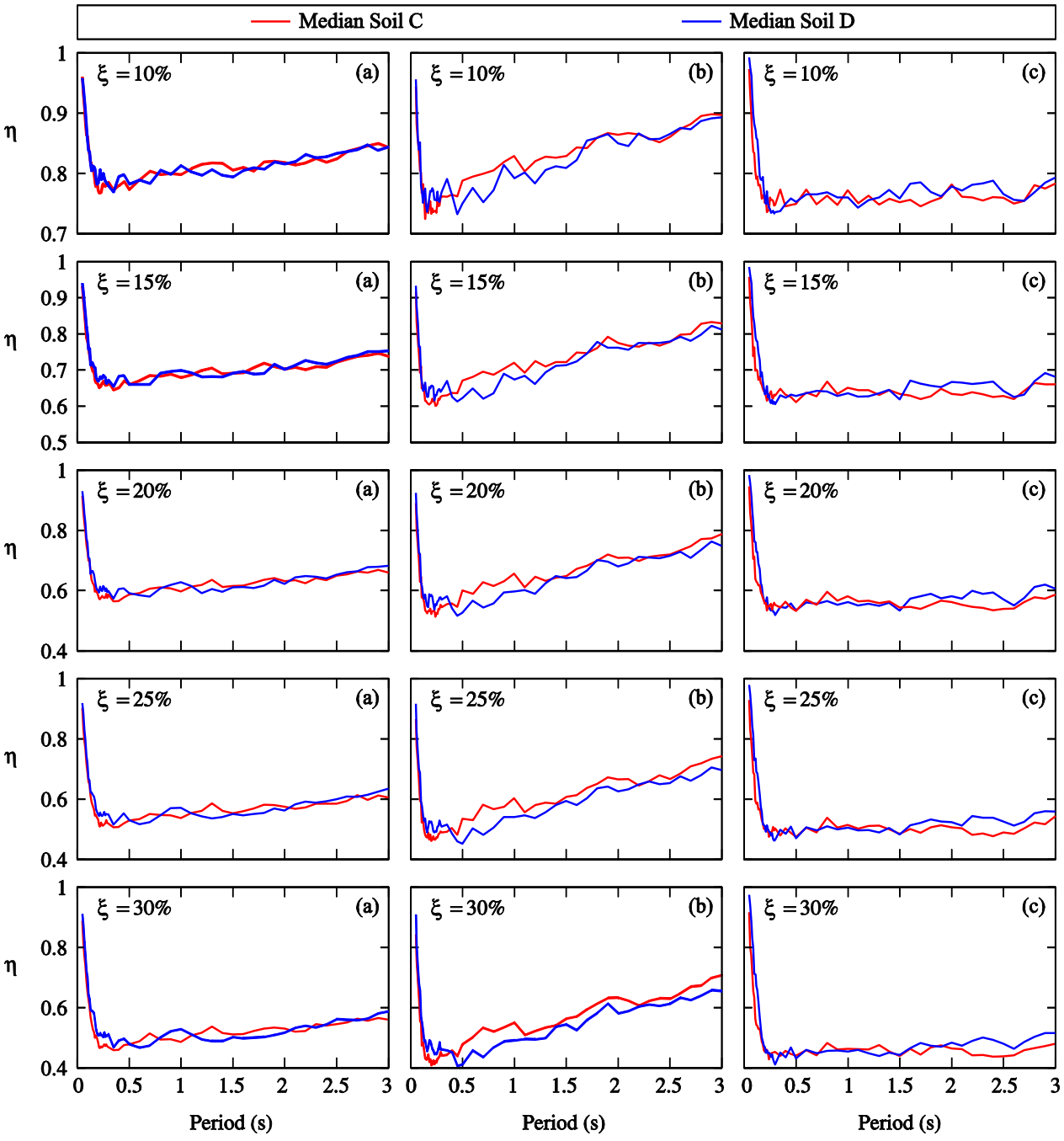

Figure 6-6: Median damping reduction factors computed by integrating all the sets of records corresponding to each T* for soil classes C and D: (a) Crustal, (b) Inslab and (c) Interface events.

As previously mentioned and illustrated in Figure 6-3 and Figure 6-4, the trends in the η factors are not significantly affected by the T^* considered. Therefore, we combined all the already selected records for different T^*s and computed the corresponding median η factors at each period T. The results are shown in Figure 6-3 and Figure 6-4 alongside those previously discussed. It can be seen that, despite some differences between the η factors computed from the Median and those from the sets of records corresponding to individual T^* for crustal events, the Median η factors can satisfactorily represent the η factors for each event. Figure 6-6 clearly illustrates that the Median η factors follow the previously observed trends in the η factors specific to each event. Figure 6-6 also reiterates the moderate effect of soil class on Median η factors for each event type and ξ considered.

6.6 Assessment of available formulations of damping reduction factors

Figure 6-3 and Figure 6-4 also compare the computed damping reduction factors of the selected crustal, inslab, and interface records to predictions of available equations from Newmark and Hall (1973, 1982) [NH1973, NH1982], Bommer et al. (2000) [BEW2000], Zhou et al. (2003) [ZWX2003], Lin and Chang (2004) [LC2004], Atkinson and Pierre (2004) [AP2004], and AASHTO (2010). The results clearly show that the majority of the available equations are not capable of predicting the computed damping reduction factors satisfactorily. The discrepancies are more evident for the η factors from inslab events, for which significant period-dependency is observed. The damping reduction factors provided by Atkinson and Pierre (2004), although they do not cover the entire period range of study, capture such period dependency and thus have acceptable agreement with those computed using crustal and inslab records, while disagreement is observed for interface events. The η factors predicted by Zhou et al. (2003) agree well with computed damping reduction factors from interface records, however, these predictions become less accurate as higher damping levels are considered. It is important to note that the available predictions are based on record datasets that do not necessarily share the same record characteristics as the ones studied herein. Therefore, it is not surprising that these equations do not satisfactorily represent the observed trends of η factors for all three event types; indeed, the anticipated discrepancy was the motivation for this investigation. Moreover, the comparisons in Figure 6-3 and Figure 6-4 highlight the need for a model equation that accounts for the distinct features of crustal, inslab, and interface earthquakes characterizing seismic hazard in south-western BC.

6.7 Proposed damping reduction factors

In this work, we develop new period-dependent equations to characterize the median damping reduction factors for the events studied. One important criterion to be satisfied by the developed equation is that its functional form can be adapted to match the computed displacements spectra of the three event types, i.e. crustal, inslab, and interface, with the least misfits possible. After several trials, the following equation is proposed to approximate the η factors:

$$\eta = 1 - (1 + a_1[-\ln \xi]^{a_2})(a_3 + T)^{a_4} \exp(a_5 T^{a_6}) \tag{6.3}$$

The coefficients in Equation (3) are determined through nonlinear regression analyses using the least squares approach. Based on the observed trends for the η factors illustrated in Figure 6-3 and Figure 6-4, one set of coefficients a_1 to a_6 for the entire period range of interest was first determined for the three event types. The results revealed that at least two sets of regression coefficients corresponding to period intervals 0 s $\leq T <$ 1 s and 1 s $< T \leq$ 3 s, respectively, are required to obtain sufficiently accurate predictions for all event types. Using more sets of coefficients corresponding to intervals below 1 s enhances the predictions at the very short period range, but at the same time complicates the use of the equation. Therefore, a compromise is made by providing coefficients a_1 to a_6 for the two period ranges 0 s $\leq T <$ 1 s and 1 s $< T \leq$ 3 s in Tables 2 and 3 for crustal, inslab, and interface events corresponding to soil classes C and D, respectively. To provide a smoother transition between the two intervals, the η factor at 1 s is calculated as the average of the outcomes of predicting expressions at periods immediately before and after 1 s.

Figure 6-7 and Figure 6-8 compare the median η factors for 10%-, 20%-, and 30%-damped displacement spectra computed from sets of records corresponding to each T^* for the three considered event types and the two soil classes with the predicted η factors obtained using proposed Equation (3). Figure 6-7 and Figure 6-8 show that there is generally a good agreement between the model predictions and the computed η factors for all the three event types. The percentages of misfit are discussed later. Slight discrepancies are observed for crustal events particularly at very short periods as illustrated in Figure 6-7 and Figure 6-8. Such misfits are neglected to allow better predictions at longer periods.

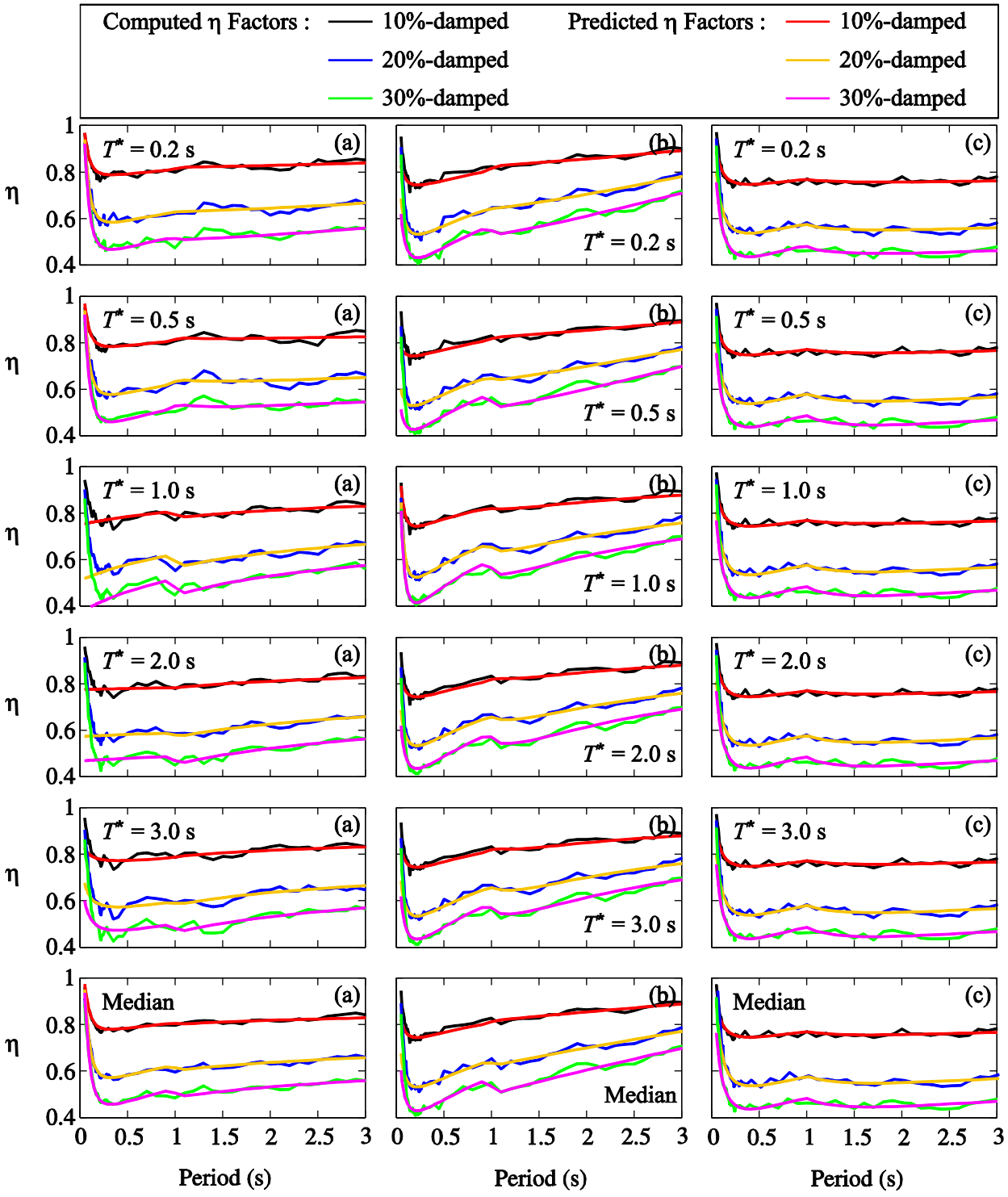

Figure 6-7: Comparison between the computed median damping reduction factors for (a) Crustal, (b) Inslab and (c) Interface events and the corresponding predictions at damping levels of 10%, 20% and 30% corresponding to soil class C.

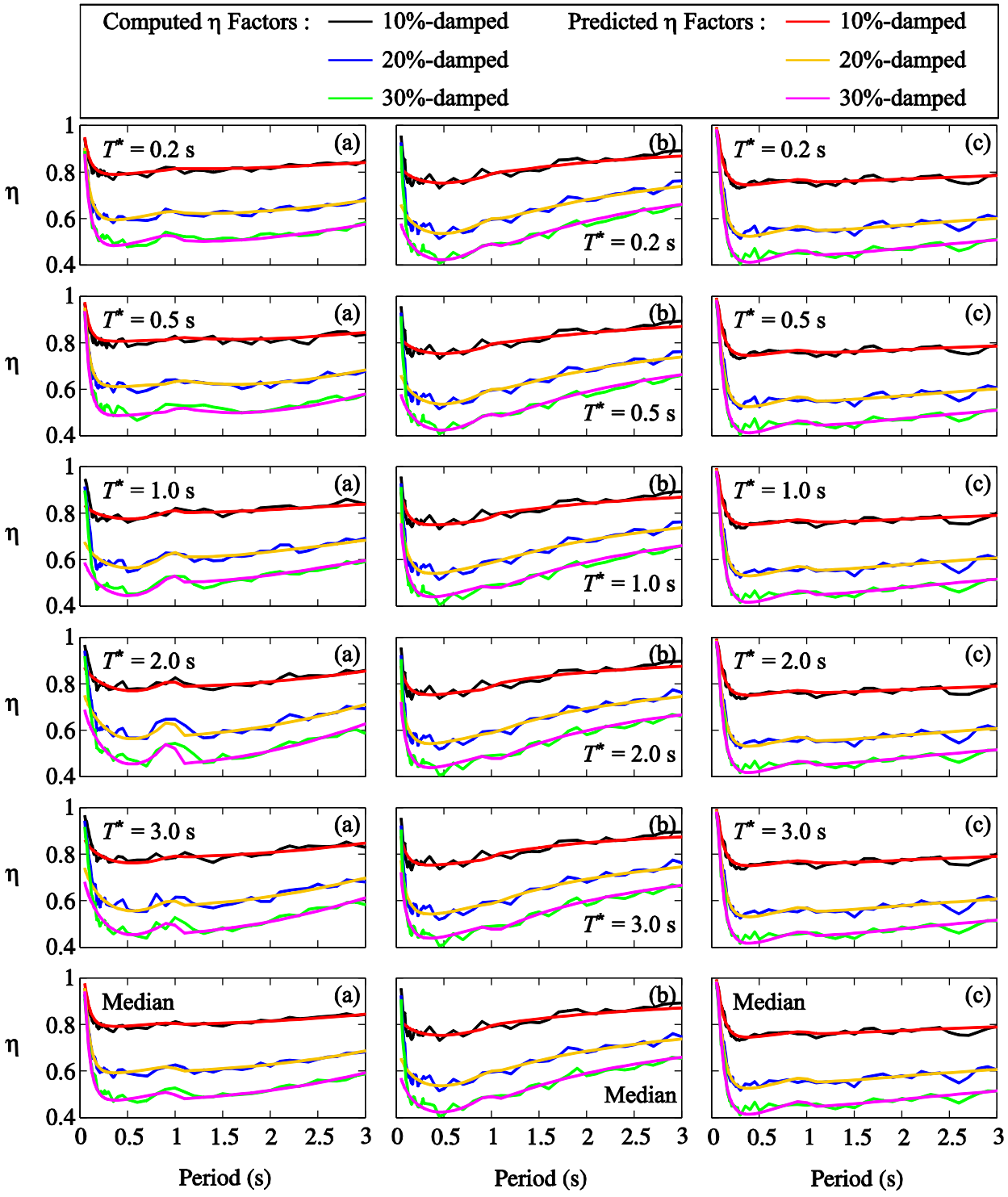

Figure 6-8: Comparison between the computed median damping reduction factors for (a) Crustal, (b) Inslab and (c) Interface events and the corresponding predictions at damping levels of 10%, 20% and 30% corresponding to soil class D.

Table 6.2 Coefficients a1 to a6 for soil class C

Event Type	T*	Period range	a_1	a_2	a_3	a_4	a_5	a_6
Crustal	0.2 s	0.05 s ≤ T < 1 s	-0.3130	1.0543	1.0	-0.3679	-0.0051	-2.0
		1 s < T ≤ 3 s	-0.4274	0.7743	1.0	-0.0282	-0.0112	2.0
	0.5 s	0.05 s ≤ T < 1 s	-0.3005	1.0924	1.0	-0.3843	-0.0051	-2.0
		1 s < T ≤ 3 s	-0.3451	0.9703	1.0	-0.1756	-0.1151	-2.0
	1.0 s	0.05 s ≤ T < 1 s	-0.3005	1.0924	1.0	-0.3843	-0.0051	-0.25
		1 s < T ≤ 3 s	-0.2860	1.1422	0.0	-0.3001	-0.1555	-0.5
	2.0 s	0.05 s ≤ T < 1 s	-0.2259	1.3561	1.0	-0.0542	-0.2860	0.0
		1 s < T ≤ 3 s	-0.2983	1.1034	0.0	-0.2611	-0.1432	-0.5
	3.0 s	0.05 s ≤ T < 1 s	-0.2001	1.4696	1.0	-0.3712	-0.1329	-0.5
		1 s < T ≤ 3 s	-0.3173	1.0473	0.0	-0.2530	-0.1338	-0.5
	Median	0.05 s ≤ T < 1 s	-0.2830	1.1469	1.0	-0.4443	-0.0057	-2.0
		1 s < T ≤ 3 s	-0.3254	1.0243	0.0	-0.2016	-0.1691	-0.5
Inslab	0.2 s	0.05 s ≤ T < 1 s	-0.1668	1.6345	1.0	-0.7997	-0.0334	-1.0
		1 s < T ≤ 3 s	-0.4102	0.8122	1.0	-0.0692	-0.0551	2.0
	0.5 s	0.05 s ≤ T < 1 s	-0.1713	1.6101	1.0	-0.8125	-0.0440	-0.75
		1 s < T ≤ 3 s	-0.4261	0.7759	0.0	-0.0436	-0.0524	2.0
	1.0 s	0.05 s ≤ T < 1 s	-0.1930	1.4987	1.0	-0.8814	-0.0033	-2.0
		1 s < T ≤ 3 s	-0.2965	1.1118	0.0	-0.6207	-0.3099	-2.0
	2.0 s	0.05 s ≤ T < 1 s	-0.1582	1.6838	1.0	-0.8783	-0.0337	-1.0
		1 s < T ≤ 3 s	-0.3170	1.0496	0.0	-0.6126	-0.3211	-3.0
	3.0 s	0.05 s ≤ T < 1 s	-0.1582	1.6838	1.0	-0.8783	-0.0337	-1.0
		1 s < T ≤ 3 s	-0.3170	1.0496	0.0	-0.6126	-0.3211	-3.0
	Median	0.05 s ≤ T < 1 s	-0.1711	1.6111	1.0	-0.7974	-0.0311	-1.0
		1 s < T ≤ 3 s	-0.4119	0.8080	0.0	-0.1661	-0.0404	2.0
Interface	0.2 s	0.05 s ≤ T < 1 s	-0.1740	1.5927	1.0	-0.4994	-0.0558	-1.0
		1 s < T ≤ 3 s	-0.1837	1.5443	0.0	-0.2009	-0.3620	-1.0
	0.5 s	0.05 s ≤ T < 1 s	-0.1740	1.5927	1.0	-0.4994	-0.0558	-1.0
		1 s < T ≤ 3 s	-0.1894	1.5162	1.0	-0.2296	-0.2111	-2.0
	1.0 s	0.05 s ≤ T < 1 s	-0.1612	1.6640	1.0	-0.5255	-0.0592	-1.0
		1 s < T ≤ 3 s	-0.1880	1.5225	1.0	-0.2340	-0.2015	-2.0
	2.0 s	0.05 s ≤ T < 1 s	-0.1612	1.6640	1.0	-0.5255	-0.0592	-1.0
		1 s < T ≤ 3 s	-0.1880	1.5225	1.0	-0.2340	-0.2015	-2.0
	3.0 s	0.05 s ≤ T < 1 s	-0.1740	1.5927	1.0	-0.4994	-0.0558	-1.0
		1 s < T ≤ 3 s	-0.1894	1.5162	1.0	-0.2296	-0.2111	-2.0
	Median	0.05 s ≤ T < 1 s	-0.1695	1.6172	1.0	-0.5019	-0.0578	-1.0
		1 s < T ≤ 3 s	-0.1882	1.5221	1.0	-0.2347	-0.2033	-2.0

Table 6.3 Coefficients a1 to a6 for soil class D

Event Type	T*	Period range	a_1	a_2	a_3	a_4	a_5	a_6
Crustal	0.2 s	0.05 s ≤ T < 1 s	-0.2860	1.1355	1.0	-0.4608	-0.0184	-1.5
		1 s < T ≤ 3 s	-0.3978	0.8381	0.5	0.5850	-0.3221	1.0
	0.5 s	0.05 s ≤ T < 1 s	-0.4368	0.7441	0.0	-0.0717	-0.0056	-2.0
		1 s < T ≤ 3 s	-0.4324	0.7597	0.0	0.3082	-0.0572	2.0
	1.0 s	0.05 s ≤ T < 1 s	-0.2885	1.1276	0.0	0.1492	-0.3686	3.0
		1 s < T ≤ 3 s	-0.2851	1.1477	0.0	0.3055	-0.2697	1.0
	2.0 s	0.05 s ≤ T < 1 s	-0.2305	1.3377	0.0	0.2708	-0.5437	3.0
		1 s < T ≤ 3 s	-0.3185	1.0434	3.0	-0.0732	-0.0136	3.0
	3.0 s	0.05 s ≤ T < 1 s	-0.1935	1.4988	0.0	0.2830	-0.4626	2.0
		1 s < T ≤ 3 s	-0.3087	1.0715	3.0	-0.0931	-0.0115	3.0
	Median	0.05 s ≤ T < 1 s	-0.3283	1.0076	1.0	-0.3143	-0.0058	-2.0
		1 s < T ≤ 3 s	-0.3482	0.9619	3.0	-0.0775	-0.0082	3.0
Inslab	0.2 s	0.05 s ≤ T < 1 s	-0.2206	1.3747	0.0	0.1755	-0.3741	2.0
		1 s < T ≤ 3 s	-0.3328	1.0053	0.0	-0.5173	-0.1317	-3.0
	0.5 s	0.05 s ≤ T < 1 s	-0.2206	1.3747	0.0	0.1755	-0.3741	2.0
		1 s < T ≤ 3 s	-0.3328	1.0053	0.0	-0.5173	-0.1317	-3.0
	1.0 s	0.05 s ≤ T < 1 s	-0.1710	1.6111	1.0	-0.5301	-0.0560	-1.0
		1 s < T ≤ 3 s	-0.3325	1.0063	0.0	-0.5041	-0.1159	-2.0
	2.0 s	0.05 s ≤ T < 1 s	-0.1882	1.5223	1.0	-0.5087	-0.0481	-1.0
		1 s < T ≤ 3 s	-0.3714	0.9045	0.0	-0.4691	-0.0332	-2.0
	3.0 s	0.05 s ≤ T < 1 s	-0.1882	1.5223	1.0	-0.5087	-0.0481	-1.0
		1 s < T ≤ 3 s	-0.3714	0.9045	0.0	-0.4691	-0.0332	-2.0
	Median	0.05 s ≤ T < 1 s	-0.2243	1.3594	0.0	0.1680	-0.3747	2.0
		1 s < T ≤ 3 s	-0.3597	0.9339	0.0	-0.4691	-0.0763	-3.0
Interface	0.2 s	0.05 s ≤ T < 1 s	-0.2089	1.4240	1.0	-0.4591	-0.0095	-2.0
		1 s < T ≤ 3 s	-0.1988	1.4716	1.0	-0.2868	-0.0886	-2.0
	0.5 s	0.05 s ≤ T < 1 s	-0.2089	1.4240	1.0	-0.4591	-0.0095	-2.0
		1 s < T ≤ 3 s	-0.1988	1.4716	1.0	-0.2868	-0.0886	-2.0
	1.0 s	0.05 s ≤ T < 1 s	-0.2204	1.3749	1.0	-0.4369	-0.0093	-2.0
		1 s < T ≤ 3 s	-0.2014	1.4600	1.0	-0.2950	-0.0893	-2.0
	2.0 s	0.05 s ≤ T < 1 s	-0.2204	1.3749	1.0	-0.4369	-0.0093	-2.0
		1 s < T ≤ 3 s	-0.2014	1.4600	1.0	-0.2950	-0.0893	-2.0
	3.0 s	0.05 s ≤ T < 1 s	-0.2204	1.3749	1.0	-0.4369	-0.0093	-2.0
		1 s < T ≤ 3 s	-0.2014	1.4600	1.0	-0.2950	-0.0893	-2.0
	Median	0.05 s ≤ T < 1 s	-0.2066	1.4343	1.0	-0.4756	-0.0097	-2.0
		1 s < T ≤ 3 s	-0.2048	1.4446	1.0	-0.2906	-0.0824	-2.0

The predictions of the proposed Equation (6.3) are then extended to the Median η factors and the results are compared to the computed ones in Figure 6-7 and Figure 6-8. To predict the Median η factors, the corresponding coefficients a_1 to a_6 are provided in Table 6.2 and Table 6.3. Figure 6-9 and Figure 6-10 illustrate the standard deviations in logarithmic scale (St. Dev.) corresponding to the median η factors for soil classes C and D, respectively. The dispersion of the η factors increases as the damping level increases. However, it does not exceed 0.3 units for both soil classes. For crustal records, the observed differences in the dispersion of η factors about the mean are due to the larger variations of the selected records at each T*. The selected inslab and interface records are quite similar for each T* and thus the corresponding dispersion about the mean does not vary significantly with T*.

For a more quantitative assessment of the performance of the model, the spectral displacements obtained using the proposed equation are compared to those given by the other available relationships described previously. The percentage of error corresponding to each expression of damping factor η in predicting computed spectral displacements $S_d(T,\xi)$ for damping ξ at period T is determined as

$$\text{Error (\%)} = \frac{\eta\, S_d(T, 5\%) - S_d(T, \xi)}{S_d(T, \xi)} \times 100 \tag{6.4}$$

The comparisons of the errors associated with the models of this study to those from the available literature are presented in Figure 6-11 to Figure 6-16. These results show that the proposed models produce the least errors for the majority of cases over the entire period range considered. The errors associated with a few combinations of T* and ξ are relatively high which is due to the jagged shape of the corresponding median η factors as discussed earlier. Overall, it is concluded that the proposed equation can be effectively used to obtain damping reduction factors corresponding to crustal, inslab, and interface earthquakes characterizing seismic hazard in the city of Vancouver.

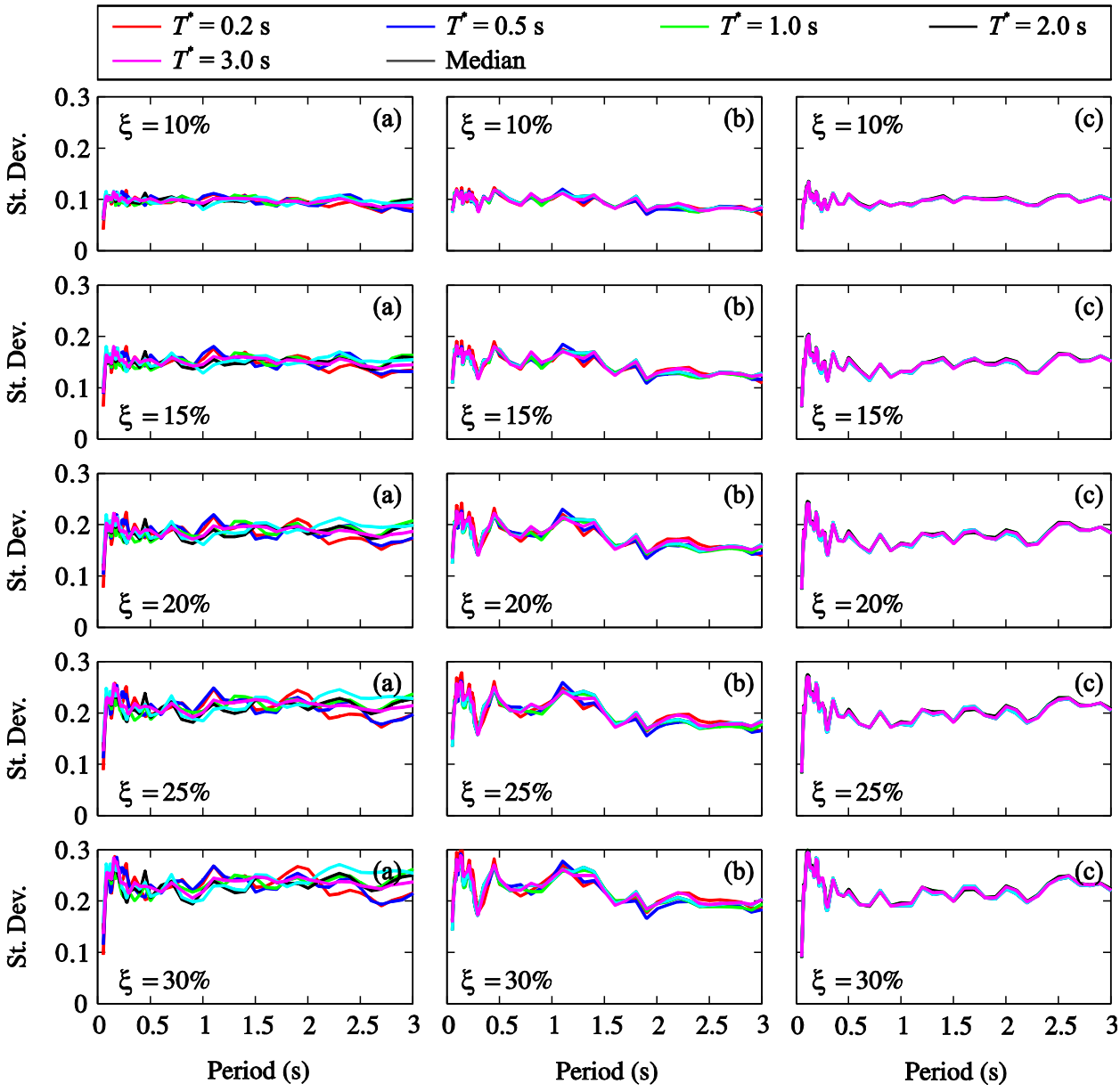

Figure 6-9: Standard deviations in logarithmic scale corresponding to median damping reduction factors for (a) Crustal, (b) Inslab and (c) Interface events corresponding to soil class C.

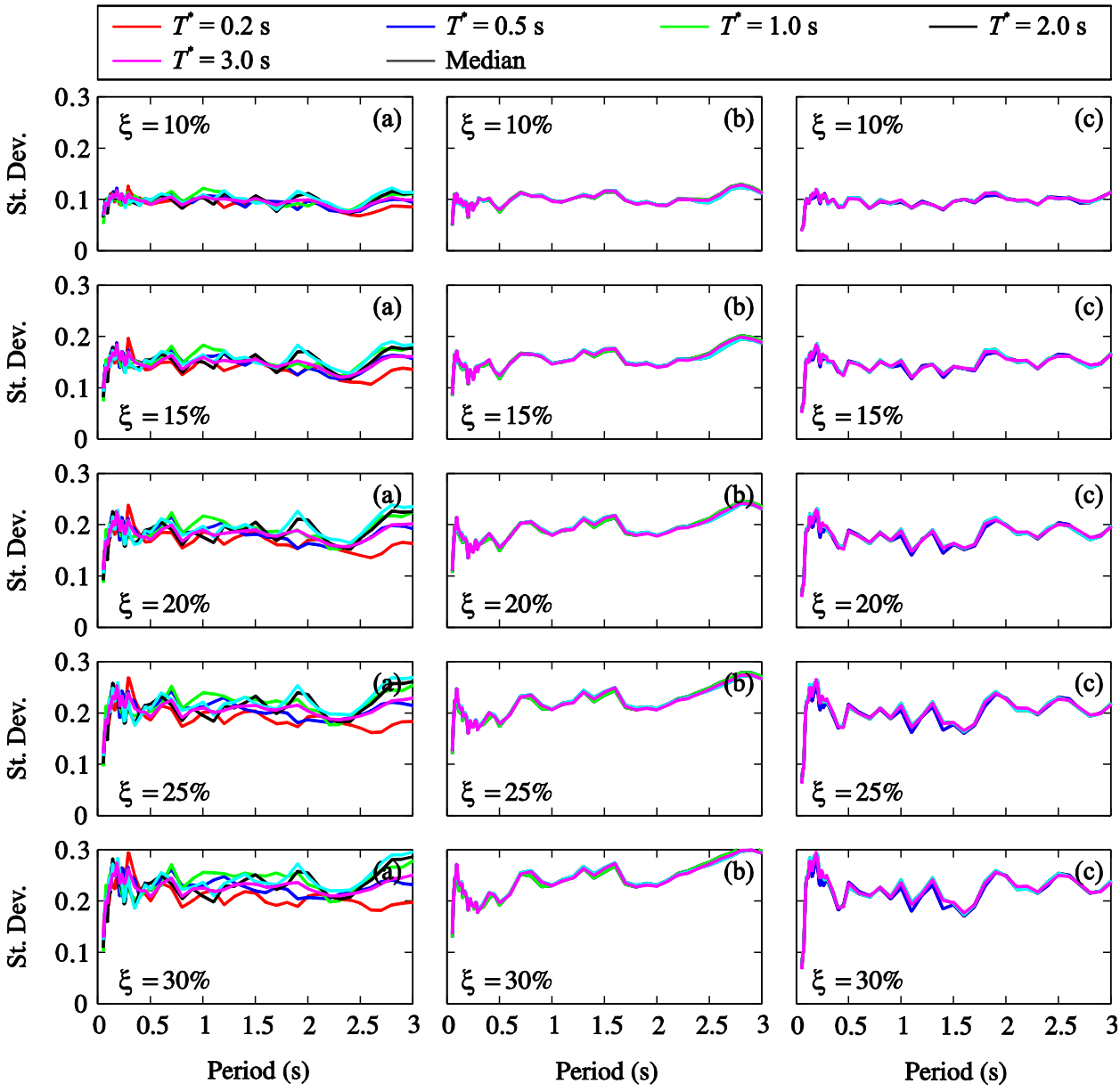

Figure 6-10: Standard deviations in logarithmic scale corresponding to median damping reduction factors for (a) Crustal, (b) Inslab and (c) Interface events corresponding to soil class D.

6.8 Summary and conclusions

High-damping displacement spectra and corresponding damping reduction factors are important ingredients for the seismic design and analysis of structures equipped with energy dissipating and/or seismic isolation systems, as well as for displacement-based design methodologies. In this paper, damping reduction factors were evaluated for three main event types (i.e. crustal, inslab, and interface) contributing to the overall seismic hazard in south-western BC.

For this purpose, a large dataset of 2302 records from the PEER-NGA, K-NET, KiK-net, and SK-net databases was first compiled. For each event type and soil type (i.e. NBCC soil classes C and D), 60 horizontal components were selected from the preliminary dataset based on seismic deaggregation results for Vancouver, the largest urban center in BC. The median damping reduction factors of this final selection of records were then determined to investigate their characteristics.

We found that the damping reduction factors of inslab records depend significantly on period, while such dependency was shown to be less pronounced for crustal records and negligible for interface records. We also observed that the damping reduction factors are practically insensitive to the period at which PSHA is performed, although a slight influence of this parameter could be seen for crustal records. Minor differences were observed in the deaggregation results for soil classes C and D, hence approximately identical damping reduction factors were obtained for both cases. These observations were further investigated by studying the frequency content and significant duration of the selected records. The rich high frequency content of inslab records results in significant period dependency of the corresponding damping reduction factors due to the more significant influence of damping ratio at shorter periods for this event type. Furthermore, the considerably longer duration of interface records for very large events (i.e. the interval of Arias intensity between 5% and 95%) results in nearly-constant damping reduction factors; this is an important consideration in seismic design for the great Cascadia subduction event. We also illustrated that the Median damping reduction factors computed from all the selected records, regardless of the period at which PSHA is conducted, can be an acceptable representative of the median damping reduction factors for each event type. A comparison between the computed damping reduction factors obtained in this study and those estimated from previous equations motivated the need of developing new model equations, capable of more accurately modeling damping reduction factors for all three types of events that contribute to the seismic hazard of south-western BC. The spectral displacements obtained using the proposed equation were validated against computed spectral displacements of the selected records. We showed that the proposed predictions provide a satisfactory evaluation of damping reduction factors corresponding to crustal, inslab, and interface earthquakes.

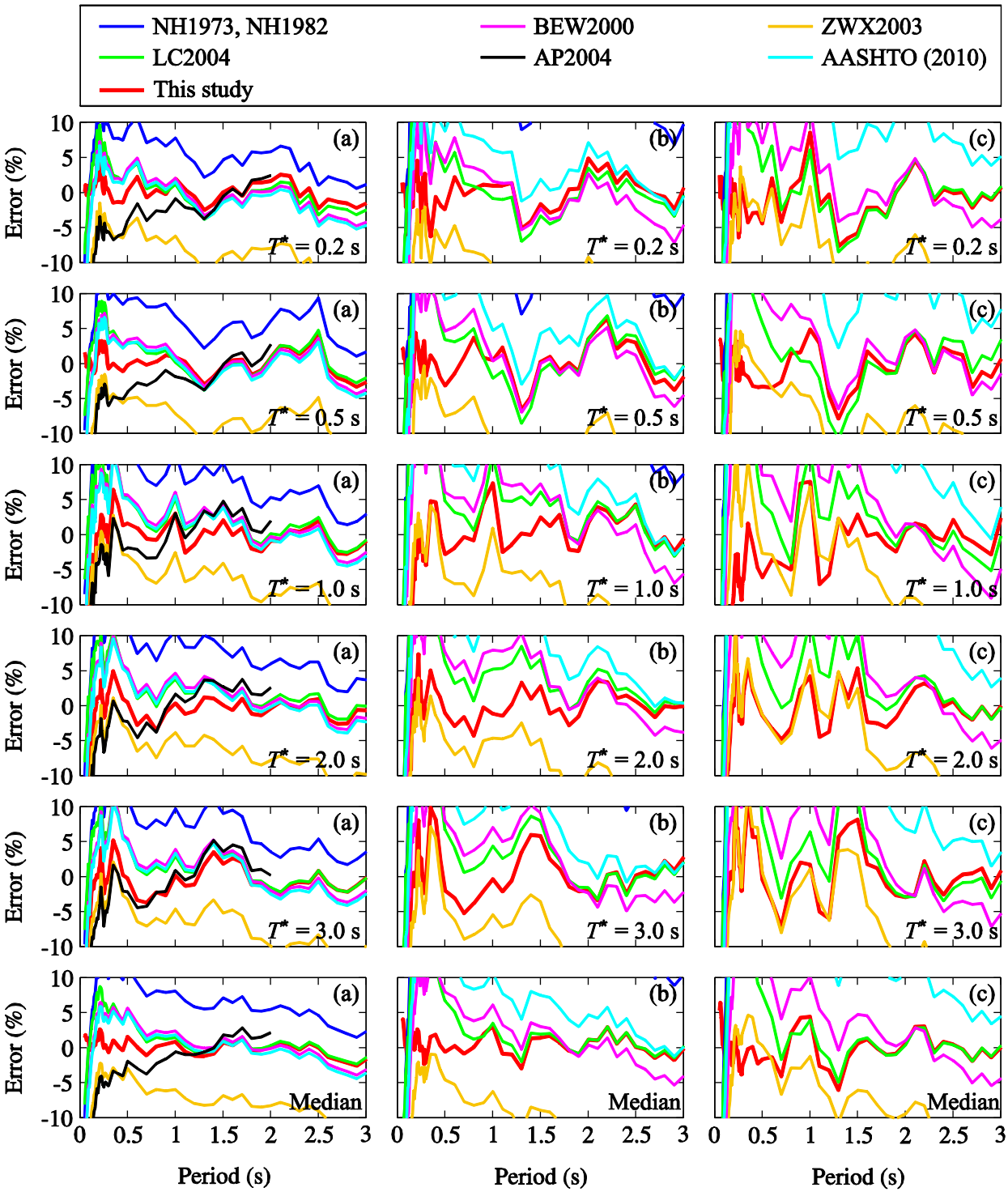

Figure 6-11: Percentages of error associated with different damping modification factor prediction equations available in the literature and the proposed equation at (a) 10%, (b) 20% and (c) 30% damping for crustal events corresponding to soil class C.

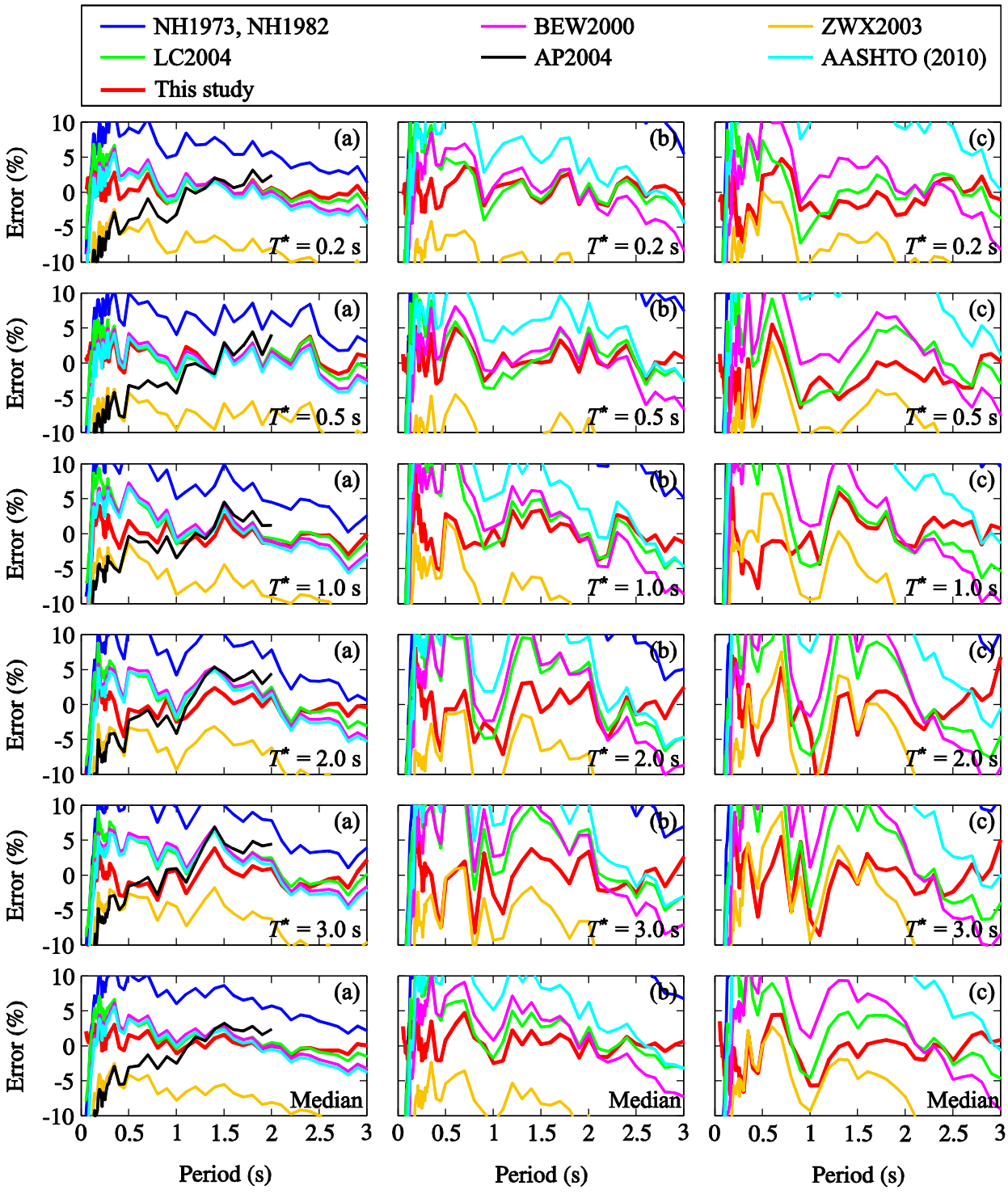

Figure 6-12: Percentages of error associated with different damping modification factor prediction equations available in the literature and the proposed equation at (a) 10%, (b) 20% and (c) 30% damping for crustal events corresponding to soil class D.

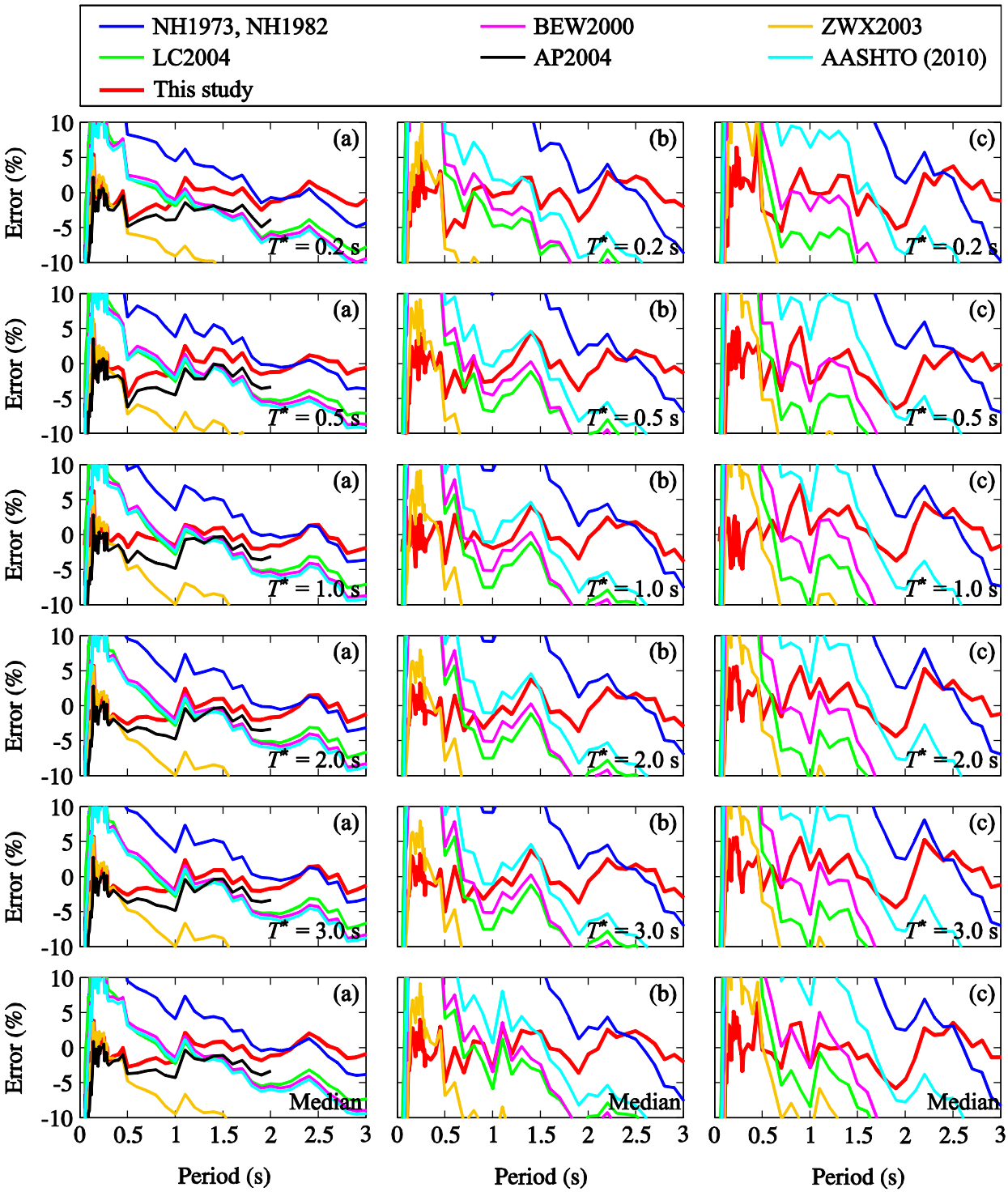

Figure 6-13: Percentages of error associated with different damping modification factor prediction equations available in the literature and the proposed equation at (a) 10%, (b) 20% and (c) 30% damping for inslab events corresponding to soil class C.

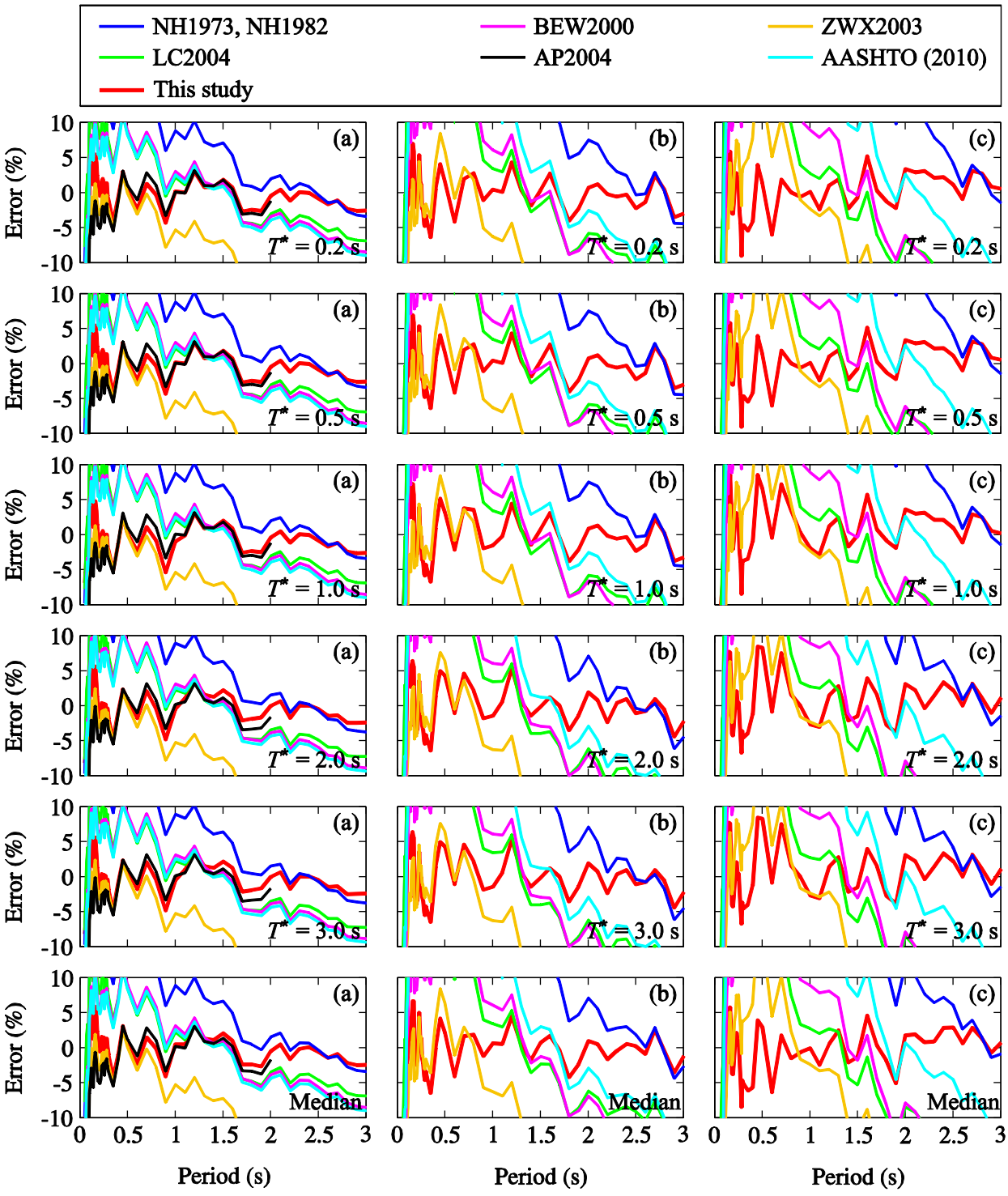

Figure 6-14: Percentages of error associated with different damping modification factor prediction equations available in the literature and the proposed equation at (a) 10%, (b) 20% and (c) 30% damping for inslab events corresponding to soil class D.

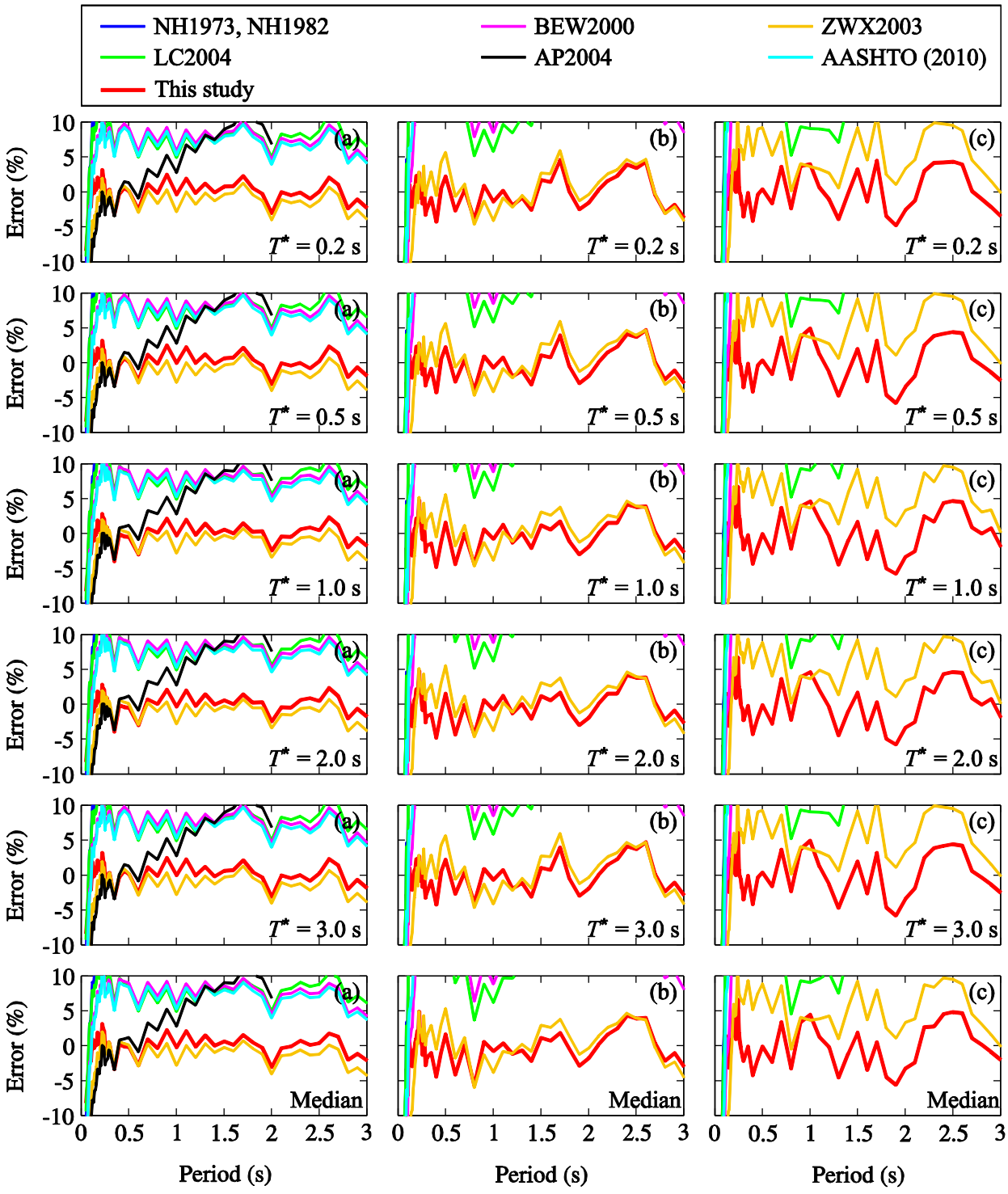

Figure 6-15: Percentages of error associated with different damping modification factor prediction equations available in the literature and the proposed equation at (a) 10%, (b) 20% and (c) 30% damping for interface events corresponding to soil class C.

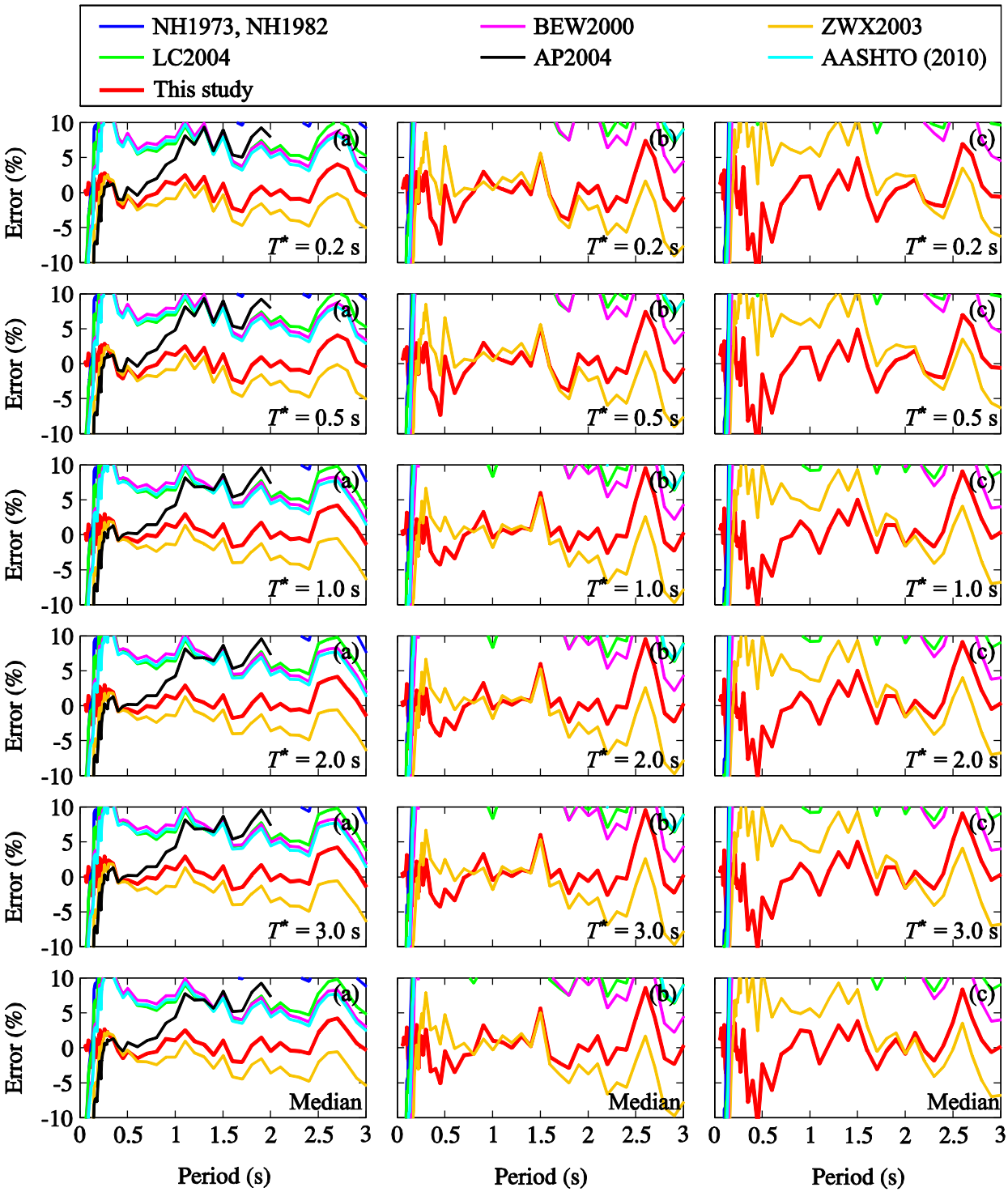

Figure 6-16: Percentages of error associated with different damping modification factor prediction equations available in the literature and the proposed equation at (a) 10%, (b) 20% and (c) 30% damping for interface events corresponding to soil class D.

Acknowledgements

The authors would like to acknowledge the financial support of the Natural Sciences and Engineering Research Council of Canada (NSERC) and the Canadian Seismic Research Network (CSRN). Strong ground-motion data were obtained from the PEER-NGA database (http://peer.berkeley.edu/nga/), the K-NET at www.k-net.bosai.go.jp, the KiK-net at www.kik.bosai.go.jp, and the SK-net at www.sknet.eri.u-tokyo.ac.jp.

References

AASHTO, American Association of State Highway and Transportation Officials, 2010. *AASHTO LRFD Bridge Design Specifications*. Washington, D.C.

Adams, J., and Halchuk, S., 2003. Fourth generation seismic hazard maps of Canada: Values for over 650 Canadian localities intended for the 2005 National Building Code of Canada. Geological Survey of Canada Open File 4459.

Akkar, S., and Bommer, J. J., 2007. Prediction of elastic displacement response spectra in Europe and the Middle East. *Earthquake Engineering and Structural Dynamics* **36**, 1275-1301.

ASCE7-10, American Society of Civil Engineers, 2010. *ASCE7-10 Minimum design loads for buildings and other structures*. Reston, Virginia.

ATC, Applied Technology Council, 2010. *Modeling and Acceptance Criteria for Seismic Design and Analysis of Tall Buildings. ATC72-1*, Redwood City, CA.

Atkinson, G. M., and Boore, D. M., 1995. Ground-motion relations for eastern North America. *Bulletin of the Seismological Society of America*, **85**, 17-30.

Atkinson, G. M., and Pierre, J. R., 2004. Ground-motion response spectra in eastern North America for different critical damping values. *Seismological Research Letters* **75**, 541-545.

Atkinson, G. M., and Goda, K., 2011. Effects of seismicity models and new ground motion prediction equations on seismic hazard assessment for four Canadian cities. *Bulletin of the Seismological Society of America*, 101, 176-189.

Baker, J. W., and Cornell, C. A., 2006. Spectral shape, epsilon and record selection. Earthquake Engineering and Structural Dynamics, **35**, 1077-1095.

Berge-Thierry, C., Cotton, F., Scotti, O., Griot-Pommera. D. A., and Fukushima, Y., 2003. New empirical spectral attenuation laws for moderate European earthquakes. *Journal of Earthquake Engineering*, **7**, 193-222.

Bommer, J. J., Elnashai, A. S., Chlimintzas, G. O., and Lee, D., 1998. *Review and development of response spectra for displacement-based design*. ESEE Research Report No. 98-3, Imperial College London.

Bommer, J. J., Elnashai, A. S., and Weir, A. G., 2000. Compatible acceleration and displacement spectra for seismic design codes. *Proceedings of the 12th World Conference on Earthquake Engineering*, Auckland, New Zealand, Paper No. 0207.

Bommer , J., J., and Mendis, R., 2005. Scaling of spectral displacement ordinates with damping ratios. *Earthquake Engineering and Structural Dynamics*, **34**, 145-165.

Boore, D. M., Joyner, W. B., and Fumal, T. E., 1993. *Estimation of response spectra and peak accelerations from western North American earthquakes: an interim report*. US Geological Survey Open-File Report.

Bradley, B. A., 2014. The influence of source- and site-specific effects on response spectrum damping modification factors. *Earthquake Spectra*, doi: http://dx.doi.org/10.1193/070213EQS189M.

Cameron, W. I., and Green, R. A., 2007. Damping correction factors for horizontal ground-motion response spectra. *Bulletin of the Seismological Society of America*, **97**, 934-960.

Cardone, D., Dolce, M., and Rivelli, M. 2009. Evaluation of reduction factors for high-damping design response spectra. *Bulletin of Earthquake Engineering*, **7**, 273-291.

Cauzzi, C., and Faccioli, E., 2008. Broadband (0.05 to 20 s) prediction of displacement response spectra based on worldwide digital records. *Journal of Seismology*, **12**, 453-475.

CHBDC, Canadian Highway Bridge Design Code, Canadian Standards Association 2006. *CAN/CSA-S6-06 Standard*, Ontario.

Chen, Y., and Yu, Y., 2008. The development of attenuation relations in the rock sites for periods ($T = 0.04 \sim 10$ s, $\xi = 0.005$, 0.02, 0.07, 0.1 & 0.2) based on NGA database. *Proceedings of Fourteenth World Conference on Earthquake Engineering*, Beijing, China, Paper No. 03-02-0029.

Chen, K. H., Kennett, B. L. N., and Furumura, T., 2013. High-frequency waves guided by the subducted plates underneath Taiwan and their association with seismic intensity anomalies. *Journal of Geophysical Research: Solid Earth*, **118**, 1-16.

EC8, European Committee for Standardization, 2004. *Eurocode 8: Design of Structures for Earthquake Resistance - Part1: General Rules, Seismic Actions and Rules for Buildings. EN 1998-1, CEN*, Brussels, Belgium.

Goda, K., and Atkinson, G. M., 2009. Probabilistic characterization of spatially correlated response spectra for earthquakes in Japan. *Bulletin of the Seismological Society of America*, **99**, 3003-3020.

Goda, K., and Atkinson, G. M., 2010. Intraevent spatial correlation of ground-motion parameters using SK-net data. *Bulletin of the Seismological Society of America*, **100**, 3055-3067.

Goda, K., and Atkinson, G. M., 2011. Seismic performance of wood-frame houses in south-western British Columbia. *Earthquake Engineering and Structural Dynamics*, **40**, 903-924.

Hong, H. P., and Goda, K., 2006. A comparison of seismic-hazard and risk deaggregation. *Bulletin of the Seismological Society of America*, **96**, 2021-2039.

Jayaram, N., Baker, J. W., Okano, H., Ishida, H., McCann, M. W., and Mihara, Y., 2011. Correlation of response spectral values in Japanese ground motions. *Earthquakes and Structures*, **2**, 357-376.

Lin, Y. Y., and Chang, K. C., 2004. Effects of site classes on damping reduction factors. *Journal of Structural Engineering*, **130**, 1667-1675.

Naiem, F., and Kircher, C. A., 2001. On damping adjustment factors for earthquake response spectra. The *Structural Design of Tall Buildings*, **10**, 361-369.

NBCC, 2010. National Building Code of Canada, Associate Committee on the National Building Code, National Research Council of Canada, Ottawa, ON.

Newmark, N. M., and Hall, W. J., 1973. *Seismic design criteria for nuclear reactor facilities*. Report No. 46, Building Practices for Disaster Mitigation, National Bureau of Standards, US Department of Commerce.

Newmark, N. M., and Hall, W. J., 1982. *Earthquake spectra and design*. Earthquake Engineering Research Institute, Oakland, CA.

Priestley, M. J. N., and Kowalsky, M. J., 2000. Direct displacement-based seismic design of concrete buildings. *Bulletin of the New Zealand National Society for Earthquake Engineering*, **33**, 421-444.

Pina, F. E., 2010. *Methodology for the seismic risk assessment of low-rise school buildings in British Columbia*. Ph.D. Thesis, The University of British Columbia, Vancouver, BC.

Priestley, M. J. N., Calvi, G. M., and Kowalsky, M. J., 2007. *Displacement-based seismic design of structures*. IUSS Press, Pavia, Italy.

Rathje, E. M., Abrahamson, N. A., and Bray, J. D., 1998. Simplified frequency content estimates of earthquake ground motions. *Journal of Geotechnical and Geoenvironmental Engineering*, **124**, 150-159**.**

Rathje, E. M., Faraj, F., Russell, S., and Bray, J. D., 2004. Empirical relationships for frequency content parameters of earthquake ground motions. *Earthquake Spectra*, **20**, 119-144.

Rezaeian, S., Bozorgnia, Y., Idriss, I. M., Campbell, K. W., Abrahamson, M., and Silva, W. J., 2014. Damping scaling factors for elastic response spectra for shallow crustal earthquakes in active tectonic regions: "Average" horizontal component. *Earthquake Spectra*, **30**, 939-963.

Tehrani, P., Goda, K., Mitchell, D., Atkinson, G. M., and Chouinard, L. E., 2014. Effects of different record selection methods on the transverse seismic response of a bridge in south western British Columbia. *Journal of Earthquake Engineering*, **18**, 611-636.

Trifunac, M. D., and Brady, A. G., 1975. A study on the duration of strong earthquake ground motion. *Bulletin of the Seismological Society of America*, **65**, 581-626.

UBC-97, Uniform Building Code, International Code Council 1997. *Uniform building code*. UBC-97, Whittier, CA.

Zhou, F., Wenguang, L., and Xu, Z., 2003. State of the art on applications, R & D and design rules for seismic isolation in China. *Proceedings of the 8th World Seminar on Seismic Isolation, Energy Dissipation and Active Vibration Control of Structures*, Yerevan, Armenia.

Zhou, J., Tang, K., Wang, H., and Fang, X., 2014. Influence of ground motion duration on damping reduction factor. *Journal of Earthquake Engineering*, DOI: 10.1080/13632469.2014.908152

CHAPTER 7 EXAMPLE APPLICATIONS TO SEISMIC DESIGN AND EVALUATION OF STRUCTURES

This chapter intends to shed more light on the findings presented through Chapters 3 to 6 and provide example applications to seismic design and evaluation of structures. For the sake of brevity only three examples are included in this chapter. First, application of the computed CMS, considering different correlation coefficients, to response spectrum analysis of a building in Eastern Canada is presented. Next, damping reduction factors are computed from the GMPEs for displacements, developed in Chapter 5, and are used in the preliminary design of a seismically isolated bridge located in Montreal. Finally, damping reduction factors determined for Vancouver in Chapter 6 are used in the preliminary design of a seismically isolated bridge in Vancouver.

7.1 Conditional mean spectrum

The application of CMS to response spectrum analysis of an eight-storey building and the comparison of the obtained inter-storey drifts, roof displacement, elastic base shear, distribution of shear force and moment on a shear wall are already presented in Chapter 3. The application of the spectral acceleration correlation coefficients $\rho(T_1, T_2)$ developed in Chapter 4 for Eastern Canada is presented in this section. To this end, the same eight-storey building, introduced in Chapter 3, is considered for the response spectrum analysis. It is assumed that the building is located on hard rock, i.e. NBCC site class A, and the NBCC 2010 UHS for Montreal is considered for the comparative study. The seismic response of the building is studied in the transverse North-South direction.

The procedure described in Section 3.3 and illustrated in Figure 4-1 is followed to construct the CMS. Four different CMS are developed for this example considering the four sets of $\rho(T_1, T_2)$ described in Chapter 3: (i) $\rho(T_1, T_2)$ developed from the entire database of records from Eastern Canada as described in Section 4.4.1; (ii) Magnitude-based $\rho(T_1, T_2)$ for Eastern Canada as explained in Section 4.4.2; (iii) Distance-based $\rho(T_1, T_2)$ for Eastern Canada as explained in Section 4.4.2; and (iv) $\rho(T_1, T_2)$ introduced as BJ08 in Chapter 4 developed based on ground motions from active tectonic regions. The CMS computed using these $\rho(T_1, T_2)$ coefficients are

referred to in this example as CMS-EC, CMS-ECM, CMS-ECR, and CMS-BJ08, respectively. The procedure reported in Section 4.4.1 is followed to account for the high frequency content of ground motions and the $\rho(T_1, T_2)$ are modified accordingly.

Response spectrum analyses of the building model is conducted using the four computed CMS as described above. The obtained results are illustrated in Figure 7-1. It can be seen in Figure 7-1(a) that, similar to the example in Chapter 3, the elastic base shear is considerably reduced when the UHS is replaced with a CMS in a response spectrum analysis. Conducting the analysis using CMS-BJ08 results in a lower base shear as the contribution of the higher modes are slightly lower for this version of CMS. This can also be observed in Figures Figure 4-17 and Figure 4-20.

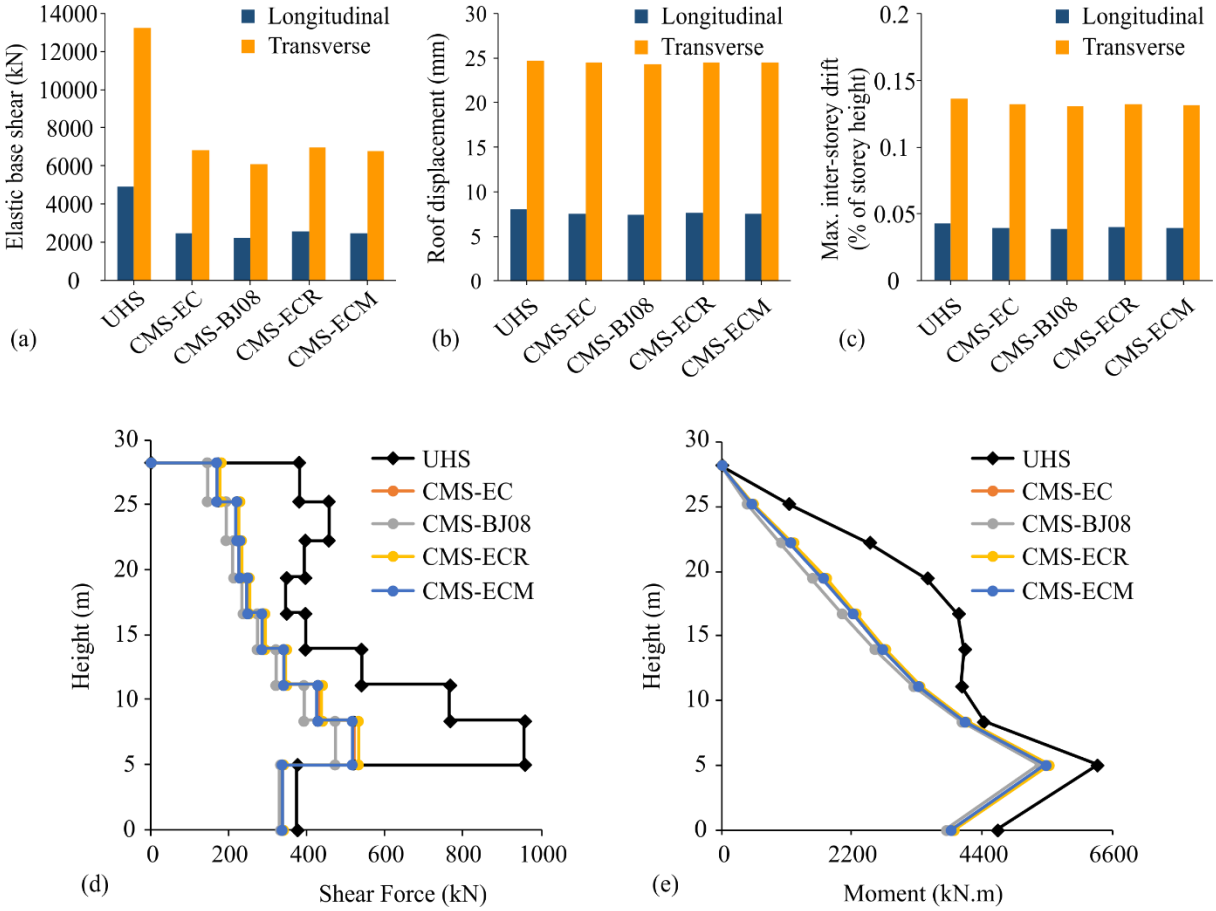

Figure 7-1: Comparison of UHS- and CMS-based response spectrum analysis results

The obtained roof displacement and inter-storey drift values, shown in Figure 7-1(b) and Figure 7-1(c), remain practically the same as the fundamental period of vibration is the major contributor

to these response indicators and all four CMS are anchored to the UHS at this period. The distributions of shear forces and bending moments in shear wall no. 4 are illustrated in Figure 7-1(d) and Figure 7-1(e). The four CMS-based shear force distributions are of lower amplitudes than the UHS-based one, with maximum differences observed at the first and second floors. CMS-based moment distributions are also lower than the UHS-based over the height of the building. Maximum differences between the two types are however concentrated from the 4th to the 6th floors. The distributions corresponding to CMS-BJ08 are slightly lower than those associated with the other CMS due to the relatively lower spectral amplitudes given by CMS-BJ08 at periods other than the fundamental period of the structure. This is illustrated in Figures Figure 4-17 and Figure 4-20.

7.2 Damping reduction factors

The Elastic Static Analysis (ESA) method is prescribed by CHBDC (2014) to determine seismic displacements and forces in isolation devices for bridges in which the first mode dominates the response to ground motions. Thus the dynamic seismic behaviour, in the direction under study, can be obtained by studying a system having a single degree of freedom: the horizontal displacement of the bridge. As ESA is a simplified and approximative method, CHBDC (2014) sets a number of limits on its application:

a) The equivalent damping ratio ξ must not be greater than 0.30, except for the case that the ratio of spectral acceleration at 0.2 s over that at 2 s is greater or equal to 8.0, i.e. S_a (0.2) / S_a (2.0) ≥ 8.0. In this case, the upper limit for ξ is increased to 0.40. ξ should include the inherent damping of the structure, the hysteresis damping of the isolators and the additional viscous damping in the case that a viscous damping device is present.

b) The obtained seismic design displacement d for the isolated bridge should be at least 1.5 times greater than the spectral displacement at the fundamental period of the non-isolated bridge. This criteria need not be satisfied in the case that the isolation system provides the minimum required lateral restoring force prescribed by CHBDC (2014), i.e. the lateral force is 0.0125W times greater than the lateral force at 50% of the seismic design displacement.

c) The effective period of vibration of the isolated bridge T_{eff} must be shorter than 3 s.

d) The bridge must not be located in site class F.

ESA method is applied to determine the displacement and forces of a considered bridge, through an iterative process. The procedure starts with an assumed seismic design displacement *d*. This value can be taken as $d = 250 \times S(T_{\text{eff}}) \times T_{\text{eff}}^2/B$ assuming T_{eff} = 1 s and B = 1 (Buckle et al. 2011) where B is the damping coefficient. Next the characteristic strength of the isolators Q_{d} and their post yield stiffness k_{d} is determined. To start the calculations, one way to determine these values is to consider the total Q_{d} as a percentage of the weight of the superstructure W and distribute it among the individual isolators based on the tributary weight of the superstructure at each support. k_{d} can also be considered as a percentage of W/d and similar to Q_{d} can be distributed among the isolators in proportion to the tributary weight of the superstructure. The effective stiffness K_{eff} at each support *j* is calculated considering the stiffness of the substructure $k_{\text{sub},j}$ as

$$K_{\text{eff},j} = \frac{\alpha_j k_{\text{sub},j}}{1 + \alpha_j} \tag{7.1}$$

where $\alpha_j$is a parameter to facilitate determination of $K_{\text{eff},j}$and is given as

$$\alpha_j = \frac{k_{\text{d},j} d + Q_{\text{d},j}}{k_{\text{sub},j} d - Q_{\text{d},j}} \tag{7.2}$$

The displacement of the isolator at each pier *j* is given by

$$d_{\text{i},j} = \frac{d}{1 + \alpha_j} \tag{7.3}$$

and thus the displacement of the substructure is determined as $d_{\text{sub},j} = d - d_{\text{i},j}$. The effective stiffness of the isolator at each support $k_{\text{eff},j}$ is determined as

$$k_{\text{eff},j} = \frac{Q_{\text{d},j}}{d_{\text{i},j}} + k_{\text{d}.j} \tag{7.4}$$

The force at each support j is given by

$$F_{\text{sub},j} = k_{\text{sub}.j} d_{\text{sub}.j} \tag{7.5}$$

The effective period of the isolated bridge is then obtained as

$$T_{\text{eff}} = \sqrt{\frac{W}{g K_{\text{eff}}}} \tag{7.6}$$

where K_{eff} is the sum of the previously determined $K_{\text{eff},j}$ and g is the gravitational acceleration taken as $g = 9.81$ m/s^2. The equivalent damping ratio is next determined

$$\xi = \frac{W_{\text{h}}}{4\pi W_{\text{s}}} = \frac{\text{EDC}}{2\pi K_{\text{eff}} d^2} = \frac{4\sum_j Q_{\text{d}}\left(d_{\text{i}} - d_{\text{i,y}}\right)}{2\pi \sum_j K_{\text{eff},j}\left(d_{\text{i},j} + d_{\text{sub},j}\right)^2} \tag{7.7}$$

where W_{h} or EDC is the energy dissipated by the isolators in one cycle of oscillation of the bridge at an amplitude d, W_{s} is the strain energy corresponding to the same cycle of oscillation of the bridge and $d_{\text{i,y}}$ is the yield displacement of the isolator. ξ is then used in determination of damping coefficient B, i.e. $1/\eta$, as prescribed by CHBDC (2014)

$$B = \left(\frac{\xi}{0.05}\right)^n \tag{7.8}$$

where n = 0.3, except for S_{a} (0.2) / S_{a} (2.0) ≥ 8.0 when n = 0.2. B is applied to the 5%-damped displacement of the bridge at T_{eff}. The resulting seismic design displacement d is compared to the one assumed at the beginning of the procedure. In the case that the two values for d are not close

enough, the obtained value replaces the assumed one and the procedure is repeated. The iterations will continue until the assumed and the obtained seismic design displacements converge.

As mentioned above, the described ESA method relies on damping reduction factors proposed by CHBDC (2015) to determine the final seismic design displacement d. The damping reduction factors developed directly and indirectly in this thesis are assessed in this section through the use of the ESA method

A computer tool CAPI (Daneshvar et al. 2015) has been developed to perform the ESA procedure for bridges equipped with isolation and/or damping devices and is presented in the form of an Excel sheet. It can perform the ESA method for straight bridges having up to 20 spans and piers of various properties. CAPI is used in Section 7.2.1 to determine the seismic design displacement of a bridge in Montreal considering the damping reduction factors determined from the GMPEs developed in Chapter 5, referred to hereafter as DB15. CAPI is also used in Section 7.2.2 to determine the seismic design displacement of a bridge considering the damping reduction factors proposed for Vancouver in Chapter 6, referred to hereafter as DBGA15.

7.2.1 Damping reduction factors for Eastern Canada

Bridge studied

A four-span bridge with single circular columns and a superstructure consisting of a box girder adapted from Tehrani and Mitchell (2012) is selected for this example. The bridge is located in Montreal on NBCC site class C soil type and is designed according to the CHBDC (2010) with the exception of adopting the NBCC 2010 UHS for design. It has an importance factor of I = 1.0. The columns are 7 m high and 2 m in diameter. The deck consists of four 50 m long spans with a weight of 200 kN/m. Figure 7-2 illustrates the studied bridge. In this work, the bridge is equipped with 5 lead-rubber isolators, one located at each substructure. The ESA method is then used through CAPI to obtain the displacements and forces for the bridge. The final seismic design displacement is obtained by means of applying the damping reduction factors determined from DB15 for Montreal.

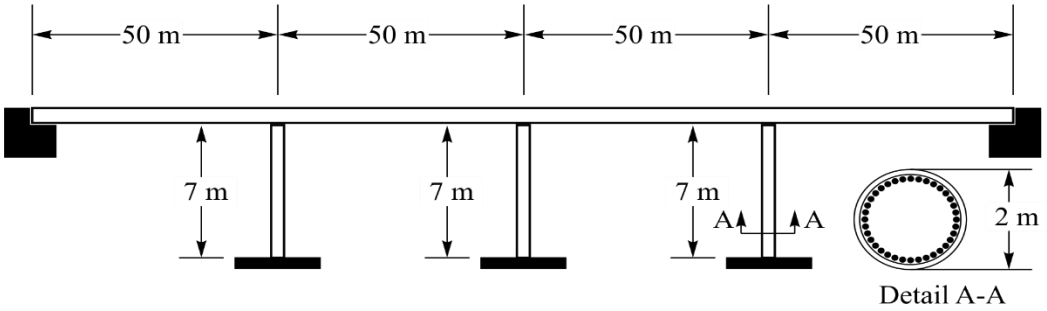

Figure 7-2 Bridge studied for Montreal (Adapted from Tehrani and Mitchell 2012)

Determination of seismic design displacements and forces

The properties of the bridge are as follows:

Weight of the superstructure W = 40000 kN;

Abutment stiffness (assumed) $k_{\text{sub1}} = k_{\text{sub5}} = 2000$ kN/mm;

Pier stiffness $k_2 = k_3 = k_4 = 177.92$ kN/mm;

Period of vibration of non-isolated bridge $T = 0.55$ s;

The period of vibration is calculated assuming only the stiffness of piers for the non-isolated bridge. The spectral acceleration and displacement corresponding to T, $S(T)$ and $S_d(T)$, respectively, are calculated according to Article 4.4.3.4 of CHBDC (2014) and are found to be $S(0.55)$ = 0.295 g, and $S_d(0.55)$ = 21.2 mm. The base shear is then calculated as $V = 0.295 \times 40000 = 11800$ kN.

The properties of the lead rubber isolators placed between the substructure and the superstructure are as follows:

At abutments:

Characteristic strength of isolator Q_d = 240 kN;

Post-yield stiffness k_d = 16 kN/mm;

Post-yield hardening ratio α = 0.15;

At piers:

Characteristic strength of isolator Q_d = 450 kN;

Post-yield stiffness k_d = 22 kN/mm;

Post-yield hardening ratio α = 0.15;

The iteration starts with an assumed $d = 250 \times S(T_{\text{eff}}) \times T_{\text{eff}}^2/B$ considering a T_{eff} = 1 s and B = 1 (Buckle et al. 2011) yielding d = 37 mm. Following a series of iterations, the calculations

result in T_{eff} = 1.03 s and ξ = 25.5% and the B coefficient prescribed by CHBDC (2014), i.e. B = 1.39, suggests d = 27.4 mm.

The same procedure was repeated for the studied isolated bridge using damping reduction factors from DB15. To obtain the appropriate damping reduction factor, the mean magnitude and distance values were taken from the deaggregation results provided by GSC (2010) and reported in Table 4.2. Linear interpolation was conducted to determine the magnitude and distance corresponding to the obtained T_{eff}. The corresponding B value is then determined as the inverse of the ξ calculated using DB15. Next, the spectral amplitude at the T_{eff} and ξ of the bridge $S_{\text{d}}(T_{\text{eff}}, \xi)$ is determined by dividing the $S_{\text{d}}(T_{\text{eff}}, 5\%)$ value by the obtained B value. For the studied bridge, the iterations and calculations result in T_{eff} = 0.92 s. The corresponding deaggregation results give a mean magnitude M = 6.77 and mean distance R = 61 km. Accordingly, DB15 predicts ξ = 27.5% and B = 2.06 which suggests d = 16.6 mm.

The obtained seismic design displacement d, the base shear V, and the force at each support F_i are presented in Table 7.1.

Table 7.1 Results obtained from application of CHBDC and DB15 damping reduction factors

	d (mm)	V (kN)	F_1(kN)	F_2(kN)	F_3(kN)	F_4(kN)	F_5(kN)
CHBDC	27.4	4157	673	937	937	937	673
DB15	16.6	3180	501.6	725.5	725.5	725.5	501.6

The results presented in Table 7.1 show a 40% and approximately a 24% reduction in the displacements and forces, respectively, when DB15 is adopted for the calculations.

7.2.2 Damping reduction factors for Vancouver

Bridge studied

A four-span bridge with single circular columns and a superstructure consisting of a box girder adapted from Tehrani et al. (2014) is selected for this example. The bridge is located in Vancouver on NBCC site class C soil type and is designed according to the CHBDC (2006). It has an importance factor of I = 1.5. The columns are 5 m high and 1.5 m in diameter. The deck consists of four 50 m long spans with a weight of 200 kN/m. Figure 7-3 illustrates the studied bridge. In

this work, the bridge is equipped with 5 lead-rubber isolators, one located at each substructure. The ESA method is then used through CAPI to obtain the displacements and forces for the bridge. The final seismic design displacement is obtained by means of applying the DBGA15 damping reduction factors developed for Vancouver in Chapter 6.

Determination of seismic design displacements and forces

The properties of the bridge are as follows:

Weight of the superstructure W = 40000 kN;

Abutment stiffness (assumed) $k_{\text{sub1}} = k_{\text{sub5}} = 2000$ kN/mm;

Pier stiffness $k_2 = k_3 = k_4 = 154.47$ kN/mm;

Period of vibration of non-isolated bridge $T = 0.59$ s;

The period of vibration is calculated assuming only the stiffness of piers for the non-isolated bridge.

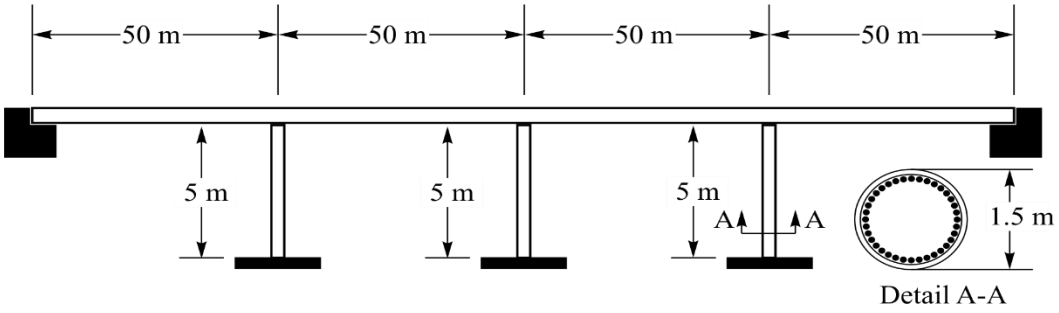

Figure 7-3 Bridge studied for Vancouver (Adapted from Tehrani et al. 2014)

The spectral acceleration and displacement corresponding to T, $S(T)$ and $S_d(T)$, respectively, are calculated according to Article 4.4.3.4 of CHBDC (2014) and are found to be $S(0.59)$ = 0.693 g, and $S_d(0.59)$ = 57.5 mm. The base shear is then calculated as $V = 0.693 \times 40000 = 27704$ kN.

The properties of the lead rubber isolators placed between the substructure and the superstructure are as follows:

At abutments:

Characteristic strength of isolator Q_d = 250 kN;

Post-yield stiffness k_d = 15 kN/mm;

Post-yield hardening ratio α = 0.15;

At piers:

Characteristic strength of isolator Q_{d} = 600 kN;

Post-yield stiffness k_{d} = 25 kN/mm;

Post-yield hardening ratio α = 0.15;

The iteration starts with an assumed $d = 250 \times S(T_{\mathrm{eff}}) \times T_{\mathrm{eff}}^2/B$ considering a T_{eff} = 1 s and B = 1 (Buckle et al. 2011) yielding d = 106.2 mm. Following a series of iterations, the calculations result in T_{eff} = 1.18 s and ξ = 16% and the B coefficient prescribed by CHBDC (2014), i.e. B = 1.42, suggests d = 93.7 mm.

The same procedure was repeated for the studied isolated bridge using damping reduction factors from DBGA15. For the studied bridge, the analysis was conducted separately for each event type contributing to the seismic hazard in Vancouver, i.e. crustal, inslab and interface events. The results obtained after the final iteration for each event type are presented in Table 7.2. The obtained seismic design displacement d, the base shear V, and the force at each support F_i corresponding to each event type are presented in Table 7.3.

Table 7.2 Results obtained from application of DBGA15 damping reduction factors

	T_{eff} (s)	ξ (%)	B	d (mm)
Crustal	1.13	19.26	1.97	63.9
Inslab	1.14	18.84	1.89	67.0
Interface	1.12	19.97	2.10	58.9

Table 7.3 Results obtained from application of CHBDC and DBGA15 damping reduction factors

		d (mm)	V (kN)	F_1(kN)	F_2(kN)	F_3(kN)	F_4(kN)	F_5(kN)
CHBDC		93.7	10884.2	1643.2	2532.6	2532.6	2532.6	1643.2
DBGA15	Crustal	63.9	8073.2	1199.5	1891.4	1891.4	1891.4	1199.5
	Inslab	67.0	8365.7	1245.7	1958.1	1958.1	1958.1	1245.7
	Interface	58.9	7602	1125	1784	1784	1784	1125

The results presented in Table 7.2 and Table 7.3 show a 32%, a 28.5%, and a 37% decrease in the seismic design displacement d for crustal, inslab, and interface events, respectively when using DBGA15. DBGA15 also reduces the base shear for approximately 35%, 30%, and 43%, for crustal, inslab and interface events, respectively.

CHAPTER 8 GENERAL DISCUSSION

8.1 Introduction

Structural engineering, in general, and seismic design and evaluation of structures, in particular, have constantly been influenced by advancement in design approaches and methodologies, development of new tools, and lessons learned from damages due to major and occasionally less significant earthquakes. This thesis discussed two main ground motion related subjects which can be reconsidered based on more recent developments in the field, considering seismic design in North America, particularly Eastern Canada.

First, the National building Code of Canada (NBCC) (2005, 2010, 2015) and also the Canadian Highway Bridge Design Code (CHBDC) (2014) assess the design adequacy of a regular structure for ground motions through determination of the induced base shear by means of a site-specific uniform hazard spectrum (UHS). Although the UHS is determined through probabilistic seismic hazard analysis (PSHA) considering the general regional seismicity (e.g., by considering return periods) and characteristics of the past events (e.g., by adopting GMPEs) (Adams et al. 2003, Atkinson and Adams 2013), the proposed spectral amplitudes are generally not representative of real ground motion records. This roots from the fact that a UHS provides spectral amplitudes considering the same hazard level at all periods. This approach neglects what one can observe from deaggregation results: spectral amplitudes considering a uniform hazard level (e.g., a exceedence of 2% in 50 years) at different periods are very likely to have been obtained from different magnitude-distance scenarios. Consequently, using a UHS as the tool for seismic design, will generally yield conservative values for forces as it cannot represent a single real ground motion record. In other words, conservative spectral amplitudes will be obtained at periods other than that considered in the analyses of the structure, e.g. the fundamental period.

Next, there is the damping reduction factors provided by design codes such as CHBDC (2006, 2014). These damping reduction factors are mainly based on the studies on ground motions from regions that have different seismic characteristics from Eastern North America (ENA), such as Western North America (WNA), and thus applying such factors in ENA might mis-predict the

damped displacement of a structure. Furthermore, these factors are commonly developed for one of the three ground motion types contributing to seismic hazard in WNA, i.e., shallow crustal earthquakes, whereas inslab and interface events have a considerable role in the seismicity of WNA, as well.

8.2 Conditional mean spectra

Baker (2011) proposed the concept of conditional mean spectrum (CMS) as a more realistic alternative to the conventional UHS. The details of computing CMS and its comparison against the UHS can be found in Chapters 3 and 4. Similar to UHS, CMS can be computed using different underlying GMPEs. CMS generated using different GMPEs are likely to differ in the produced spectral amplitudes. As a result, the influence of the selected GMPEs on CMS was illustrated in Chapter 4 for three Canadian cities.

The correlation coefficient ρ between spectral amplitudes is necessary to obtain CMS at a location. However, such coefficients have only been developed for regions of high seismicity such as WNA. Thus in Chapter 3, we first analyzed a building using the available and frequently used predicting equation for ρ values proposed by Baker and Jayaram (2008). Then a database of records from ENA was compiled and ρ values were determined for ENA. Determination of ρ coefficients requires consideration of the differences between the WNA ground motion records and those from ENA, most importantly the high frequency content of records in ENA. This was done following the procedure suggested by Carlton and Abrahamson (2014). The resulting CMS generated using ENA-based ρ values produced different spectral amplitudes at short periods than those generated using the equation given by Baker and Jayaram (2008).

8.3 Damping reduction factors

There are two approaches to determine spectral amplitudes at high damping levels. The first approach which is more cumbersome is to directly develop GMPEs to obtain spectral amplitudes at different damping levels. Several of such equations are found in the literature and are mainly for spectral accelerations at 5%-damping level. As mentioned previously in Section 7.1, displacement-based methods are gradually introduced in design procedures such as the one proposed for design of isolated bridges by CHBDC (2014). To this end, ground motion prediction equations for high-damping spectral amplitudes were developed for Eastern North America. The proposed equations

can further be used (i) in determination of damping reduction factors, i.e, by dividing the high-damping spectral amplitudes by those at 5%-damping; and (ii) in conducting PSHA in Canada based on displacements such as in developing seismic hazard maps for spectral displacements in Canada.

Several equations predicting damping reduction factors for shallow crustal earthquakes in active tectonic regions such as WNA have already been proposed (e.g., Newmark and Hall 1982, Lin and Chang 2004, Rezaeian et al. 2012). However, there is a lack of damping reduction factors for inslab and interface event types which have considerable contributions to the seismicity of WNA. It was shown in this thesis that the trends in the damping reduction factors differs from one event type to another and thus the same equation cannot satisfactorily predict this factors for all event types. As Vancouver is one of the densely populated cities in an active tectonic region Western Canada, a great seismic risk is associated with it. In this thesis, a period-based model equation was developed to predict damping reduction factors for Vancouver based on a thorough magnitude- and distance-based selection of a large database of ground motion records. The effect of the event type on the damping reduction factors was clearly demonstrated. It was also shown that the site condition and the period at which PSHA is performed have minor effects on the damping reduction factors.

8.4 Remarks

Studying the seismic hazard in the regions with moderate seismic activity, such as ENA, is always associated with uncertainties and difficulties. The principal reason for this is the lack of ground motion records which are of interest for the engineering community. There exist numerous ground motion records of low magnitude at long distances, however, such records do not truly serve the purpose of structural seismic analysis as they do not have the level of energy required for such studies. Furthermore, a large database of records has recently been compiled under the NGA-East project. However, most of these records are also from events of moment magnitudes lower than 5.5 and far field epicentral distances higher than 50 km (Goulet et al. 2013). This problem can contribute to the differences found between the correlation coefficients predicted by Baker and Jayaram (2008) and those determined in Chapter 5 of this thesis. Nevertheless, the extent of this contribution should be evaluated in light of new ground motions.

As a result of the mentioned paucity of ground motion records in ENA, simulated and hybrid records are normally used as alternatives which may introduce some bias in the results and

conclusions as these records are normally required to be scaled or matched to a target spectrum. Nonetheless, the extent of such bias in the results depends on the nature of the analysis and can be reduced by careful selection of the target spectrum accordingly.

CHAPTER 9 CONCLUSIONS AND RECOMMENDATIONS

9.1 Conclusions

This doctoral thesis aimed at investigating uniform hazard spectrum (UHS) and damping reduction factors as two main ground motion-related design tools provided by National Building Code of Canada and the Canadian Highway Bridge Design Code. The current code-prescribed practice of UHS-based seismic design and evaluation of structures can lead to over-conservative results. To investigate the applicability of the recent mostly Western North America-based developments in this regard, i.e. conditional mean spectrum (CMS), to Eastern Canada, coefficients representing correlations between spectral amplitudes at two different periods are needed. Such coefficients have to consider seismic characteristics of the region under consideration, e.g. very high frequency content of ground motions in Eastern Canada in comparison to those occurring in Western Canada. Moreover, the effect of the predicted ground motion amplitudes on CMS computed for Eastern Canada needs to be investigated. Simplified seismic design and evaluation methods mainly apply damping reduction factors obtained from the studies based on ground motions from regions of high seismicity. These ground motions do not necessarily share the same characteristics as those occurring in Eastern Canada. Furthermore, although Western Canada is a region of high seismicity, these commonly used damping reduction factors are not developed considering all the ground motion types contributing to the seismic hazard of this region. As a result, the following contributions have been made throughout this doctoral thesis:

- A step-by-step demonstration of computation of Conditional Mean Spectrum (CMS) for Eastern Canadian localities using (i) the underlying ground motion model for NBCC 2005 and NBCC 2010 UHS; and (ii) the available correlation coefficients in the literature; and subsequently application of the developed CMS to response spectrum analysis of a building located in Montreal, Quebec.
- Demonstration of the influence of (i) the most commonly used ground motion prediction equations (GMPEs) on the resulting CMS in three major Eastern Canadian cities; (ii) the adopted computation approach on the obtained CMS; and (iii) accounting for the frequency

content of the database of records used to develop correlation coefficients on the computed CMS; and development of Eastern Canadian-specific correlation coefficients based on historical ground motions.

- Development of GMPEs capable of predicting spectral displacements at damping levels of between 5% and 30% accounting for the most recent developments in prediction of spectral amplitudes in Eastern North America.
- Development of site specific damping reduction factors for Vancouver, British Columbia considering the three major event types contributing to the seismic hazard in the region.

The conclusions drawn for each of the mentioned contributions, are briefly recalled below:

9.1.1 Computation of CMS in Eastern Canada and its application to a building in Montreal

This part of research was presented in Chapter 3 and consisted of an original study to assess the application of CMS to conduct response spectrum analyses of an existing 8-storey reinforced concrete shear wall building located in eastern Canada (Montreal). The construction of the CMS was reviewed and adapted to take account of seismic hazard in Montreal. The developed CMS at the fundamental period of the building, the bracketing periods, and their envelope were used to conduct modal response spectrum analyses of the building and the results were compared to those obtained from the NBCC 2005 UHS. It was seen that for those response parameters which are greatly dependent on the fundamental period of the structure, replacing UHS with CMS does not change the results considerably. On the other hand, when a response parameter is also affected by other vibration modes, particularly at periods where there is a significant difference between the CMS and UHS amplitudes, CMS provides lower results than UHS. For the building studied, a 33% reduction in the base shear was observed when the CMS, anchored to the UHS at the fundamental period of the building, was used in the analyses. This reduction varied between 3% and 40% for bending moment along one of the shear walls. However, CMS- and UHS-based roof displacements and maximum inter-storey drifts were found to be practically the same.

9.1.2 Comparative study on the ingredients of CMS and development of correlation coefficients specific to Eastern Canada

Having demonstrated the procedure and the required ingredients for computation of CMS in Eastern Canada, a more detailed study on computation of CMS was performed and presented in Chapter 4. This work assessed the main parameters required to construct CMS in Eastern Canada and investigated the effect of their variations on the obtained CMS taking account of the seismic hazard in three different Eastern Canadian cities: Toronto, Montreal, and Quebec. It was shown that the selected GMPE can considerably affect the spectral amplitudes of the CMS mainly at shorter periods which might have an impact on the seismic analysis or evaluation of structures with relatively short fundamental periods and also those for which higher mode effects are significant. The CMS computed using two approximate methods were found to be moderately different only at short period ranges mainly due to the weights associated with the GMPEs for Eastern Canada. The applicability to Eastern Canada of spectral correlation models developed based on WNA ground motions was evaluated through studying the correlation coefficients computed for a database of ground motions recorded in Eastern Canada using an up-to-date GMPE developed for ENA and by considering the effects of higher frequency content of ground motions on correlation coefficients. The results suggest higher spectral correlations for Eastern Canada than those predicted by a WNA-based model. Finally, the dependency of correlation coefficients in Eastern Canada on magnitude and epicentral distance was investigated. Records of lower magnitude demonstrated higher correlations at short periods for longer conditioning periods T^*. The dependency of obtained correlation coefficients on magnitude is found to be generally pronounced as one of the two periods is shifted towards the longer period range. Distance-dependency was found to be less significant for distances of interest in structural engineering applications. We also showed that the effects of magnitude- or distance-based correlation coefficients on the CMS developed for the three cities are generally negligible at long periods, and significant at shorter periods particularly when the conditioning period is less than approximately 0.5 s. This work is the first study addressing in detail the ingredients and construction of CMS in Eastern Canada. The methodology and results discussed are expected to enhance the application of CMS in this region.

9.1.3 Development of equations to predict high-damping spectral displacements in Eastern North America

This part of research, as presented in Chapter 5, aimed at assessing seismic demands and associated damping reduction factors corresponding to ENA horizontal ground motions with moment magnitudes larger than M_W = 6.0, which are of more interest to structural engineering applications. For this purpose, a database of 552 horizontal hybrid empirical records having a magnitude range of $6.0 \leq M_W \leq 7.6$ and and epicentral distance range of $1 \leq R_{EPI} \leq 250$ km was first compiled to and next each spectrally matched to the 5%-damped spectral pseudo-accelerations provided for the same M_W and R_{EPI} combination by GMPEs accounting for recent developments related to ENA seismic hazard. The 5%-, 10%-, 15%-, 20%-, 25%- and 30%-damped spectral displacements were computed from the matched records. Nonlinear regression analyses were conducted on the 5%- to 30%-damped displacement spectra to obtain a magnitude- and distance-based prediction equation for periods up to 2.0 s. The results confirmed the expected direct (respectively reciprocal) relation between displacement demands and magnitude (resp. distance). The proposed equation was also used to characterize damping reduction factors considering the effects of moment magnitude, epicentral distance and site condition. The period dependency of damping reduction factors was shown to be more significant than the effect of distance and particularly at shorter periods. We also observed that the effect of distance and magnitude on damping reduction factors is more pronounced for soil sites. The results of this work will contribute to an improved assessment of seismic demands considering the particularities of seismic hazard in ENA while accounting for added-damping in the design of structures equipped with energy dissipation systems. Application of the resulting magnitude- and distance-based damping reduction factors to the analysis of a seismically isolated bridge in Montreal revealed a 40% and a 24% reduction in the overall displacement and base shear, respectively, in comparison to the values obtained when CHBDC (2014) damping reduction factors were applied.

9.1.4 Development of damping reduction factors for Vancouver considering the seismic hazard and the three contributing ground motion event types

Considering the recent popularity of adding energy dissipating and/or seismic isolation systems to structures and also emergence of displacement-based methodologies, for which high-damping

displacement spectra and corresponding damping reduction factors are important design or evaluation ingredients, in this part of research as presented in Chapter 6, damping reduction factors were evaluated for three main event types (i.e. crustal, inslab, and interface) contributing to the overall seismic hazard in south-western BC. For this purpose, a large dataset of 2302 records from the PEER-NGA, K-NET, KiK-net, and SK-net databases was first compiled. For each event type and soil type (i.e. NBCC soil classes C and D), 60 horizontal components were selected from the preliminary dataset based on seismic deaggregation results for Vancouver, the largest urban center in BC. The median damping reduction factors of this final selection of records were then determined to investigate their characteristics.

It was found that contrary to crustal and interface records the damping reduction factors of inslab records depend significantly on period. Furthermore, it was seen that the damping reduction factors are practically insensitive to the period at which PSHA is performed. Minor differences were observed in the deaggregation results for soil classes C and D, hence approximately identical damping reduction factors were obtained for both cases. A further study on the frequency content and significant duration of the selected records revealed that the rich high frequency content of inslab records results in significant period dependency of the corresponding damping reduction factors due to the more significant influence of damping ratio at shorter periods for this event type. Furthermore, the considerably longer duration of interface records for very large events (i.e. the interval of Arias intensity between 5% and 95%) results in nearly-constant damping reduction factors; this is an important consideration in seismic design for the great Cascadia subduction event. We also illustrated that the median damping reduction factors computed from all the selected records, regardless of the period at which PSHA is conducted, can be an acceptable representative of the median damping reduction factors for each event type. A comparison between the computed damping reduction factors obtained in this study and those estimated from previous equations motivated the need of developing new model equations, capable of more accurately modeling damping reduction factors for all three types of events that contribute to the seismic hazard of south-western BC. The spectral displacements obtained using the proposed equation were validated against computed spectral displacements of the selected records. Application of the resulting event-type-based damping reduction factors to the analysis of a seismically isolated bridge in Vancouver revealed a 32%, a 28.5 and a 37% reduction in the overall displacement for crustal, inslab and interface events, respectively, in comparison to the values obtained when CHBDC (2014) damping

reduction factors were applied. For crustal, inslab and interface events, a 35%, a 30% and a 43%reduction in the base shear was observed, respectively.

9.2 Recommendations

Considering the above-mentioned developments and contributions, this research work has addressed a number of issues and necessary tools towards amelioration of seismic design and evaluation of structures in North America, Canada in particular. It has also opened doors to many further research areas some of which are presented below.

9.2.1 CMS

It was shown in Chapter 3 and Chapter 4 that CMS, due to its more realistic nature of considering exceedance rates associated with spectral amplitudes, in comparison to the UHS, provides considerably lower seismic demands at periods other than the fundamental period of the structure. The study of application of CMS in response analysis of a building in Chapter 3 and Chapter 7 verified that adoption of CMS for seismic analysis will considerably influence the response parameters which are dominated by higher mode effects. It was also shown that correlation coefficients used to construct the CMS need to be modified to account for regional seismic characteristics. Nevertheless, due to lack of significant earthquakes in Eastern Canada, the study of trends and values for ground motion related parameters are always accompanied with uncertainties.

The obtained coefficients for Eastern Canada have to be verified with possible future events. Furthermore, in the case that a structure is sensitive to excitations at multiple periods, computation of CMS at the fundamental period will not produce satisfactory results. Further investigation is needed to address this issue. Application of CMS for bidirectional excitation of structures is also a subject that still needs to be further investigated.

9.2.2 High-damping spectral displacements

Equations predicting spectral displacements were developed in Chapter 5. These equations were predicted using ground motions proposed for Central and Eastern United States, a region with similar seismic hazard characteristics to Eastern Canada. The predicted displacements when applied to design of a seismically isolated bridge in the form of damping reduction factors, resulted

in considerably lower displacements and forces in comparison to the equation for damping reduction factors prescribed by NBCC 2014. Nevertheless, as already stated in Chapter 5, due to the low number of records at magnitudes higher than 7 and short epicentral distances, the predictions of the proposed equation at these magnitude-distance combinations are less reliable. Thus further research in light of future ground motions is needed to improve such predictions. In addition, with advances in construction techniques and the increasing interest in structures with longer periods of vibration, developing equations that can cover longer period ranges seem inevitable. This, indeed, requires spectral displacements reliable enough to be used in derivation of such equations. Finally, the proposed equations can be developed further to include damping levels lower than 5%.

9.2.3 Damping reduction factors accounting for different event types

In Chapter 5 damping reduction factors specific to Vancouver, British Columbia, were developed which take account of the three ground motion types contributing to the seismic hazard in the region. Application of these damping reduction factors to seismic design of a seismically isolated bridge in Chapter 7, results in lower displacements and base shear in comparison to the case where CHBDC 2014 prescribed damping reduction factors were used. However, application of the developed factors is not straight forward. Most of the damping reduction factors used in different codes and guidelines are based on those obtained from crustal events. Application of other types of damping reduction factors requires knowing the detailed deaggregation results of the location of interest and accordingly including the weight associated with each of the three event types in the underlying probabilistic seismic hazard model, in the final damping reduction factor. In addition, damping reduction factors can be developed for other major Canadian cities having a high seismic risk particularly for cities that are affected by different ground motion types. Finally, similar to the case of the high damping spectra in Eastern Canada, the equations proposed in Chapter 6, can be modified to include damping levels lower than 5%.

BIBLIOGRAPHY

AASHTO. American Association of State Highway and Transportation Officials, 2010. AASHTO LRFD Bridge Design Specifications. Washington, D.C.

Abrahamson, N. A., and Silva, W. J. (2008). Summary of the Abrahamson & Silva NGA ground-motion relations. Earthquake Spectra, 24, 67-97.

Abrahamson, N. A., and Silva, W. J. (1997). Empirical response spectral attenuation relations for shallow crustal earthquakes, Seismological Research Letters, **68**, 94-127.

Adams, J., and Atkinson, G. M. (2003). Development of seismic hazard maps for the proposed 2005 edition of the National Building Code of Canada. Canadian Journal of Civil Engineering, 30, 255-271.

Akkar, S., and Bommer, J. J. (2007). Prediction of elastic displacement response spectra in Europe and the Middle East. Earthquake Engineering and Structural Dynamics, 36, 1275-1301.

ASCE7-10. American Society of Civil Engineers, 2010. ASCE7-10 Minimum design loads for buildings and other structures. Reston, Virginia.

ATC. Applied Technology Council (2010). Modeling and Acceptance Criteria for Seismic Design and Analysis of Tall Buildings. ATC72-1, Redwood City, CA.

Atkinson, G. M. (2008). Ground-motion prediction equations for Eastern North America from a referenced empirical approach: Implications for epistemic uncertainty. Bulletin of the Seismological Society of America, 98, 1304-1318.

Atkinson, G. M. (2009). Earthquake time histories compatible with the 2005 National building code of Canada uniform hazard spectrum. Canadian Journal of Civil Engineering, 36(991-1000).

Atkinson, G. M., and Adams, J. (2013). Ground motion prediction equations for application to the 2015 Canadian national seismic hazard maps. Canadian Journal of Civil Engineering 40, 988-998.

Atkinson, G. M., and Beresnev, I. A. (1998). Compatible ground-motion time histories for new national seismic hazard maps. Canadian Journal of Civil Engineering, 25, 305-318.

Atkinson, G. M., and Boore, D. M. (1995). New ground motion relations for eastern North America. Bulletin of Seismological Society of America, 85, 17-30.

Atkinson, G. M., and Boore, D. M. (2006). Earthquake ground-motion prediction equations for Eastern North America. Bulletin of Seismological Society of America, 96, 2181-2205.

Atkinson, G. M., and Boore, D. M. (2011). Modifications to existing ground-motion prediction equations in light of new data. Bulletin of Seismological Society of America, 101, 1121-1135.

Atkinson, G. M., and Goda, K. (2011). Effects of seismicity models and new ground-motion prediction equations on seismic hazard assessment for four Candaian cities. Bulletin of Seismological Society of America, 101, 176-189.

Atkinson, G. M., and Pierre, J. R. (2004). Ground-motion response spectra in eastern North America for different critical damping values. Seismological Research Letters, 75, 541-545.

Baker, J. W. (2011). Conditional mean spectrum: tool for ground motion selection. Journal of Structural Engineering, 137(3), 322-331.

Baker J. W., and Cornell, C. A. (2005) Vector-valued ground motion intensity measure for probabilistic seismic demand analysis. John A. Blume Earthqukae Engineering Center, Report No. 150, Stanford, California.

Baker, J. W., and Jayaram, N. (2008). Correlation of spectral acceleration values from NGA ground motion models. Earthquake Spectra, 24(1), 299-317.

Baker J. W., and Cornell, C. A. (2006). Correlation of response spectral values for multi-component ground motions. Bulletin of the Seismological Society of America, 96, 215 – 227.

Bolt, B. A. (1989). The nature of earthquake ground motion. In F. Naeim (Ed.), The Seismic Design Handbook (pp. 1-31). New York, USA: Chapman & Hall.

Bommer, J. J., Elnashai, A. S., and Weir, A. G. (2000). Compatible acceleration and displacement spectra for seismic design codes. Proceedings of the 12th World Conference on Earthquake Engineering, Auckland, New Zealand, Paper No. 0207.

Boore, D. M. (1983). Stochastic simulation of high-frequency ground motions based on seismological models of the radiated spectra. Bulletin of the Seismological Society of America, 73, 1865-1894.

Boore, D. M., and Atkinson, G. M. (2008). Ground-motion prediction equations for the average horizontal component of PGA, PGV, and 5%-damped PSA at spectral periods between 0.01 s and 10.0 s. Earthquake Spectra, 24(1), 99-138.

Bozorgnia, Y., and Bertero, V. V. (2004). Earthquake Engineering: From Engineering Seismology to Performance-Based Engineering Boca Raton, USA: CRC Press LLC.

Bradley, B. A. (2014). The influence of source- and site-specific effects on response spectrum damping modification factors. *Earthquake Spectra*, doi: http://dx.doi.org/10.1193/070213EQS189M.

Burks, L. S., and Baker, J. W. (2012). Occurrence of negative epsilon in seismic hazard analysis deaggregation, and its impact on target spectra computation. Earthquake Engineering and Structural Dynamics, 41(8):1241–1256.

Campbell, K. W. (1997). Empirical near-source attenuation relationships for horizontal and vertical components of peak ground acceleration, peak ground velocity, and pseudo-absolute acceleration response spectra. Seismological Research Letters, 68, 154-179.

Campbell, K. W. (2003). Prediction of strong motion using the hybrid empirical method and its use in the development of ground-motion (attenuation) relations in Eastern North America. Bulletin of the Seismological Society of America, 93, 1012-1033.

Campbell, K. W., and Bozorgnia, Y. (2003). Updated near-source ground-motion (attenuation) relations for the horizontal and vertical components of peak ground acceleration and acceleration response spectra, Bulletin of the Seismological Society of America, 93, 314-331.

Campbell, K. W., and Bozorgnia, Y. (2008). NGA ground motion model for the geometric mean horizontal component of PGA, PGV, PGD and 5% damped linear elastic response spectra for periods ranging from 0.01 to 10 s. Earthquake Spectra, 24, 139-171.

Carballo, J. E., and Cornell, C. A. (2000). Probabilistic seismic demand analysis: spectrum matching and design: Department of Civil and Environmental Engineering, Stanford University.

Cardone, D., Dolce, M., and Palermo, G. (2009). Direct displacement-based design of seismically isolated bridges. Bulletin of Earthquake Engineering, 7, 391-410.

Cauzzi, C., and Faccioli, E. (2008). Broadband (0.05 to 20 s) prediction of displacement response spectra based on worldwide digital records. Journal of Seismology, 12, 453-475.

CHBDC. (2000). Canadian Highway Bridge Design Code. CAN/CSA-S6-00. Ontario: Canadian Standard Association.

CHBDC. (2006). Canadian Highway Bridge Design Code. CAN/CSA-S6-06. Ontario: Canadian Standard Association.

CHBDC. (2014). Canadian Highway Bridge Design Code. CAN/CSA-S6-14. Ontario: Canadian Standard Association.

Chen, Y., and Yu, Y. (2008). The development of attenuation relations in the rock sites for periods ($T = 0.04 \sim 10$ s, $\xi = 0.005$, 0.02, 0.07, 0.1 & 0.2) based on NGA database. Proceedings of Fourteenth World Conference on Earthquake Engineering, Beijing, China, Paper No. 03-02-0029.

Chiou, B. S. J., and Youngs, R. R. (2008). An NGA model for the average horizontal component of peak ground motion and response spectra. Earthquake Spectra, 24, 173-215.

Condie, K. C. (2003). Plate Tectonics and Crustal Evolution (4 ed.). London, England: Butterworth-Heinemann.

CSA. (1966). Design of Highway Bridges. CSA Standard S6. Ontario: Canadian Standards Association.

CSA. (1974). Design of Highway Bridges. CSA Standard S6. Ontario: Canadian Standards Association.

CSA. (1978). Design of Highway Bridges. CSA Standard S6. Ontario: Canadian Standards Association.

CSA. (1988). Design of Highway Bridges. CAN/CSA-S6-M88. Ontario: Canadian Standard Association

Daneshvar, P., Bouaanani, N., and Tremblay, R. (2015). CAPI. Version 1.0. [Computer Program]. Polytechnique Montreal.

Dion, K. (2010). Étude numérique et expérimentation du comportement dynamique des ponts avec isolateurs et amortisseurs sismiques. Master of Applied Science, École Polytechnique de Montréal, Montreal.

EC8, European Committee for Standardization (2004). Eurocode 8: Design of Structures for Earthquake Resistance - Part1: General Rules, Seismic Actions and Rules for Buildings. EN 1998-1, CEN, Brussels, Belgium.

Field, E. H. (2011). Probabilistic Seismic Hazard Analysis (PSHA) A Primer Retrieved 20 March, 2011, from http://www.opensha.org/sites/opensha.org/files/PSHA_Primer_v2_0.pdf

Filiatrault, A. (2002). Elements of Earthquake Engineering and Structural Dynamics (Second ed.). Montreal, Canada: Polytechnic International Press.

Hanks, T., and McGuire, R. (1981). The character of high-frequency strong ground motion. Bulletin of the Seismological Society of America, 71, 2071-2095.

Harmsen, S. C. (2001). Mean and modal epsilon in the deaggregation of probabilistic ground motion. Bulletin of the Seismological Society of America, 91(6), 1537-1552.

Idriss, I. M. (2008). An NGA empirical model for estimating the horizontal spectral values generated by shallow crustal earthquakes. Earthquake Spectra, 24, 217-242.

Lamontagne, M. (1987). Seismic activity and structural features in the Charlevoix region, Quebec. Canadian Journal of Earth Sciences, 24, 2118-2129.

Lamontagne, M., Keating, P., and Perreault, S. (2003). Seismotectonic characteristics of the Lower St. Lawrence seismic zone, Quebec: insights from geology, magnetics, gravity, and seismics. Canadian Journal of Earth Sciences, 40(2), 317-336.

Lee, W. H. K., Bennett, R. E., and Meagher, K. L. (1972). A method of estimating magnitude of local earthquakes from signal duration. United States Geological Survey Open File Report 72-223.

Lin, Y. Y., and Chang, K. C. (2004). Effects of site classes on damping reduction factors. Journal of Structural Engineering, 130, 1667-1675.

Lin, T., Harmsen, S. C., Baker, J. W., Luco, N. (2013) Conditional spectrum computation incorporating multiple causal earthquakes and ground motion prediction models. Bulletin of the Seismological Society of America 103(2A), 1103-1116.

Massicotte, B. (2011). Conception et évaluation des ponts: course notes: course CIV6511 École Polytechnice de Montreal.

McGuire, R. K. (1995). Probabilistic seismic hazard analysis and design earthquakes: closing the loop. Bulletin of the Seismological Society of America 85(5), 1275-1284

Miao, Q., and Langston, C. A. (2008). Spatial distribution of earthquake energy release in the Central United States from a global point of view. Seismological Research Letters, 79(1), 33-40.

Milne, W. G., Rogers, G. C., Riddihough, R. P., McMechan, G. A., & Hyndman, R. D. (1978). Seismicity of western Canada. Canadian Journal of Earth Sciences, 15(7), 1170-1193.

Mitchell, D., Paultre, P., Tinawi, R., Saatcioglu, M., Tremblay, R., Elwood, K., et al. (2010). Evolution of seismic design provisions in the National building code of Canada. Canadian Journal of Civil Engineering, 37, 1157-1170.

Naeim, F., Alimoradi, A., and Pezeshk, S. (2004). Selection and scaling of ground motion time histories for structural design using genetic algorithms. Earthquake Spectra, 20(2), 413-426.

Natural Resources Canada. (2013a). Earthquake zones in Eastern Canada Retrieved 15 February, 2015, from http://earthquakescanada.nrcan.gc.ca/zones/eastcan-eng.php

Natural Resources Canada. (2013b). Western Canada Earthquakes of the Last 5 Years Retrieved 15 February, 2015, from http://earthquakescanada.nrcan.gc.ca/recent/maps-cartes/index-eng.php?maptype=5y&tpl_region=west

Natural Resources Canada. (2015) Retrieved 27 February, 2015, from http://earthquakescanada.nrcan.gc.ca/histor/caneqmap-eng.php

NBCC. (1941). National Building Code. Ottawa: National Research Council of Canada.

NBCC. (1953). National Building Code of Canada. Ottawa: National Research Council of Canada.

NBCC. (1960). National Building Code of Canada. Ottawa: National Research Council of Canada.

NBCC. (1965). National Building Code of Canada. Ottawa: National Research Council of Canada.

NBCC. (1975). National Building Code of Canada. Ottawa: National Research Council of Canada.

NBCC. (1978). National Building Code of Canada. Ottawa: National Research Council of Canada.

NBCC. (1980). National Building Code of Canada. Ottawa: National Research Council of Canada.

NBCC. (1985). National Building Code of Canada. Ottawa: National Research Council of Canada.

NBCC. (1990). National Building Code of Canada. Ottawa: National Research Council of Canada.

NBCC. (2005). National Building Code of Canada. Ottawa: National Research Council of Canada.

NBCC. (2010). National Building Code of Canada. Ottawa: National Research Council of Canada.

NBCC. (2015). National Building Code of Canada. Ottawa: National Research Council of Canada.

Newmark, N. M., and Hall, W. J. (1973). Seismic design criteria for nuclear reactor facilities. Report No. 46, Building Practices for Disaster Mitigation, National Bureau of Standards, US Department of Commerce.

Newmark, N. M., and Hall, W. J. (1982). Earthquake spectra and design. Earthquake Engineering Research Institute, Oakland, CA.

Pezeshk, S., Zandieh, A., and Tavakoli, B. (2011). Hybrid empirical ground-motion prediction equations for Eastern North America using NGA models and updated seismological parameters. Bulletin of the Seismological Society of America, 101, 1859-1870.

Priestley, M. J. N., and Kowalsky, M. J. (2000). Direct displacement-based design of concrete buildings. Bulletin of the New Zealand Society for Earthquake Engineering, 33(4), 421-444.

Priestley, M. J. N., Calvi, G., and Kowalsky, M. J. (2007). Displacement-Based Seismic Design. Pavia: IUSS Press.

Rezaeian, S., Bozorgnia, Y., Idriss, I. M., Campbell, K. W., Abrahamson, M., and Silva, W. J. (2014). Damping scaling factors for elastic response spectra for shallow crustal earthquakes in active tectonic regions: “Average” horizontal component. Earthquake Spectra, 30, 939-963.

Sadigh, K., Chang, C. Y., Egan, J. A., Makdisi, F., and Youngs, R. R. (1997). Attenuation relationships for shallow crustal earthquakes based on California strong motion data. Seismological Research Letters, 68, 180-189.

Scholz, C. H. (1972). Crustal movements in tectonic areas. Tectonophysics, 14(3-4), 201-217.

Silva, W., Gregor, N., and Darragh, R. (2002). Development of regional hard rock attenuation relations for Central and Eastern North America. Technical Report, Pacific Engineering and Analysis, El Cerrito, California.

Turcotte, D. L., and Schubert, G. (2002). Geodynamics. New York, USA: Cambridge University Press.

UBC-97. Uniform Building Code, International Code Council 1997. Uniform building code. UBC-97, Whittier, CA.

USGS. 2010. United States Geological Survey. Available from https://geohazards.usgs.gov/deaggint/2008/.

Zhang, R. (2003). Seismic Isolation and Supplemental Energy Dissipation. In W. F. Chen and L. Duan (Eds.), Bridge Engineering Handbook. Boca Raton: CRC Press LLC.

Zhou, F., Wenguang, L., and Xu, Z. (2003). State of the art on applications, R & D and design rules for seismic isolation in China. Proceedings of the 8th World Seminar on Seismic Isolation, Energy Dissipation and Active Vibration Control of Structures, Yerevan, Armenia.